Title: Mechanisms of androgen-induced hypertrophy: Lessons from muscle cell models

Name: David Conway Hughes

Mechanisms of androgen-induced hypertrophy: Lessons from muscle cell models

David Conway Hughes

PhD

2014

UNIVERSITY OF BEDFORDSHIRE

Mechanisms of androgen-induced hypertrophy: Lessons from muscle cell models

By

David Conway Hughes

A thesis submitted to the University of Bedfordshire in partial fulfillment of the requirements for the degree of Doctor of Philosophy

April 2014

ABSTRACT

Androgen endocrine physiology is responsible for many processes in the body, from bone metabolism to skeletal muscle maintenance. Testosterone is one of the most potent androgens produced, with decades of research highlighting its androgenic-anabolic effect on skeletal muscle growth. The research has been further driven through the emergence of pharmaceutical derivates (steroids) of testosterone and their use in interventions for muscle wasting associated with disease and advancing age (sarcopenia). However, the molecular regulation of testosterone and the influence it has on cellular processes in promoting muscle development, hypertrophy and satellite cell activation (proliferation, differentiation) remain poorly understood.

In summary, this thesis has highlighted the impact of testosterone in rescuing an aged phenotype in myoblast cells (PD cells) displaying prior reductions in regeneration and hypertrophy vs. relevant 'un-aged' controls (Sharples *et al*., 2011, Sharples *et al*., 2012). Importantly, the results provide evidence towards the mechanisms for testosterone induced hypertrophy, where in the presence of testosterone and a functional androgen receptor (shown via AR antagonism/ flutamide administration) testosterone is fundamental in regulating appropriate myoD, myogenin and myostatin expression in the control of myotube differentiation and hypertrophy. Increases in androgen receptor protein levels in PD myoblasts under a testosterone stimulus highlight the intrinsic responsiveness of aged myoblasts to a hypertrophic stimulus which may somewhat explain the use of testosterone as an effective clinical treatment in muscle wasting disease. Finally, myotube hypertrophy occurred in both aged and un-aged myoblasts with testosterone administration even in the presence of an IGF-I receptor inhibitor (Picropodophyllin) suggesting a limited role of the IGF-IR and associated signaling in testosterones mediated increases in differentiation and hypertrophy.

Testosterone did appear however to increase Akt phosphorylation in cells that show a prior impaired regenerative capacity (PD cells), even in the presence-IGF-IR inhibitor suggesting that testosterone can directly activate Akt independently of upstream IGF-IR a novel finding that is presented in chapter 5. This interaction maybe mediated by myostatin, where increases in myostatin has

been linked with directly inhibiting Akt (Dubois *et al*., 2014, Léger *et al*., 2008, Morissette *et al*., 2009), and in the present study we see an increase in myostatin mRNA and corresponding decrease in phospho-Akt when AR's (via flutamide) action is inhibited and the protein level of AR is low (chapter 5). Furthermore in chapter 6 we further showed that inhibition of PI3K/AKT using LY294002 was sufficient to remove the prior rescuing of differentiation and hypertrophy in aged cells after testosterone administration. This was coupled with reductions in myostatin and increases in mTOR with testosterone administration. Overall AR seems to be the most fundamental pathway in testosterones induction of myotube differentiation and hypertrophy with important roles for myogenin, Akt, mTOR and myostatin in mediating these processes.

DECLARATION

I declare that this thesis is my own unaided work. It is being submitted for the degree of Doctor of Philosophy at the University of Bedfordshire.

It has not been submitted before for any degree or examination in any other University.

Name of candidate: David Hughes Signature:

Date:

Contents

List of Figures

List of Tables

ACKNOWLEDGEMENTS

Firstly, I want to thank my director of studies, Professor Mark Lewis and Dr Nicholas Sculthorpe for accepting me as a PhD student and to undertake this project of work as well as the opportunity to pursue my career in academia. I also thank Professor Claire Stewart and Dr. Adam Sharples for their continued support, advice and guidance throughout my PhD journey. I'd also like to thank the Institute for Sport and Physical Activity Research (ISPAR) and Research in Sport and Exercise Sciences (RISES) for their support in helping me complete my PhD studies.

I would also like to thank the members of the Muscle Cellular and Molecular Physiology research group (MCMPRG) and Stem Cells, Ageing and Molelcular Physiology (SCAMP) unit at the University of Bedfordshire and Liverpool John Moores respectively, with whom I've had the great pleasure of working with during my time there. Specific thanks to Miss Colleen Deane and Miss Claire Potter who have been priceless sources of support throughout my journey. I'd also like to acknowledge Dr Sharples and Dr Amarjit Saini as influential role models in my research endeavors.

I am grateful to Miss Lucy Ditzel and Miss Natalie Fitch, both of whom have always provided me with the support and strength to continue in the pursuit of my dreams. To Miss Emma Storey-Gordon, your passion and own determination always inspired me and helped a lot at the end of my PhD journey.

Finally, to my parents and brother, Dr Thomas Hughes, who have gave me so much support and guidance in my life, this is for you.

Publications and Presentations

Deane, C.S., **Hughes D.C**., Sculthorpe, N., Lewis, M.P., Stewart, C.E. & Sharples, A.P (2013). Impaired hypertrophy in myoblasts is improved with testosterone administration. *Journal of Steroid Biochemistry and Molecular Biology, 138,* 152-161. (ATTACHED see appendix 3).

Sharples, A.P, Al-Shanti, N., **Hughes, D.C**., Lewis, M.P. & Stewart, C.E. (2013). A potential role for the insulin-like growth factor binding protein 2 (IGFBP2) and phosphatase and tensin homologue (PTEN) in the regulation of myoblast differentiation and hypertrophy. *Growth Hormone and IGF-I research, 23,* 53-61.

Hughes, D.C., Sculthorpe, N., Sharples, A.P. & Lewis, M.P. (2012). Testosterone and the molecular regulation of skeletal muscle (pg 27-55). In: Perspectives on Anabolic Androgenic Steroids (AAS) and doping in Sport and Health. Nova Publisher. ISBN: 978-1-62081-243-3

Hughes, D.C., Day, S.H., Ahmetov, I.I. & Williams, A.G. (2011). Genetics of muscle strength and power: Polygenic profile similarity limits skeletal muscle performance. *Journal of Sport Sciences, 29,* 1425-1434.

Hughes, D.C., Deane, C.S., Sculthorpe, N., Lewis, M.P., Stewart, C.E., & Sharples, A.P. European College of Sports Sciences Annual Conference (Barcelona 2013): Impaired Hypertrophy in myoblasts is improved with testosterone administration.

Hughes, D.C., Sculthorpe, N., Sharples A.P. & Lewis, M.P. Physiological Society Meeting "Biomedical Basis of Elite Performance" (London 2012): The effects of testosterone on molecular markers of hypertrophy in C_2C_{12} skeletal muscle cells.

List of Abbreviations

AAS	Androgenic-Anabolic Steroids
ANOVA	Analysis of variance
AR	Androgen Receptor
ARE	Androgen Response Elements
BSA	Bovine serum albumin
CNS	Central Nervous System
CSA	Cross-Sectional Area
DHEA	dehydroepiandrosterone
DHT	dihydrotestosterone
DM	Differentiation Media
DMSO	Dimethyl Sulphoxide
DNA	Deoxyribonucleic Acid
ECL	Enhanced chemiluminescence
ERK	Extracellular signal-regulated kinases
FBS	Foetal Bovine Serum
FSH	follicle-stimulating hormone
GM	Growth Media
GnRH	gonadotropin-releasing hormone
Hrs	Hours
IGF-I	insulin-like growth factor I
IGF-IR	insulin-like growth factor I receptor
LH	Lutenizing hormone
JNK	c-Jun N-terminal kinases
mTOR	mechanistic/mammalian target of rapamycin
mRNA	messenger Ribonucleic acid
µg	Microgram
µM	Micrometer
ml	Milliliter
MAPK	Mitogen-activated Protein Kinase
MyHC	Myosin Heavy Chain

PBS	Phosphate Buffered Saline
PCR	Polymerase Chain Reaction
PCNA	Proliferating cell nuclear antigen
PPP	Picropodophyllin
RNA	Ribonucleic acid
T	Testosterone
TGF-β	Transforming Growth Factor-beta
TBS	Tris Buffered Saline
TNF-α	Tumor necrosis factor-alpha

1. GENERAL INTRODUCTION

Testosterone (17β-Hydroxyandrost-4-en-3-one: $C_{19}H_{28}0_2$) is a potent naturally occurring steroid hormone (androgen) produced from cholesterol. Within the body, testosterone (T) is responsible for regulating many physiological processes such as muscle maintenance, sexual and cognitive function, plasma lipids and bone metabolism (Bhasin *et al*., 1996, Evans, 2004). For decades, testosterone has been researched from the perspective of these physiological processes, with muscle growth, development and maintenance receiving predominant attention. Furthermore, such attention to muscle growth has been highlighted through the emergence of chemical and pharmaceutical derivates of T called Androgenic-Anabolic Steroids (AAS) (Evans, 2004, Hartgens and Kuipers, 2004). The molecular regulation of T and its pharmaceutical derivatives remain poorly understood. Recent research however, has begun to delve into these mechanisms alongside the emergence of new cellular and molecular technologies.

The aging process correlates with a gradual decline in the production of testosterone and a subsequent reduction in serum T levels (Dillon *et al*., 2010). In healthy young men, serum T levels range from 400-1000 ng/dl (Sinha-Hikim *et al*., 2003, Traish *et al*., 2011) whereas for elderly men, serum testosterone levels range from 150-550 ng/dl (Wierman, 2007). Any serum T levels below this range for elderly men are defined as hypogonadism (Dillon *et al*., 2010). Declining serum levels highlight the effects that T may have on peripheral tissues where sarcopenia and osteoporosis have been previously associated with the reduced levels (Dillon *et al*., 2010, Sattler *et al*., 2011). Testosterone administration has been utilised as a treatment for such conditions, and more importantly the development of T derivatives and selective androgen receptor modulators (SARMs) has provided a more specific target of action within the treatment of tissues (Dillon *et al*., 2010, Ting and Chang, 2008). However, due to its clinical importance it is fundamentally important to first understand the mechanisms and signalling pathways that T and androgens activate, to reduce the risk of cross talk with other signalling pathways and thus potential side effects that could be incurred with such pharmaceutical treatments (discussed below).

1.1 TESTOSTERONE PRODUCTION *IN-VIVO*

Testosterone is produced predominately in the leydig cells located in the testes of males, with a small amount being additionally secreted from the adrenal cortex and ovaries in females. The nature of the hormone prevents it from being stored in the cells that produce it and thus on production it is immediately released from the cells. The signalling for the production of T within the gonads is through the hypothalamic-pituitary-gonadal-axis (**Fig 1.1.**) (Kim, 2007, Vingren *et al*., 2010). The signal originates in the hypothalamus by innervations of the Central Nervous System (CNS) which leads to specialized neurons secreting gonadotropin-releasing hormone (GnRH). GnRH is then transported from the hypothalamus to the anterior pituitary gland and subsequently to the pituitary target cells, via the hypothalamic-hypophysical portal vein. At this location, GnRH activates the production and release of lutenizing hormone (LH) and follicle-stimulating hormone (FSH) from the gonadotropes, with both hormones consequently circulating to the gonads (**Fig1.1**).

Lutenizing hormone is responsible for testosterone production in the leydig cells in men and in the theca calls of women. This production is brought about by LH binding to a G-protein coupled membrane receptor (Miller, 1988, Payne and Hales, 2004). Furthermore, the binding process initiates a rate-limiting step in testosterone production by way of cyclic adenosine monophosphate dependant protein kinase (protein kinase A) stimulation (Miller, 1988, Payne and Hales, 2004). On the other hand, in terms of variations between men and women, FSH appears to have no direct effect on testosterone stimulation in men but stimulates production of pregnenolone in women. Pregnenolone is further processed into testosterone upon leaving the granuolsa cells. Another role of FSH, which appears in both men and women, is the stimulation of steroid binding proteins in the liver. These proteins (primary being sex-hormone binding globulin) are especially important for the T produced to be circulated within the body, due to testosterone's hydrophobic nature and thus not being readily dissolved in the systemic circulation (Vingren *et al*., 2010). Although this cascade of signalling events is the predominant source for T and androgen production, about 30 to 50%

of androgens are further produced in peripheral tissues (Labrie, 1991, Labrie, 2010).

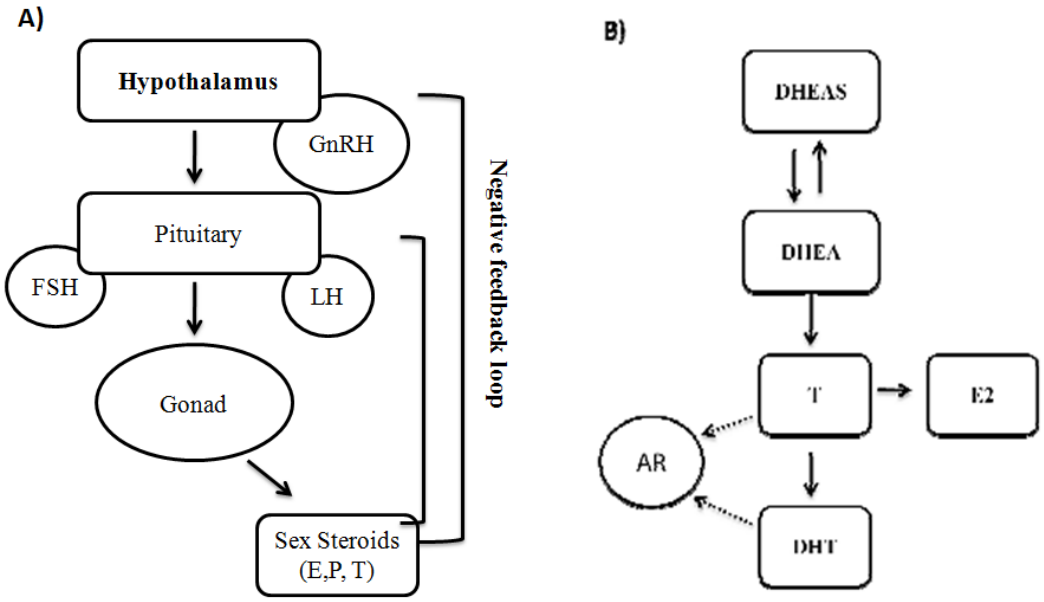

Fig 1.1. Testosterone is produced through the signalling events of the Hypothalamus-pituitary-gondal axis (A) and alternatively synthesised in target tissues via androgen metabolism (B). E, estrogen; P, progesterone; T, testosterone; E2, estradiol; AR, androgen receptor; DHEA, dehydroepiandrosterone; DHEAS, dehydroepiandrosterone sulphate. Adapted from (Vandenput and Ohlsson, 2010); (Wierman, 2007).

1.1.2 Peripheral Tissue Expression

Androgen production in peripheral tissue, such as bone and skeletal muscle, is synthesized locally from the sex steroid precursor's dehydroepiandrosterone (DHEA) and DHEA sulphate (**Fig 1.1**) (Sato *et al*., 2008, Vandenput and Ohlsson, 2010). The transformation of both steroid precursors involves steroidogenic enzymes to produce T and various other androgens (**Fig 1.1**). Of these steroidgenic enzymes, 5-α reductase is critical in converting T to dihydrotestosterone (DHT) (Labrie, 2010, Vandenput and Ohlsson, 2010). In both male and female rats, a single bout of exercise has been show to increase all of these metabolites and enzymes (DHEA, DHEAS, T, DHT and 5-α reductase type 1 isoenzyme) and thus the activation of local bioactive androgen metabolism (Aizawa *et al*., 2010). Ultimately, the conversion creates a more potent androgen in DHT and is more readily available within the tissue compared to testosterone

(Bennett *et al*., 2010). A characteristic for DHT being more potent is the higher binding affinity to the androgen receptor within the cells (Bennett *et al*., 2010). Although within skeletal muscle, DHT levels are considerably low compared to T due to the low levels of 5-α reductase (Chen *et al*., 2005). Furthermore, it has recently been shown that the conversion of T to DHT is not a requisite for T to exert its anabolic effect, as suppressed levels of DHT still brought about changes in skeletal muscle strength with T administration (Bhasin *et al*., 2012).

In bone tissue, bio-available testosterone is converted to estradiol through aromatization (**Fig 1.1**), with estradiol being observed to be important for regulation of bone loss and bone metabolism (Gennari *et al*., 2003, Khosla *et al*., 2005, Vandenput and Ohlsson, 2010). Therefore, a reduced level with increasing age or even a testosterone/estradiol deficiency within individuals has been associated with rapid bone loss, in turn impacting on bone mineral content and density, leading to a more prevalent incidence of osteoporosis in elderly men and women (Fink *et al*., 2006). Estradiol has repeatedly been associated as the main predictor of bone morphology, with T frequently showing no association in bone structural parameters. Testosterones role within bone remodeling is believed to be primarily centered on its availability for conversion to estradiol (Ward *et al*., 2011). Although, a recent study by Ward *et al*. (2011) suggests that bio-available T may influence bone health through its effect on skeletal muscle mass reducing mechanical load inducing bone remodeling. For a more detailed review on sex steroid metabolism and influences on bone, refer to Vandenput and Ohlsson (2010) or Callewaert, Boonen and Vanderschueren (2010).

1.2 TESTOSTERONE AND SKELETAL MUSCLE

Testosterone is thought to elicit an anabolic effect on skeletal muscle via increases in protein synthesis and decreases in protein degradation (Ahtiainen *et al*., 2011, Brodsky *et al*., 1996, Sheffield-Moore *et al*., 1999). These adaptations culminate in a hypertrophic (increased size via increased protein synthesis) response occurring in skeletal muscle. Indeed, a dose dependant increase in the size of skeletal muscle, shown by increases in cross sectional area (CSA), is observed following administration of testosterone enanthate at doses of 25-600

mg (Bhasin *et al*., 1996, Bhasin *et al*., 2001, Sinha-Hikim *et al*., 2002). Another form of growth within skeletal muscle, besides hypertrophy, is muscle cell hyperplasia. Skeletal muscle fibre number is set at gestation (*in-utero*) due to mature fibres that are unable to divide (i.e. terminally differentiated or post mitotic). Skeletal muscle's change in size occurs as a result of a specialised cell type (the satellite cell) that resides underneath the basal lamina. These cells can undergo hyperplasia (cell division/ mitosis) and fuse to the existing fibres to increase size or repair damage from trauma, injury or exercise. Testosterone has been shown to increase satellite cell number and increase activation and fusion of these cells indicated by an increase in myonuclear incorporation in skeletal muscle *in-vivo* following testosterone administration (100-600 mg) (Chen *et al*., 2005, Kadi and Thornell, 2000). The analysis of skeletal muscle morphology in power lifters demonstrates significant positive correlations between the number of myonuclei per area and fibre area size (Eriksson *et al*., 2005). Indeed, with the use of androgenic-anabolic steroids, muscle hypertrophy adaptations in power lifters are amplified compared to non-users (Eriksson *et al*., 2005). Despite these intriguing physiological observations, the molecular mechanisms by which testosterone initiates anabolic processes for a hypertrophic response remain poorly understood.

To investigate androgen signalling, various experimental approaches have been utilized. Commonly, the administration of exogenous T (Ferrando *et al*., 2002) is implemented, employed in either an in vivo or in vitro model. Alternatively the suppression of endogenous testosterone within in vivo models, via injections (goserelin), are performed (Kvorning *et al*., 2007). Other molecular techniques have enabled research to gain an insight into T's mechanisms using androgen receptor antagonists (Inoue *et al*., 1994, Masiello *et al*., 2002) and transgenic or knock out animal models (MacLean *et al*., 2008, Ophoff *et al*., 2009). Another approach within in vivo studies is the elevation in endogenous serum T levels (up to 38 $nmol.L^{-1}$ (1100 ng/dl)) through resistance training (Spiering *et al*., 2009). This response is commonly elicited through a high volume and high intensity program (Spiering *et al*., 2009, Vingren *et al*., 2010). Although, recent evidence would suggest post-exercise elevations in T have no causal effect on muscle hypertrophy and myofibrillar protein synthesis rates, likely due to exercise inducing only small and transient increases in free testosterone compared to pharmacological administration (West *et al*., 2009, West *et al*., 2010, West and Phillips, 2010, Wilkinson *et al*., 2006). The use of human muscle biopsies can be taken pre and post resistance training to enhance our understanding of molecular

events associated with this specific stimulus and the role of T. However, due to ethical considerations, assessing the role of T in the activation of satellite cells is difficult with the processing and sampling of biopsies, as such this particular approach has been relatively unavailable in human studies. Therefore, animal and in vitro models currently allow for the most in depth investigation of the molecular targets involved in androgen signalling, with the identification of potential target pathways to be triggered through a T stimulus. Below are some of the mechanisms indicated by these models.

T(Brodsky *et al*., 1996, Ferrando *et al*., 1998, 2002, Smith *et al*., 2013, Urban *et al*., 1995)*et al.et al.*T*et al.*(Ferrando *et al*., 2002)(Vingren *et al*., 2010)(Kraemer and Ratamess, 2005, McCall *et al*., 1999, McCaulley *et al*., 2009, Rønnestad *et al*., 2011)(Mitchell *et al*., 2013, West *et al*., 2009, 2010, Wilkinson *et al*., 2006)(Wilkinson *et al*., 2006)*et al*(2012)(2012)(Atkinson *et al*., 2010, Ferrando *et al*., 2002)(Bhasin *et al*., 2001, Basaria *et al*., 2010, Fernandez-Balsells *et al*., 2010)(Basaria *et al*., 2010)(Bhasin *et al*., 2001)(Atkinson *et al*., 2010, Bhasin *et al*., 2001, Sinha-Hikim *et al*., 2002)

1.3 DIRECT PATHWAY (TESTOSTERONE-AR COMPLEX)

Androgens interact with muscle tissue via the androgen receptor (AR), a member of the steroid receptor superfamily and nuclear transcription factors (Chen *et al*., 2005, Kadi, 2008). The AR is detectable within hormone-sensitive cells e.g. bone and muscle cells (Gentile *et al*., 2010). Within target cells, un-ligand bound AR is located in the cytoplasmic compartment of the cell, in the form of a multi-complex protein consisting of heat shock proteins and immunophilins (**Fig 1.2.**) (Bennett *et al*., 2010, Gobinet *et al*., 2002). Once testosterone is bound to AR, a conformational change occurs leading to AR dissociating from its multi-protein complex and recruiting co-activators such as importin-α, androgen receptor-associated protein-70 (ARA70) and filamin-α, enabling the ligand-bound AR to translocate to the nucleus (Figure 2.) (Bennett *et al*., 2010, Wannenes *et al*., 2008). In the nucleus, AR acts as a transcription factor and thus interacts with androgen responsive elements (ARE) within the genome (Ahtiainen *et al*., 2011) e.g. specific target genes such as insulin-like growth factor I, MyoD, myosin heavy chains (Gentile *et al*., 2010). As these specific gene targets described above have fundamental functions in muscle cell proliferation, differentiation, maturation, and survival. The activation of the AR has been

proposed to mediate fundamental processes in skeletal muscle cells (Bennett *et al*., 2010).

Fig 1.2. Overview of the human androgen receptor gene, protein and the conformational change once bound to an androgen. The gene consists of 8 exons which code for a functional protein (approx. 920 amino acids) with four domains. Exon 1 encodes for the N-terminal transactivation domain (NTD); Exon 2-3 encodes the DNA-binding domain (DBD); Exon 4 encodes the small hinge region, finally exons 5-8 encode for the C-terminal ligand-binding domain (LBD). The LBD represent the domain where androgens bind to the receptor protein, resulting in the release of heat shock proteins (HSP) and immunophilins plus the recruitment of co-activators, ARA70 and filamin-α, thus enabling translocation to the nucleus. Adapted from Bennett *et al*.(2010) and Chen *et al*.(2005).

Satellite cells (discussed above) within skeletal muscle provide the predominant location for AR expression and thus androgens can act directly through these cells (Chen *et al*., 2005, Lee, 2002, Sinha-Hikim *et al*., 2004). Satellite cells once activated are termed myoblasts and can proliferate, enter differentiation or even return to quiescence (**Fig 1.3.**) (Chen *et al*., 2005, Cornelison and Wold, 1997, Kadi *et al*., 2005, Sinanan *et al*., 2006, Smith *et al*., 1994). In addition, as mentioned satellite cells provide a major source for the addition of new myonuclei within the skeletal muscle (Kadi, 2008) and thus the myonuclei addition increases the focal points for AR expression as well as helping maintain nuclear-to-cytoplasmic balance (Kadi *et al*., 1999). In terms of muscle hypertrophy, the differentiation/fusion of cells into the existing fibres allows for a further increase in size (**Fig 1.3.**). Plus the addition of more satellite cells, as previously mentioned, leading to an increased in myonuclei would aid in the availability of androgen receptors to interact with testosterone more readily (Sinha-Hikim *et al*., 2003). The availability of the androgen receptor and testosterone levels is highlighted by gender differences, as males produce ten times more testosterone and equally have an increased AR protein content than in females (Vingren *et al*., 2009).

Fig 1.3. Location of the Satellite cell and its involvement in muscle fibre modeling. Adapted from Kadi *et al*.(2005).

In mediating T's effects, the increase (up-regulation) or decrease (down-regulation) in *AR* mRNA expression is an important consideration (Ratamess *et al*., 2005, Vingren *et al*., 2009). Commonly with resistance exercise, where acute elevations in testosterone levels are observed, there is an initial stabilisation of the AR, followed by a down-regulation (1hr post exercise) (Ratamess *et al*., 2005) before finally an up-regulation (3hr post exercise (Spiering *et al*., 2009)). This type of phase response is further highlighted by Ferrando *et al*. (2002) where the (6 months) administration of exogenous T produced a significant increase in AR protein expression after 1 month, yet after 6 months of administration, AR protein expression levels returned to near baseline values. Additionally, in females, this phase response occurs more quickly than in males (Vingren *et al*., 2009). The phase response or paradigm was suggested to be the result of a steady-state adaptation with the administration of T. Interestingly though, Insulin-Like Growth Factor I (IGF-I) protein expression, remained elevated for the same time frame after exogenous T administration. Thus, posing the question; does T's interaction revolve predominately around the AR or an indirect pathway, for which; in the in vivo environment, the administration of T may be more beneficial to patients in a cycling pattern (Ferrando *et al*., 2002)?

Two more recent in vivo studies investigated the role of androgen receptor expression by suppressing endogenous T (by injecting goserelin) (Kvorning *et al*., 2007) or applying a resistance training stimulus to elevate endogenous T (Ahtiainen *et al*., 2011). Through the implementation of a 21 week resistance training program (60-90% of 1 RM, 5-12 reps per set, 5 sets total), Athtianen *et al*. (2011) observed no statistically significant changes in *AR* mRNA expression and AR protein content between young and old training groups. However, when individual changes within groups were further analysed, significant relationships were observed in AR protein concentrations and training-induced changes (1 repetition maximum, fibre CSA) within the skeletal muscle i.e. increased AR protein concentration with increase in fibre CSA. Thus, AR protein concentrations may have a role training induced skeletal muscle adaptations. Contrary to this, Korvning *et al*, (2007) suppressed testosterone (administration of goserelin) which limited the increase in muscle strength being observed post-strength training but

more importantly endogenous testosterone did not appear to be involved in the regulation of *AR* mRNA expression as similar expression was observed in suppressed *verses* placebo groups. Indeed, recent research has suggested that testosterone may influence skeletal muscle growth via a different pathway to AR interaction (Gentile *et al*., 2010, Kovacheva *et al*., 2010, Ratamess *et al*., 2005).

From the perspective of in vitro studies, the androgen receptor has commonly been inhibited using either flutamide or biclutamide (AR antagonist) (Basualto-Alarcón *et al*., 2013, Sculthorpe *et al*., 2012, Serra *et al*., 2011, Wannenes *et al*., 2008). Certain studies in particular have highlighted the variation of levels in AR expression within mouse C_2C_{12} skeletal muscle cells (Altuwaijri *et al*., 2004, Sheppard *et al*., 2011). Recently Sheppard and colleagues (2011) demonstrated the affect of sequence variation within the AR receptor on C_2C_{12} cell development. They addressed the polyglutamine repeat for *AR* 14, 24 and 33 CAG repeats involvement in cell proliferation and differentiation. The transcriptional activity increased with repeating CAG length, and in response to T administration. Furthermore, ligand activation was increased for *AR*33 compared to *AR* 14 and 24. These alterations resulted in reduced cell proliferation in AR33 transfected cells, reduced creatine kinase activity in AR14 cells and myonuclear fusion index being lower in AR14 and AR33 cells compared to wild type (non-transfected) cells. Sheppard and colleagues highlight the role which this polymorphism plays in altered growth and development, but most importantly, their observations show that within mouse C_2C_{12} cells (wild type) there is a low expression of AR as previous studies have adopted a similar technique of AR transfection to address the role of androgen treatment where total AR expression appears low (Lee, 2002, Wu *et al*., 2010a) compared to various species and muscle groups (De Naeyer *et al*., 2014, Kadi *et al*., 2000).

Contrary to these previous studies though, Wannenes *et al*. (2008) used multiple techniques (western blotting, immunofluorescence and polymerase chain reaction (PCR)) to demonstrate that the cellular model of C_2C_{12} cells implemented clearly expressed the androgen receptor within their study. The authors highlighted the translocation of the AR from the cytoplasm to the nucleus, which was accompanied by increases in myogenin, myosin heavy chain isoforms and

GRIP-1 (steroid receptor coactivator) expression, supporting T's role in driving muscle differentiation (Lee, 2002, Sculthorpe *et al*., 2012). The expression levels of AR would suggest the importance of AR in skeletal muscle development and mediating T's action. Indeed, between muscle groups in vivo, the expression of AR differs between the upper and lower limbs of the body (Kadi *et al*., 2000). However, it may be that where AR expression levels are low, T's action is mediated via another signaling cascade which is more prominent (White *et al*., 2012). Most recently in C_2C_{12} muscle cells, it has been observed that with incremental increases in T doses, there is indirect activation of the Akt/mTORC1 pathway in stimulating muscle protein synthesis, a potential T-mediator which is discussed below.

Fig 1.4. Two potential pathways testosterone may use to interact with skeletal muscle cells**.** Testosterone can act directly via the AR pathway (right side) or indirectly through the IGF-I signalling pathway (left side). Akt, protein kinase B; AR, Androgen receptor; ARE, Androgen response elements; DHT, dihydrotestosterone; ERK, extracellular signal-regulated kinase; eiF2B, the guanine nucleotide-exchange factor for eukaryotic initiation factor 2; 4E-BPP-1, eukaryotic translation initiation factor 4E binding protein 1; FOXO, forkhead homebox type O; GSK-3, Glycogen Synthase Kinase-3; HSP, Heat shock proteins; IGF-I, insulin-like growth factor-I; IRS-1, insulin receptor substrate-1; MAFbx, Muscle atrophy f-box; MAPK, mitogen activated protein kinase; mTOR, mammalian target of rapamycin; MuRF1, muscle RING-finger protein-1; P70S6K, P70S6 Kinase- a serine/threonine kinase (phosphorylation of S6 induces protein synthesis at the ribosome); Ras, Ras Protein; Raf, MAP Kinase Kinase Kinase (MAP3K). Adapted from Bennett *et al* (2010); (Sharples and Stewart, 2011).

1.4 INDIRECT PATHWAYS

1.4.1 Role of IGF-I and Its Downstream Pathways

IGF-I regulates several biochemical pathways (**Fig 1.4.**), involved in protein synthesis within skeletal muscle cells (Rommel *et al*., 2001, Yin *et al*., 2009). The downstream pathways of Pi3K/Akt/mTOR play a fundamental role in myotube hypertrophy (Fig 1.4.) (Rommel *et al*., 2001), with recent evidence that mTOR can be also activated independently of IGF-I through mechanical stimulation and amino acid supplementation (Miyazaki *et al*., 2011, Spangenburg *et al*., 2008). The binding of IGF-I to its receptor, activates a cascade of signalling, initiated with the activation of Pi3K. The release of a phosphate group by Pi3K allows for the phosphorylation and activation of Akt. Once at this step in the pathway, Akt mediates the phosphorlaytion of mTOR. Through mTOR, protein synthesis is promoted through mitigating eukaryotic initiation factor 4E– binding protein 1 (4E-BP1)-mediated inhibition of eukaryotic initiation factor 4E (eIF-4E) (Rommel *et al*., 2001, Yin *et al*., 2009). Supplementary to mTOR promoting protein synthesis through eIF-4E, the activation of mTOR further promotes protein synthesis via the phosphorylation of p70S6k and subsequent S6K downstream target (Yin *et al*., 2009). Another downstream target, GSk-3β is a substrate of Akt and thus once Akt is phosphorylated, GSk-3β becomes phosporylated and

inhibited. This inhibition of GSk-3β in turn activates eukaryotic translation factor eIF-2B leading to further increases in protein synthesis (Fig 1.4.). There is evidence that testosterone mediates its androgenic effects through Insulin-like growth factor (IGF-I) and its associated downstream signaling (Serra *et al*., 2011). For example, with a T deficiency, a reduced level of IGFI in humans has been observed which may suggest an activation/synergistic behaviour by testosterone on IGF-I (Bhasin *et al*., 2001, Yin *et al*., 2009). The suggested synergistic behaviour is further supported through T supplementation, where the addition of exogenous androgens is accompanied by an increase in IGFI protein and mRNA expression (MacLean *et al*., 2008, Sculthorpe *et al*., 2012, Serra *et al*., 2011). Furthermore, IGFI and its splice variants, IGFIEa and MGF, stimulate both satellite cell proliferation and differentiation with a unique temporal expression following resistance exercise (Ates *et al*., 2007, Hill and Goldspink, 2003, Hameed *et al*., 2003). There is emerging evidence within skeletal muscle cells for IGF-I activation of the AR through a ligand-independent mechanism (Kim and Lee, 2009a, Kim and Lee, 2009b, Lee, 2009).

The androgen receptor is considered a ligand dependant receptor, yet recent research by Kim and Lee (2009a; 2009b) suggests that total AR and increases in *AR* mRNA expression can be induced through the addition of endogenous IGF-I in C2C12 skeletal muscle cells. These investigators observed (through immunocytochemistry fluorescence staining) an increase in *AR* DNA binding activity in murine skeletal muscle cells (C2C12) in a time-dependant manner after being treated with IGF-I.. Therefore, in the presence of IGF-I, it was observed that AR localization in the nucleus increased along with binding to ARE, in the absence of ligand. A follow up study by Kim and Lee (2009b) addressed the MAPK pathway (discussed in more detail below) as being a mechanism for AR activation and localization in the absence of the ligand. Through the use of MAPK pathway inhibitors (p38 MAPK, SB203580; ERK1/2 PD98059; JNK SP600125), total AR and AR phosphorylation response to IGF-I was blocked. Through a near identical approach, yet addressing the Pi3K/Akt pathway (inhibitor LY294002) similar results were seen by Lee (2009) suggesting that both MAPK and PI3K/Akt pathways stimulate AR activity and as these pathways have been shown to be

involved in proliferation (MAPK) and differentiation (PI3K/Akt) (Coolican *et al*., 1997). Therefore, in conjunction with Testosterone binding to AR to initiate activation, IGF-I also activates AR through the MAPK and Pi3K/Akt pathways suggesting a dual regulation of AR through previously distinct pathways. The activation/synergist behaviour by testosterone on IGF-I may facilitate competition between T binding directly to AR or increased IGF-I levels activating the AR first, in a ligand-independent manner.

The utilization of animal models has further allowed research to address the role which T may play in the activation/mediation of IGF-I and its downstream pathways (Wu *et al*., 2010a, Yin *et al*., 2009). Yin *et al*.(2009) employed a catabolic mouse model (dexamethasone administration) to investigate the effect of T on reversing muscle atrophy. It was observed that T reversed the effects of atrophy via the activation of the IGF-I downstream targets, Akt, GSk-3β and p70S6K (**Table 1.1**). The activation of downstream target p70S6K has further been associated with androgen-mediated muscle hypertrophy in castrated rats (Xu *et al*., 2004). The role of T supplementation in reversing muscle wasting/loss was further supported by Kovacheva *et al*.(2010), in similar findings to Yin *et al*.(2009) in using a mouse model, T supplementation reversed muscle loss via activation of Akt signalling pathway.

The exact mechanisms for T-induced hypertrophy to occur through IGF-I remain controversial due to recent research suggesting that the IGF-I/Growth hormone axis is not necessary to mediate the effects of T on skeletal muscle in vitro (Serra *et al*., 2011). Testosterone was observed by Serra *et al*. (2011) to rescue muscle-specific mass in the absence of both GH and IGF-I, through use of GH-deficient rats that also show suppressed IGF-I levels. A possible explanation for this observation may be due to mTOR, a key regulator of satellite cell growth and proliferation (Sarbassov *et al*., 2005). Previously the use of rapamycin, an inhibitor of mTOR, blocked overload-induced and IGF-I induced skeletal muscle hypertrophy in vivo and in vitro respectively (Bodine *et al*., 2001, Rommel *et al*., 2001). The activity of mTOR has been observed to play a key role in mediating the effects of T-induced muscle hypertrophy, independently of IGF-I and Akt

after mechanical stimulation (Miyazaki *et al*., 2011, Spangenburg *et al*., 2008, Wu *et al*., 2010a).

In rat L6 myoblasts, Wu *et al*.(2010a) utilized various inhibitors for mTOR, AR, IGF-I and its receptor (IGF-IR) as well as inhibitors for Akt and Erk to address their roles in T-induced hypertrophy. The authors observed that Erk and mTOR play an important role in hypertrophy occurring through T with both being activated under this stimulus. The activation of mTOR and Erk by T administration was observed independently of IGF-I, as the inhibition of IGF-I and IGF-IR still lead to the phosphorylation of mTOR and Erk. The increased activation of mTOR, may further be attributed to T's action on REDD1 (inhibitor of mTOR) which has been observed to have reduced protein levels upon T's administration (Wu *et al*., 2010b). Recently White and colleagues (2012) further supported the findings of Wu *et al*., showing that with testosterone administration there is a direct effect on mTOR activity. They observed an increase in phosphorylation of mTOR with increasing doses of T in C_2C_{12} myotubes, highlighting the role of the AKT/mTOR pathway in T's action. However, in slight opposition to the findings of Wu *et al*. (2010a), Brown *et al*. (2009) observed no activation within Erk in T supplementation of a mouse model, suggesting varying results between cell lines and in vivo models. Thus further investigation is warranted with other cell lines and in vivo experimentation to see if T-induced hypertrophy is dependent on Erk and mTOR activity. To note, Wu and colleagues observed no activation of IGF-IR or Akt with T, highlighted through no increases in expression and protein content in rat L6 myoblasts. The inactivation of IGF-IR may aid in the evidence for IGF-I not mediating the effects of T, as Wu *et al*. (2010a) observed unaltered changes in *Igf1* mRNA levels with T administration.

Most recently, Basulto-Alarcon and colleagues (2013) have highlighted a link between mTOR and the androgen receptor in signaling the effects of a T-stimulus. The authors used primary rat cultures in combination with various inhibitors for ERK1/2, PI3K/Akt, mTOR/S6K1 and the androgen receptor. They observed acute increases in ERK1/2, Akt and S6K1 with a T-stimulus. Additionally increases in myotube cross sectional area after 12 hours were abolished through inhibition of PI3K/Akt pathway (using LY294002) and the AR.

Their findings highlight the role of fast intracellular signaling and the role of the androgen receptor in T induced skeletal myotube hypertrophy. Of course the interactions for how the cross talk occurs remain to be elucidated; however Basulto-Alcarcon and colleagues (2013) provide more evidence for the role of key proteins and signals which T stimulates to promote muscle hypertrophy.

Table 1.1 Various androgen treatments and their interactions with the downstream targets of IGF-I signalling pathway

Signalling Proteins	Published Papers	Androgen Treatment	Activation Level	Target Cells
IGF-IR	Wu *et al*. 2010a	100 nM T	No effect.	Rat L6 myoblasts
MAPK	Kovacheva *et al*. 2010	0.5cm or 1.0cm T Implant	No effect.	Young vs. Old Mice
	Brown *et al*. 2009	2cm T Implant (supraphysiologial dose)	↑	Mouse Model.
ERK1/2	Wu *et al*. 2010a	100nM T	↑	Rat L6 myoblasts
	Brown *et al*. 2009	2cm T Implant (supraphysiologial dose)	No effect.	Mouse Model
Akt	Yin *et al*. 2009	0.5 mg/100g/day T	↑	Rat Model
	Wu *et al*. 2010	100 nM T	No effect.	Rat L6 myoblasts
	Kovacheva *et al*. 2010	0.5 or 1.0cm T implant	↑	Young vs. Old Mice
mTOR	Wu *et al*. 2010a	100 nM T	↑	Rat L6 myoblasts
p70s6k	Yin *et al*. 2009	0.5 mg/100g/day T	No effect.	Rat model
	Xu *et al*. 2004	0.3mg/kg or 3.0mg/kg DHT	↑	Rat model (Castrated)
	Wu *et al*. 2010a	100nM T	↑	Rat L6 myoblasts
GSk-3β	Yin *et al*. 2009	0.5 mg/100g/day T	↑	Rat model
	Gentile *et al*. 2010	3mg/kg per day DHT	↑	Rat model (Castrated)

1.4.2 MAPK/JNK/Notch Signalling

As previously mentioned, mitogen-activated protein kinases (MAPK's) are another family of downstream proteins activated by IGF-I (**Fig 1.4.**) and consists of three subfamilies, ERK (1/2), p38 MAPK and JNK (Brown *et al*., 2009, Kim and Lee, 2009b). ERK (1/2) is activated in response to a growth stimuli and thus involved in promoting cell growth where as p38 MAPK and JNK are involved in growth inhibition and promoting apoptosis (cell death) through either inflammatory or environmental signals (Brown *et al*., 2009). However, p38 MAPK has dual roles and has been implicated as a differentiation regulator with different isoforms having distinct functions. Where p38-α promotes differentiation and inhibis proliferation where as p38-β has the opposite actions on activated

satellite cells (Lassar, 2009). Testosterone supplementation has been observed to influence all these proteins in inducing muscle fibre hypertrophy and rescuing muscle mass size in an aging model (Brown *et al*., 2009, Kovacheva *et al*., 2010). More specifically, Brown *et al*. (2009) utilised a mouse model of T-induced hypertrophy where it was observed that after 2-4 weeks of T supplementation (**Table 1.1 and 1.2**), p38 MAPK was activated (high levels of phosphorylated p38 MAPK) and JNK inhibited (decreased levels of phosphorylated JNK). Kovacheva *et al*. (2010) further supported these observations using the same mouse model. Notch signalling represents another alternative pathway as the pathway is responsible for the activation, proliferation and the myogenic progression of satellite cells (Conboy *et al*., 2003, Sinha-Hikim *et al*., 2006). Thus testosterone supplementation may increase satellite cell number via the activation of this pathway. T has indeed been observed to increase the expression of Delta, the ligand which binds to activate the Notch receptor (Brown *et al*., 2009). Notch signalling is mediated via the activation of p38 MAPK, which has been observed to be induced through a T stimulus in young mice (Brown *et al*., 2009). Using inhibitors for p38 MAPK Brown and colleagues (2009) highlighted a reduction in the activation of Notch signalling in the presence of T. The impact of reduced Notch signalling resulted in decreased expression of Notch 1 and Notch 2 as well as decreased expression of myogenin (muscle specific transcription factor and promoter of expression of creatine kinase and cytoskeletal proteins e.g. titin and desmin). As the increase in all these factors resulted in muscle fibre hypertrophy, it may be suggested that p38 MAPK can activate Notch signalling contributing to hypertrophy via a T stimulus. In comparison, T appeared not to activate p38 MAPK in aged mice. However, through the increased expression of Notch 1, T still reversed age-related effects on skeletal muscle i.e. decreased the levels of myostatin and increased inhibition of JNK contributing to rescuing muscle mass size (Kovacheva *et al*., 2010). Therefore, it may be suggested that the signalling pathways mediating this process may vary with age per se or p38 MAPK is not fundamental in T action which may suggest an alternative mechanism maybe more important.

1.4.3 Myostatin/TGF-β Signalling

The molecular mechanism for how T-induces the promotion of muscle growth and hypertrophy is one aspect considered so far. An alternative aspect to consider is the possible role of action testosterone exerts on pathways (see **table 1.2.**) involved in growth inhibition, protein degradation and programmed cell death (apoptosis). Transforming growth factor-β (TGF-β) signalling pathway is responsible for the inhibition of myogenic differentiation (Beggs *et al*., 2004). Follistatin is a Wnt target gene, expressed following β-catenin nuclear localisation and subsequently plays a role in binding to TGF-β family members. One such family member is myostatin and thus Follistatin inhibits the activity of myostatin (endogenous inhibitor of growth) (Amthor *et al*., 2004). Myostatin is responsible for the up-regulation of p21, an inhibitor of cyclin-dependant kinase (CDK) and subsequently cell cycle withdrawl in G1 and thus differentiation with the subsequent inhibition of cell proliferation (Kovacheva *et al*., 2010, McCroskery *et al*., 2003). In addition, myostatin has been observed to reduce myotube size and differentiation of myoblasts via Akt/mTOR and p70S6K signalling (pathways suggested to be activated by T) (Trendelenburg *et al*., 2009).

Testosterone supplementation has been observed to down-regulate the expression of myostatin (Kovacheva *et al*., 2010, Mendler *et al*., 2007). Through the suggested AR/β-Catenin cross talk leading to the expression of Wnt target genes, follistatin is up-regulated following T administration and thus the regulation of TGF-β signalling (Brown *et al*., 2009). Most recently, Braga and colleagues (2012) have highlighted the potential role of follistatin in mediating testosterone's action in mice. They assessed growth and differentiation on satellite cells which had been isolated from the levator ani muscle of mice. T up-regulated follistatin expression which resulted in TGF-β induced inhibition of growth and differentiation being blocked and thus highlighting T's role in inhibiting this particular pathway via increased follistatin expression. Furthermore, T inhibits JNK (Brown *et al*., 2009), which besides MAPK interaction with T, is a possible consequence of the reduction in myostatin expression. The inactivation of JNK may further play a role through stimulating cellular proliferation by reducing the up-regulation of p21 (Huang *et al*., 2007). These potential events influenced by T

may offer a potential mechanism of action for T through a reduction in cell apoptosis causing increased cell growth instead. Therefore with age, T's action may be a protective function (Qin *et al*., 2010, Zhao *et al*., 2008), that is more specific towards sarcopenia and muscle wasting diseases, where metabolites associated with grown inhibition, reduced regenerative capacity and cell apoptosis are highly expressed (Degens, 2010).

Table 1.2. The interaction of Androgens with alternative (growth inhibition/cell development) signalling pathways

Proteins	Published Paper	Androgen treatment	Activation Level	Target Cells
Myostatin	Mendler *et al*. 2007	T propionate 100ug/100g body weight for 4 weeks	↓	Male Wister rats (Castrated)
JNK	Brown *et al*. 2009	2cm T Implant	↓	Mouse Model
	Kovacheva *et al*. 2010	0.5cm/1.0cm T Implants	↓	Young vs. Old Mice
Notch 1 and 2	Brown *et al*. 2009	2cm T Implant (supraphysiologial dose)	Increased expression after 1 and 8 weeks	Mouse Model
Delta	Brown *et al*. 2009	2cm T Implant	Increased expression after 2 and 8 weeks	Mouse Model
β-Catenin	Singh *et al*. 2009	100nM T and 10nM DHT	↑ Plus translocation to the nucleus.	Mouse C3H 10T1/2 cells
	Gentile *et al*. 2010	3mg/kg per day DHT.	Acute increase after 1-7 days treatment.	Rat Model (Castrated)
Cyclin D1	McClung *et al*. 2005	6mg/kg body weight, Nandrolone Decanoate	↓ mRNA levels.	Rat soleus muscle
REDD1	Wu *et al*. 2010b	28mg/kg/day and 100-500nM T	↓ Protein and mRNA expession	Dexamethasone - treated Wister rats and rat L6.AR myoblasts
4E-BP-1	Wu *et al*. 2010b	28mg/kg/day T	↓	↓
FOXO1	Qin *et al*. 2010	↓	↓	
MAFbx	Zhao *et al*. 2008	↓	↓ mRNA levels.	↓

1.5 SKELETAL MUSCLE WASTING

Muscle wasting occurs within many life-threatening diseases such as cancer (termed cancer cachexia), AIDS (Dudgeon *et al*., 2006), SEPSIS (Hasselgren *et al*., 2005), heart failure (Conraads *et al*., 2007) and ageing (sarcopenia) (Cruz-Jentoft *et al*., 2010, Mitchell *et al*., 2012, Saini *et al*., 2009, Sharples *et al*., 2011). Individuals that experience muscle loss during these various disease states have a reduced physiological and functional capacity, altered metabolism (Russ and Lanza, 2011, Tisdale, 2009) and a reduction in circulating levels of growth hormone, insulin-like growth factor-I (IGF-I) and testosterone (Dudgeon *et al*., 2006). These factors accumulate in increased frailty and morbidity and therefore reduced quality of life that subsequently leads to earlier mortality (Deans and Wigmore, 2005, Rantanen *et al*., 2000). In the instance of cancer cachexia, muscle loss (also termed atrophy) can reach 75% at which point leads to fatality (Dillon *et al*., 2012, Muscaritoli *et al*., 2006). Furthermore this occurs in 50% of cancer patients, with cachexia alone causing 25% of cancer deaths (Argilés *et al*., 2005).

Within the literature, the highlighted catabolic mediators of muscle loss in wasting diseases are tumor necrosis factor-alpha (TNF-α) and interleukin-6 (IL-6) (Sakuma and Yamaguchi, 2013). There is an increase in systemic inflammation and the levels of IL-6 and TNF-α (Degens, 2010), with these levels correlating with weight loss and even a reduced survival in cancer cachexia patients (Argilés *et al*., 2005). Indeed the exogenous addition of both these cytokines in animal models has been observed to result in increased protein breakdown and reduced rates of protein synthesis (Li *et al*., 2003, Li *et al*., 2005b). The breakdown in protein has been observed in cultured myotubes to be mediated by the E3 ligase genes (e.g. MuRF-1 and MaFbx) in the ubiqutin-proteasome pathway (Frost *et al*., 2007, Li *et al*., 2005b). The combination of these factors leads to an overall reduction in muscle strength and mass.

Using the example of the ageing process, the ability of skeletal muscle to regenerate becomes less efficient especially in response external stimuli such as exercise (Dreyer *et al*., 2006, Kadi *et al*., 2004), with several studies highlighting

the importance that the cell niche plays in the wasting phenotype (Chakkalakal *et al*., 2012, Carlson and Conboy, 2007, Conboy *et al*., 2003, 2005). Indeed, seminal work has shown that when aged mice undergo parabiotic sharing of their circulatory system with young mice, the activation of delta (notch ligand) is restored in association with the proliferative and regenerative capacity of the aged satellite cells (Conboy *et al*., 2005). The enhancement of muscle regeneration through a change in systemic environment suggests stem cells (satellite cells) retain regenerative potential (Conboy *et al*., 2005). Alternatively, the role of intrinsic alterations in the satellite cells ability to proliferate and differentiate in muscle wasting with age, have also been shown to be influential in contributing to the reduced capacity for regeneration (Beccafico *et al*., 2011, George *et al*., 2010, Pietrangelo *et al*., 2009).

T replacement therapy has been observed to increase muscle strength and mass in various clinical populations such as AIDS, COPD and sarcopenia (Bhasin *et al*., 2000, Casaburi *et al*., 2004, Dillon *et al*., 2012, Ferrando *et al*., 2002, Lewis *et al*., 2007, Sattler *et al*., 2011). In these clinical populations, the suggested mechanisms for skeletal muscle hypertrophy have focused on the expression of androgen receptor, IGF-I and myogenic regulatory factors, with increases being observed in proteins with testosterone administration (Casaburi *et al*., 2004, Ferrando *et al*., 2002, Lewis *et al*., 2007). There is however a limited number of studies which have investigated the role of T in restoring skeletal muscle atrophy at the cellular level (Serra *et al*., 2013, White *et al*., 2012, Wu *et al*., 2010a).

1.5.1 Cellular Models to investigate ageing phenotypes

In recent years, cell culture models have been implemented which are representative of the ageing process and atrophic phenotypes. These models have attempted to address the regulatory programme for myoblast proliferation and differentiation from the intrinsic perspective. Bigot and Colleagues (2008) aged human satellite cells in vitro in order to address the effect of replicative senescence (terminal growth arrest) on the myogenic programme. They observed that senescent myoblasts were still able to form functional multinucleated myotubes, yet these were statistically smaller in size. These morphological

observations were explained by Bigot and colleagues to be due to the delay regulation of the myogenic program. For example, myogenin (terminal differentiation marker) had a 15 hour delayed expression which was accompanied by a 7-fold decrease. The observations of Bigot *et al*. contribute evidence towards the role intrinsic factors play in myotube formation/regeneration.

Most recently, two myoblast models to study reduced differentiation capacity have been highlighted (Sharples *et al*., 2010, Sharples *et al*., 2011). The first investigated the parental mouse C_2 myoblasts vs. their subclone, the C_2C_{12} cells. Despite their shared origins, we observed differences in morphological and biochemical responses between the C_2 and C_2C_{12} cells. The C_2 cells displayed slower and diminished differentiation profiles compared to the C_2C_{12} cells and were also more susceptible to TNF-α-induced inhibition of differentiation and induction of apoptosis. Because muscle wasting is associated with reduced muscle mass (Degens and Alway, 2003, Morse *et al*., 2005) and increased susceptibility to TNF-induced muscle protein degradation (Bruunsgaard *et al*., 2003, Lees *et al*., 2009), this comparative model provides an excellent representation of muscle atrophy, hypertrophy and adaptability, thus, enabling the determination of potential regulators associated with muscle wasting.

The second model utilises C_2C_{12} cells that have undergone multiple population doublings (PD) vs. parental control cells (undergoing no doublings relative to the PD cells) (Sharples *et al*., 2011). These cells also display impaired differentiation in monolayer and in three dimensional culture systems (Sharples *et al*., 2012) *verses* their parental controls. It was reported that the MPD cells had significantly reduced numbers of cells exiting the cell cycle in G_1, a prerequisite for fusion, with corresponding decreases in transcript expression of *Igf1*, *myoD*, *myogenin* and reduced activation of Akt with increases in *Igfbp5* mRNA and JNK activation *verses* control cells (Sharples *et al*., 2011). Interestingly, similar morphology, transcript and signalling processes are also observed in cells isolated from elderly human muscle (Beccafico *et al*., 2011, Bigot *et al*., 2008, Pietrangelo *et al*., 2009) and in whole tissue biopsies (Cuthbertson *et al*., 2005, Léger *et al*., 2008). Thus, these cells can be used as a representative model to investigate

mechanisms of atrophic phenotypes (PD) *verses* hypertrophic phenotypes (CON) (Sharples *et al*., 2011).

1.6 AIMS AND OBJECTIVES

Based on the review of the literature, the aims of this thesis are to: 1) investigate the role of testosterone in skeletal muscle cell differentiation and myotube hypertrophy in vitro; 2) investigate whether T administration can restore differentiation and myotube hypertrophy in population doubled skeletal muscle cells that show impaired differentiation and hypertrophy (ageing phenotypes). 3) Elucidate the most predominant molecular pathways in T's action i.e. the androgen receptor and/or IGF-I and its associated cell signalling). Ultimate objectives and hence aims are to highlight key cellular and molecular mechanisms involved in testosterone-induced hypertrophy and regeneration in skeletal muscle cells with a view to enhancing future therapeutic interventions for clinical populations where muscle wasting is apparent.

1.7 THESIS OVERVIEW

To address our aims **chapter 2** will define methodology undertaken in the following four data chapters; **chapter 3** will determine a dose response of testosterone in skeletal muscle (C_2C_{12}) myoblasts. T will be administered to both proliferating and early differentiating cells as well as onto differentiated myoblasts (myotubes/myofibres). This chapter will thus help to establish a characterisation of morphological adaptation of C_2C_{12} cells to T administration of differing doses vs. basal conditions i.e. myotube number, diameter, nuclei per myotube, myonuclear accretion) and transcript expression of key genes involved in differentiation and hypertrophy (myogenin, IGF-I, AR, myostatin etc) in order to take the relevant dose forward to subsequent chapters. **Chapter 4** will establish an effective dose to inhibit the AR (flutamide) and IGF-I receptor (Picropodophyllin: PPP) in order to determine their role in T's molecular regulation of differentiation and hypertrophy in subsequent chapters. Here CON and PD cells will be incubated with T in the absence or present of flutamide or PPP with AR total protein and IGF-I signaling (pERK, pAKT) measured respectively to confirm inhibition. In **Chapter 5** CON and PD cells will be

administered with testosterone, T plus AR inhibitors (flutamide), IGF-I receptor inhibitor (Picropodophyllin) (alone and in combination) dependant on dose determined in the above chapters) to address if whether the direct AR or indirect IGF pathways are the predominant routes for testosterone's role in muscle cell differentiation and hypertrophy and whether this is altered/impaired in an aged muscle cell model (PD cells). Morphological analysis (desmin staining, myotube number and diameter, myonuclear accretion and nuclei per myotube), gene expression (myogenin, IGF-I receptor, AR, MyoD, myostatin) and key cell signaling (pERK, pAKT, p70S6K) processes will be investigated. **Chapter 6** will finally investigate the IGF-I downstream target, Akt as this protein has recently been suggested to be involved in mediating testosterone induced-hypertrophy and low levels have been observed in aged mammals. Therefore this chapter will attempt to discover if Akt is involved in improving skeletal muscle regeneration when testosterone is administered. **Chapter 7** will provide a final summary, discussion of the work and future directions.

2. MATERIALS AND METHODS

2.1 GENERAL EQUIPMENT AND SPECIALISED SOFTWARE

2.1.1 Cell Culture

All cell culture was performed in a microbiological safety cabinet (Herasafe^{TM} KS Class II, Thermo Fisher Scientific, Rosklide, Denmark). All cells were incubated in a Thermo scientific Hera Cell 150i CO_2 Air Jacketed Incubator (Loughborough, UK). Liquid handling for cell culture was performed using an IBS Integra Biosciences Vacusafe Comfort (Chur, Switzerland). Distilled water from an Milli-Q intergral water purification system (Merck Millipore, Oxford, UK) was used in the preparation for all solutions.

2.1.2. Biochemical Assays

Total Protein assays were performed using a Thermo Labsystems Multiskan spectrum microplate reader (Franklin, MA, USA). Reagents for protein assays were purchased from Pierce (Division of Thermo Fisher Scientific, Rosklide, Denmark).

2.1.3. Real Time PCR

RNA concentration and purity were assessed by UV spectroscopy using a Nanodrop Spectrophotometer 3000 (Fisher, Rosklide, Denmark). Real-time PCR was performed using a Qiagility automated pipetting machine and Rotor-Gene Q PCR machine (Qiagen Inc, Valencia, CA, USA). Reagents for real time PCR (2x Quantifast SYBR Green RT-PCT master mix, 100 µl Quantifast RT mix) were supplied by Qiagen (Valencia, CA, USA).

2.1.4 SDS page and Western Ligand Blotting

Gels were prepared and run using a Mini-PROTEAN Tetra Cell Electrophoresis Unit (Bio-Rad Laboratories, Inc. Hercules, CA, USA; Figure 2.5). Transfer of proteins from gels to nitrocellulose membrane was performed using semi dry Trans Blot turbo transfer system (Bio-Rad Laboratories, Inc. Hercules,

CA, USA; Figure 2.6). Detection of proteins was achieved using enhanced chemiluminescence (ECL) with a West Pico Supersignal kit (Pierce, Rockford, IL, USA). Chemiluminescence detection was achieved using the Bio-rad Imaging System (Hercules, CA, USA) supported by Quantity One 4.6.2 (Bio-Rad Laboratories, Inc. Hercules, CA, USA).

2.2 PLASTICWARE

Tissue culture flasks (T75) and 6 well plates for cell culture use were purchased sterile from Nunc Life Sciences, Thermo Fisher Scientific (Rosklide, Denmark). 96 well plates for protein assays from Nunc Life Sciences, Thermo Fisher Scientific (Rosklide, Denmark). 1 ml Cryogenic vials were originally produced by Biosigma (Venice, Italy) and purchased from Fisher Scientific UK (Loughborough, UK). Cell scrapers were also purchased from Fisher Scientific UK (Loughborough, UK). Syringe's and syringe filters (0.20 μM) were from Fisher Scientific UK (Loughborough, UK). 0.5, 1.5 and 2 ml tubes were purchased from Eppendorf (Hamburg, Germany) and 0.25, 0.5, 1.5 ml RNase Free Microfuge tubes for use in RNA extraction, isolation and Real-Time PCR were purchased from Ambion (Cheshire, UK). Pipette tips for tissue culture, biochemistry and aerosol resistant tips (ART^{TM}) for use with RNA extraction, isolation and RT-PCR were purchased from Fisher Scientific UK (Loughborough, UK).

2.3 TISSUE CULTURE REAGENTS

Sterile cell and tissue culture media and supplements were purchased as follows: Dulbecco's modified Eagle's medium (DMEM, High glucose, with L-glutamine Cat no. D6429) from Sigma-Aldrich (Poole, UK), foetal bovine serum (FBS) from PAA (Buckinghamshire, UK). The following supplements were purchased non-sterile and therefore sterilised through a syringe using a 0.20 μM filter: penicillin streptomycin solution and trypsin from Gibco (Paisley, UK) and Sigma-Aldrich (Poole, UK) respectively. Gelatin type A from porcine skin was purchased from Sigma-Aldrich (Poole, UK) and phosphate buffered saline (PBS) from Fisher Scientific UK (Loughborough, UK). The FBS, penicillin-

streptomycin and trypsin were stored in -20°C in suitable aliquots until required to make up either growth media (GM) or differentiation media (DM). GM constituted: 395 ml bottle of DMEM plus 20% FBS (100 ml), and 1% penicillin - streptomycin solution (5 ml). DM (50 ml) constituted; DMEM (48.5 ml) plus 2% FBS(1 ml), and 1% penicillin- streptomycin solution (500 µl). This sterile GM and DM were stored at 4°C and used within 4 weeks.

2.4 C_2C_{12} SKELETAL MUSCLE MYOBLASTS

The murine C_2C_{12} cells are a subclone of the C_2 line (Blau *et al*., 1985) where C_2 cells were originally established by Yaffe and Saxel (Yaffe and Saxel, 1977) from adult C3H mouse leg muscle that was crush-injured to induce satellite cell proliferation. C_2C_{12} cells are commercially available and were obtained from the American Tissue Culture Collection (ATCC; Rockville, MD, USA) and stocks were maintained and stored in liquid nitrogen (LN_2) within our laboratories. These cells undergo spontaneous differentiation into myotubes on serum withdrawal, and do not require additional growth factors to stimulate the process (Blau *et al*., 1985).

2.4.1 Cell Culture of C_2C_{12} skeletal muscle myoblasts

C_2C_{12} cells were brought up in 1.0 ml cryovials from LN_2 at 1×10^6 cells.ml^{-1}. Once the cryovial contents had thawed, C_2C_{12} cells were plated at 7-9 $\times 10^5$ cells (700-900 µl of total cell suspension in a cryovial) per T75 flask. T75s were pre-gelatinised with 5 ml of 0.2% gelatin for 15 mins before aspirating off excess gelatin. GM was added to the cell suspension to make a total of 15 ml GM in T75 flasks. Flasks were incubated in a humidified 5% CO_2 atmosphere at 37°C, for 72 hrs.

Once the cells were ~ 80% confluent after a total of 72 hrs. Cells were washed twice with PBS to remove any serum (an inhibitor of trypsin) and trypsinised using 1 ml (per 75 cm^2) 0.05% Trypsin/0.02% Ethylenediaminetetraacetic acid (EDTA) for 5 minutes at 37^{o}C. Disassociation of the cells from the base of the flask was checked under the microscope (Phase contrast light microscope; CETI inverted light microscope, Thermo Fisher). 5 ml of GM was added (6 ml total,

including 1 ml trypsin) to inactivate the trypsin; this was collected into a test tube and gently dispersed using a 21 gauge needle and syringe to prevent cell clumping. The cell suspension was prepared in a 1:1 dilution in trypan blue stain (Gibco, Paisley, UK). Between 20 and 50 µl cell suspension was mixed with the equivalent amount of trypan blue stain and dispensed into a haemocytometer (Weber Scientific International, Hove, UK); for cell counting procedure see 2.6 below. Cells were seeded at the required density (80,000/ml) in GM onto relevant pre-gelatinised (0.2%) 2 ml six well plates (total 160,000 cells per well) for 24 hours to attach. Following washing, cells were further cultured until 80% confluency was attained (**Fig 2.1**). Any remaining cells from the original cell suspension were re-suspended at 1×10^6 cells.ml^{-1} in growth medium and 10% dimethyl sulphoxide (DMSO; BDH, Poole, UK) for 24 hrs cold storage at -80^{o}C before long term storage in liquid nitrogen (for cryopreservation see 2.7).

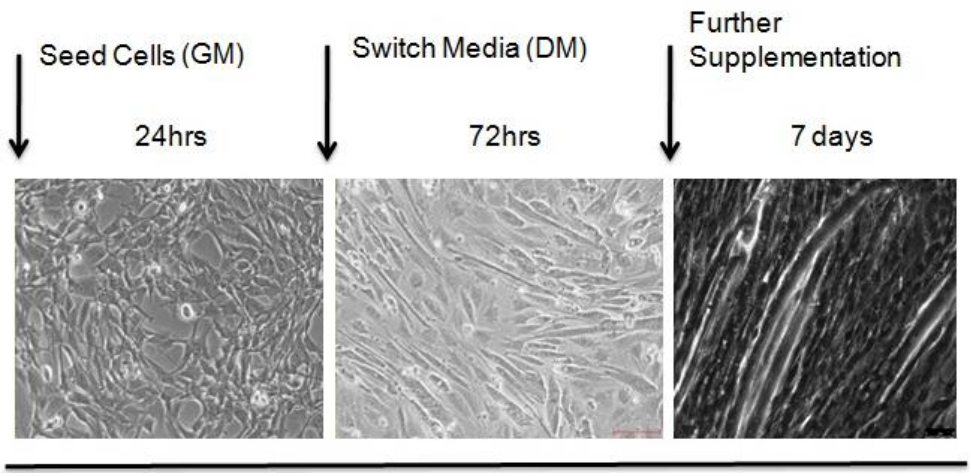

Fig 2,1 The time course for C2C12 skeletal muscle cells from confluence (24hrs GM) to differentiating (72hrs) to myotube maturation (7 days DM). Cells were seeded at 80,000 per ml (0hrs) and cultured in growth media (GM) for 24hrs before being switched to differentiation media (DM) for 7 days.

C_2C_{12} skeletal muscle myoblasts were induced to differentiate by aspirating GM, washing with 1 ml of PBS and replacing with low serum media (DM). 2 ml of DM was added to each well. The cells were induced to differentiate for up to 72 hrs and 7 days with morphological, biochemical, transcript and protein analyses taking place at 0, 72 hrs and 7 days, as detailed below. The media was

further topped up at 72hrs with 1 ml DM plus relative treatment (for treatments see below).

2.4.2 Mean Population Doubled (PD) C_2C_{12} myoblasts

C2C12 mouse myoblasts (CON) were used fresh or had previously undergone 58 population doublings (PD). (For a more detailed explanation, refer to Sharples *et al*. (2011)). In brief, cells had previously been doubled and numbers recorded throughout. This cycle was repeated 20 times over 49 days, creating a stock of cells that had undergone population doublings, compared with the original stock that were retained in liquid nitrogen and had undergone no doublings (CON) relative to the PD cells and were used as the controls in all experiments reported here. Thus, the same ‘‘parental cells’’ that had produced their progeny were used as control cells. There was no observable cell death between cell expansions (determined upon counting by trypan blue exclusion) as previously reported (Sharples *et al*., 2011). Furthermore, the cells display an impairment in skeletal muscle regeneration due to an inability to exit the cell cycle (Sharples *et al*., 2011). Overall, CON cells were used between passages 5-7 and PD cells were used between passages 25-27. Both cell types were resurrected as outlined in section 2.7 and cultured as detailed in section 2.4.1.

2.5 Cell Counting by Trypan Blue Exclusion

A haemocytometer was used for cell counting. This consists of a glass cover slip resting on a counting chamber. The cells were prepared as a 1:1 suspension in 0.4% trypan blue stain and loaded into the haemocytometer. Cells in the four corner grids were counted under a microscope at × 10 magnification. Viable cells were identified as small, round and clearly visible, while non-viable cells were generally misshapen, slightly larger and had lost their membrane integrity and hence were trypan blue positive. If the standard deviation was high between the initial four counts, the same sample was loaded and counted on the opposite side of the haemocytometer and a further 4 grids used in the calculation. The resultant mean of 4 or 8 grids was calculated, which represented average cell numbers occupied 0.1 mm^3. This value was then multiplied by 2 to take account of the

dilution factor of 1:1. A further multiplication by 10^4 was undertaken to extrapolate the number of cells in 0.1 mm^3 to 1 cm^3 (equivalent to 1 ml of cell suspension) (Equation 2.1). The total number of cells contained in the cell suspension could be calculated by multiplying by the total volume of cell suspension (ml).

$$Cells.ml^{-1} = \text{Average 4-8 grids} \times \text{dilution factor (2)} \times 10^4 \text{ cells.ml}^{-1}$$

Equation 2.1 Calculation of viable and dead cell number following haemocytometer counting.

2.6 CELL CRYOPRESERVATION AND RESURRECTION

Viable cells that had been passaged were preserved in Liquid Nitrogen (LN_2) by supplementing GM with 10% Dimethyl sulphoxide (DMSO), a cryoprotectant that penetrates the cell membrane and functions by replacing part of the cells water and subsequently reducing ice crystal formation that can cause damage to the cells (Lovelock and Bishop, 1959, Rubinsky, 2003). Once cells were 80% confluent in T75 flasks they were trypsinised and counted (as above 2.5). The cell suspension was then supplemented with additional GM to ensure the density of cells was 1×10^6 cells.ml^1, or if the cells suspension was populated with less than 1×10^6 cells.ml^1 they were centrifuged for 5 minutes at 2500 rcf and then re-suspended with the correct amount of GM to ensure density of 1×10^6 cells.ml^{-1}. The cell suspension was dispersed using a 21 gauge needle and syringe to avoid cell clumping. 10% DMSO was added in a drop-wise manner and slowly agitated up and down using a pipette. 1 ml of this cell suspension was transferred to a 1.0 ml cryovial labeled with cell type, passage number upon resurrection, treatment condition (if any), and date of storage. The vials were then placed into freezing chamber "Mr Frosty" purchased from Fisher Scientific (Loughborough, UK) containing isopropyl alcohol and placed into a freezer at -80°C. This chamber is designed to cause a rate of freezing of -1°C.min^{-1} which slowly allows the reduction in metabolism of the cells and thus enhanced survival. After 24 hrs the cells were transferred into a liquid nitrogen storage tank, Biostore (Tyne & Wear, UK). For resurrection, frozen vials containing cells were obtained from LN_2 and the exterior cleaned with 70% industrial methylated spirits (IMS). Cells were

placed inside a flow hood and thawed at room temperature. Cells were then plated onto plasticware as described in section 2.4.1 for initiation of specific investigations.

2.7 DOSING CELLS

2.7.1 Reconstitution of Testosterone

50 mg Testosterone (Tocris Bioscience, Bristol, UK) was purchased and initially prepared by adding 5 ml of DMSO to 7.2 mg T making a 5 mM stock solution (0.0072 g (1 mol/288.42 g)/ 0.005 L= 0.00499 M) in DMSO. The stock was aliquoted into 200 µl eppendorfs. These were frozen at -20^{o}C in 20 µl aliquots for storage. The working stock was kept for a month until a fresh stock was made. Concentrations of 50, 100 and 500nM were used on mouse C_2C_{12} cells, with 100 nM being used in CON and PD myoblasts.

2.7.2 Reconstitution of Flutamide (AR inhibitor)

1g of flutamide (Tocris Bioscience, Bristol, UK) was purchased and initially prepared as a 10 mg.ml^{-1} stock in 1ml of DMSO. The stock was aliquotted into 200 µl eppendorfs. These were frozen at -20^{o}C in 50 µl aliquots for storage until use. Concentrations of 20 and 40 µM were used on CON and PD cells (see Chapter 4 & 5).

2.7.3 Reconstitution of Picropodophyllin (IGF-IR inhibitor)

1mg of Picropodophylin (Calbiochem, Nottingham, UK) was purchased and initially prepared as a 1 mg.ml^{-1} stock in 1ml of DMSO. The stock was aliquotted into 200 µl eppendorfs. These were frozen at -20^{o}C in 50 µl aliquots for storage until use. Concentrations of 30, 90 and 150 nM were used on CON and PD cells (see Chapter 4 & 5).

2.7.4 Reconstitution of LY294002 (Pi3K/Akt inhibitor)

1mg of LY294002 (Calbiochem, Nottingham, UK) was purchased and initially prepared as a 20 mg.ml^{-1} stock in 1ml of DMSO. The stock was aliquotted into 200 µl eppendorfs. These were frozen at -20^{o}C in 20 µl aliquots for

storage until use. A concentration of 5 μM was used on CON and PD cells (see Chapter 6). The LY294002 inhibitor has been extensively shown to be highly specific and effective in C_2C_{12} cells in inhibiting PI3K and downstream Akt (Al-Shanti *et al*., 2011, Coolican *et al*., 1997, Frost *et al*., 2009, Lee, 2009, Li *et al*., 2005a, Zeng *et al*., 2012).

2.7.5 Reconstitution of IGF-I

50 ug of recombinant human insulin-like growth factor I (IGF-I) was purchased from Sigma Aldrich (Poole, UK) and reconstituted in 100 mM hydrochloric acid to generate a 10 $ng.ml^{-1}$ useable stock. The stock was aliquoted into 200 μl eppendorfs. These were frozen at -20^{o}C in 20 μl aliquots for storage until use. A 10 $ng.ml^{-1}$ concentration was used in experiments described in Chapter 3 and 4.

2.7.6 Procedure for dosing cells

For experimental protocols involving the dosing of CON and PD C_2C_{12} skeletal myoblasts (prior to the induction of differentiation by placing cells in DM) the DM was pre-dosed with testosterone 50, 100 and 500 nM, Flutamide at 20 and 40 μM, Picropodophylin at 30, 90 and 150 μM and LY294002 at 5 μM. For small quantities as highlighted in the example below, then serial dilution was performed. The following equation was used to determine amount of the stock solutions required:

Amount of stock required (μl) = (RC ÷ SC) × DM required (ml)

Where: RC = Required Concentration

SC = Stock Concentration

e.g.

Amount of Stock Required (μl)= 100 nM Testosterone ÷ 5000000 nM × 50 ml

Amount of Stock Required (μl) = 1 μl of Testosterone stock to be added to 50 ml of DM.

Equation 2.2. An equation to calculate amount of stock required when dosing skeletal muscle cells with testosterone and inhibitors in DM.

2.8 LYSING CELLS FOR USE WITH TOTAL PROTEIN ASSAY

Cells were induced to differentiate for up to 72 hrs and 7 days in DM ± dosing conditions detailed above. At the relevant time points cells were washed twice in 1 ml/well PBS and lysed in 300 µl.well^{-1} for 6 well plates using 10 mM TrisHCl, 5mM EDTA, 50 mM sodium chloride, 30 mM sodium pyrophosphate, 50 mM sodium fluoride, 100 µM sodium orthovanadate, 1 mM PMSF and 1% Triton X-100 (Cell lysis buffer). Cells were lysed at room temperature for 10 minutes, and lysates were scraped and collected into 1.5 ml eppendorf tubes. Tubes were labelled with cell type, condition, time point and date, and subsequently stored at -20^{o}C for at least 24 hrs prior to protein assays (see below 2.9). Protein assays were all completed within 2 weeks of the sample being obtained.

2.9 TOTAL PROTEIN ASSAY

2.9.1 Principle

The total protein that was present in a single well of 6 well plates was determined using a highly sensitive reagent for dilute aqueous solutions; Bicinchoninic acid (BCA), which detects Cu^{+1}, and is created when Cu^{+2} is reduced by protein in an alkaline environment (Smith *et al*., 1985). When the reagent was mixed with a sample; two molecules of BCA join with one cuprous (Cu^{+1}) molecule and the reaction becomes purple coloured. This purple colour is due to the macromolecular structure of protein, the number of protein bonds and the presence of the four amino acids: Cysteine, Cystine, Tryptophan and Tyrosine (Wiechelman *et al*., 1988). The darker the colour the more protein present. The absorbance of this complex was measured between 540 and 590 nM which is linear with increasing protein concentrations (Equation 2.3).

1. Protein (peptide bonds) + Cu^{2+} → tetradentate-Cu^{+} complex

2. Cu^{+} complex + Bicinchoninic Acid (BCA) → BCA-Cu^{+} complex
(Purple Coloured)

↓

Read at absorbance 540 nM-590nM

Equation 2.3. Chemical reactions underlying the protein assay (Smith *et al.*, 1985).

2.9.2 Procedure

Standards made with bovine serum albumin (BSA) were used to determine the concentration of protein ($mg.ml^{-1}$) based on standard curve generated using a Bio-Tek ELISA plate reader (Winooski, VT, USA). BSA protein standards were prepared at 4, 2, 1, 0.5, 0.25, 0.125, 0.0625 and 0 $mg.ml^{-1}$ initially by diluting 200 mg BSA (in 0.9% sodium chloride and sodium azide a preservative; Pierce, Rockford, IL, USA) with 4.8 ml cell lysis buffer (detailed in section 2.8) providing a working stock solution (× 10) at 40 $mg.ml^{-1}$ of BSA. 200 µl of stock solution was then diluted with 1.8 ml cell lysis buffer providing the first standard of 4 $mg.ml^{-1}$ BSA. All subsequent standards were prepared by mixing 1 ml of the previous standard with 1 ml cell lysis buffer, apart from the preparation of the 0 standard, which was the cell lysis buffer alone.

BCA reagents A & B were purchased from Pierce (Rockford, IL, USA). Reagent B was made up of 4% cupric sulphate and was mixed thoroughly in a multichannel trough with reagent A (sodium carbonate, sodium bicarbonate, bicinchoninic acid and sodium tartrate in 0.1 M of sodium hydroxide) at a ratio of 1:50. 10 µl of standard, sample and a blank (distilled water) were pipetted in duplicate into a 96 well plate. 200 µl of the working reagent was added to all wells using a multichannel pipette (excluding the blank), and the plate was incubated at 37°C for up to 60 mins. Following background subtraction, the absorbance was recorded at 30 and 60 minutes at 630 nM using a Thermo

Labsystems Multiskan spectrum microplate reader. The standard curve was generated by plotting the average blank-corrected 630 nM measurement of each BSA standard against its pre-programmed known concentration in $mg.ml^{-1}$. Sample concentrations were calculated from the standard curve.

2.10 IMMUNOCYTOCHEMISTRY AND MICROSCOPY

2.10.1 Principal

Antibodies can be used to probe and detect specific molecules of interest in cells. This is achieved by the antibodies being specific for antigens which are present on the protein of interest. The addition of fluorescent dyes allows for these proteins to be visualised by fluorescence microscopy.

Firstly, the cells must be fixed. Two types of fixatives can be used- organic solvents and cross-linking agents. For this thesis, an organic solvent is used. This type works by dehydrating the cells and removing lipids, yet the cell architecture remains intact. Alternatively, the cross-linking agent such as paraformaldehyde allows for a network of linked antigens to be created via intermolecular bridges and thus preserves the cell structure. In order for the antibodies to infiltrate the cell and access the intracellular protein of interest, the cell membranes need to be first permeablised. This is normally achieved using a detergent such a Triton. In unison with permeablisation being performed, blocking is performed. This step is necessary in order to prevent the binding of the primary antibody to non-specific sites with the cell structure. Serum is used for the blocking of non-specific binding as this also allows for the avoidance of background fluorescence when image collection is performed (detailed in 2.10.3). Subsequently, after the steps of fixation, permablisation and blocking, the cells can be incubated with the desired antibodies. There are two types of antibodies which can be used in ICC and IHC:

i) Polyclonal antibodies- These are produced from the sera of animals, by injecting the antigen of interest into the animal. The animal's B-lymphocytes produce an antibody specific to the protein of interest. These antibodies are then harvested and purified for subsequent use in ICC/IHC.

ii) Monoclonal antibodies- These antibodies are more expensive and take longer to produce. A similar procedure occurs to the polyclonal antibodies where the animal is injected again with the antigen of interest, however this time; the B-lymphocytes are fused *in vitro* with myeloma cells to form hydrodimas. These hydrodimas are isolated and allowed to multiply, formulating a large stock of identical antibodies to the antigen of interest.

Therefore, the process of indirect immunofluorescence was utilised in this thesis, which required the use of an initial primary antibody to bind to the protein of interest within the cell. This followed by a secondary antibody against the IgG of the animal in which the primary antibody was raised. The conjugation of the secondary antibody with a fluorescent dye (e.g. TRITC or FITC) allows for visualisation upon excitation at the correct wavelength.

2.10.2 Procedure

Cells were fixed by first, media being aspirated from the wells and replaced with PBS (1ml per Well) and 1ml of methanol/acetone (50:50mix) ice-cold. The mix was incubated in the wells for 10mins. Upon the incubation time being complete, this mix was aspirated and a further 2ml methanol/acetone was added carefully to each well and incubated for another 10mins. Finally PBS (2ml/well) was added after removal of the methanol/acetone mix and plates were stored in 4^{o}c until further analysis. The process of immunofluorescence was performed directly in the wells of 6 well plates or on glass cover slips. In general, cover slips/wells were stained for desmin and nuclei using 1:200 desmin primary antibodies (Abcam, Cambridge, UK), 1:200 TRITC secondary antibody (Sigma, St Louis, USA) and 1:2000 Sytox Green (Life Technologies, CA, USA) nuclei stain using the protocol illustrated in **fig 2.2**. The blocking/permeabilisation solution consisted of 1x TBS (pH 8.5), 5% goat serum (Sigma Aldrich, Poole, UK) and 0.2% Triton-X 100 (Fisher Scientific, Loughborough, UK) with 100 and 500 µl added to cover slips and wells respectively. The antibody solutions consisted of 1x TBS, 2% goat serum and 0.2% Triton-X100 plus either the

primary or secondary antibody at concentrations highlighted above. Cover slips were mounted on to slides using Mowiol and left in the dark, overnight to dry. Wells were covered in 2 ml of 1x TBS and stored in 4^{o}C until fluorescent microscopy was performed. All incubation periods were performed at room temperature.

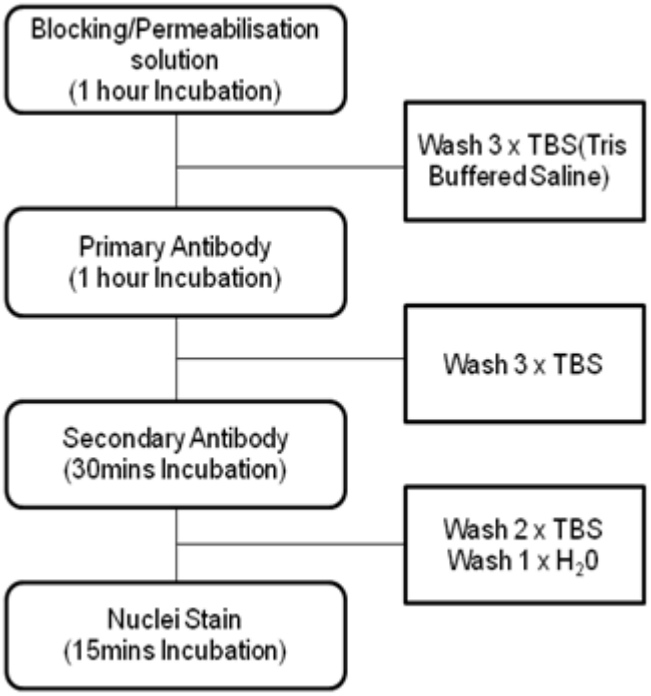

Fig 2.2 Immunocytochemistry protocol implemented for cover slips and wells.

2.10.3 Image Quantification

A total of 30 fields per condition for each time point were captured with a cell imaging system at x10 magnification for light microscope (Inverso-TC, CETI, Medline Scientific Limited, Oxon, UK) and x40 (chapter 3) and x 20 (chapter 5) fluorescent microscopy (DM6000 FS, Leica, Germany). Images were analysed using Image J (Java) software (National Institutes of Health, USA). Morphology was assessed by determination of myotube diameter, number of myotubes per view, mean number of nuclei per myotube per field of view, fusion index (cell fusion) and total nuclei counts (changes in total cell number and therefore an indices for proliferation). A myotube was defined as containing 3^{+} nuclei

encapsulated within cellular structures, so to avoid counting of single cells undergoing mitosis. Myotube diameter (μm) was determined by measuring the diameter of 3 equidistant points on each myotube (left end, middle, right end) and determining the mean of the 3 values as previously described (Stevenson *et al*., 2005, Trendelenburg *et al*., 2009). An indicator of myonuclear accretion (fusion index) was calculated by dividing myotubes into two classes; myotubes which expressed 3-4 nuclei or myotubes which expressed 5+ nuclei, with the data expressed as percentages.

2.11 RNA EXTRACTION

2.11.1 Procedure

Following the required experimental incubation period, murine C_2C_{12} myoblasts had their existing media aspirated, were washed with PBS and lysed for 5 min at RT in 300 μl TRIZOL reagent/well (Sigma-Aldrich, Poole, UK). TRIZOL is a mono-phasic solution of phenol guanidine isothiocyanate that disrupts cells and dissolves all cell components other than RNA and DNA and protein. 2 wells of a 6 well plate per condition were harvested using a scraper and then collected into 1.5 ml RNase free tubes. Samples were agitated by vortexing for 10 seconds to ensure cells were totally lysed and were then stored at -20ºC for up to 1 week before homogenates were supplemented with 0.1 ml chloroform per 0.5 ml of TRIZOL reagent prior to vigorous mixing for 15 seconds. Resulting mixtures were kept at room temperature for 10 minutes then centrifuged at 12000 g for 15 mins at 4˚C. Following centrifugation the mixture separates into a lower red phenol-chloroform phase containing cell debris and components of TRIZOL, a milky-coloured interphase containing DNA and protein, and a colourless aqueous upper phase that houses the RNA and chloroform. The colourless aqueous phase was carefully extracted into new RNase free tubes, without disturbing the interphase. RNA was precipitated from the aqueous phase by mixing with isopropanol at a ratio of 1:2 (with the starting amount of 300 μl TRIZOL). Samples were stored at room temperature for 5-10 mins and centrifuged at 12000 g for 10 minutes at 4 °C. Supernatant was removed and the RNA pellet washed by adding 1 ml of 75% ethanol. The samples were centrifuged

at 7500 g for 5 minutes at 4 ˚C. Ethanol was removed and the RNA pellet air-dried until it was invisible in the tube. RNA was dissolved in 30-50 µl RNA storage solution (Ambion- The RNA Company, Cheshire, UK) and vortexed for 10 seconds. All procedures above were carried out using RNA-free pipette tips and pipettes that were handled for RNA use only. A different tip was used for every sample to ensure no cross contamination. All work surfaces and equipment were sprayed with 70% IMS and then RNase ZAP (Ambion- The RNA Company, Cheshire, UK) before commencing work with RNA. The samples were either stored in -80°C or analysed immediately for RNA concentration (see section 2.12.2.).

2.11.2 RNA Concentration

RNA concentration and purity were assessed through UV spectroscopy at ODs of 260 and 280 nm, using the Nanodrop spectrophotometer 3000 (Fisher, Rosklide, Denmark). Only samples with a 260:280 ratio of between 1.9 and 2.15 were carried forward for reverse transcription and PCR amplification (detailed in section 2.13).

2.12 ONE STEP, REAL TIME POLYMERASE CHAIN REACTION (PCR) USING SYBR GREEN DYE

2.12.1 Principal

The use of real time PCR allows for gene expression levels to be quantified. This molecular biology technique allows for the amplification of specific gene sequences in order to quantify the original amount of starting material e.g. RNA or DNA. Therefore, a sequence of RNA expression can be targeted to see if it is up or down regulated with a particular treatment e.g. testosterone administration. The first initial step is to extract RNA from the sample (see section 2.12). The isolated RNA can then be reverse transcribed into complimentary DNA (cDNA). The reverse transcription is achieved by oligo primers binding to the poly-A tail at the 3’ end of the mRNA molecule, and the enzyme reverse transcrisptase generates the complimentary sequence. The process of reverse transcription

usually occurs between 40 to 60^{o}C and in this thesis, 50^{o}C. The following three steps of PCR occur:

i) Denaturation: This step involves the heating of reaction tubes to 95^{o}C, allowing for the disruption of hydrogen bonds on the complementary DNA strands.

ii) Annealing: Specific primers which are complementary to the sense and anti-sense strands of the DNA, bind (anneal) to the sequence of interest. A reduction in temperature occurs at this stage, which is optimal for the primers that were designed (See **table 2.1**)

iii) Extension: A Taq polymerase enzyme is used to synthesize a new strand of the target DNA sequence. The enzyme achieves synthesis of new DNA by attaching to the primary sites on the primers and uses dNTP's to extend the target sequence. The process generally occurs at an optimal temperature of 72^{o}C, and in this thesis was performed at 60^{o}C.

The completion of all three steps combined indicates one cycle has been performed. Generally, PCR is carried out for 40 cycles, generating millions of copies of specific gene sequence that is of interest for quantification. Finally, the technique uses fluorescence in order to detect the amount of cDNA which has been amplified in real-time. Particular to this thesis, SYBR green was used as the fluorescent dye which binds to double stranded DNA and the subsequent fluorescence is detected by the PCR machine. The amount of fluorescence is measured at the end of the extension step for each cycle, and thus as the number of cycles increases and the products is amplified, then the level of fluorescence will increase accordingly. The quantification of fluorescence and relative gene expression is outlined in section 2.13.4.

2.12.2 Primer Design

Primer sequences were identified using Gene (NCBI, www.ncbi.nlm.nih.gov/gene) and designed using both web-based OligoPerfect™ Designer (Invitrogen, Carlsbad, CA, USA) and Primer-BLAST (NCBI, http://www.ncbi.nlm.nih.gov/tools/primer-blast). Sequence homology searches ensured specificity. Three or more GC bases in the last 5 bases at the 3' end of the primer were avoided. Secondary structure interactions (hairpins, self-dimer and cross dimer) within the primer were avoided. All primers ranged between 18 and 23 bp and amplified a product between 173 and 197 bp. GC content was between 36.3 and 60%. Primers without the requirement of further purification were purchased from Sigma (Suffolk, UK).

Table 2.1 Primer Sequences for Genes of interest

Gene	Primer Sequence (5'-3')	Ref. Sequence Number	Amplicon Length (bp)	GC% Content
AR	**F:**GCCTCCGAAGTGTG GTATCC **R:**CCTGGTACTGTCCA AACGCA	NM_013476.3	138	60 55
IGF-IR	**F:**CTACCTCCCTCTCTG GGAATG **R:**GCCCAACCTGCTGT TATTTCT	NM_010513	185	47.4 47.4
IGF-I	**F:**ATCAGCAGCCTTCC AACTC **R:**AAGGTGAGCAAGCA GC	NM_010512	116	45 47.4
MyoD	**F:**CATTCCAACCCACA GAAC **R:**GGCGATAGAAGCTC CAA	NM_010866	125	59.7 50
MAFbx	**F:**GTCGCAGCCAAGAA GAGAA **R:**CGAGAATCCAGTCT GTTGAA	NM_026346.3	155	52.7 47.7
Myostatin	**F**:TACTCCGAATAGAA GCCATAA **R**: GTAGCGTGATAACGTCAT C	NM_010834	194	36.3 45
mTOR	**F:** CACTCCACTATCCT GTTACCT **R:** GAGATCCTTGGCAC ACCT	NM_020009	190	47.6 55.5
Myogenin	**F:**CCAACTGAGATTGT CTGTC **R:** GGTGTTAGCCTTATGTGA AT	NM_031189	173	47.3 40
RP-IIβ	**F:**GGTCAGAAGGGAA CTTGTGGTAT **R:**GCATCATTAAATG GAGTAGCGTC	NM_153798.1	197	50 44.4

2.12.3 Procedure

PCR reaction tubes were prepared using the QIAGility automated pipetting system (Qiagen, Crawley UK). Reactions (20 µl) were made up in transparent, optically clear RNA free tubes which consisted 0.15 µl of both forward and

reverse primers at 100 µM concentration (sigma), 0.2 µl of Quantifast reverse transcription kit (Qiagen), and 10 µl of SYBR green dye (Qiagen) plus 9.5 µl of 70 ng RNA/Sample (concentrated at 7.3 ng.ul^{-}1). Upon completion, reaction tubes were loaded into a Rotogene 3000 (Qiagen, Crawley, UK). RT-qRT-PCR was performed as follows: 10 min, 50^{o}C (reverse transcription), 5 min 95^{o}C (transcriptase inactivation and initial denaturation), Followed by: 10 secs, 95^{o}C (denaturation), 30 secs, 60^{o}C (annealing and extension) for 40 cycles (see section 2.12.1). Following completion, melting curve analyses were performed to exclude primer-dimer and non-specific amplification (**Fig 2.3**).

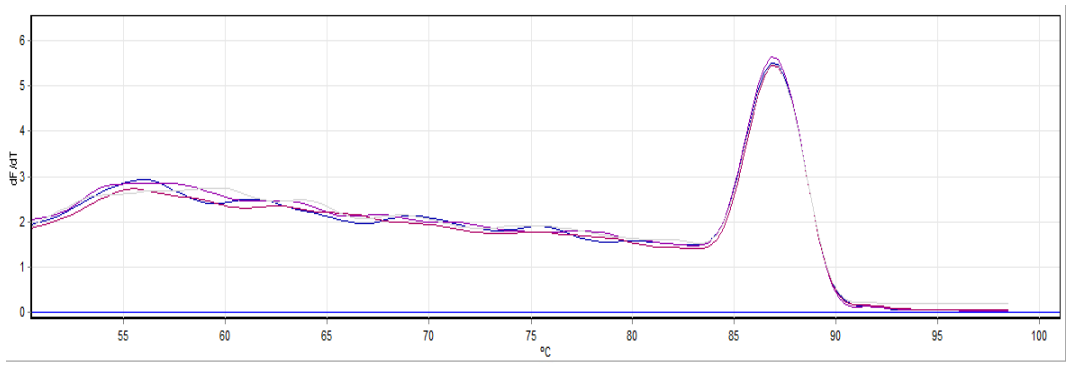

Fig 2.3 Melt curve analysis showing peak confirms primer set specificity. The melt curve shown is from primers designed for mouse (mus musculus) mTOR.

2.12.4 qPCR analysis

Relative mRNA expression was quantified by using the comparative C_T method (also known as the $2^{-\Delta\Delta CT}$ method) as described previously (Livak and Schmittgen, 2001, Schmittgen and Livak, 2008). The cycle threshold (C_T) for an individual sample is defined as the cycle at which the sample's fluorescence produced by the reaction exceeds the background fluorescence (**Fig 2.4**). Therefore, the numerical value of the C_T inversely represents the amount of amplicon in the reaction i.e the lower the C_T value, the greater amount of gene expression. Subsequently, gene expression can be normalised to the CT value for a housekeeping gene (e.g. RP-IIβ) which is selected based on being stable under all conditions in the experiment. Finally, this methods requires that the data is made relative to a control condition (e.g. CON DM 0hrs). The following equation was implemented:

e.g. $2^{-\Delta\Delta CT}$ = [(C_T gene of interest – C_T internal control) Treatment sample – (C_T gene of interest - C_T internal control) Untreated sample)]

Equation 2.4 The comparative C_T method used to quantify relative mRNA expression (Adapted from Schmittgen and Livak (2008))

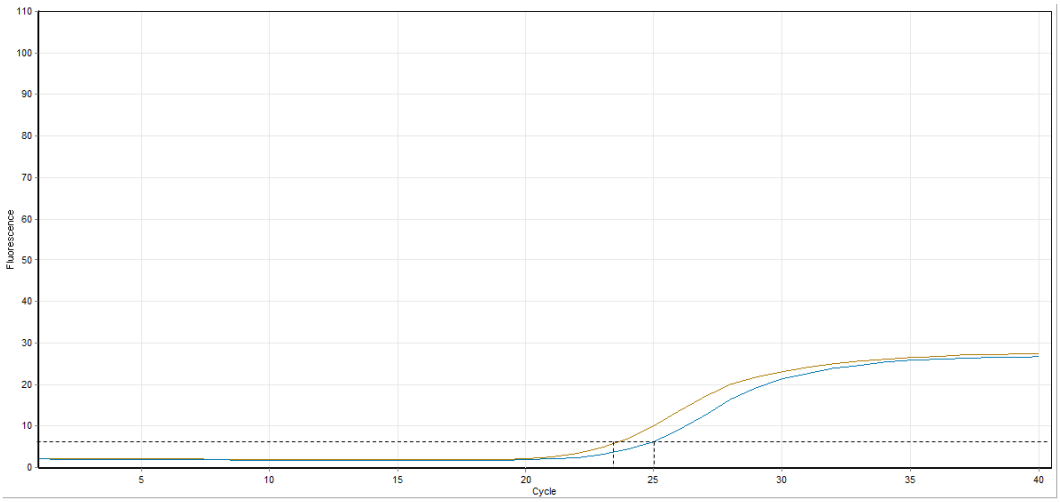

Fig 2.4 The determination of the threshold cycle (C_T) for gene expression quantification. Identification of the threshold cycle is used to quantify the starting expression level for the gene of interest. For example, the brown line (above) has a lower C_T value compared the blue line, meaning heightened expression.

2.13 SDS-PAGE (Sodium Dodceyl Suplhate-polyacryladmide gel Electrophoresis) and Immunoblotting

2.13.1 Principal

Separation of complex protein structures is performed using discontinuous sodium dodecyl sulphate polyacrylamide gel electrophoresis (SDS-PAGE) according to their molecular weight in kilo Daltons (kDa) (Laemmli, 1970). Different concentrations of acrylamide can be used for polymerisation depending on the size of interest e.g. 12% gel for proteins of low molecular weight vs. 7% gels for a protein of high molecular weight. The use of bis-acrylamide allows for the polymerisation of the gel by forming cross-links between the acrylamide polymers. The process of polymerisation is catalysed by mixing ammonium per

sulphate (APS) and N, N, N', N'-Tetramethylethylenediamine (TEMED). Two discontinuous gels are generated: i) the resolving gel (10%) which separates the protein by size and ii) the stacking gel (5%) which enables large volume of dilute sample to be loaded in to lanes and thus align at the gel interface, prior to separation occurring in the resolving gel.

2.13.2 Sample preparation

After transfer to DM or relevant dosing conditions cell monolayers were washed twice in PBS and lysed in 200 µl/ well of a 6 well plate in cell lysis buffer containing: 10 mM TrisCl, 5mM EDTA, 50 mM sodium chloride, 30 mM sodium pyrophosphate, 50 mM sodium fluoride, 100 µM sodium orthovanadate, 1 mM PMSF and 1% Triton X-100 and 1 cOmplete Protease Inhibitor cocktail tablet (Roche, Hertfordshire, UK). After 5 minutes on ice, the cells were scraped with a cell scraper, transferred to a 1.5 ml eppendorf tubes and stored at -80˚C until required. Protein concentrations were assessed using methodology in Section 2.9 above prior to preparation for loading.

5X Sample buffer (Laemmili Buffer) was prepared (3 ml 1M Tris-HCl pH 6.8, 0.5 g SDS, 5 ml Glycerol, 2 ml dH_2O, gel loading solution (Sigma Aldrich, Poole, UK) and 2 ml β-mercaptoethanol. 30 µg of protein per cell lysate was added to sample buffer. Approximately 60 µl of supernatant sample per condition was loaded with 8 µl of loading buffer. Molecular weights were determined by the incorporation of 10 µl rainbow molecular weight protein standards. Rainbow marker was purchased from Sigma-Aldrich (Color Burst Electrophoresis Marker, Sigma, Poole, UK). Containing myosin (violet; 200 kDa), BSA (red; 100 kDa), GDH (blue; 60 KDa), ADH (red; 45 kDa), Carbonic Anhydrase (orange; 30 kDa), 200 mM Tris, SDS and formamide (amount not specified). The samples were boiled at 90˚C for 5 minutes in a beaker of water placed on a hotplate (to reduce disulphide bonds) before loading onto the gel with a 20 µl loading tip (Fisher Scientific, Loughborough, UK).

2.13.3 Gel preparation

Gels were prepared using a Mini-PROTEAN Tetra Cell Electrophoresis Unit (Bio-Rad Laboratories, Inc. Hercules, CA, USA; Fig 2.5). The glass plates were assembled as per manufacturer's instructions. The resolving gel (30% acrylamide 1% BIS, 1.5M Tris base pH 8.9, 0.1M EDTA pH 7.4, 10% SDS, 0.1% (w/v) APS and 0.1% (v/v) TEMED) was poured between the clamped plates in the Tetra Cell unit (Fig 2.5). Ethanol: dH_2O (1:1) gel overlay buffer, was poured over the top of the gel which enables uniform polymerisation by preventing air from inhibiting the process at the surface of the gel. Once polymerized, the ethanol was thoroughly washed away with dH_2O and the stacking gel (30% acrylamide 1% BIS, 54mM Tris HCl pH 6.8, 0.1M EDTA pH 7.4, 0.1% (w/v) SDS, 0.1% (w/v) APS and 0.1% (v/v) TEMED) was over-layed. A 10 well-comb was inserted into the stacking gel whilst un-polymerised to ensure loading of samples could take place. The combs were removed once the staking gel had polymerized and the gels were transferred the gel running tank (shown in Fig 2.5). The upper and lower chambers were filled with 1X running buffer (25 mM Tris base, 192 mM glycine, 2 mM EDTA and 0.1% (w/v) SDS in dH_2O pH 9.65).

2.13.4 Electrophoretic separation

Samples subjected to 10% SDS-PAGE were electrophoresed at 200 volts using a PowerPac^{TM} HC high-current power (Bio-Rad Laboratories, Inc. Hercules, CA, USA) until the sample buffer tracking dye reached the bottom of the gel.

2.13.5 Transfer of proteins to Nitrocellulose Membrane

The glass plates (Fig 2.5) were carefully disassembled without ripping the gels. The stacking gel removed using a scraper leaving the resolving gel. Meanwhile, a piece of Hybond-C nitrocellulose and 4 sheets of Whatman filter paper (Bio-Rad Laboratories, Inc. Hercules, CA, USA) were cut to the size of the gel (7.5 x 8 cm) and immersed in transfer buffer final pH 8.3 (114 nM glycine, 19 mM Tris base and 33% methanol). Two sheets of pre-immersed Whatman filter paper were placed on the green semi dry trans blot turbo transfer system (Bio-Rad Laboratories, Inc. Hercules, CA, USA; Fig 2.6), the gel was placed on top of the

filter paper followed by the nitrocellulose membrane paper and a further 2 layers of pre-immersed Whatman filter paper added. Finally, the combined layers were rolled to ensure no air bubbles were retained between each layer. The lid of the electrode cell was placed on top of the gel sandwich stack. The proteins were transferred to the nitrocellulose membrane support for use in western ligand blotting for 30 minutes at 25 V using a PowerPac^{TM} HC high-current power (Bio-Rad Laboratories, Inc. Hercules, CA, USA).

2.13.6 Ponceau S staining

It is possible to view the transfer efficiency of the proteins and view any unstained molecular weight markers by staining the membrane with a non-permanent dye called Ponceau S. Membranes were incubated in 0.1% Ponceau S solution in 5% acetic acid (Sigma, Poole, U.K) for 5 minutes, washed with dH_2O and the markers marked with a soft pencil. Membranes were completely de-stained following prolonged washing with dH_2O and 1 × TBS (containing 1% Tween-20).

2.13.7 Immunoblotting

Immunoblotting was performed using a fast western supersignal west pico rabbit substrate kit (Pierce, Rockford, IL, USA). The western blotting was performed based on manufacturer's instructions. Initially, the nitrocellulose membranes were soaked in wash buffer (containing blocking solution twice) for 10 minutes. Next, membranes were sealed in plastic bags containing primary antibodies (1:1000-2000) in an antibody diluent liquid for 1 hour incubation at room temperature. Primary antibodies (rabbit polyclonal) were purchased from New England Bio labs (Santa Cruz, USA) (**Table 2.2**). Post primary antibody incubation, membranes were washed in 1 x TBS (containing 0.05% Tween). Then, membranes were incubated for 30 minutes in HRP-conjugated secondary antibody (1ml in 10ml) at room temperature. Then membranes were washed with 1 x wash buffer supplied in the kit for 5 minutes each. All washes and incubations were performed on a rocking platform in boxes and sealed bags respectively.

Table 2.2 Primary antibodies for proteins of interest and loading control

Protein	Cat no.	Concentration	Molecular Wt. (kDa)
Androgen receptor	Sc-816	1:500	110
IGF-I receptor	Sc-713	1:500	97
Total Akt	9272	1:1000	60
Akt^{ser473}	4058	1:1000	60
Total ERK ½	9102	1:1000	42, 44
ERK 1/2$^{thr202/tyr204}$	9101	1:1000	42, 44
Total p70S6K	9202	1:1000	70
p70S6K^{thr389}	9205	1:1000	70
GAPDH	5174	1:4000	37

2.13.8 ECL detection

Detection of proteins was achieved using enhanced chemiluminescence (ECL) with a West Pico Supersignal kit (Pierce, Rockford, IL, USA). The ECL substrate was made up from reagent A and B in a ratio of 1:1 (2.5 ml each) and incubated for 5 minutes (Supersignal kit) with gentle agitation according to manufacturer's instructions. Membranes were drained bags resealed and light emission captured using the Biorad Imaging System (Hercules, CA, USA). Briefly, reagent A decays to H_2O_2, the substrate for peroxidase. Reduction of the enzyme HRP is coupled to a light producing reaction by detection with reagent B. This contains luminol, which upon oxidation, produces blue light that can be detected on an imaging system.

2.14 Statistical Analysis

All statistical analysis performed in this thesis was done using SPSS version 19 (IBM, Armonk, NY, USA) and Graph Pad Prism Software (San Diego, USA). All data was checked for normal distribution and being parametric. The statistical tests performed will be detailed in the methods section of each results chapter.

3. THE DOSE EFFECTS OF TESTOSTERONE ADMINISTRATION IN C_2C_{12} SKELETAL MUSCLE CELLS

3.1 INTRODUCTION

Testosterone elicits an anabolic effect on skeletal muscle via increases in protein synthesis, decreases in protein degradation and the reutilization of amino acids (Ahtiainen *et al*. 2011; Brodsky *et al*. 1996; Sheffield-Moore *et al*. 1999). These adaptations culminate in a hypertrophic (increased size via increased protein synthesis) response occurring in the skeletal muscle. An increase in size of skeletal muscle, shown by increases in cross sectional area (CSA) has been observed following administration of testosterone enanthate (derivative of T through the addition of an ester) at doses of 25-600 mg, with corresponding strength increases being dose dependant (Bashin *et al*. 1996; Bashin *et al*. 2001; Sinha-Hikim *et al*. 2002). Testosterone has been shown to increase satellite cell number and increase activation and fusion of these cells indicated by an increase in myonuclear incorporation in skeletal muscle in vivo following testosterone administration (100-600 mg) (Chen *et al*. 2005; Kadi & Thornell, 2000). Power lifters known to be users of androgenic-anabolic steroids demonstrate an amplified muscle hypertrophy response (Eriksson *et al*. 2005). However, the molecular mechanisms by which testosterone stimulate anabolic processes for hypertrophic responses remain poorly understood.

3.1.1 Molecular targets from human studies involved in Testosterone-induced muscle hypertrophy

In the last decade, human studies have investigated potential molecular and cellular targets which may mediate the effects of testosterone administration in enhancing skeletal muscle mass. Ferrando and colleagues (2002) observed increases in AR protein expression after 1 month administration of testosterone enanthate (dose adjusted to maintain individuals within 17-28 $nmol.l^{-1}$ range), but these levels reduced to pre-treatment after 6 months treatment in elderly men. Furthermore, IGF-I protein expression increased after 1 month, and continued to increase following continued 6 month administration. The alterations in AR and

IGF-I protein levels accompanied increases in leg lean body mass, muscle volume and muscle strength (leg and arm). In a study using graded doses (25, 50, 125, 300 and 600 mg) of testosterone, Sinha-Hikim and colleagues (2006) investigated testosterone induced hypertrophy looking specifically at satellite cell influence. They observed doses from 125 mg and above, increased satellite cell number (PCNA+), along with activation of Notch and increased myogenin expression. The authors providence evidence for testosterone restoring skeletal muscle mass in elderly individuals, with a dose effect above 125 mg. To note, AR was not measured within this cohort, although the satellite cell is the main location for AR expression in humans (Kadi *et al*., 2000, Kadi, 2008).

3.1.2 Molecular targets investigated in animal/in-vitro studies with testosterone administration.

In-vitro studies have further enhanced our understanding of potential molecular targets which may be involved in testosterone induced hypertrophy. The majority of testosterone related studies have centered around the AR, IGF-I, myostatin and myogenin expression (marker of terminal differentiation) in relation to myotube differentiation and hypertrophy (Kovacheva *et al*., 2010, Braga *et al*., 2012, Singh *et al*., 2009, Sculthorpe *et al*., 2012, Wannenes *et al*., 2008, Lee, 2002, Serra *et al*., 2011). In human craniofacial muscle cells, Sculthorpe and colleagues (2012) observed significant increases in *Igf1* mRNA expression with 500 nM T compared to 100 nM T, with this observation being abrogated through AR inhibition using flutamide. In comparison, Wannenes *et al*. (2008) used 0.1, 1 and 10 nM testosterone on C_2C_{12} skeletal muscle cells, to investigate the role of the AR in muscle cell differentiation. The authors observed a dose-response increase in AR (protein and mRNA expression), myogenin, myosin heavy chains (MyHC: IIb, IIx/d and I) and GRIP-1 (co-regulator of the AR) expression. These observations provide evidence towards testosterone and the AR role in myogenesis, even at a low dose.

Further studies have addressed the role of IGF-I and its downstream pathways in mediating the effects of testosterone (Serra *et al*., 2011, Wu *et al*., 2010a). Serra and colleagues utilized both a knock out (IGF-I receptor/IGF-IR)

animal model and primary human myoblasts to address the impact of circulating IGF-I and associated signaling in testosterone mediated processes. IGF-I receptor knock outs were treated with a GnRH antagonist to suppress endogenous T. The administration of exogenous testosterone enanthate enhanced body weight and *levator ani* muscle weight (androgen-responsive which is due to abundance of AR expression present). Furthermore, testosterone treatment enhanced primary human myotube morphology through myonuclear accretion, diameter and increased MyHC expression in the presence of small interference RNA for IGF-I receptor. The author's observations highlight variables (morphological and biochemical) which testosterone can enhance in vitro and potentially how these effects are mediated.

Therefore, based on literature above, the temporal action of testosterone on pre-existing myotubes *verses* differentiating myoblasts is yet to be investigated along with the impact of high and low doses in C_2C_{12} muscle cells. By addressing these two factors, the findings will inform a suitable dose to be used later in the thesis as well as the impact of testosterone on muscle differentiation and hypertrophy.

3.1.3 Aims and Objectives

Therefore in light of the literature discussed above, the aims of this chapter were to characterize high and low testosterone doses (50 and 500 nM) in C_2C_{12} skeletal muscle myoblasts, with administration at two points in time: differentiating (myoblast pre-fusion/upon transfer to low serum media/ denoted 0hrs) vs. differentiated (pre-existing myotubes/72 hrs in low serum media) defined as T_1 and T_2 respectively. The investigation of both dose and time point administration would allow for the determination of the effects of testosterone on myotube formation (differentiation) and hypertrophy as well as a suitable dose for subsequent experiments (chapter 5 and 6). Thus morphological (myotube number, myotube diameter, myonuclear accretion) and transcriptional (myogenin, AR, IGF-I and myostatin) alterations to testosterone administration were measured. It was hypothesized that there would be dose responsive increase in morphological

and transcriptional differentiation and hypertrophy as well as myotube hypertrophy and differentiation.

3.2 METHODOLOGY

3.2.1 Cell Culture

Mouse C_2C_{12} skeletal muscle myoblasts were resurrected as described in section 2.6 and cultured as outlined in section 2.4.1. Once cells were ~80% confluence, they were seeded at 80,000 cells per ml in 2 ml of growth media (GM) per well onto 0.2% porcine gelatin-coated 6-well plates and grown in a humidified 5% CO_2 atmosphere at 37^{o}C. Once confluent, the myoblasts were changed from growth media to low serum media/differentiation media (DM), which promotes the fusion of the myoblasts into multinucleated myotubes. C_2C_{12} myoblasts undergo spontaneous differentiation into myotubes on serum withdrawal, and do not require growth factor addition to stimulate the process (outlined in section 2.4.1). Cells were incubated in DM for 30 minutes at 37^{o}C in a 5% CO_2 atmosphere with this period of equilibration denoted as the 0 hour time point.

For T_1 experiments, cells at the time points of 0, 72 hrs and 7 days were fixed and isolated for RNA (outlined in sections 2.10.2 and 2.12). For T_2 experiments, cells were cultured in DM for 72 hrs (defined as 0hrs for T_2) and then transferred to treatments as described below. Extraction and fixation for T_2 was performed at 24hrs and 72hrs post administration to analyze morphology and transcriptional changes using reverse transcription quantitative real-time polymerase chain reaction (RT-PCR) (described in sections 2.10.2 and 2.12 respectively).

Due to observations from investigations into 50 nM and 500 nM (detailed below) a further dosing condition (100 nM) was investigated, primarily in CON myoblasts, and then this dose was taken forward to characterize the basal adaptation in cells that display prior reductions in regeneration/ageing phenotypes, the PD myoblasts. In brief, population doubled (PD) myoblasts have previously undergone 58 doublings and the process results in impaired regeneration (Sharples *et al*., 2011), where as CON myoblasts have undergone relatively few population doublings vs. the daughter population doubled cells (See section 2.4.2 for more

detail). Cell culture was performed as outlined in section 2.4.1 (same as the T_1 methodology) and myotube morphology (myotube number, nuclei per myotube, myotube diameter) was reported in this chapter (with transcriptional and signaling data reported in chapter 5 and 6). It should be noted that for 100 nM conditions different microscopes, and therefore microscope objectives were used for morphological images (detailed in 3.2.5 section). Therefore, absolute numbers for 100 nM dosing conditions were unable to be directly compared to 50 and 500 nM, however, we were able to be compare to the DM control ran in the same experiments.

3.2.2Cell Treatments

All treatments were administered in DM described above (detailed in section 2.7.6). The treatments comprised of a vehicle control (DMSO at a concentration of 0.01%), Testosterone doses (T) 50, 100 nM and 500 nM i.e. DM + T (outlined in section 2.7). DMSO was used as the solvent for T reconstitution at the same concentration as the vehicle (0.01%). For results and figure legends the following nomenclature will be used control (DM) (50 nM T, 100 nM T, 500 nM T. All treatments were added at 0 hrs and existing media was further supplemented at 72 hrs for T_1 and only at 72 hrs for T_2.

3.2.3 RNA Isolation

6 well plates for each time point (T_1: 0hrs, 72hrs, 7 days; T_2: 0hrs, 24hrs, 72hrs) were washed with 1 ml per well of Phosphate Buffer Saline (PBS) and extracted for RNA by placing 300 µl of TRIzol^{TM} Reagent (Sigma, St Louis) in each well. Total RNA was extracted as outlined in section 2.12.1. RNA concentration and purity were assessed through UV spectroscopy at ODs of 260 and 280 nM, using the Nanodrop spectrophotometer 3000 (outlined in section 2.11.2).

3.2.4 Real time, Reverse Transcriptase Polymerase Chain Reaction (rt-RT-PCR)

Seventy nanograms of RNA was taken from each sample and real time, reverse transcription polymerase chain reaction (RT-rt-PCR) was performed as detailed in section 2.12.3. Primer sequences for genes of interest are shown in **table 2.1** and were checked for specificity according to section 2.12.2. The relative mRNA expression of AR, IGF-I, myogenin and myostatin was quantified using the comparative Ct ($^{\Delta\Delta}$ct) Method against a reference gene of RP-IIb and calibrator of control treatment (after 72hrs exposure in both T_1 and T_2 (72hrs = 0hrs in T_2) experiments). Raw C_T for qPCR conducted in this chapter of work can be viewed in appendix 1 (**Table 9.1**). To note, for the T_2 experiment, gene expression was made relative to reference point of 0hrs (time of administration on pre-cultured myotubes) and thus value equals ~1 (not shown in figures for **Fig 3.6**).

3.2.5 Immunocytochemistry Analysis

For 50 and 500 nM doses, cells were fixed and immunocytochemistry was performed as described in section 2.10.2. Myotubes were stained for desmin (intermediate filament found in skeletal muscle near Z line of sarcomeres) and images captured on x40 oil magnification confocal microscopy. Quantification of morphology was performed as outlined in section 2.10.3. For 100 nM dosing, cells were fixed and immunocytochemistry was performed as outlined in section 2.10.2. Images were captured on x20 magnification fluorescence microscope (due to a laboratory move) and are presented in Chapter 5.

3.2.6 Statistical Analysis

Experiments were performed 3 x (n=3) in triplicate. Data are presented as Mean $\pm$ S.D unless stated otherwise. Shapiro-Wilk and Levenes tests were used to test for normal distribution and homogeneity of variation respectively. A two way mixed ANOVA was performed (for main effects and interactions for time, dose and cell type) with subsequent bonferonni post-hoc test to determine where significant differences lay. Subsequently, Gene expression data was assessed using a (2x4) mixed two-way factorial ANOVA for interactions between time

(72hrs and 7 days) and treatments (Control, 50 nM T, 500nM T and IGF-I). Morphology data was assessed using a one-way ANOVA for interactions between time (7 days) and treatments. For 100 nM dose experiment, Morphology was assessed using a two way mixed (2x2) ANOVA was performed in CON myoblasts for interactions between time (72hrs and 7 days) and treatments (DM and 100 nM T). In PD myoblasts, Independent T-tests were performed to compare treated vs. untreated cells in myotube morphology variables. A p-value of ≤ 0.05 was considered statistically significant. All statistical analyses were performed using SPSS version 19 and GraphPad Prism Software (detailed in section 2.14).

3.3 RESULTS

3.3.1 The effects of testosterone treatment on myotube morphology at different administration points

In the T_1 experiment, the administration of testosterone at 0hrs and 72hrs lead to both doses of testosterone significantly increasing myotube diameter (50 nM T 20.7 ± 5.9μm; 500 nM T 20.4 ± 4.9 μm ($P \leq 0.001$ respectively)) compared to control (17.5 ± 3.4 μm) treatment (**Fig 3.1A**) after 7 days exposure. Interestingly, there was no significant difference observed between the two testosterone doses for the increased myotube diameter. To note, in cover slips fixed at 72hrs there was no quantifiable myotubes present in any of the treatments for the T_1 experiment. No statistical differences were observed for mean number of nuclei per myotubes in any of the treatments (control 5.08 ± 1.89; 50 nM 5.66 ± 2.00; 500 nM 5.89 ± 2.08; P=N.S.). Testosterone induced (50 nM 3.53 ± 2.34; 500 nM 3.10 ± 1.24) increases in myotube number were not significantly different from the control treatment (2.89 ± 1.71), shown in **Fig 3.1B**.

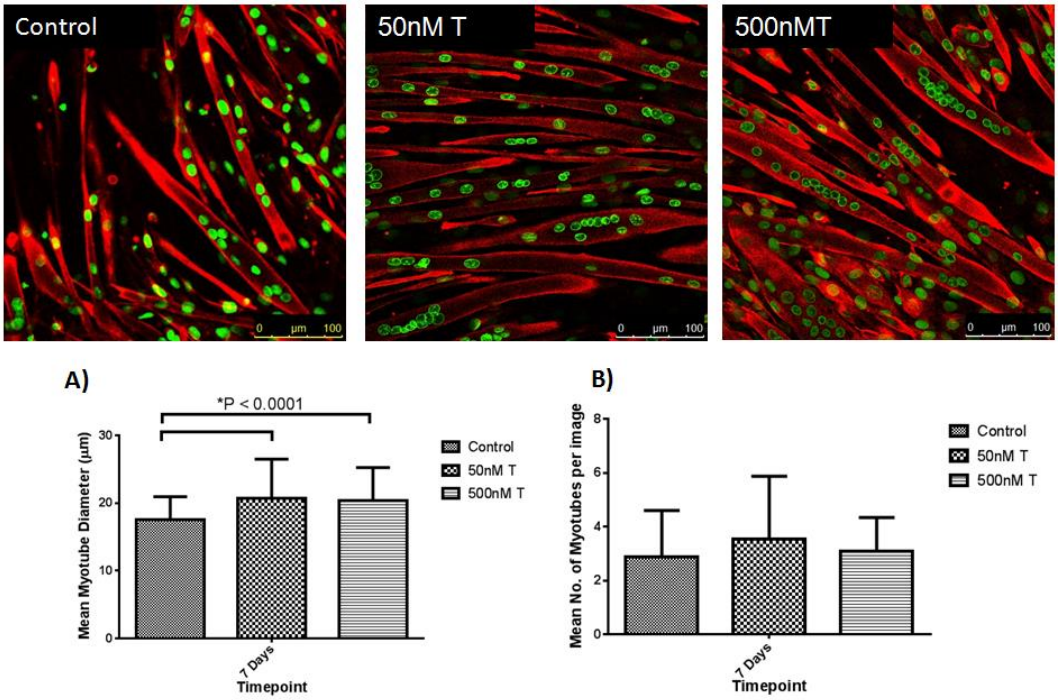

Fig 3.1 The effects of 50 and 500 nM testosterone doses on morphological parameters. Myotubes stained for desmin (red) and nuclei (green) in the T_1 experiment after 7 days culture. **A**) Doses of 50 and 500 nM testosterone significantly increased myotube diameter compared to control. **B**) Testosterone doses (50 and 500 nM) did not significantly increased the number of myotubes per image compared to control treatment (P=N.S).

However, when myotubes in the T_1 experiment were analysed for variation in number of nuclei per myotube (myonuclear accretion) and expressed as a percentage, both testosterone treatments (50 nM 62.0 ± 4.6%; 500 nM 59.8 ± 4.7%) had significantly increased the percentage of myotubes expressing 5+ nuclei (**Fig 3.2**) verses control (39.3 ± 4.8%). Whereas the control (60.7 ± 4.8%) treatment had a significantly higher percentage of myotubes with 3-4 nuclei incorporated ($P \leq 0.05$) (**Fig 3.2**) compared to 50 nM (38.0 ± 4.7%) and 500 nM (40.2 ± 4.7%) testosterone.

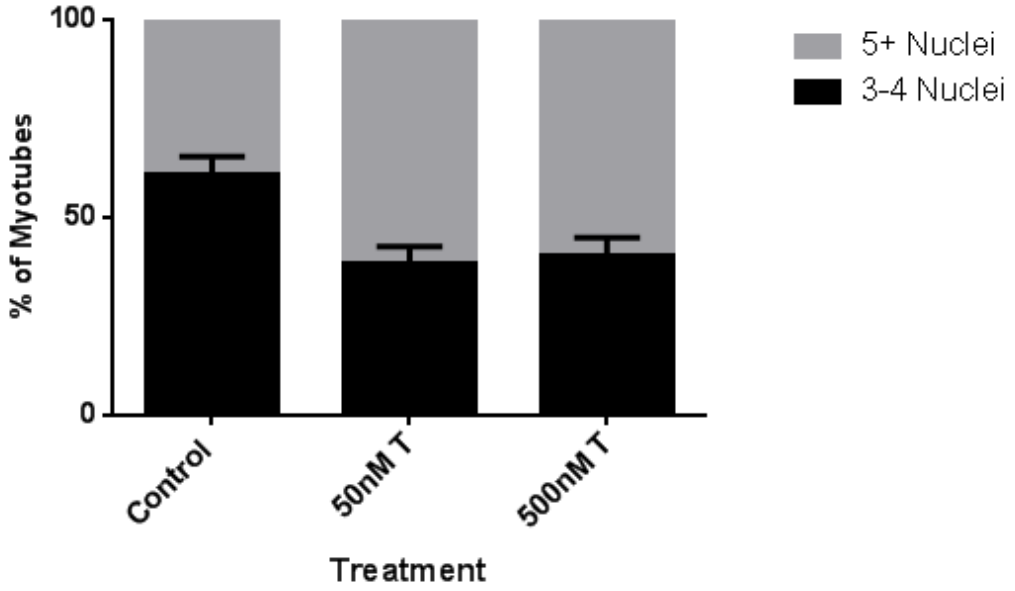

Fig 3.2 The effect of testosterone administration (T_1) after 7 days exposure on the incorporation of nuclei into myotubes. Testosterone doses significantly increased the percentage of myotubes expressing 5+ nuclei ($p \leq 0.05$). Data represented as Mean ± S.E.M.

In the T_2 experiment, increases in myotube size of pre-existing myotubes ($T_{2\,=}$ 72hrs in DM after transfer into low serum media) after 24hrs testosterone administration vs. the control treatment (50 nM 16.80 ± 2.22 μm; 500 nM 16.58 ± 2.17 μm vs. control 14.54 ± 1.64 μm; $P \leq 0.001$, **Fig. 3.3A**). Additionally, the testosterone-induced increases in myotube diameter were observed after 72 hrs exposure (50 nM 16.99 ± 3.00 μm; 500nM 16.54 ± 2.07 μm vs. control 14.87 ± 1.44 μm; $P \leq 0.001$, **Fig. 3.3A**), although there was no significant main effect for time (P= N.S). To note again, opposite to the original hypothesis, there was no difference observed between a low and high dose as testosterone doses resulted in similar increases in myotube diameter. In terms of mean nuclei per myotube, testosterone induced an increase in myonuclei compared to control treatment after 24 hours exposure (T_2) (50 nM 4.94 ± 1.32; 500 nM 4.32 ± 0.83 vs. control 3.76 ± 0.67; $P \leq 0.001$, **Fig. 3.3B**). As for myotube number, there were no alterations after 24hrs exposure, but 500 nM testosterone did increase moytube number after 72hrs exposure compared to the control treatment (500 nM T 2.82 ± 1.02 vs. control 2.00 ± 0.64; $P \leq 0.02$, **Fig 3.3C**).

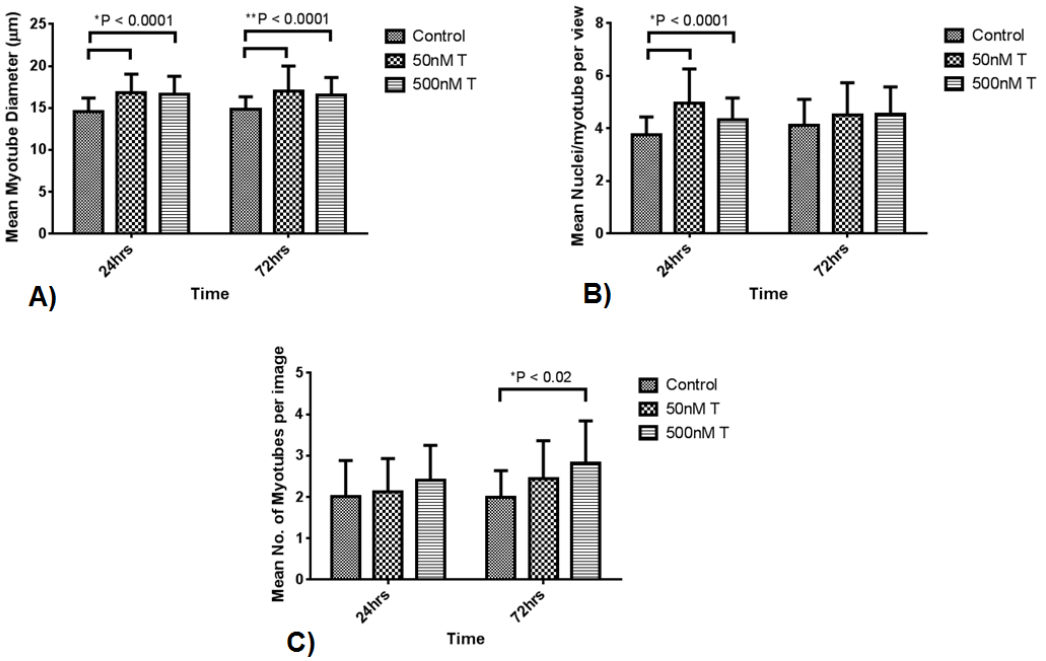

Fig 3.3 The effects of testosterone administered to pre-existing myotubes (T_2 experiment) on myotube morphology. **A**) A Significant increase in myotube diameter was observed with the administration of testosterone (50 and 500 nM) compared to the control treatment after 24 and 72hrs ($P \leq 0.0001$) **B**) At 24hrs, both testosterone doses increased the number of nuclei per myotube compared to the control treatment ($P \leq 0.0001$) **C**) There were no significant differences in myotube number after 24hrs exposure. 500 nM testosterone only increased myotube number compared to the control treatment after 72hrs ($P \leq 0.02$).

Interestingly and in comparison to the T_1 experiment, the addition of testosterone on to differentiated myoblasts (T_2) didn't lead to an increase in myonuclear accretion as the percentage of myotubes expressing 3-4 and 5+ nuclei was similar after 24 hrs and 72 hrs for all treatments (**Fig 3.4**).

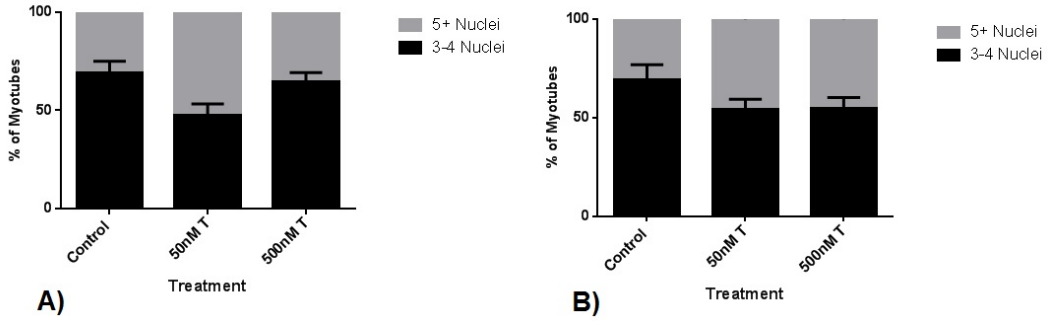

Fig 3.4 The addition of treatments to pre-existing myotubes for 24 hrs (**A**) and 72hrs (**B**) exposure (T_2 experiment) on myonuclear accretion. There were no significant differences in the alterations of myotubes expressing 3-4 nuclei vs. 5+ nuclei for all treatments at both time points.

3.3.2 The effect of Testosterone doses on gene mRNA expression levels at different administration time points.

In order to assess the effects of testosterone on differentiation, the steroid was added to confluent C2C12 cells after transfer to low serum media (T_1). After 72 hrs exposure, a significant increases in myogenin were observed in 50 and 500 nM testosterone treatments compared to control (50 nM 1.27 ± 0.36; 500 nM 1.16 ± 0.40 vs. control 0.97 ± 0.40; $P \leq 0.01$, **Fig 3.5A**). However, there was no statistical difference between the two T treatments suggesting no further increases in myogenin at the higher dose of 500 nM vs. 50 nM. No statistically significant changes occurred in myogenin mRNA levels after 7 days exposure in any of the treatments (P=N.S, **Fig 3.5A**), which is not surprising seen as myogenin is involved in myoblast fusion not maturation of existing myotubes.

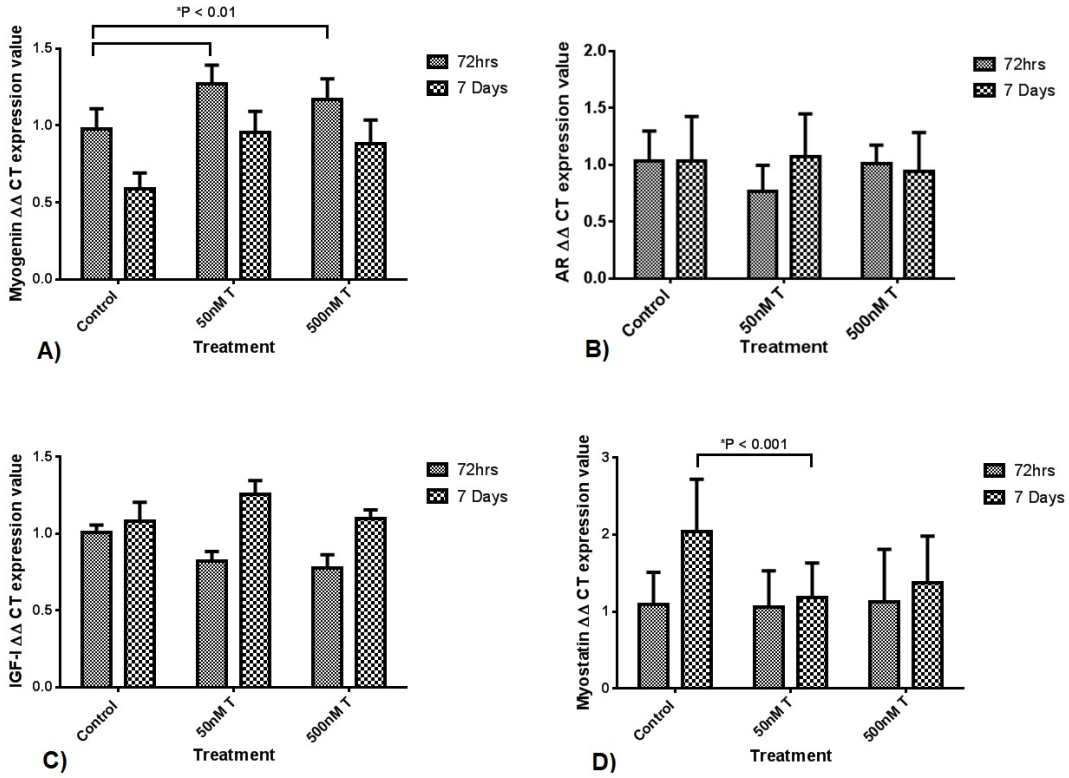

Fig 3.5 The effect of testosterone doses on selected gene transcripts in differentiating myoblasts (T_1 experiment). **A**) Both *50 and *500 nM testosterone increased myogenin expression after 72 hrs exposure compared to control treatment ($P \leq 0.01$). **B**) Exogenous $^{\lambda}$IGF-I significantly increased AR mRNA expression after 72 hrs ($P \leq 0.01$). Testosterone doses did not significantly alter AR expression levels at any time point. **C**) Testosterone doses also did not significantly alter IGF-I mRNA expression after 72 hrs and 7 days exposure. The addition of exogenous $^{\#}$IGF-I significantly down regulated IGF-I mRNA after 72 hrs exposure ($P \leq 0.01$) **D**) The 50 nM testosterone significantly down regulated myostatin expression after 7 days exposure compared to the control treatment (*$P \leq 0.001$).

After 7 days exposure, the largest increase in *Igf1* mRNA expression was observed in the 50 nM T condition, although no statistical differences were observed between treatments in IGF-I expression (P=N.S, **Fig 3.5C**). As for *AR* mRNA expression (**Fig 3.5B**), there were no significant changes between testosterone doses at either time points (P=N.S). In terms of myostatin mRNA expression, the 50 nM testosterone treatment significantly down regulated myostatin levels compared to the control treatment after 7 days exposure (50nM 1.18 ± 0.45 vs. control 2.04 ± 0.68; $P \leq 0.001$, **Fig 3.5D**)

In comparison to the T_1 observations, the administration of testosterone on pre-existing myotubes (T_2) resulted in slightly different results. Only the 50 nM dose of testosterone had an effect on *myogenin* mRNA expression (**Fig 3.6A**). After 24 hours exposure, myogenin expression remained significantly elevated compared to the control treatment (50 nM 0.90 ± 0.09 vs. control 0.67 ± 0.20; $P \leq 0.01$, **Fig 3.6A**). However, after 72 hrs exposure, there was a significant reduction in *myogenin* expression with 50nM testosterone compared to the control treatment (50nM 0.60 ± 0.19 vs. control 0.87 ± 0.12; $P \leq 0.01$, **Fig 3.6A**). In terms of the 500 nM dose, there were no significant alterations in *myogenin* expression at either time point (24 hrs control 0.67 ± 0.20 vs. 500 nM 0.80 ± 0.14; 72hrs control 0.87 ± 0.12 vs. 500 nM 0.75 ± 0.22; P=N.S. Fig 3.6A). Interestingly, there were no alterations in *AR* mRNA expression levels between treatments (**Fig 3.6B**). However, a main effect for time was observed, where a reduction in *AR* mRNA significantly decreased after 24 hrs to 72 hrs culture time ($P \leq 0.001$, **Fig 3.6B**).

For *Igf1* mRNA expression, 50 nM testosterone maintained levels after 24 hours exposure compared to the control treatment (50 nM 0.86 ± 0.17 vs. Control 0.62 ± 0.20; $P \leq 0.05$, **Fig 3.6C**). After 72 hrs exposure, 500 nM testosterone administration resulted in statistically significant reductions in *Igf1* mRNA expression (500 nM 0.98 ± 0.11 vs. control 1.29 ± 0.32; $P \leq 0.01$, **Fig 3.6C**). Finally, for *myostatin* mRNA expression, testosterone doses administered to pre-existing myotubes had no significant effect on reducing levels in comparison to the results observed in differentiating myoblasts in the T_1 experiment (P=N.S, **Fig 3.6D**).

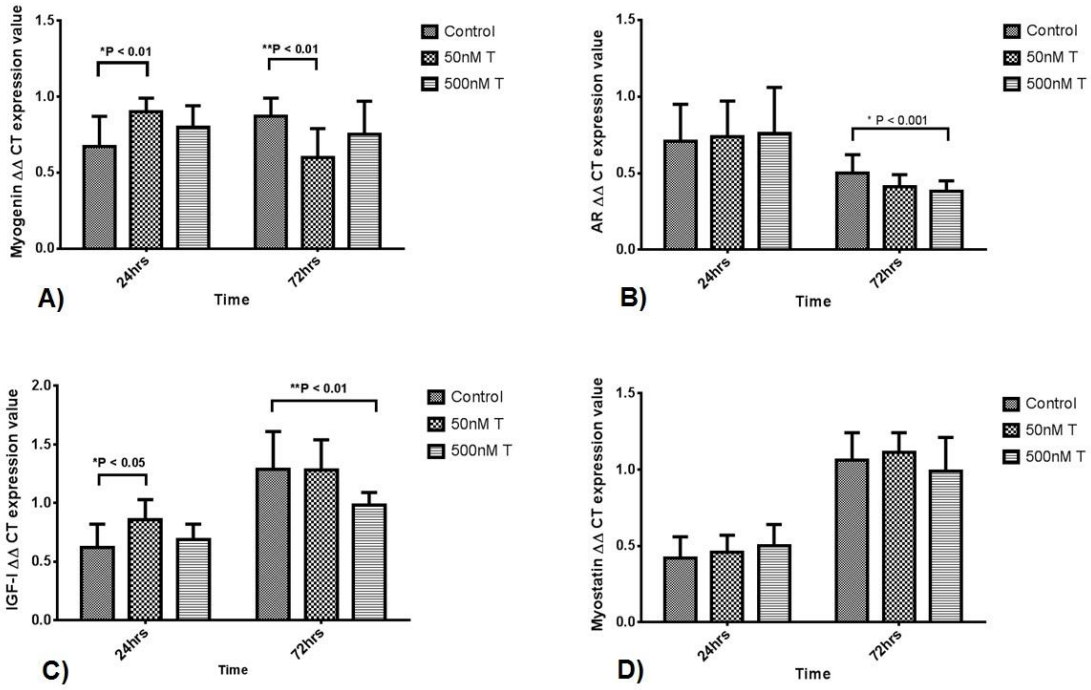

Fig 3.6 The effect of testosterone administration on mRNA expression levels in pre-existing myotubes (T_2). **A**) *50 nM testosterone significantly increased myogenin mRNA expression after 24hrs exposure ($P \leq 0.01$). However after 72 hrs exposure myogenin was significantly down regulated in the 50 nM testosterone treatment compared to other treatments (**$P \leq 0.01$). **B**) Treatments administered to pre-existing myotubes did not alter AR mRNA expression levels. However, with time, there was a significant decrease in AR mRNA in all treatments at 72 hrs compared to 24 hrs ($P \leq 0.001$). **C**) *50 nM testosterone statistically elevated IGF-I expression after 24 hrs exposure compared the control treatment ($P \leq 0.05$). There was a significant reduction observed with 500 nM after 72 hrs exposure (**$P \leq 0.01$). **D**) There were no alterations in myostatin expression levels after 24 and 72 hrs with any treatments administered (P=N.S).

3.3.3 The effect of a 100 nM dose in CON and PD myoblasts on myotube morphology

As there was little difference between the high and low dose testosterone with respect to a hypertrophic response an intermediary 100 nM dose was implemented (similar to T_1) firstly in the CON myoblasts as this dose has previously been extensively used in myoblast in vitro studies in the literature ((Basualto-Alarcón *et al*., 2013, Serra *et al*., 2011, White *et al*., 2012, Wu *et al*., 2010a), then subsequently in the PD myoblasts to characterise their response to testosterone administration. The 100 nM dose had a significant effect on myotube hypertrophy. After 7 days exposure, testosterone increased myotube number in

CON myoblasts (CON 3.27 ± 0.72 vs T 4.73 ± 0.87; P ≤ 0.0001, **Fig 3.7A**). In terms of myotube diameter, testosterone significantly increased size after 72 hrs (CON 16.18 ± 1.57 μm vs T 19.04 ± 2.07 μm; P ≤ 0.05, **Fig 3.7B**) and 7 days (CON 16.34 ± 1.11 μm vs T 19.54 ± 1.77 μm; P ≤ 0.05, **Fig 3.7B**) exposure. In CON myoblasts, increases nuclei number per myotube were observed after 72 hrs (CON 3.38 ± 0.50 vs. T 4.68 ± 0.92; P ≤ 0.05, **Fig 3.7C**) and 7 days (CON 4.93 ± 0.92 vs. T 6.80 ± 1.51; P ≤ 0.05, **Fig 3.7C**) exposure.

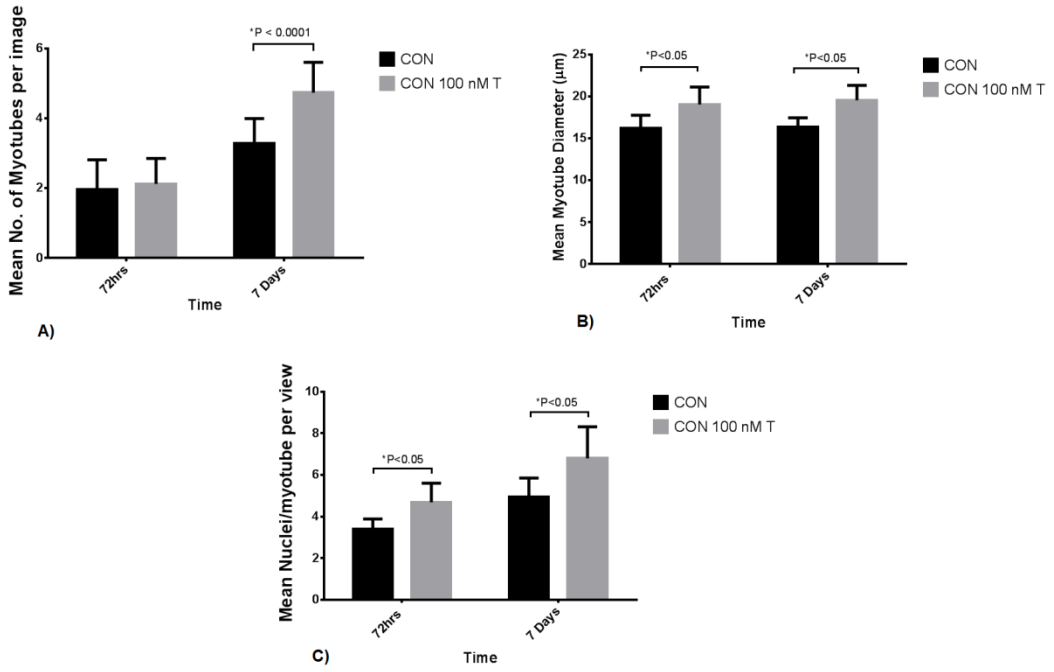

Fig 3.7 The effect of 100 nM T dose on myotube morphology in CON myoblasts. **A)** Testosterone significantly increased myotube number compared to basal conditions (*P ≤ 0.0001). **B)** Testosterone significantly increased myotube diameter in CON (*P ≤ 0.05) myoblasts after 72 hrs and 7 days compared to untreated cells. **C)** Testosterone increased nuclei per myotube after 72 hrs and 7 days culture (*P ≤ 0.05).

As the 100 nM dose elicited a positive hypertrophic response in CON myoblasts, it was carried forward and investigated in the PD myoblasts. The amount of myotubes present at 72 hrs was sparse and thus myotube number and nuclei number per myotube were not quantified after 72 hrs culture. There were no alterations in myotube number after 7 days testosterone treatment compared to basal conditions (PD vs. T; P=N.S, **Fig 3.8A**). Testosterone significantly increased myotube diameter after 72hrs (PD 13.40 ± 0.37 vs. T 17.57 ± 1.28; P ≤

0.05) and 7 days (PD 15.52 ± 1.89 vs. T 18.79 ± 2.10; P ≤ 0.05) exposure compared to untreated PD myoblasts (Fig 3.8B). Finally, testosterone increased the number nuclei per myotube in both CON and PD myoblasts. After 7 days exposure, 100 nM testosterone significantly increased nuclei per myotube compared to un-treated PD myoblasts (PD 4.14 ± 0.79 vs. T 6.58 ± 1.54; P ≤ 0.05, **Fig 3.8C**). Overall, the 100 nM T dose appear to have a positive hypertrophic response in both cell types.

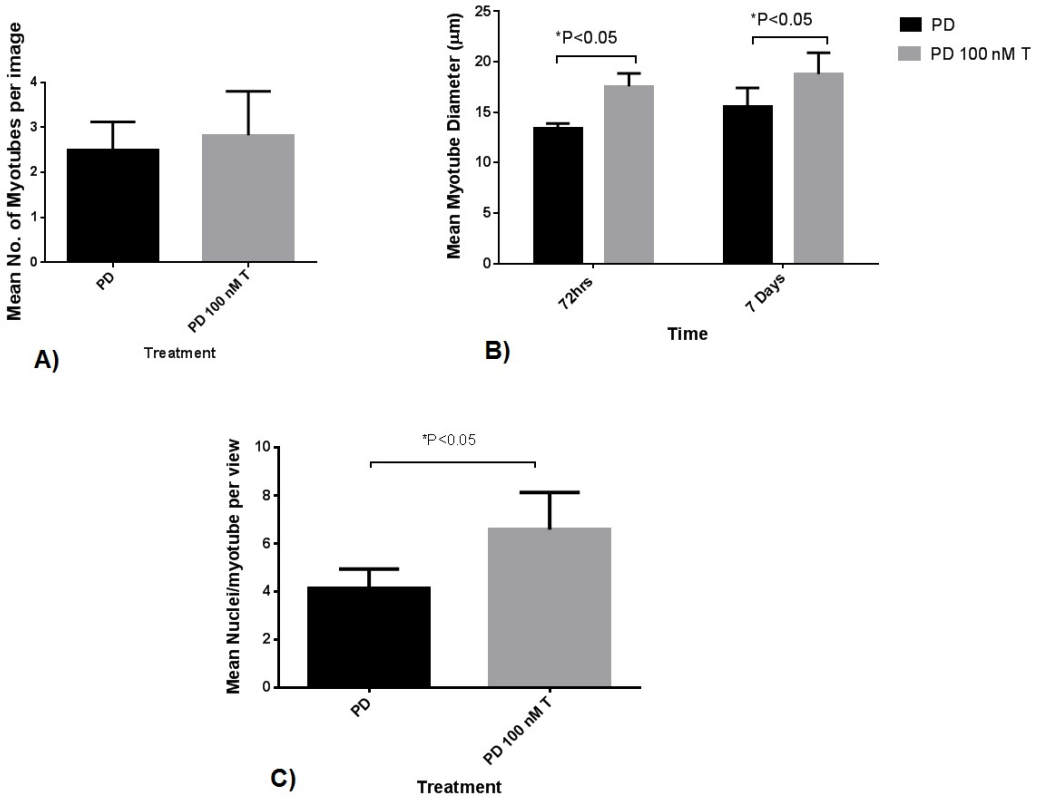

Fig 3.8 The effect of 100 nM testosterone dose on myotube morphology in PD myoblasts **A**) Testosterone had no significant impact on myotube morphology after 7 days culture (P=N.S) **B**) Increases in myotube diameter was observed in testosterone treated PD myoblasts after 72 hrs and 7 day culture compared to untreated cells (*P ≤ 0.05) **C**) Testosterone significantly increased the number of nuclei per myotube in PD myoblasts after 7 days treatment (*P ≤ 0.05).

3.4 DISCUSSION

3.4.1 Characterization of testosterone on myogenesis and hypertrophy

In the present study, the use of testosterone significantly enhanced myotube hypertrophy when administered to both differentiating and differentiated

myoblasts. These observations support *in-vitro* and *in-vivo* data which has repeatedly shown the hypertrophic effect of testosterone administration on skeletal muscle (Sculthorpe *et al*., 2012, Bhasin *et al*., 2001, Sinha-Hikim *et al*., 2002, Sinha-Hikim *et al*., 2006, Serra *et al*., 2011, Wannenes *et al*., 2008). The administration of testosterone to differentiating myoblasts increased myonuclear accretion (myotubes expressing 5+ nuclei) in the T_1 experiment only, highlighting the steroids role in differentiation (cell fusion) and contribution towards myotube hypertrophy. In the T_1 experiment, the significant increase in myogenin (promotes differentiation/cell fusion) expression with testosterone at 72hrs provides evidence towards confirmation of testosterone's role in enhancing muscle differentiation and myonuclear accretion, resulting in enhance myotube hypertrophy. Further, this pattern of heightened myogenin expression was observed in the T_2 experiment after 24 hrs exposure of testosterone. These observations are supported by earlier studies in C_2C_{12} muscle cells, although their focus was on the androgen receptor itself, instead the role of a testosterone stimulus (Lee, 2002, Wannenes *et al*., 2008).

Contrasting to previous studies, testosterone administration did not significantly increase endogenously expressed IGFI mRNA when exposed to differentiating myoblasts (Sculthorpe *et al*., 2012). In the T_2 experiment, 50 nM testosterone maintained local IGFI expression after 24 hrs exposure, a factor which might help explain the enhanced myotube hypertrophy, without increased myonuclear accretion, as T has been observed to enhance muscle protein synthesis (Brodsky *et al*., 1996, Ferrando *et al*., 2002, Urban *et al*., 1995). Another possibility where testosterone may interact with the IGF-I/Pi3K/Akt pathway is through myostatin, as decreases were observed with 50 nM testosterone in the T_1 experiment after 7 days exposure. In vitro myostatin has been observed to inhibit IGF-I induced myotube hypertrophy through Akt (myostatin inhibited Akt phosphorylation). Plus myostatin appears to reduce Akt/TORC1/p70S6K signaling, myoblast differentiation and myotube size (Morissette *et al*., 2009, Trendelenburg *et al*., 2009). Thus the reductions in myostatin mRNA expression under a testosterone stimulus may have contributed to the enhanced myotube size

observed.(Léger *et al*., 2008)(Aversa *et al*., 2012)(Atkinson *et al*., 2010, Bhasin *et al*., 2005, Dillon *et al*., 2012)

3.4.2 The effect of low and high doses towards testosterone-induced hypertrophy

Interestingly, there was no difference between high and low dose responses in mRNA expression changes and morphological parameters between testosterone treatments. A low level of AR in C_2C_{12} cells has previously been reported (Altuwaijri *et al*. 2004) and thus no dose response may likely be due to androgen receptor saturation. Within the C_2C_{12} cell line, previous literature has reported low endogenous levels of AR expression (Altuwaijri *et al*., 2004). To overcome this factor, the AR has been over expressed (transfection) to address the action of testosterone (Altuwaijri *et al*., 2004, Lee, 2002, Sheppard *et al*., 2011) due to these potential low levels. Recently Sheppard *et al*. (2011) illustrated the variability in AR level in C_2C_{12} cells with a low expression in single myoblasts cells and heightened expression in formed myotubes, where the expression decreased with time (myotube maturation).

Indeed, the T_2 experiment provides evidence towards a decrease in *AR* expression, as the mRNA level significantly reduced with myotube maturation (independent of treatment condition between 24 hrs to 72 hrs). Wannenes *et al*and Colleagues (2008) exposed wild type C_2C_{12} cells (no AR transfection performd) to low doses of T (1-10 nM) for 0,2,4 days and observed a dose-response in the activation of *AR* mRNA expression plus the translocation of AR from the cytoplasm to the nucleus, while investigating T's role in muscle differentiation. Thus the differing results between the current study and Wannenes *et al* (2008), maybe due to the different dose exposures, the length of exposure time and possibly the variability in *AR* expression levels. Overall, these two experiments (T_1 and T_2) and the 100 nM dose in CON and PD myoblasts, provide an indication for a suitable dose to be used in subsequent experiments as in-vitro testosterone administrations have ranged from low dose (1-100 nM) (Basualto-Alarcón *et al*., 2013, Wannenes *et al*., 2008, Wu *et al*., 2010a) to high dose (400-500 nM) (Sculthorpe *et al*., 2012, Serra *et al*., 2011).

3.4.3 Chapter Summary

In summary, this chapter of work has characterized the cellular and transcriptional effects of testosterone-induced hypertrophy in skeletal muscle C_2C_{12} myoblasts and myotubes. Furthermore, a temporal response has been observed by administrating testosterone on to differentiating myoblasts vs. pre-existing myotubes. Testosterone induced hypertrophic alterations in myotube morphological characteristics such as diameter and myonuclear accretion. These alterations were accompanied by the up regulation of *myogenin*, *Igf1* mRNA and the down regulation of *myostatin* mRNA expression levels, although these changes were dependant on the point of testosterone administration. Commonly, increases in muscle mass and myotube size with testosterone administration are observed with a dose response effect. However within this cell type, there was no difference between the 50 and 500 nM testosterone, a factor potentially explained by previously reported low levels of androgen receptor expression. Due to this observation, a 100 nM dose was administered to the CON myoblasts and carried forward into PD myoblasts to characterize this dose in cells that display impaired regeneration. A hypertrophic response (myotube number and diameter) was observed in both cell types with the 100 nM dose. Overall, this chapter provides evidence of the cellular and molecular targets involved in testosterone-induced hypertrophy, indicating a suitable dose for use in subsequent experiments, as well as targets which may mediate this action.

3.4.4 Linking Summary

In order to investigate the role of direct AR *verses* indirect IGF-I signaling, a dose response of AR inhibitors and IGF-IR inhibitor was needed to be established. Although an increase in local IGF-I expression did not occur compared to previous literature (Sculthorpe *et al*., 2012, Serra *et al*., 2011), a mean increase with testosterone administration was observed. Furthermore, the decrease in myostatin levels with testosterone administration in the current chapter, and potential activation of downstream IGF-I signalling (i.e. via Akt), make it pertinent to investigate if IGF-I signalling as such signalling may still be involved in mediating testosterone-induced muscle hypertrophy.

4. THE CHARACTERIZATION OF INHIBITOR DOSES FOR THE ANDROGEN RECEPTOR AND IGF-I RECEPTOR

4.1 INTRODUCTION

There are two potential pathways which may mediate the action of testosterone induced skeletal muscle hypertrophy; binding to the androgen receptor (direct) and the IGF-I/Akt/mTOR/p70s6k pathway (indirect). In vivo, androgen receptor expression has been investigated in numerous studies implementing resistance exercise to mechanically overload skeletal muscle (Spiering *et al*., 2009, Ratamess *et al*., 2005, Vingren *et al*., 2009, Hulmi *et al*., 2008). Resistance exercise elicits an increase in circulating levels of anabolic hormones such as IGF-I and testosterone, which may contribute to muscle hypertrophy (Borst *et al*., 2001, Kraemer and Ratamess, 2005, Spiering *et al*., 2009). Although the recent evidence casts doubt on the importance of post-exercise circulating in muscle hypertrophy (West *et al*., 2009, West *et al*., 2010, Wilkinson *et al*., 2006), yet increases in androgen receptor protein content have been correlated with muscle hypertrophy, specifically mean fibre cross-sectional area (Mitchell *et al*., 2013). In comparison, IGF-I has been extensively shown to stimulate muscle protein synthesis and enhance muscle hypertrophy (Rommel *et al*., 2001, Sacheck *et al*., 2004, Kalista *et al*., 2011). Although it may still be under debate as to whether IGF-I receptor is/is not required for load induced hypertrophy ((Spangenburg *et al*., 2008), it does, however, appear critical in skeletal muscle development (Fernández *et al*., 2002, Philippou *et al*., 2007) satellite cell activation and differentiation (Crown *et al*., 2000, Heron-Milhavet *et al*., 2010, Lawlor *et al*., 2000, Sharples *et al*., 2010).

4.1.1 The role of the androgen receptor in skeletal muscle differentiation and hypertrophy

Testosterone is a ligand of the androgen receptor and thus binds to the receptor to form a complex which binds promoter or androgen response elements (ARE) of target genes to regulate their transcription (Chen *et al*., 2005). The classical view is that un-ligand bound receptor resides in the cytoplasm, once bound it translocates to the nucleus (Bennett *et al*., 2010). Most recently in C212

muscle cells, the AR has been observed to be sub-localized in the mitochondria and microsomal (Pronsato *et al*., 2013). The satellite cell is the predominant location for AR expression and thus the AR may contribute to muscle hypertrophy via differentiation and/or proliferation of these cells (Doumit *et al*., 1996, Lee, 2002, Wannenes *et al*., 2008, Sinha-Hikim *et al*., 2004). The AR and IGF-I both have androgen response element present upon their promoter regions (Grad *et al*., 1999, Wu *et al*., 2007). Interestingly, myogenin does not have an response element present but has been observed to have increased expression following testosterone-administration and subsequent binding to the AR (Lee, 2002). This factor is highlighted in a study by Lee (2002), where AR transfection into C_2C_{12} muscle cells, lead to enhance muscle differentiation under a testosterone stimulus.

The effects on skeletal muscle by inhibiting the AR have been investigated in vitro using chemical inhibitors (flutamide & bicalutamide) (Sculthorpe *et al*., 2012, Wannenes *et al*., 2008, Basualto-Alarcón *et al*., 2013) and animal knockout models (MacLean *et al*., 2008, Ophoff *et al*., 2009). Animal knockout models illustrate the importance of the androgen receptor in skeletal muscle development as these models exhibit decreases in muscle mass and impairment i.e. reduced muscle force production (Chambon *et al*., 2010, MacLean *et al*., 2008, Ophoff *et al*., 2009). The uses of flutamide and bicalutamide in vitro cell culture are designed as substrate competitors (AR antagonists) and thus compete with Testosterone for binding to the androgen receptor (Bennett *et al*., 2010, Singh *et al*., 2003). Indeed the co-incubation of testosterone and an AR antagonist in vitro leads to reduced muscle differentiation and hypertrophy (Basualto-Alarcón *et al*., 2013, Sculthorpe *et al*., 2012, Wannenes *et al*., 2008).

4.1.2 The role of the IGF-I receptor and downstream signaling in skeletal muscle.

The binding of IGF-I to its receptor, activates a cascade of signalling, initiated with the activation of Pi3K. The release of a phosphate group by Pi3K allows for the phosphorylation and activation of Akt. Once at this step in the pathway, Akt mediates the phosphorylation of mTOR. The activation of mTOR promotes protein synthesis via the phosphorylation of p70S6k and S6K targets (Yin *et al*.,

2009). The activation of this signaling cascade leads to increased muscle protein synthesis and subsequently muscle/myotube hypertrophy (Bodine *et al*., 2001, Rommel *et al*., 2001). Similar to the AR, the inhibition of IGF-IR has been performed using substrate competitors (Picropodophyllin) (Girnita *et al*., 2004, Duan *et al*., 2009), small interference RNA and animal knockout models (Deldicque *et al*., 2007, Galluzzo *et al*., 2009, Heron-Milhavet *et al*., 2010, Liu *et al*., 1993, Serra *et al*., 2011, Spangenburg *et al*., 2008). IGF-I stimulates both proliferation and differentiation via the IGF-I receptor and mice lacking the IGF-I receptor have diminished muscle size (Clemmons, 2009, Liu *et al*., 1993).

4.1.3 Aims and Objectives

Therefore in light of the literature discussed above, the aims of this chapter were to characterize doses for inhibitors of the AR (20 and 40 μM) and IGF-IR (30, 90 and 150 nM) in C_2C_{12} skeletal muscle myoblasts, specifically utilizing the population doubling (PD) model (Sharples *et al*., 2011). The investigation of all the inhibitor doses will allow for the determination of an effective dose to be identified for use in a subsequent chapter (5). Thus morphological (myotube diameter and number) and transcriptional (myogenin, AR and IGF-I) and biochemical (Akt and ERK1/2) alterations to these doses were measured. It was hypothesized that a detrimental dose response effect would be observed towards cellular and molecular signalling involved in myotube differentiation and hypertrophy.

4.2 METHODOLOGY

4.2.1 Cell Culture

Mouse C_2C_{12} skeletal muscle myoblasts (CON and PD; outlined in 2.4.2) were resurrected as described in 2.6 and cultured as outlined in 2.4.1. Cells were cultured as detailed in section 2.4 and chapter 3. Cells at the time points of 0, 72 hrs and 7 days were fixed for histology, isolated for RNA (outlined in 2.12.2 and 2.12) for rt-PCR and lysed for protein analysis (western blots, as outlined in 2.9). For the IGF-I receptor stimulation experiment, cells were stimulated for 15

minutes in treatments detailed below (4.2.2) and then lysed for protein analysis (detailed in 2.9).

4.2.2Cell Treatments

All treatments were administered in DM described above (detailed in 2.7.6). The treatments comprised of a vehicle control (DMSO at a concentration of 0.01%), Flutamide doses (F) 20 and 40 μM, Picropodophyllin (PPP) 30, 90 and 150 nM i.e. DM + PPP and DM + F. For the IGF-I receptor stimulation study to address downstream signalling of the receptor, exogenous IGF-I (10 $ng.ml^{-1}$) and PPP were incubated alone and together i.e. DM + IGF-I and DM + PPP (outlined in section 2.7). The IGF-I stimulation was conducted to address whether PPP was still effective in the presence of exogenous IGF-I. The exogenous IGF-I dose was selected based on previously published work (Saini *et al*., 2008). DMSO was used as the solvent for flutamide and picropodophyllin reconstitution at the same concentration as the vehicle (0.01%). For results and figure legends the following nomenclature will be used Control, F, PPP and IGF-I respectively. All treatments were added at 0 hrs and existing media was further supplemented at 72 hrs for flutamide and Picropodophyllin experiments.

4.2.3 RNA Isolation

6 well plates for each time point (0hrs, 72 hrs and 7 days) were washed with 1 ml per well of Phosphate Buffer Saline (PBS) and extracted for RNA by placing 300 μl of TRIzol™ Reagent (Sigma, St Louis) in each well. Total RNA was extracted as outlined in section 2.12.1. RNA concentration and purity were assessed through UV spectroscopy at ODs of 260 and 280 nM, using the Nanodrop spectrophotometer 3000 (outlined in 2.11.2).

4.2.4 Real time, Reverse Transcriptase Polymerase Chain Reaction (rt-RT-PCR)

Seventy nanograms of RNA were taken from each sample and real time, reverse transcription polymerase chain reaction (RT-rt-PCR) was performed as detailed in section 2.12.3. Primer sequences for genes of interest are shown in

table 2.1 and were checked for specificity according to 2.12.2. The relative mRNA expression of AR, IGF-I, myogenin was quantified using the comparative Ct ($^{\Delta\Delta}$ct) Method against a reference gene of RP-IIb and calibrator of Control treatment (after 0hrs in all experiments). Raw C_T for real time qPCR conducted in this chapter of work can be viewed in appendix 2 (**Table 9.2**).

4.2.5 Immunoblotting

Samples were prepared as outlined in 2.13.2. Gels were made up of a 10% resolving gel and a 5% stacking gel. Samples were electrophoresed at 200 volts until the sample buffer tracking dye reached the bottom of the gel (detailed in2.13.4). The proteins were transferred to the nitrocellulose membrane for use in Immunoblotting for 30 minutes (described in 2.13.5). The western blotting was performed based on manufacturer's instructions (described in 2.13.7). Membranes were sealed in plastic bags containing primary antibodies for Akt (total and phosphorylation (Ser473)), ERK ½ (total and phosphorylation (Thr202/Tyr204)) at a concentration of 1:1000, and GAPDH (loading control; 1:4000) in an antibody diluent liquid for 1 hour incubation at room temperature. Detection of proteins was achieved using enhanced chemiluminescence (ECL) with a West Pico Supersignal kit as described in 2.13.8.

4.2.6 Microscope Analysis

Cells were fixed using the protocol detailed in 2.10.2. PBS (2ml/well) was added after removal of the methanol/acetone mix and plates were stored in 4^{o}c until further analysis. Quantification of myotube diameter and myotube number was captured using an x10 light microscope (Inverso-TC, CETI, Medline Scientific Limited, Oxon, UK). In total 30 fields per condition for each time point were acquired and analyzed using image J (Java) software (National Institutes of Health, USA) as detailed in section 2.10.3.

4.2.6 Statistical Analysis

Experiments were performed in triplicate, with 3 separate repeats (n=3). Data are presented as Mean $\pm$ S.D unless stated otherwise. Gene expression data was assessed using a mixed three-way factorial ANOVA for interactions between time

(72 hrs and 7 days), treatments (DM, 40μM F; DM, 150nM PPP) and cell types (CON and PD). Morphology data was assessed using an ANOVA for interactions between time (72 hrs and 7 days), treatments and cell types. If significant interactions were present, independent t-tests were conducted to confirm statistical significance between variables of interest. For the IGF-I stimulation experiment, a one way ANOVA was performed for western blots analyses. A p-value of <0.05 was considered statistically significant. All statistical analyses were performed using SPSS version 19 and GraphPad Prism Software (detailed in 2.14).

4.3 RESULTS

4.3.1 The impact of flutamide doses on myotube morphology

There was a significant difference between the CON and PD cell types for myotube diameter and number after 7 days culture (**Fig 4.1**). After 72hrs, there were no visible myotubes observed in the PD myoblasts for all treatments highlighting basally impaired regeneration as previously described by Sharples *et al*., 2011; 2012. The CON myoblasts resulted in a significantly greater number of myotubes (CON 4.29 ± 0.77 vs. PD 2.29 ± 0.61, $P \leq 0.001$) and increased myotube size (CON 16.69 ± 1.09 μm vs. PD 12.94 ± 1.04 μm, $P \leq 0.001$) verses PD myoblasts (**Fig 4.2**) after 7 days.

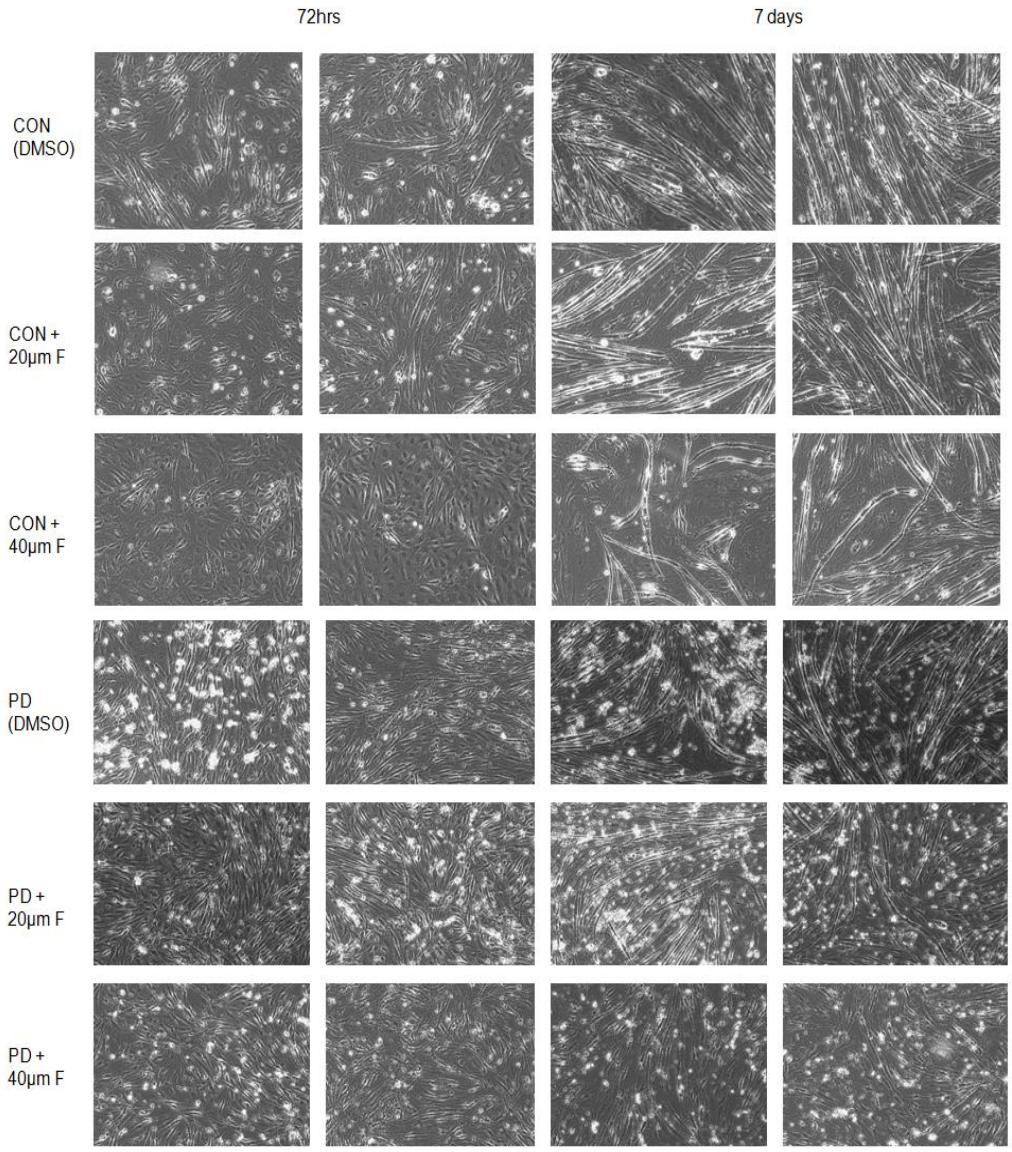

Fig 4.1 Light microscope images (10x magnification) of CON and PD myoblasts administered 20 and 40 µM doses for 72 hrs and 7 days. The administration of both flutamide doses resulted in decreases in differentiation (72hrs) and hypertrophy (7 days) in CON and PD myoblasts.

There was a detrimental impact on myotube morphology in a dose response manner in the presence of flutamide (**Fig 4.1**) in both cell types. In CON myoblasts, there was a significant reduction in myotube number (CON DM 2.46 ± 0.66 vs. 40 µM F 1.22 ± 0.44; $P \leq 0.01$, **Fig 4.2A**) and diameter (CON DM 15.20 ± 0.85 µm vs. 40 µM F 12.67 ± 1.27 µm; $P \leq 0.01$, **Fig 4.2B**) with the highest flutamide dose after 72hrs exposure. After 7 days exposure, the reduction in myotube number (CON DM 4.29 ± 0.77 vs. 40 µM F 1.93 ± 0.59; $P \leq 0.01$) and diameter (CON DM 16.69 ± 1.09 µm vs. 40 µM F 14.78 ± 1.12µm; $P \leq 0.01$) with

40 μM flutamide was still observed (**Fig 4.2**). In PD myoblasts, a similar trend was observed after 7 days exposure as 40 μM flutamide was detrimental to the myotube formation and hypertrophy with no measurable myotubes being observed vs. DM conditions and 20 μM flutamide that did have measurable myotubes (7 days myotube diameter: PD 12.94 ± 1.04 vs 20 μM F 10.89 ± 1.64; **Fig 4.2B**). Overall in terms of PD myoblasts, there was a ~45% decrease in myotube number and ~16% in diameter with the presence of 20 μM flutamide alone. Subsequently the 40 μM dose was carried forward for *AR* gene expression and total AR protein analyses.

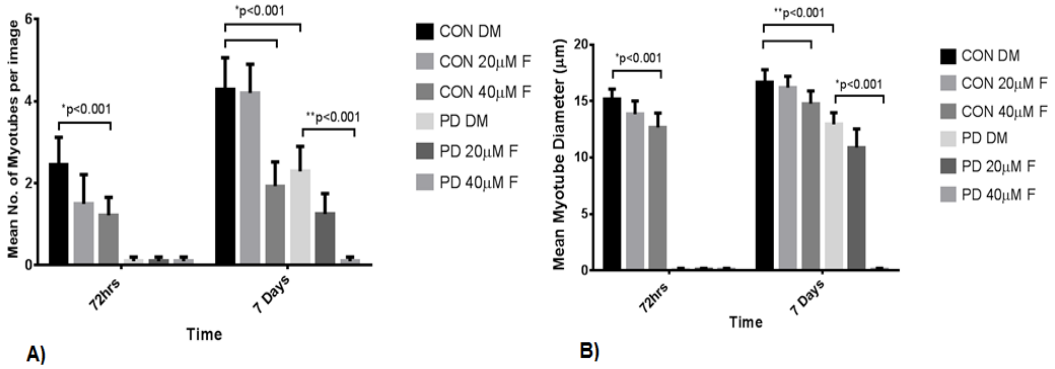

Fig 4.2. The quantification of myotube morphology with flutamide administration in CON and PD myoblasts after 72 hrs and 7 days exposure. **A)** The administration of flutamide had a detrimental effect on myotube number after 72 hrs and 7 days in CON cells (*P ≤ 0.001). In the PD cells, flutamide was detrimental to myotube formation with 40 μM inhibiting myotube formation after 7 days exposure **B)** Myotube diameter was significantly reduced at 72hrs (*P ≤ 0.001) and 7days (**P ≤ 0.001) with flutamide administration in CON cells. In PD cells, the addition of 40 μM flutamide resulted in no myotubes being formed after 7 days exposure. Furthermore, at 7 days there was a significant difference in basal CON and PD mean myotube diameter (**P ≤ 0.001).

4.3.2 Androgen receptor protein and related gene transcript alterations with flutamide administration

In basal conditions between CON and PD cells, myogenin mRNA expression was significantly down-regulated in PD cells after 72 hrs (CON DM 28.94 ± 3.28 vs. PD DM 8.12 ± 1.33; P ≤ 0.05, **Fig 4.3A**) and 7 days (CON DM 29.37 ± 3.04 vs. PD DM 17.78 ± 1.78; P ≤ 0.05, **Fig 4.3A**). Similarly IGF-I mRNA expression was down-regulated in PD cells compared to CON basal conditions after 72 hrs

(CON DM 3.14 ± 0.68 vs. PD DM 0.62 ± 0.27; P ≤ 0.05, **Fig 4.3B**) and 7 days (CON DM 7.10 ± 3.10 vs. PD DM 3.94 ± 1.61; P ≤ 0.05, **Fig 4.3B**). Finally, androgen receptor mRNA expression exhibited the same pattern of down-regulation after 72 hrs (CON DM 1.51 ± 0.76 vs. PD DM 0.64 ± 0.12; P ≤ 0.05, **Fig 4.3C**) and 7 days (CON DM 1.39 ± 0.38 vs. PD DM 0.81 ± 0.39; P ≤ 0.05, **Fig 4.3C**) between PD and CON myoblasts. The *AR* mRNA observations highlight that in basal conditions, PD myoblasts have a lower expression of *AR* initially compared to CON myoblasts.

The administration of the 40 μM flutamide dose significantly reduced *myogenin* expression in both CON and PD cells after 72 hrs (CON DM 28.94 ± 3.28 vs. 40μM F 19.44 ± 1.99; PD DM 8.12 ± 1.33 vs. 40 μM F 1.17 ± 0.52; P ≤ 0.05, **Fig 4.3A**) and 7 days (CON DM 29.37 ± 3.04 vs. 40 μM F 18.22 ± 6.12; PD DM 17.78 ± 1.78 vs. 40 μM F 0.39 ± 0.18; P ≤ 0.05, **Fig 4.3A**). In comparison, *Igf1* mRNA expression with only significantly reduced in PD cells after 7 days exposure (PD DM 3.94 ± 1.61 vs. 40μM F 0.74 ± 0.26; P ≤ 0.05, **Fig 4.3B**). There were no significant alterations in *AR* mRNA expression in the presence of flutamide at either time points in CON and PD myoblasts (P=N.S, **Fig 4.3C**). However, there was a reduction in total androgen receptor protein with flutamide in both cell type at72 hrs and 7 days (**Fig 4.3D**).

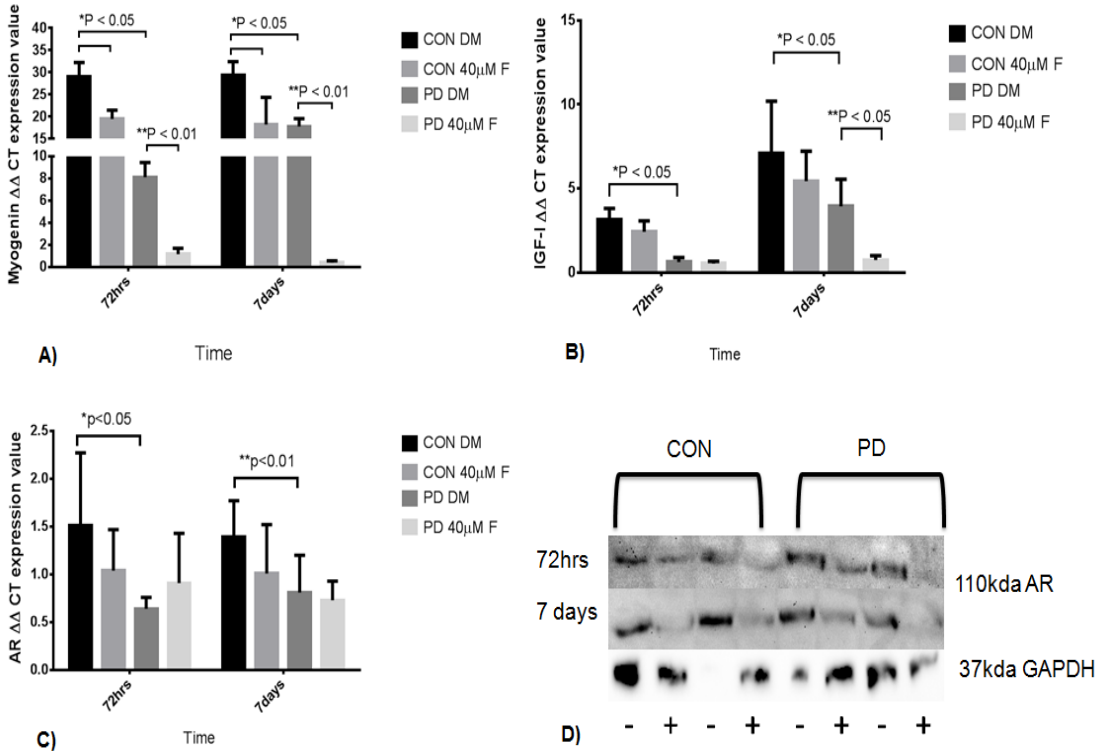

Fig 4.3. The effects of flutamide administration on specific gene transcripts and total androgen receptor protein levels after 72 hrs and 7 days exposure. **A)** Myogenin mRNA expression was significantly down regulated in PD cells after 72 hrs and 7days compared to basal CON cells (*P < 0.05). The addition of flutamide significantly decreased myogenin levels in both CON (*P < 0.05) and PD (**P < 0.01) cells at both time points. **B)** IGF-I expression was significantly lower in basal PD cells compared to CON cells at both time points (*P < 0.05). Flutamide significantly reduced IGF-I expression in the PD cells after 7 days exposure (**P < 0.05). **C)** There was a significant decrease between CON and PD myoblast basal AR levels after 72hrs (*P < 0.05) and 7 days (**P < 0.01) culture. **D)** Interestingly, flutamide appeared to reduce total AR protein levels in both cell types for both time points (Flutamide +; DM -). Images are representative blots (n=3).

4.3.3 Alterations in myotube morphology with the addition of Picropodophyllin

The IGF-I receptor inhibitor (PPP) was administered to both CON and PD myoblasts for 72 hrs and 7 days. With increasing doses, there appeared to be a detrimental effect on myotube morphology in both cell types (**Fig 4.4**). At 72 hrs, similar to the flutamide experiment, there were no quantifiable myotubes present in the PD cell type. The following absolute data is different as different samples were generated for the PPP dose experiment. There were significant differences between basal CON and PD myoblasts for myotube number (CON DM 4.18 ±

0.61 vs. PD DM 2.54 ± 0.66; P ≤ 0.01, **Fig. 4.5A**) and diameter (CON DM 16.06 ± 0.65μm vs. PD DM 13.24 ± 0.59μm; P ≤ 0.01, **Fig. 4.5A**) after 7 days culture.

There was a significant detrimental effect with increasing doses of PPP on CON myoblasts after 72 hrs (CON DM 2.30± 0.73 vs. 30 nM 1.92 ± 0.67; 90 nM 1.38 ± 0.51; 150 nM 1.33 ± 0.49; P ≤ 0.01, **Fig. 4.5A**) and 7 days (CON DM vs. 30 nM 3.32 ± 0.61; 90 nM 3.21 ± 0.57; 150 nM 2.46 ± 0.58; P ≤ 0.01, **Fig. 4.5A**) in mean myotube number. The same pattern was evident in the PD myoblasts after 7 days culture (PD DM 2.54 ± 0.66 vs. 30 nM 1.68 ± 0.65; 90 nM 1.59 ± 0.59; 150 nM 1.50 ± 0.58; P ≤ 0.01, **Fig. 4.5A**). In terms of myotube diameter, the increasing doses reduced the diameter in CON myoblasts after 72 hrs (CON DM 15.11 ± 0.81 vs. 30 nM 14.09 ± 1.02; 90 nM 13.77 ± 1.34; 150 nM 13.37 ± 0.62; P ≤ 0.01, **Fig. 4.5B**) and at 7 days (CON DM 16.06 ± 0.65 vs. 30 nM 15.32 ± 0.73; 90 nM 15.38 ± 0.71; 150 nM 15.17 ± 0.65; P ≤ 0.01, **Fig. 4.5B**). In the PD cell type, myotube diameter was also significantly reduced with increasing PPP dose at 7 days (PD DM 13.24 ± 0.59 vs. 30 nM 12.92 ± 1.11; 90 nM 12.81 ± 0.59; 150 nM 11.54 ± 1.08; P ≤ 0.01, **Fig. 4.5B**). The alterations in myotube morphology provides evidence towards the PPP inhibiting the IGF-I receptor, highlighted by the reduction in muscle differentiation (myotube number ~41% decrease) and hypertrophy (myotube diameter ~7% reduction). Subsequently, IGF-I signalling and gene transcripts involved in muscle differentiation are investigated below.

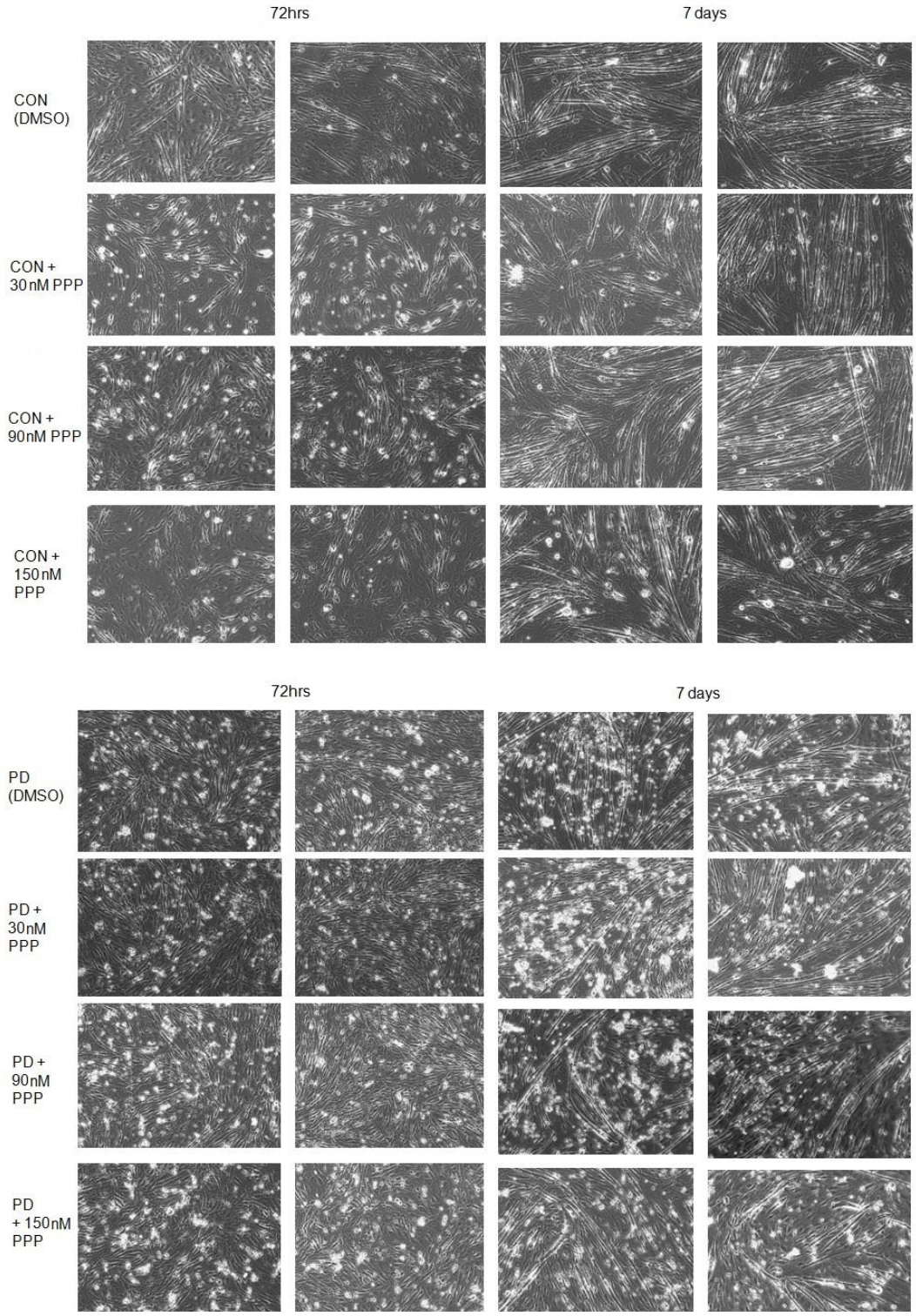

Fig 4.4 Representative light microscope (x10 magnification) images of CON and PD myoblasts administered with 30, 90 and 150 nM doses of PPP for 72 hrs and 7 days culture. The 150 nM dose of PPP appeared to have the most detrimental effect on cell differentiation and hypertrophy in both cell types at each time point.

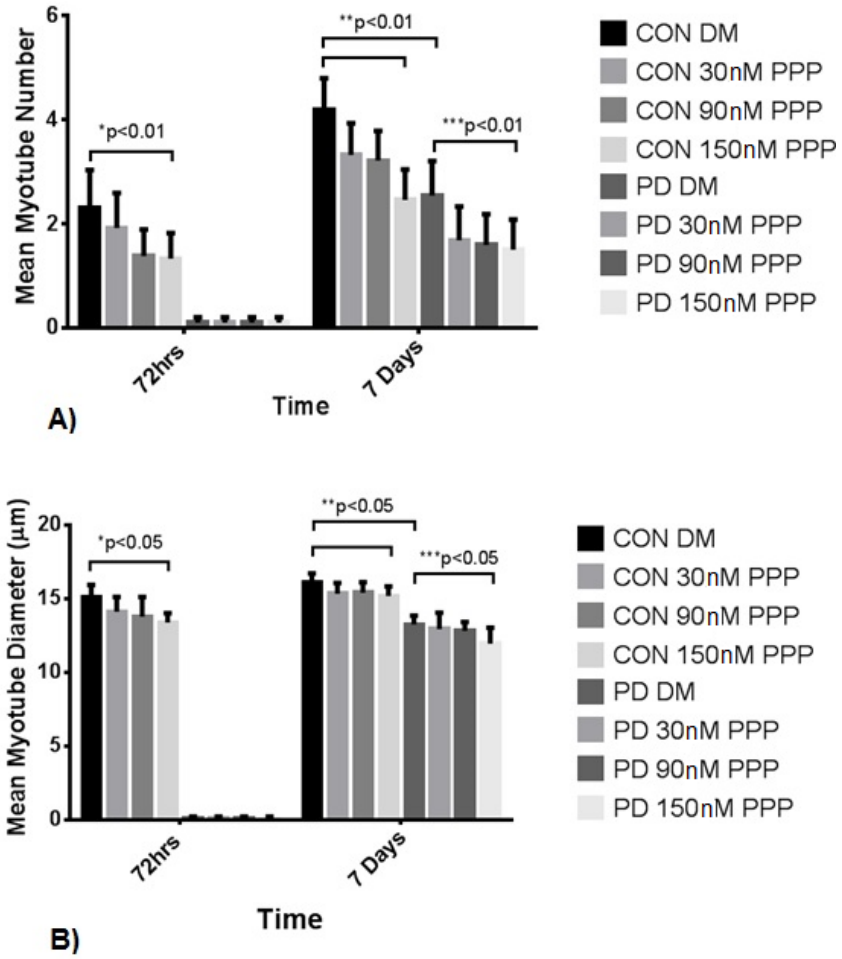

Fig 4.5 The effect of Picropodophyllin (PPP) doses on CON and PD myotube morphology after 72 hrs and 7 days. **A**) A detrimental effect in myotube number was observed with increasing doses of PPP in CON myoblasts after 72hrs (*P < 0.01) and 7 days (**P < 0.01). In PD myoblasts, PPP was also detrimental to myotube formation after 7 days culture (***P < 0.01). **B**) Additionally PPP reduced myotube diameter in both CON and PD myoblasts after 72hrs and 7 days culture (P < 0.05). To note, no quantifiable myotubes were observed in PD myoblasts after 72hrs culture hence no data presented for the above morphological analyses.

4.3.4 No effect of Picropodophyllin administration on IGF-I receptor protein and gene expression

Interestingly, compared to the alterations in myotube morphology, the addition of 150 nM PPP resulted in no differences between DM and treatments in either cell type for *myogenin*, *MyoD*, *Igf1* and the *Igf1* receptor (**Fig 4.6**). Furthermore, similar to the flutamide experiment, there were significant

differences between basal CON and PD myoblasts for myogenin mRNA expression (CON DM 65.85 ± 29.14 vs. PD DM 23.52 ± 9.89; P ≤ 0.01 **Fig 4.6A**) and MyoD mRNA expression (CON DM 5.67 ± 2.04 vs. PD DM 2.79 ± 1.16; P ≤ 0.01 **Fig 4.6A**) after 72 hrs cell culture. Furthermore, Picropodophyllin administration had no effect on total protein levels for the IGF-IR in either cell type at 72 hrs and 7 days (**Fig 4.7**).

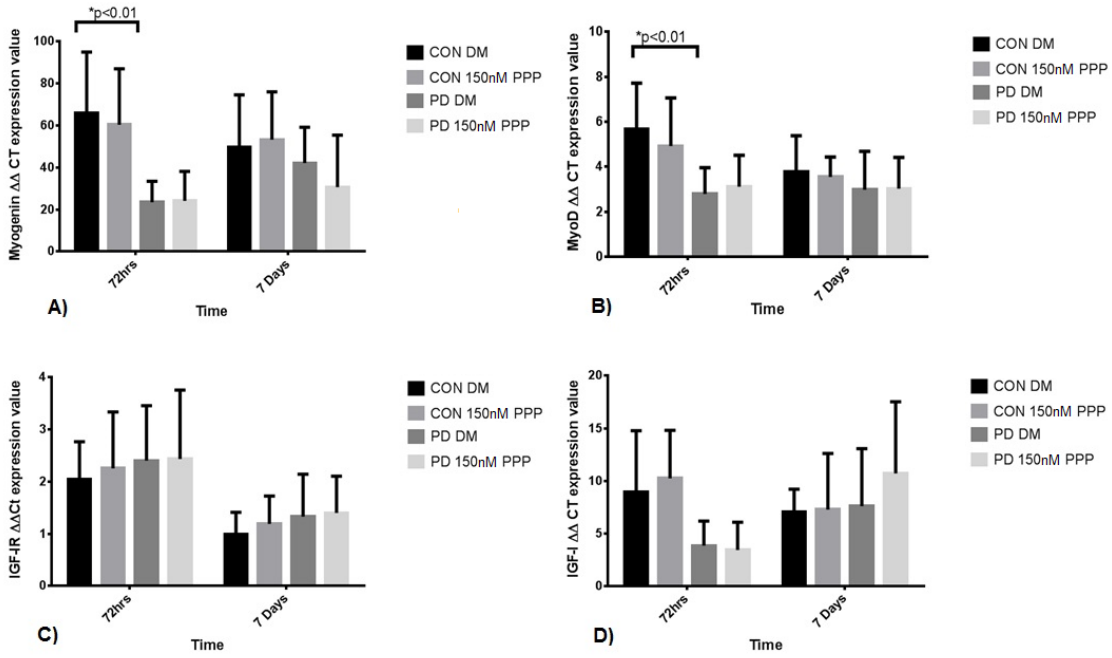

Fig 4.6 The effect of Picropodophyllin (PPP) on myogenin (**A**), MyoD (B) IGF-I (**C**) and IGF-IR (**D**) in CON and PD myoblasts. **A**) There was a significant decrease in myogenin expression between basal CON and PD cells after 72 hrs (*P < 0.01). **B**) A significant decrease in MyoD expression between CON and PD cells was observed after 72 hrs as well (*P < 0.01). **C & D**) Similar to myogenin and MyoD, there were no effects of PPP administration on IGF-I and its receptor in either cell type during culture time (P=N.S.).

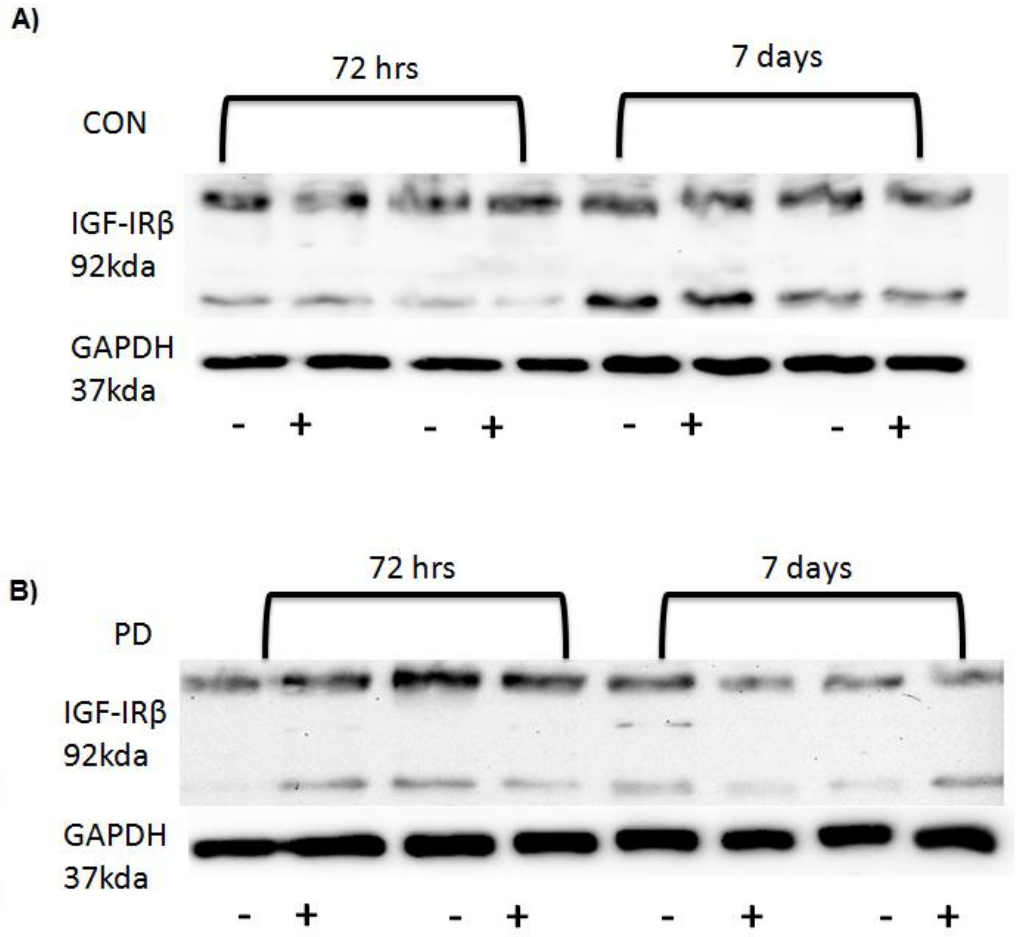

Fig 4.7 Representative western blots for the IGF-I receptor (β sub-unit) (n=3) in CON and PD myoblasts after 72 hrs and 7 days exposure with (+) and without (-) the inhibitor, Picropodophyllin (150 nM). GAPDH (37kda) was blotted as a loading control. There appeared to be no alterations in IGF-IR protein levels in either cell type with administration of the inhibitor.

4.3.5 Effects of exogenous IGF-I stimulation in combination with Picropdophyllin on downstream protein signalling.

Due to the no changes observed in gene transcripts and IGF-IR protein levels in the presence of the IGF-IR inhibitor (PPP) the downstream signalling (pERK1/2 and pAkt) of IGF-IR was investigated in order to confirm that PPP was impacting on the function of the receptor to relay to intracellular signalling. We also included the addition of exogenous IGF-I in the presence of the PPP in order to further substantiate its role in the inhibition of IGF-IR function. The addition of exogenous IGF-I for 15 minutes in PD myoblasts lead to a statistically significant increase (~90%) in Akt phosphorylation levels compared basal PD myoblasts (PD

DM 9.0 ± 1% vs. PD IGF-I 102.5 ± 12.5%; P ≤ 0.01, Fig 4.8C). The co-incubation of PPP with exogenous IGF-I abrogated the effect of IGF-I alone (PD IGF-I 102.5 ± 12.5% vs. IGF-I+PPP 41 ± 9%; P ≤ 0.01, **Fig 4.8C**). However, there was no significant effect observed between basal PD and PPP alone. In CON myoblasts, a similar trend was observed for exogenous IGF-I alone (CON DM 1 ± 1% vs. CON IGF-I 31.5 ± 3.5%; P ≤ 0.05, **Fig 4.8C**) increasing Akt phosphorylation. However, the PPP inhibitor when co-incubated with IGF-I did not abrogate the exogenous IGF-I stimulation of Akt (CON IGF-I 31.5 ± 3.5% vs. CON IGF-I+PPP 25.5 ± 5.5%; P ≤ 0.05, **Fig 4.8C**). The ineffectiveness of the PPP in combination with exogenous IGF-I may be due to IGF-I being having a higher affinity to the receptor than PPP, although in the PD myoblasts, the Akt response is blunted. There were no changes in Akt total protein levels in either cell type for any of the treatments administered.

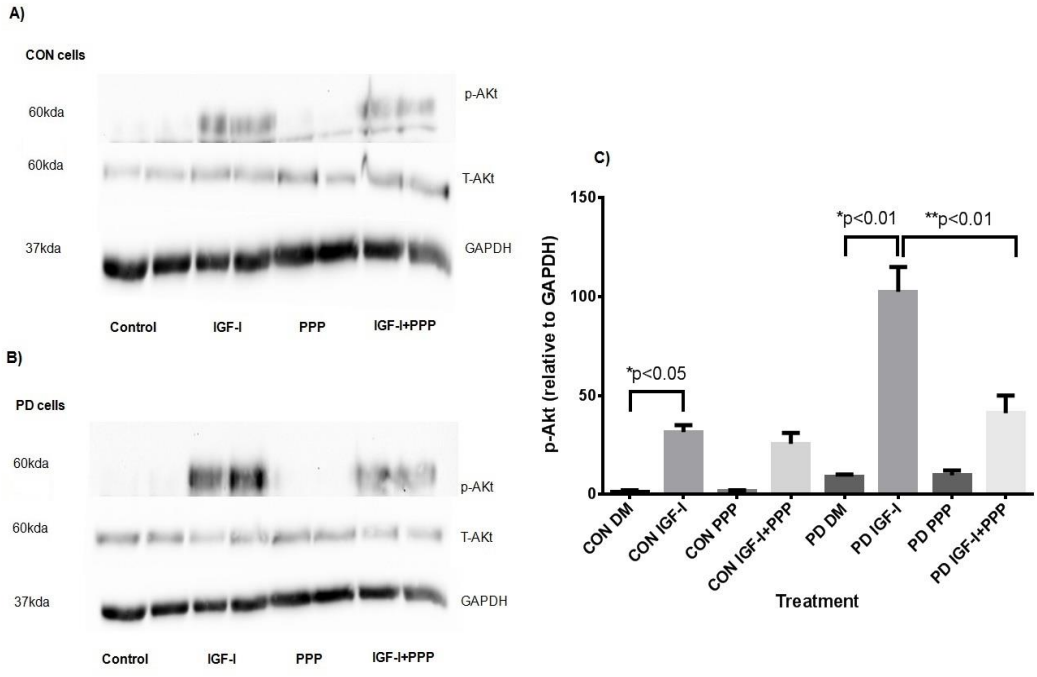

Fig 4.8 Immunoblots for Akt (total and phosphorylation ($_{Ser473}$)) after 15 minutes exposure to various treatments in CON (**A**) and PD (**B**) myoblasts. **C**) Exogenous IGF-I stimulated Akt phosphorylation in CON (*P < 0.05) and PD (*P < 0.01) myoblasts after 15 minutes. The effect of exogenous IGF-I was reduced in the PD myoblasts only when co-incubated with PPP (**P < 0.01). Values expressed as Mean ± S.E.M. Samples are duplicates for one experiment (n=1)

Furthermore, the activation of ERK1/2 was investigated after exogenous IGF-I stimulation for 15mins in PD and CON myoblasts. In both CON and PD myoblasts, exogenous IGF-I significantly increased ERK1/2 phosphorylation compared to basal treatments (CON IGF-I 86 ± 2% vs. CON DM 48 ± 13%; PD IGF-I 61 ± 0% vs. PD DM 30.5 ± 0.5%; $P \leq 0.01$, **Fig 4.9C**). The co-incubation of IGF-I and PPP, reduced ERK1/2 phosphorylation significantly compared to IGF-I alone in both cell types (CON IGF-I 86 ± 2% vs. CON IGF-I+PPP 38.5 ± 12.5%; PD IGF-I 61 ± 0% vs. PD IGF-I+PPP 45 ± 1%; $P \leq 0.01$, **Fig 4.9C**). However, PPP alone had no significant effect on ERK 1/2 phosphorylation compared to DM alone in CON and PD myoblasts (P=N.S.), although there was a mean reduction observed. There were no alterations in ERK1/2 total protein levels in either cell type. Overall, the abrogation of pAkt and pERK 1/2 phosphorylation with PPP in combination of exogenous IGF-I provides evidence for 150 nM dose being sufficient to inhibit the function of the IGF-I receptor and its downstream intracellular signalling.

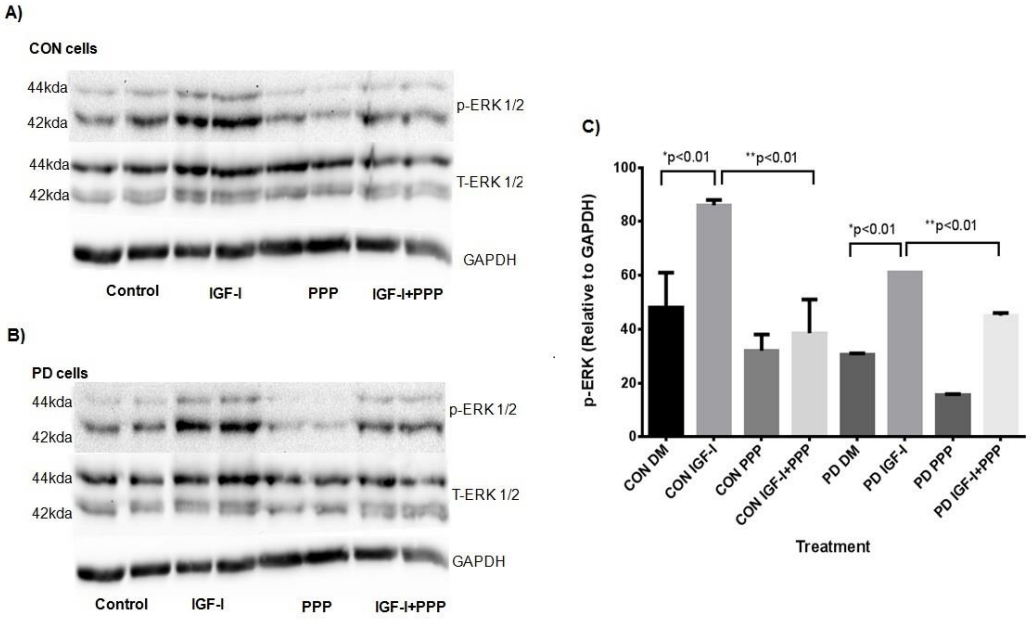

Fig 4.9 Immunoblots for ERK1/2 (total and phosphorylation ($_{Thr202/Tyr204}$)) after 15 minutes exposure to various treatments in CON (**A**) and PD (**B**) myoblasts. **C**) Exogenous IGF-I significantly increased ERK1/2 phosphorylation in CON and PD myoblasts after 15 minutes exposure (*P < 0.01). The co-incubation of IGF-I and PPP lead to reduced levels in ERK1/2 phosphorylation in both cell types (**P < 0.01). There was a mean reduction in PPP alone in ERK1/2 phosphorylation in CON and PD myoblasts, although this observation was not statistically significant. Values expressed as Mean ± S.E.M. Samples are duplicates for one experiment (n=1)

4.4 DISCUSSION

The androgen receptor and IGF-I receptor have been linked to play roles in muscle mass and development (Fernández *et al*., 2002, MacLean *et al*., 2008, Philippou *et al*., 2007). The current chapter of work investigated the effects of two inhibitors, one for each receptor; flutamide and Picropodophyllin respectively. Furthermore, the doses for the inhibitors were characterized in cells which display hypertrophic (CON) and aged/reduced differentiation (PD) phenotypes, as these cells will be used in chapter 5 and 6 in order to address the role of testosterone in a model of ageing muscle cells. In PD myoblasts, reductions in myotube number and diameter for morphology and *myogenin* and *MyoD* for gene transcripts were observed compared to CON myoblasts, confirming previously published observations (Sharples *et al*., 2011, Sharples *et al*., 2012).

4.4.1 The impact of Flutamide on the androgen receptor and muscle differentiation

Flutamide is an anti-androgen drug which competes with testosterone and its derivative, DHT for the binding to the androgen receptor (AR) (Bennett *et al*., 2010). Flutamide has been used in numerous studies to investigate the impact of the AR on muscle differentiation and hypertrophy (Singh *et al*., 2003, Diel *et al*., 2008, Sculthorpe *et al*., 2012). In the current study, an increasing flutamide dose resulted in reduced myotube formation and hypertrophy in both CON and PD myoblasts. The 40 μM dose resulted in alterations in myogenin and IGF-I mRNA expression, for which IGF-I has been reported to have an androgen response element in the promoter region of the gene (Grad *et al*., 1999, Wu *et al*., 2007).

There appeared to be a reduction in total AR protein levels with flutamide administration, although there were no alterations at the mRNA level. These observations combined provide evidence for the inhibition of the androgen receptor and thus a dose to be used the later experiment (Chapter 5). To note, the detection of the androgen receptor at the protein level (although the mRNA being lowly expressed (i.e. low Ct values of 28.45 ± 2.20) the use of the C2C12 muscle cell line, as earlier studies have occasionally transfected in AR due to previously reported low levels in this cell type (Altuwaijri *et al*., 2004, Lee, 2002, Sheppard *et al*., 2011). Overall, despite low mRNA levels, inhibiting the *AR* appeared to have catastrophic effects on morphological and transcriptional markers of differentiation and hypertrophy, eluding to the importance of a functional AR in myotube formation and hypertrophy in skeletal muscle (Mitchell *et al*., 2013, Sheppard *et al*., 2011)

4.4.2 The effect of Picropodophyllin on the IGF-I receptor and muscle differentiation

There is limited evidence on the impact of Picropodophyllin in skeletal muscle differentiation (Deldicque *et al*., 2007, Galluzzo *et al*., 2009). In the current study, the 150 nM dose was detrimental to myotube formation and hypertrophy in both cell types. These alterations in the muscle phenotype were accompanied by

decreases in IGF-I downstream signalling (pAkt and pERK1/2) as picropodophyllin acts a substrate competitor for the IGF-IR to inhibit tyrosine phosphorylation of the receptor (Vasilcanu *et al*., 2004). Both ERK ½ and Akt and ERK1/2 downstream of the IGF-I receptor have been highlighted to contribute towards muscle proliferation and differentiation respectively (Adams, 2002, Al-Shanti and Stewart, 2008, Coolican *et al*., 1997, Sarbassov and Peterson, 1998) and thus the ~40% (pERK ½) and ~60% (pAkt) decreases in signalling with the administration of PPP in the presence of exogenous IGF-I may explain the reductions in myotube number and diameter.

Previous doses of Picropodophyllin used in C2C12 muscle cells have ranged from 1-100 nM (Deldicque *et al*., 2007, Galluzzo *et al*., 2009), although the effect on muscle cellular process such as differentiation were not reported. The inhibition of the IGF-IR has previously been observed to delay skeletal muscle differentiation in myoblasts in vitro and mice lacking a functional IGF-I receptor have diminished muscle size and development (Cheng *et al*., 2000, Clemmons, 2009, Fernández *et al*., 2002, Heron-Milhavet *et al*., 2010, Liu *et al*., 1993, Kim *et al*., 2005). Alternatively small interference RNA has been used to inhibit the function of the IGF-I receptor, with a reduction in myotube area being observed in cultured human muscle cells (Serra *et al*., 2011). Overall, the administration of Picropodophyllin at a 150 nM dose is detrimental to myotube formation and hypertrophy, providing evidence for effective inhibition of the IGF-I receptor through alterations in the downstream signalling cascade.

4.4.3 Chapter Summary

In summary, this chapter of work has investigated the use of two inhibitors for the androgen receptor (Flutamide) and IGF-I receptor (Picropodophyllin) on skeletal muscle differentiation and hypertrophy in both control and population doubled cells that show a prior aged phenotype. These two receptors, as eluded to previously are suggested to mediate testosterone-induced muscle hypertrophy. The administration of flutamide (40 μM) significantly reduced myotube hypertrophy and differentiation in cells expressing hypertrophic CON and atrophic (PD) phenotypes. The detrimental effect was accompanied by alterations

in gene transcripts for muscle differentiation, IGF-I and the androgen receptor itself. In the instance of Picropodophyllin administration, a 150 nM dose had a negative effect on muscle differentiation and hypertrophy in both cell types. There were no alterations in gene transcripts or IGF-I receptor protein levels. However, close inspection highlighted reductions in Akt and ERK1/2 phosphorylation with Picropodophyllin treatment. Therefore, the 40 μM of flutamide and 150 nM doses were carried forward for co-incubation experiments with testosterone.

4.5 THESIS DIRECTION

In the current chapter and previous (chapter 3), both testosterone and inhibitors for AR and IGF-IR have been characterized in mouse C_2C_{12} skeletal muscle cells and cells that show prior impaired reductions in regenerative capacity (aged phenotype/PD cells). Subsequently, going forward, a 100 nM testosterone dose will be used (highlighted in section 3.3.3) as this has been utilized in other cell lines/primary cultures (Basualto-Alarcón *et al*., 2013, Serra *et al*., 2011, Wu *et al*., 2010a). The evidence reported in the current chapter has identified appropriate doses which will be carried forward in the co-incubations of testosterone (100 nM) with flutamide (40 uM) and Picropodophyllin (150 nM) in order to elucidate the most predominant pathway (direct AR vs. indirect IGF-IR) in testosterones role in increasing differentiation and hypertrophy in muscle cells (Chapter 5). As testosterone administration has been implemented in ageing populations to enhance muscle mass, (Atkinson *et al*., 2010, Bhasin *et al*., 2000, Lewis *et al*., 2007, Sinha-Hikim *et al*., 2006), chapter 5 will also focus on the restoration of a hypertrophic phenotype in cells that show prior impaired regeneration/differentiation and the mechanisms controlling this process. Chapter 6 will investigate the role of Akt in the restoration in the ageing phenotype observed in chapter 5.

5. TESTOSTERONE ACTS VIA THE AR AND NOT THE IGF-IR IN THE INDUCTION OF DIFFERENTIATION AND HYPERTROPHY AND RE AN AGED PHENOTYPE IN MYOBLASTS.

5.1 INTRODUCTION

The regulation of skeletal muscle mass is reliant on the balance between hypertrophy (e.g. protein synthesis/anabolism) and atrophy (e.g. protein breakdown/catabolism). A potential clinical intervention for promoting a positive net balance in the favour of protein synthesis is Testosterone administration (Brodsky *et al*., 1996, Sheffield-Moore *et al*., 1999). Testosterone replacement therapy has been observed to increase muscle strength and mass in various clinical populations including patients with AIDS, COPD and sarcopenia (Bhasin *et al*., 2000, Casaburi *et al*., 2004, Dillon *et al*., 2012, Ferrando *et al*., 2002, Sattler *et al*., 2011). However, a limited number of studies have investigated the role of testosterone in skeletal muscle hypertrophy and during periods of atrophy i.e. following ageing (Serra *et al*., 2013, Wu *et al*., 2010a, White *et al*., 2012) at the cellular level. Recently, Serra and colleagues (2013) observed increases in skeletal muscle regeneration in young and aged rats post injury, which culminated in increased satellite cell activation and proliferation under a testosterone stimulus. These observations highlight the potential of testosterone administration in rescuing aged muscle mass and ageing phenotypes, with the mechanisms remaining to be elucidated.

5.1.1 Myoblast models to investigate skeletal muscle hypertrophy and atrophy.

Recent studies have highlighted two myoblast models to study reduced differentiation capacity (Sharples *et al*., 2010, 2011, 2012). The first investigated the parental mouse C_2 myoblasts vs. their subclone, the C_2C_{12} cells. Despite their shared origins, we observed differences in morphological and biochemical responses between the C_2 and C_2C_{12} cells. The C_2 cells displayed slower and diminished differentiation profiles compared to the C_2C_{12} cells and were also more susceptible to TNF-α-induced inhibition of differentiation and induction of

apoptosis (Sharples *et al*., 2010). Because muscle wasting is associated with reduced muscle mass (Degens and Alway, 2003, Morse *et al*., 2005) and increased susceptibility to TNF-induced muscle protein degradation (Bruunsgaard *et al*., 2003, Lees *et al*., 2009), this comparative model is an excellent representation of muscle atrophy, hypertrophy and adaptability, thus, enabling the determination of potential regulators associated with muscle wasting. The second model utilised C_2C_{12} cells that had undergone multiple population doublings (PD) *verses* parental control cells (CON), which have undergone no doublings relative to the PD cells (Sharples *et al*., 2011). These cells also display impaired differentiation in monolayer (Sharples *et al*., 2011) and in three dimensional culture systems (Sharples *et al*., 2012) *verses* their parental controls.

5.1.2 Potential mediators of testosterone-induced muscle hypertrophy

Commonly in studies, testosterone has been co-incubated with inhibitors for the AR, IGF-IR, Akt, mTOR in a multitude of cell lines and primary cultures to investigate testosterone-induced hypertrophy (Basualto-Alarcón *et al*., 2013, Serra *et al*., 2011, Sculthorpe *et al*., 2012, Wannenes *et al*., 2008, Wu *et al*., 2010a). The AR, Akt, ERK1/2 and mTOR have all been observed to be involved in testosterone-induced hypertrophy in rat L6 myoblasts and primary cultures (Wu *et al*., 2010a, Basualto-Alarcón *et al*., 2013), however these pathways are usually studied in isolation and there is no information about the most predominant/important pathway in testosterone induced hypertrophy. Indeed, *in-vivo* the AR and p70S6K (downstream of IGF-I/mTOR), measured by increases in protein expression, have been correlated with increased muscle hypertrophy (Baar and Esser, 1999, Mitchell *et al*., 2013). Furthermore, Akt and mTOR have been observed to prevent muscle atrophy (highlighted by using genetic activation animal models) (Bodine *et al*., 2001). However there is limited data on the potential role of upstream factors (IGF-IR) and the AR in mediating testosterone rescuing muscle atrophy. Studies which have investigated both these receptors in relation to myotube hypertrophy, predominately inhibit the pathways independently, and there is controversy around the most important pathway in testosterones action via the indirect IGF-I pathway (Serra *et al*., 2011, White *et*

al., 2012) or the direct AR pathway (Lee, 2002, Wannenes *et al*., 2008) is fundamental in testosterone induced hypertrophy.

5.1.3 Aims and Objectives

Therefore in light of the literature discussed above, the aims of this chapter were to: (1) investigate the role the predominant pathway (androgen receptor vs. the IGF-I receptor) in mediating testosterones hypertrophic effects in CON and MPD cells using specific substrate competitors for AR and IGF-IR (flutamide and Picropodophyllin respectively) in the absence and presence of testosterone. (2) Investigate the role of testosterone in cells that display prior reductions in regeneration/aged phenotypes and the associated signaling compared with 'un-aged' controls. It was initially hypothesized that: (i) The inhibition of the AR and IGF-I receptor would both be fundamental in testosterones induced increases in myotube differentiation and hypertrophy and; (ii) that aged cells (although may respond to testosterone, as alluded to in chapter 3), the impact of T would be dampened in aged cells *verses* un-aged controls.

5.2 METHODOLOGY

5.2.1 Cell Culture

Mouse C_2C_{12} skeletal muscle myoblasts (CON and PD; outlined in 2.4.2) were resurrected as described in section 2.6. Cells were cultured as detailed in section 2.4, chapters 3 and 4. Cells at the time points of 0, 72 hrs and 7 days were fixed for immunocytochemistry (outlined in 2.10.2), isolated for RNA (outlined in 2.10.2 and 2.11) and lysed for protein analysis (outlined in 2.9).

5.2.2Cell Treatments

All treatments were administered in DM described above (detailed in 2.7.6). The treatments comprised of a vehicle control (DMSO at a concentration of 0.01%), testosteron*et al*one (100 nM), Flutamide (F) alone (40 μM), Picropodophyllin (PPP) alone (150 nM), co-incubations of the inhibitors with T (i.e. T + F, T + PPP) and finally all three (T + F + PPP). DMSO was used as the solvent for reconstitution of testosterone and inhibitors (detailed in 2.7), at the

same concentration as the vehicle (0.01%). For results and figure legends the following nomenclature will be used Control (DMSO), T, F, and PPP respectively. All treatments were added at 0 hrs and existing media was further supplemented at 72 hrs as outlined (chapter 2 sections).

5.2.3 RNA Isolation

6 well plates for each time point (0hrs, 72hrs and 7 days) were washed with 1 ml per well of Phosphate Buffer Saline (PBS) and extracted for RNA by placing 300 µl of TRIzol^{TM} Reagent (Sigma, St Louis) in each well. Total RNA was extracted as outlined in 2.11.1. RNA concentration and purity were assessed through UV spectroscopy at ODs of 260 and 280 nM, using the Nanodrop spectrophotometer 3000 (outlined in 2.11.2).

5.2.4 Real time, Reverse Transcriptase Polymerase Chain Reaction (rt-RT-PCR)

Seventy nanograms of RNA were taken from each sample and real time, reverse transcription polymerase chain reaction (RT-rt-PCR) was performed as detailed in 2.12.3. Primer sequences for genes of interest are shown in **table 2.1** and were checked for specificity according to 2.12.2. The relative mRNA expression of AR, myogenin, MyoD, IGF-IR and myostatin was quantified using the comparative Ct ($^{\Delta\Delta}$ct) method against a reference gene of RP-IIb and calibrator of control treatment (after CON 0hrs in all experiments).

5.2.5 Immunoblotting

Samples were prepared as outlined in 2.13.2. Gels were made up of a 10% resolving gel and a 5% stacking gel. Samples were electrophoresed at 200 volts until the sample buffer tracking dye reached the bottom of the gel (detailed in 2.13.4). The proteins were transferred to the nitrocellulose membrane for use in immunoblotting for 30 minutes (described in 2.13.5). The western blotting was performed based on manufacturer's instructions (described in 2.13.7). Membranes were sealed in plastic bags containing primary antibodies (outlined in **table 2.1**) for total proteins and related phosphorylation sites of the following proteins: Akt($_{ser473}$), ERK1/2($_{Thr202/Tyr204}$), p70S6K($_{Thr389}$) at a concentration of 1:1000, the

AR (1:500) and GAPDH (loading control; 1:4000) were diluted in an antibody diluent liquid for 1 hour incubation at room temperature. Detection of proteins was achieved using enhanced chemiluminescence (ECL) with a West Pico Supersignal kit (Pierce, Rockford, IL, USA) as described in 2.13.8. It was observed that the total levels of Akt and p70S6K changed in some conditions, however this was not repeatable and variable (discussed in chapter 7). ERK1/2 total protein was unchanged across the conditions (Fig 5.10 and 5.11). Therefore the phosphorylated proteins were assessed relative to the GAPDH that was unchanged between conditions. Although proteins (p-Akt, p-ERK1/2 and p-p70S6K) were analyzed on separate membranes between cell types i.e. (CON vs. PD when mean ± S.D were calculated globally for the arbitrary units (following detection), these were found to be non-significant between cell types (e.g. p-p70S6K 72hrs: CON 0.21 ± 0.18 vs. PD 0.17 ± 0.17; P=N.S.). Thus comparisons between cell types were enabled to be made. For the AR protein, the same exposure times were selected for densitometry analysis allowing for comparison between cell types.

5.2.6 Immunocytochemistry

Cells were fixed using the protocol detailed in 2.10.2. PBS (2ml/well) was added after removal of the methanol/acetone mix and plates were stored in 4^{o}c until further analysis. Immunocytochemistry was performed as described in 2.10.2. Myotubes were stained for desmin (intermediate filament found in skeletal muscle near Z line of sarcomeres) and defined as 3+ nuclei encapsulating a desmin positive structure so to rule out cells undergoing mitosis. A total of 30 images per condition were captured on x20 oil magnification fluorescence microscope. Quantification of morphology was performed as outlined in 2.10.3.

5.2.7 Statistical Analysis

Experiments were performed in triplicate, with separate repeats (n=3). Data are presented as Mean $\pm$ S.D unless stated otherwise. Gene expression data was assessed using a mixed three-way factorial ANOVA for interactions between time (72hrs and 7 days), treatments (DM, T, F, PPP, T+F, T+PPP T+F+PPP) and cell types (CON and PD). Morphology data was assessed using an ANOVA for

interactions between time (72 hrs and 7 days), treatments and cell types. Bonferroni post hoc analyses were performed where main effects for treatment or cell type occurred. A one way ANOVA was performed for western blots analyses to compare the effect of treatments within each cell type at 72 hrs and 7 days. A p-value of <0.05 was considered statistically significant. All statistical analyses were performed using SPSS version 19 and GraphPad Prism Software (detailed in section 2.15).

5.3 RESULTS

5.3.1 Testosterone administration enhances hypertrophy in control myoblasts and cells displaying aged phenotypes.

Myotubes were stained for desmin (**Fig 5.1-5.4**) to allow for the quantification of hypertrophic variables addressed in previous chapters (3 & 4). In CON cells, testosterone significantly increased myotube diameter after 72 hrs (CON DM 16.18 ± 1.57 vs. CON+T 19.04 ± 2.07; $P \leq 0.05$, **Fig. 5.5A**) and 7 days (CON DM 16.34 ± 1.11 vs. CON+T 19.54 ± 1.77; $P \leq 0.05$, **Fig. 5.5A**) administration. The enhanced myotube diameter was accompanied by significant increases in mean nuclei per myotube (72 hrs CON DM 3.38 ± 0.50 vs. CON+T 4.68 ± 0.92: 7 days CON DM 4.93 ± 0.92 vs. CON+T 6.80 ± 1.51; $P \leq 0.05$, **Fig 5.6A**). After 72 hrs exposure, there was limited myotubes present in PD myoblasts for the various treatments, although the administration of testosterone significantly increased the myotube diameter (μm) in treated vs. un-treated PD myotubes (PD DM 13.40 ± 0.47 vs. PD+T 17.57 ± 1.28; $P \leq 0.05$, **Fig. 5.5A**) that were present.

After 7 days, testosterone administration significantly increased myotube diameter (PD DM 15.52 ± 1.89 vs. PD + T 18.79 ± 2.10; $P \leq 0.05$, **Fig. 5.5A**) in PD myoblasts compared to un-treated cells. Similar to CON myoblasts, the hypertrophic increase was accompanied by mean nuclei per myotube (PD DM 4.14 ± 0.79 vs. PD+T 6.58 ± 1.54; $P \leq 0.05$, **Fig 5.6B**). In terms of myotube number there were no significant differences between testosterone treated and un-treated PD myoblasts (P=N.S). Between the two cell types (CON and PD), there were significant differences in myotube number and diameter ($P \leq 0.05$)

confirming the impaired differentiation already observed in chapter 4 and previously published (Sharples *et al*., 2011, Sharples *et al*., 2012). Interestingly, the magnitude of change in myotube diameter under a testosterone stimulus between CON and PD myoblasts was the same at 72 hrs (CON 15%; PD 23%) and 7 days (CON 16%; PD 17%) (**Fig 5.5E**). Similarly for nuclei per myotube a similar magnitude was observed between treated *v*s. untreated CON (27%) and PD (37%) myoblasts after 7 days culture. Indeed, these findings were reproduced in chapter 6 and highlight the ability of testosterone to rescue PD myoblasts to the hypertrophic level of basal CON myoblasts (in DM).

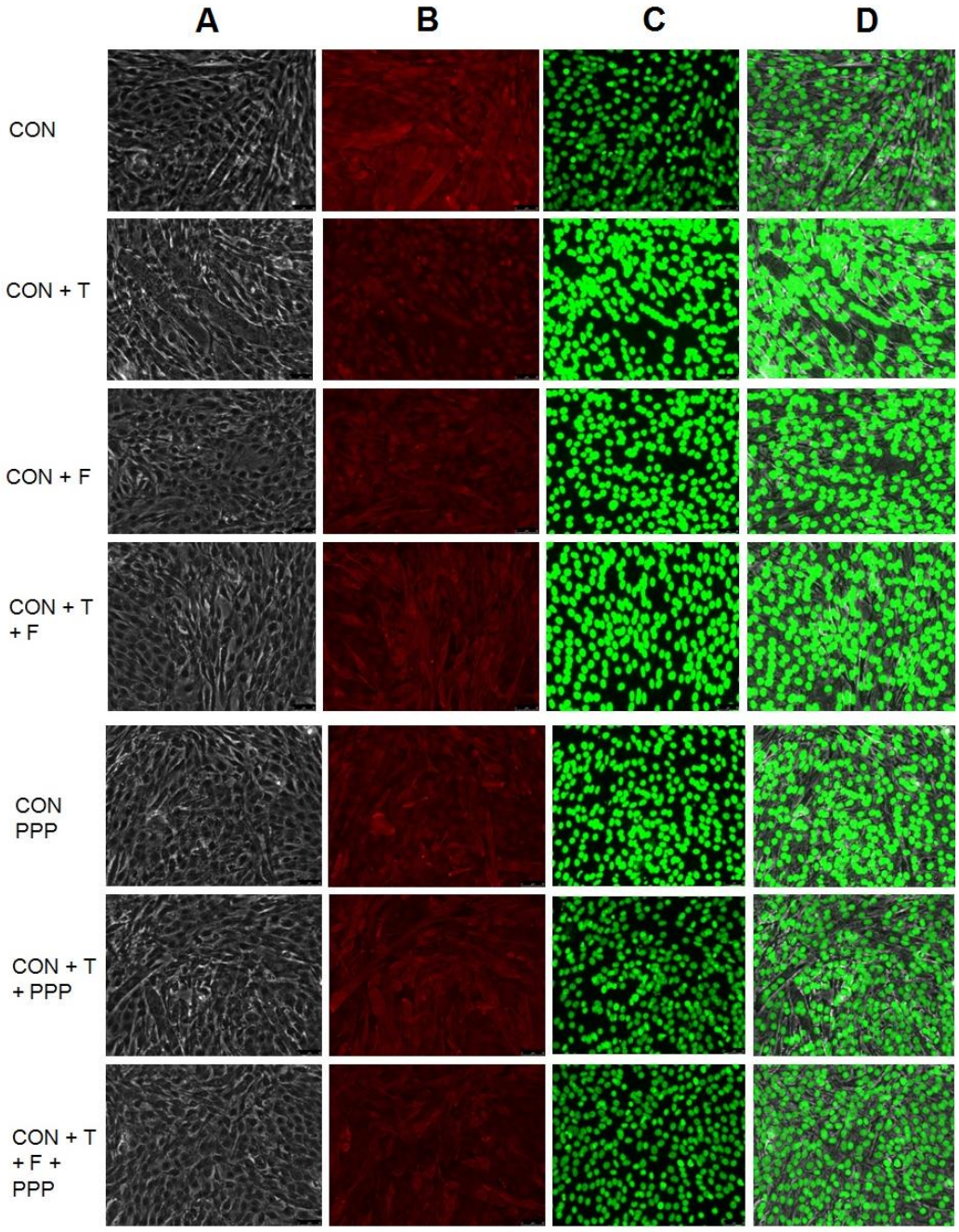

Fig 5.1 Representative microscope (x20) images for CON myotube morphology after 72 hrs culture. Myotubes were stained for desmin (**B**: red) and nuclei (**B**: green). Combined Light (**A**) and green images are presented too (**D**: last column). The presence of T resulted in larger myotubes compared to control conditions, with flutamide negating the increase in myotube size. Furthermore, T had positive effect on myotube size even in the presence of PPP.

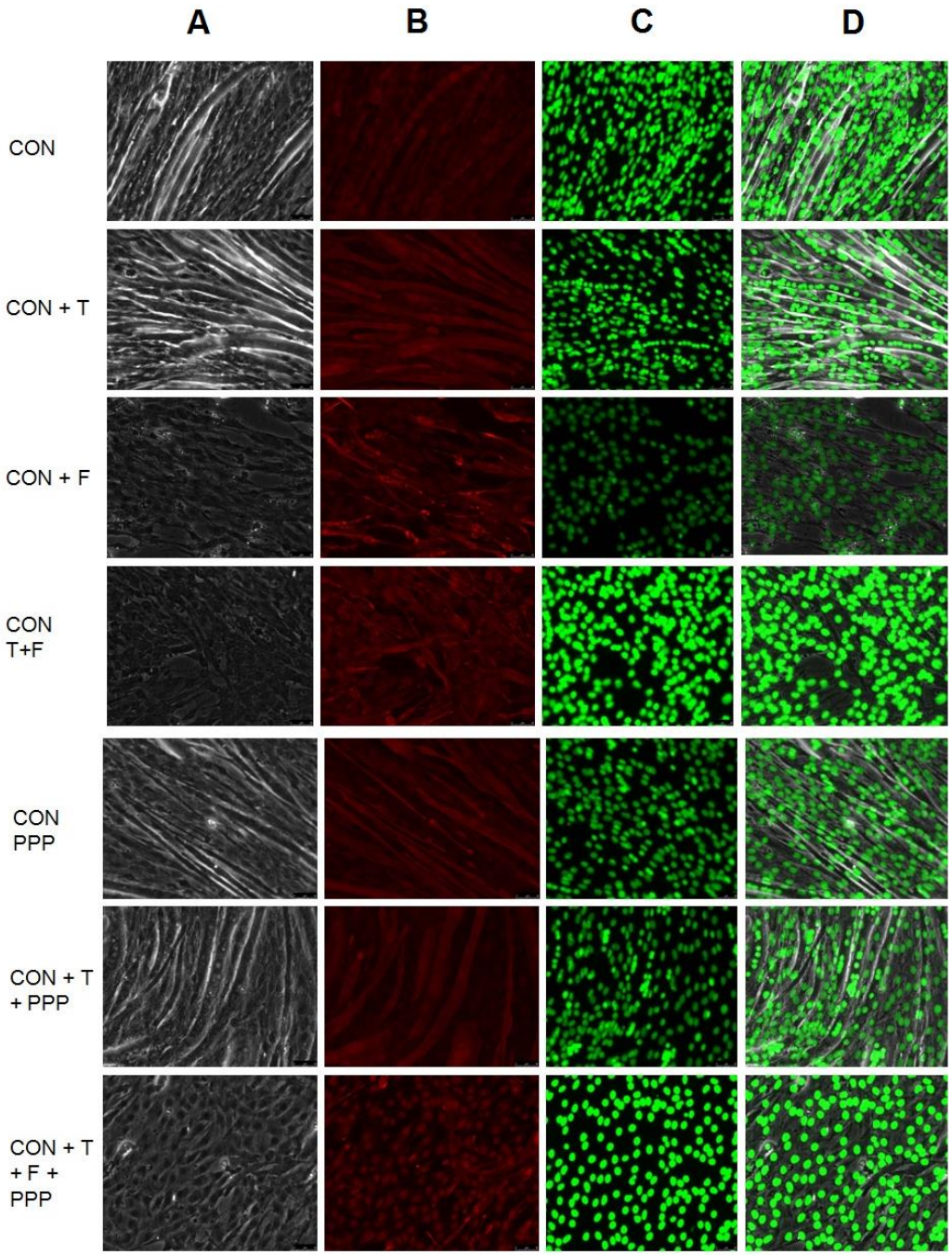

Fig 5.2 Representative microscope (x20) images for CON myotube morphology after 7 days culture. Myotubes were stained for desmin (**B**: red) and nuclei (**C**: green). Combined Light (**A**) and green images are presented too (**D**: last column). The presence of T resulted in larger myotubes compared to control conditions, with flutamide negating the increase in myotube size and myotube number. Furthermore, T had positive effect on myotube size even in the presence of PPP, suggesting limited involvement of the IGF-I receptor in mediating T's effect.

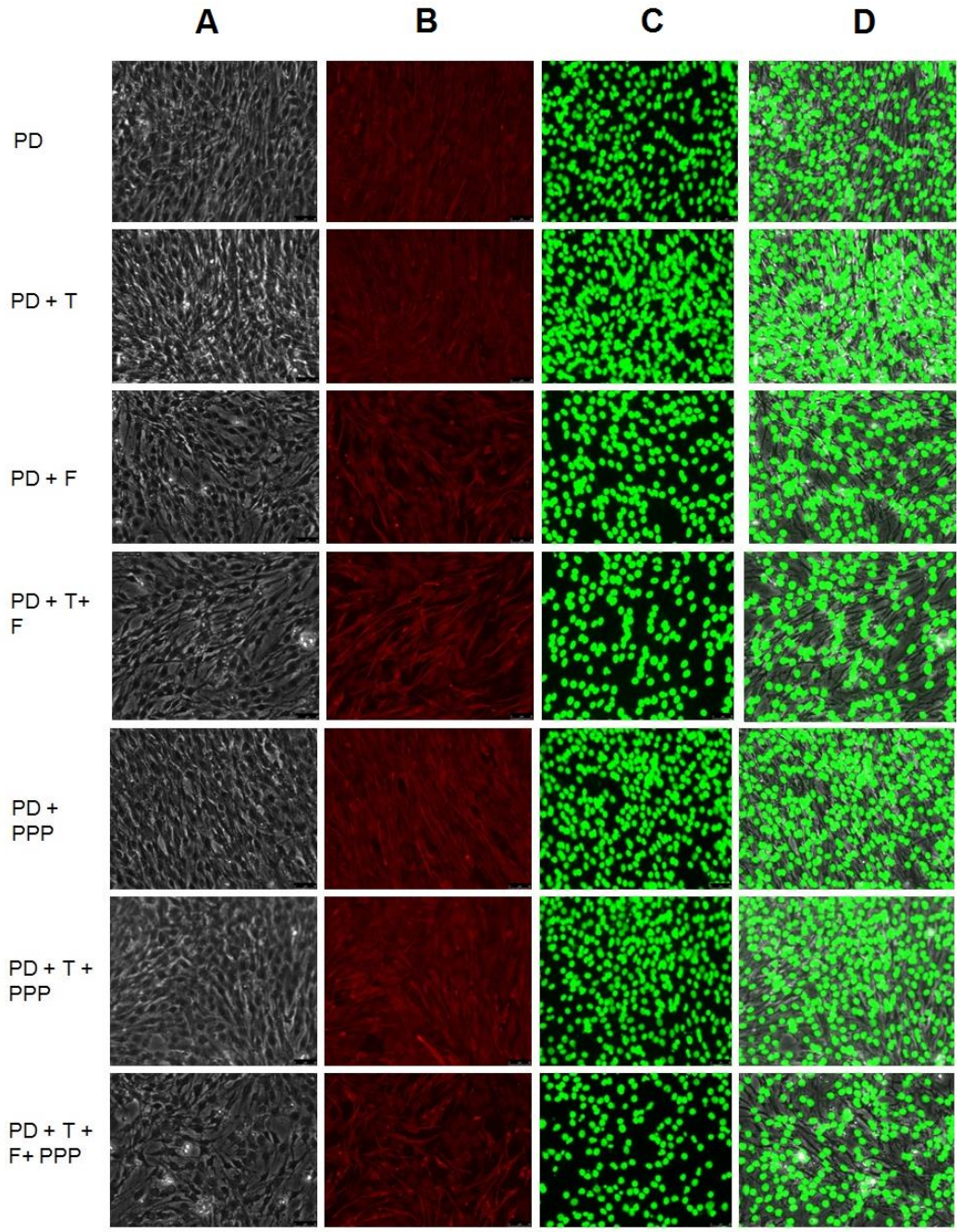

Fig 5.3 Representative microscope (x20 magnification) images for PD myotube morphology after 72 hrs culture. Myotubes were stained for desmin (**B**: red) and nuclei (**C**: green). Combined Light (**A**) and green images are presented too (**D**: last column). The presence of T appeared to reverse the aged phenotype as increases in myotube size were observed, yet flutamide negated the increase in myotube size. Furthermore, T had positive effect on myotube size even in the presence of PPP.

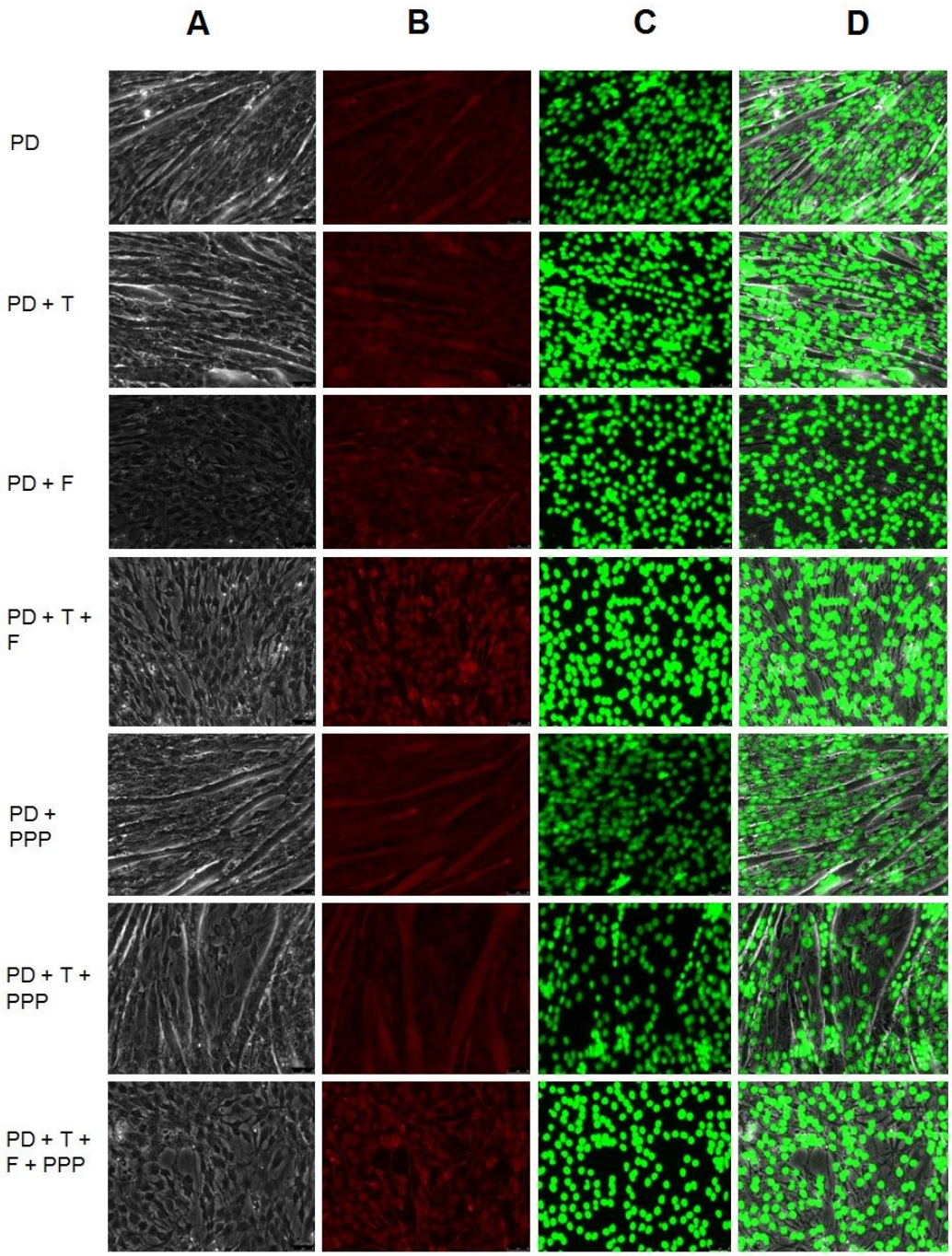

Fig 5.4 Representative microscope (x20 magnification) images for PD myotube morphology after 7 days culture. Myotubes were stained for desmin (red) and nuclei (green). Combined Light and green images are presented too (last column). The presence of T resulted in larger myotubes compared to control conditions, even in the presence of PPP. However flutamide abrogated the increases in myotube size in PD myoblasts, highlighting a critical role of the AR in reversing the aged phenotype.

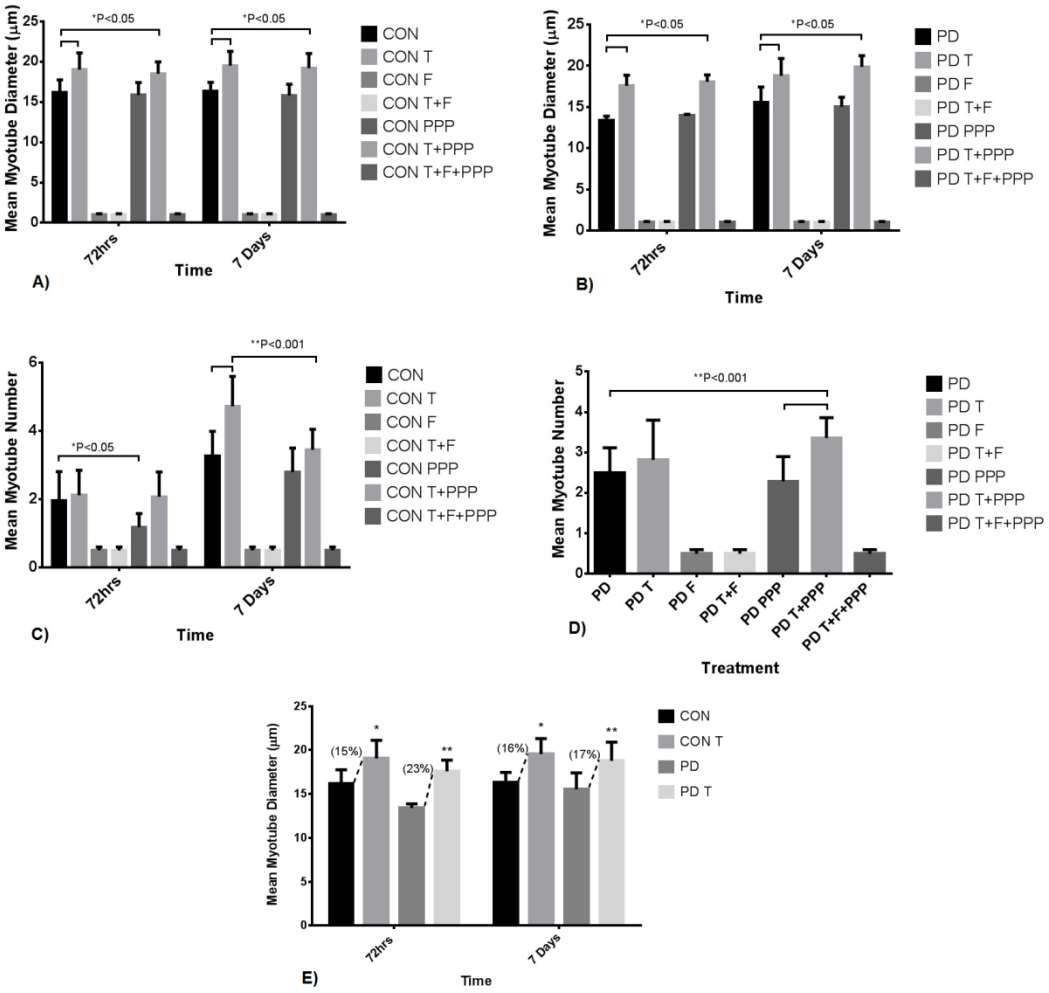

Fig 5.5. The effect of testosterone administration, along with co-incubations of flutamide and Picropodophyllin on myotube formation and hypertrophy. **A**) In CON cells, testosterone significantly increased myotube diameter at 72 hrs and 7 days exposure. The co-incubation of testosterone with Picropodophyllin did not abrogate testosterone increases in myotube diameter at either time point (*P ≤ 0.05) **B**) A similar trend occurred in PD myoblasts with testosterone treatment significantly increasing myotube diameter compared to un-treated cells (*P ≤ 0.05). The observed increases in testosterone induced hypertrophy continued at 7 days treatment (**P ≤ 0.05). The addition of Picropodophyllin had no effect on altering the observed increases in hypertrophy at either time point in PD myoblasts. **C**) The addition of PPP alone significantly reduced myotube number in CON myoblasts after 72 hrs (*P ≤ 0.05). Testosterone significantly increased myotube number after 7 days exposure (**P ≤ 0.001) in CON myoblasts, but the addition of Picropodophyllin abrogated this increase. **D**) The myotube number at 7 days in PD myoblasts was increased with the co-incubation of testosterone and Picropodophyllin compared to untreated and Picropodophyllin treated cells (*P ≤ 0.001). **E**) The magnitude of change between testosterone treated CON (72 hrs 15%; 7 days 16%) and PD (72 hrs 23%; 7 days 17%) myoblasts in myotube diameter was the same, highlighting a similar intrinsic response to a testosterone stimulus.

5.3.2 The impact of flutamide and Picropodophyllin on testosterone-induced hypertrophy

The addition of flutamide to both CON and PD myoblasts had an extensive detrimental effect on myotube formation at each time point as no quantifiable myotubes were observed (**Fig 5.1-5.4**). Testosterones function was rendered inactive in its ability to promote myotube formation and hypertrophy following its co-incubation with flutamide suggesting that the successful binding of testosterone to the AR is fundamental in these processes. Picropodophyllin (PPP) alone significantly decreased myotube number compared to DM conditions in CON myoblasts after 72hrs (CON DM 1.95 ± 0.86 vs. CON+PPP 1.18 ± 0.40; $P \leq 0.05$, **Fig 5.5C**). Although after 7 days there was still a mean decrease present with Picropodophyllin, this was not statistically significant (CON DM 3.27 ± 0.72 vs. CON+PPP 2.80 ± 0.70; P=N.S, **Fig 5.5C**). The co-incubation of Picropodophyllin with testosteron*et al*so abrogated the increase in myotube number after 7 days exposure (CON+T 4.73 ± 0.87 vs. CON+T+PPP 3.45 ± 0.60; $P \leq 0.05$, **Fig 5.5C**).

In terms of myotube diameter in CON cells, there was no significant effect at 72 hrs and 7 days between treated and un-treated myoblasts (P=N.S, **Fig 5.5A**). The co-incubation of testosterone and Picropodophyllin still resulted in significant hypertrophic increases in myotube diameter along with testosteron*et al*one at each time point (72 hrs CON+T 19.04 ± 2.07 vs. CON+T+PPP 18.54 ± 1.45: 7 days CON+T 19.54 ± 1.77 vs. CON+T+PPP 19.23 ± 1.82; P=N.S, **Fig 5.5A**). Additionally, Picropodophyllin alone did not significantly alter mean nuclei per myotube in CON myoblasts after 72hrs and 7 days compared to DM treated cells (P=N.S., **Fig 5.6A**). The co-incubation of testosterone with Picropodophyllin did not abrogate the significant increases in mean nuclei per myotube with testosterone administration alone at each time point (72 hrs CON+T 4.68 ± 0.92 vs. CON+T+PPP 3.86 ± 0.52: 7 days CON+T 6.80 ± 1.51 vs. CON+T+PPP 6.50 ± 1.22; P=N.S, **Fig 5.6A**).

Similarly, Picropodophyllin addition resulted in no significant differences in myotube number for PD myoblasts compared to un-treated cells after 7 days exposure (P=N.S, **Fig. 5.6B**). A significant difference was detected between

Picropodophyllin and the co-incubation with testosterone group for myotube number (PD+PPP 2.29 ± 0.61 vs. PD+T+PPP 3.36 ± 0.50; P ≤ 0.01, **Fig. 5.5D**). For myotube diameter, the presence of Picropodophyllin was ineffective in preventing testosterone-induced hypertrophy in PD myoblasts after 72 hrs and 7 days co-incubation (72 hrs PD+PPP 14.00 ± 0.10 vs. PD+T+PPP 18.06 ± 0.83: 7 days PD+PPP 15.03 ± 1.14 vs. PD+T+PPP 19.87 ± 1.35; P ≤ 0.01, **Fig. 5.5B**). In addition, the co-incubation of Picropodophyllin with testosterone had no effect on abrogating the increases in mean nuclei per myotube with testosterone administered alone (PD+T 6.58 ± 1.54 vs. PD+T+PPP 5.85 ± 0.86; P=N.S, **Fig 5.6B**). There were no significant differences observed between CON and PD treatments for PPP alone, T+PPP and T+F+PPP (no myotubes present) at either time point (P=N.S.). Overall, in terms of myotube morphology, it appears that testosterone-induced hypertrophy is not mediated via the IGF-I receptor in both cell types as testosterone still induced appropriate increases in myotube formation and hypertrophy in the presence of the IGF-IR inhibitor. The data suggests above that Testosterones effects are fully inhibited in the presence of flutamide, the AR inhibitor, in both cell types, providing initial evidence for the more predominant role of the AR in testosterone mediated myotube formation/differentiation and myotube hypertrophy *verses* the IGF-IR. This should however be viewed with some caution as PPP was not as effective alone on reducing the above parameters *verses* flutamide.

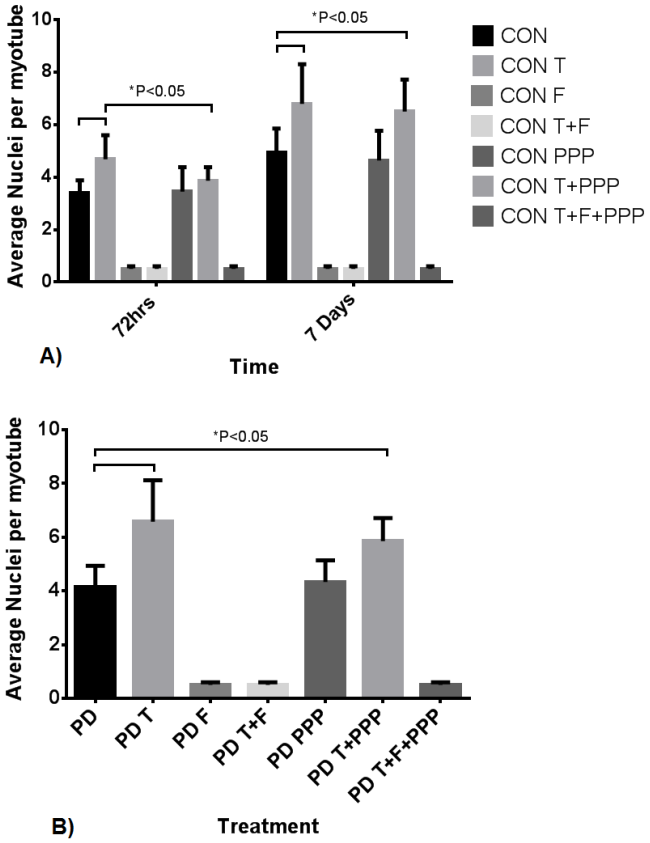

Fig. 5.6 Effect of testosterone treatment and AR/IGF-IR inhibitors (Flutamide/PPP respectively) on average nuclei per myotube in both CON and PD myoblasts. To note, AR inhibition resulted in all parameters measured being abolished in both cell types. Additionally, between CON and PD cells, there were no significant differences in PPP alone, T+PPP and T+F+PPP treatments at either time point. **A**) Testosterone significantly increased the mean nuclei observed in each myotube after 72 hrs, with Picropodophyllin negating the observed increase in CON myoblasts (*P ≤ 0.05). After 7 days, testosterone treatment continued to increase myotube nuclei content, with co-incubation of Picropodophyllin (**P ≤ 0.05) **B**) After 7 days in PD myoblasts, testosterone treatment significantly increased myotube nuclei content with Picropodophyllin co-incubation having no effect on these parameters measured compared to un-treated cells (*P ≤ 0.05).

5.3.3 The effect of testosterone administration on Androgen receptor protein levels.

A testosterone dose (100 nM) was sufficient to increase androgen receptor protein levels in both CON and PD myoblasts for each time point. In CON myoblasts, although not statistically significant, testosterone increased AR protein levels alone and even with co-incubation of Picropodophyllin after 72 hrs (CON+T 18 ± 6%; CON T+PPP 13.5 ± 4.5% vs. CON DM 7 ± 2%; P=N.S. **Fig.**

5.7) and 7 days (CON+T 15 ± 7%; CON T+PPP 12 ± 3% vs. CON DM 6 ± 1%; P=N.S. **Fig. 5.7**). The presence of AR protein with flutamide administration alone seemed to be completely abolished on first inspection on both 72 hrs and 7 day blots (**Fig. 5.7A** and **5.7B** respectively). However, this was not statistically significant across all three experimental repeats. Testosterone in the presence of flutamide increased AR vs. flutamide alone (72 hrs CON T+F 5 ± 0% vs. CON F 1 ± 0%; 7 days CON T+F 3 ± 0.5% vs. CON F 1 ± 0%; P=N.S.) but again this was not significant. It was interesting that in the testosterone plus IGF-IR inhibitor (PPP), AR total protein was seemingly restored back to basal levels suggesting that testosterone administration (similar to T alone) (72 hrs CON T 18 ± 6% vs. CON T+PPP 13.5 ± 4.5%; 7 days CON T 15 ± 7% vs. CON T+PPP 12 ± 3%; P=N.S.) induces increases in AR that is not dependant on IGF-IR/signaling.

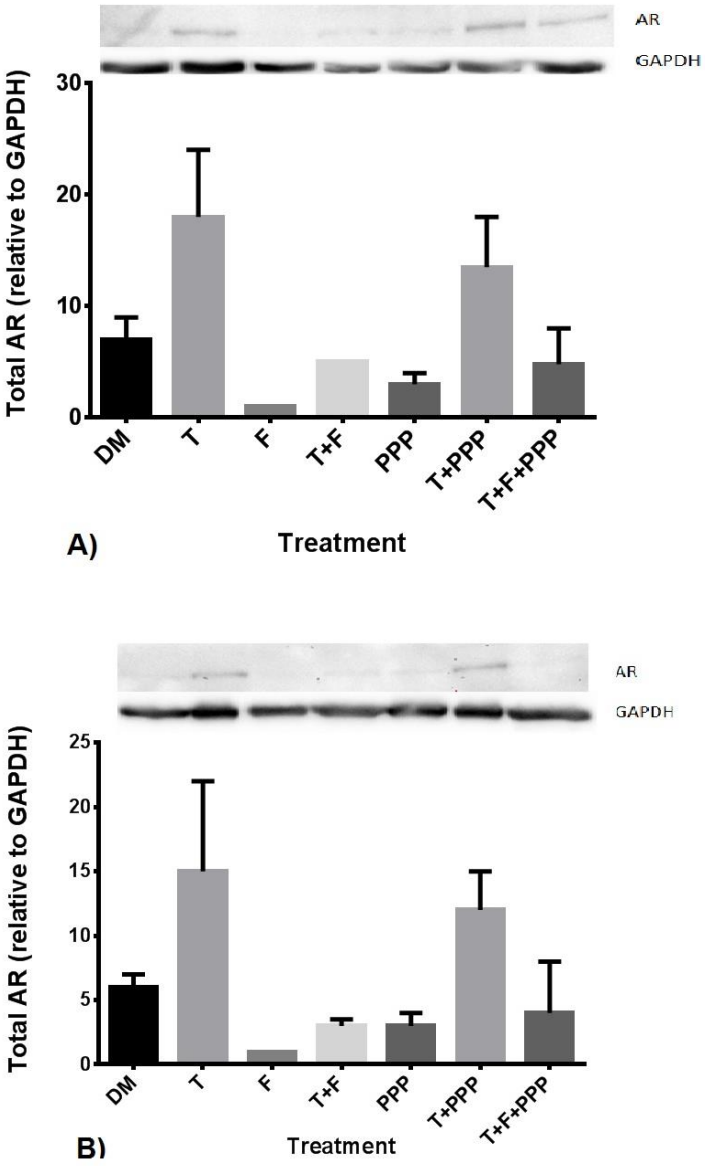

Fig 5.7 The effect of testosterone and co-incubations treatment on total AR protein levels in CON myoblasts after 72 hrs (**A**) and 7 days (**B**). Values presented as Mean ± S.E.M. Although not statistically significant, the presence of T appeared to increase total AR abundance even in the presence of PPP. This was however abrogated with the introduction of flutamide.

In the PD myoblasts, testosterone significantly increased the AR protein levels, even in the presence of Picropodophyllin after 72 hrs (PD+T 41 ± 2%; PD T+PPP 44 ± 11% vs. PD DM 11 ± 6%; $P \leq 0.05$, **Fig. 5.8**) and 7 days (PD+T 42 ± 2%; PD T+PPP 52 ± 5% vs. PD DM 6 ± 1%; $P \leq 0.05$ **Fig. 5.8**) administration. Flutamide significantly abrogated testosterone increases in AR protein levels after 72hrs (PD+T 41 ± 2%vs. PD T+F 3 ± 2%; $P \leq 0.05$, **Fig.5.8**) and 7 days (PD+T

42 ± 2% vs. PD T+F 3 ± 2%; $P \leq 0.05$, **Fig. 5.8**). Furthermore, the presence of flutamide in combination with testosterone and Picropodophyllin, decreased AR protein levels compared to testosterone incubated with Picropodophyllin (72hrs PD T+PPP 44 ± 11% vs. PD T+F+PPP 10 ± 2%: 7 days PD T+PPP 52 ± 5% vs. PD T+F+PPP 14 ± 7%; $P \leq 0.05$, **Fig. 5.8**) at both time points. Together with morphological findings these data provide evidence that testosterone increases AR total protein and this increase is abrogated in the presence of flutamide but not PPP, again suggesting an important role for AR and not the IGF-IR/associated signalling in testosterones impact on the morphological parameters measured in CON and PD cells.

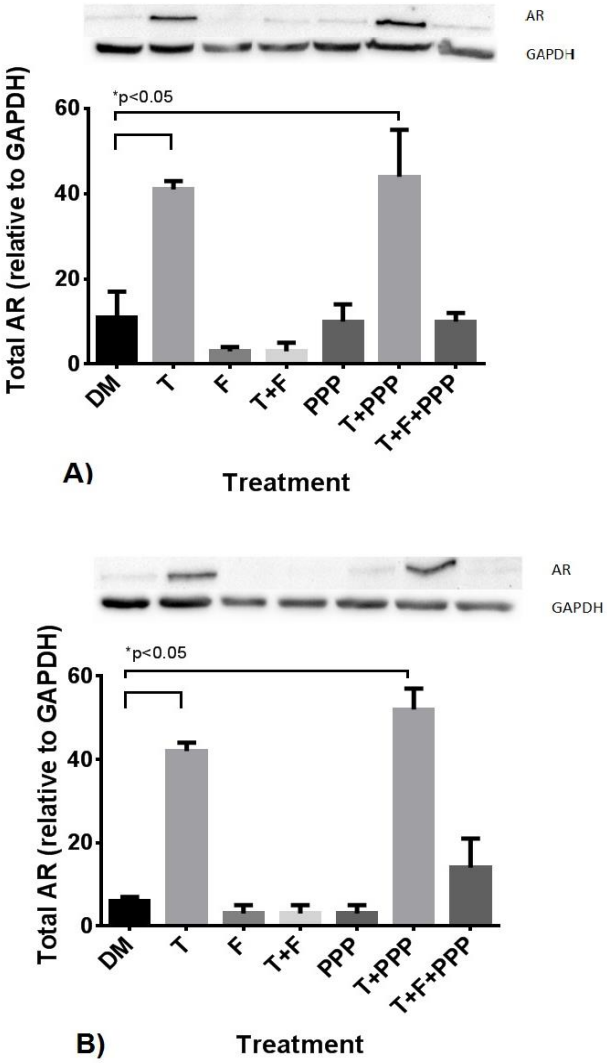

Fig 5.8 The effect of testosterone and co-incubations treatment on total AR protein levels in PD myoblasts after 72 hrs (**A**) and 7 days (**B**). Values presented as Mean ± S.E.M. **A**) Testosterone treatment significantly increased AR protein level, even in the presence of Picropodophyllin for PD myoblasts (*P < 0.05). Flutamide administration inhibited testosterone increases in AR protein levels. **B**) Testosterone treatment significantly increased AR protein level, even in the presence of Picropodophyllin (*P < 0.05). The presence of flutamide abrogated these increases in AR protein levels under a testosterone stimulus.

It was interesting that between cells that display prior reductions in myotube formation/hypertrophy after 72 hrs there were no significant differences between basal CON and PD myoblasts for AR total protein expression (CON DM 7 ± 2% vs. PD DM 11 ± 6%; P=N.S, **Fig 5.9A**). However, there was a significant increase in AR in testosterone treated PD myoblasts verses CON treated cells (PD T 41 ±

2% vs. CON T 18 ± 6%; P ≤ 0.05) after 72 hrs culture. It is also worth noting this larger increase in AR with testosterone in the PD cells *verses* CON cells was also shown when in the presence of IGF-IR inhibitor (PPP) (PD T+PPP 44 ± 11% vs. CON T+PPP 13.5 ± 14.5%; P ≤ 0.05, **Fig 5.9A**). At 7 days, Testosteron*et al*so induced a larger increase in AR PD *verses* CON myoblasts (PD T 42 ± 2% vs. CON T 15 ± 7%; PD T+PPP 52 ± 5% vs. CON T+PPP 12 ± 3%; P ≤ 0.05, **Fig 5.9B**). These observations provide evidence towards a heightened response in PD myoblasts to testosterone stimulated increases in AR protein expression which may contribute to the rescuing of the aged phenotype back to control cells in basal conditions as reported above.

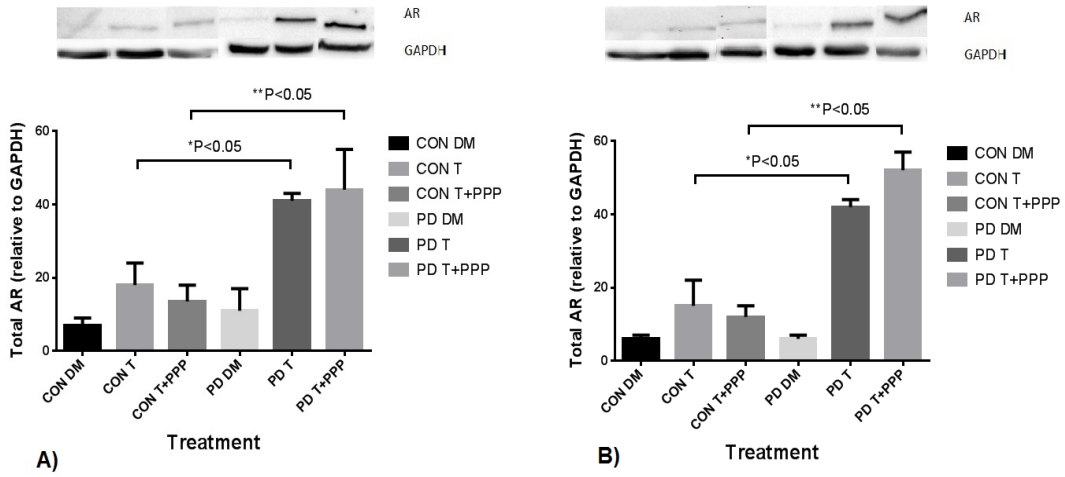

Fig 5.9 Comparison between total AR levels in CON and PD myoblasts exposed to testosteron*et al*one and in combination with Picropodophyllin after 72 hrs (**A**) and 7 days (**B**). **A**) Testosterone significantly increased AR levels in PD myoblasts vs. CON myoblasts after 72 hrs (*P ≤ 0.05). These increases in AR remained in the PD cells co-incubated with picropodophyllin compared to the same treatment in CON cells (**P ≤ 0.05). **B**) At 7 days culture, the same pattern was evident, where by Testosteron*et al*one (*P ≤ 0.05) and co-incubated with picropodophyllin (**P ≤ 0.05) significantly increased AR levels compared the same treatments in CON myoblasts. Values presented as Mean ± S.E.M.

5.3.4 Impact of testosterone and inhibitor administration on downstream IGF-I signalling proteins.

Supplementary to assessing the androgen receptor protein levels with a testosterone stimulus and inhibitors, downstream proteins of IGF-I signalling (Akt, ERK1/2 and p70S6K) were investigated. Despite the IGF-IR being

seemingly un-important in testosterones impact on morphology shown above, downstream signaling to IGF-IR has been shown to be increased with T administration in the literature therefore warranting further investigation (Basualto-Alarcón *et al*., 2013, Serra *et al*., 2011, White *et al*., 2012, Wu *et al*., 2010a). Especially as i.e. p70s6K is fundamental in protein synthesis in hypertrophy (Baar and Esser, 1999, Bodine *et al*., 2001, Mitchell *et al*., 2013) and hypertrophy occurs in the presence of T in the present studies.

For ERK1/2 phosphorylation, the presence of testosterone and flutamide co-incubation treatments significantly reduced levels at both 72 hrs (CON DM 30 ± 6% vs. T+F 3 ± 2%; T+F+PPP 5 ± 2%; $P \leq 0.05$, **Fig. 5.10**) and 7 days (CON DM 20 ± 8% vs. T+F 3 ± 2%; T+F+PPP 1 ± 0%; $P \leq 0.05$, **Fig. 5.10**). There were no alterations in total ERK1/2 protein levels in any of the treatments at either time point. In the PD myoblasts, testosterone was ineffective in significantly increasing ERK1/2 phosphorylation at either time point. However there was a trend towards the presence of flutamide being detrimental towards ERK1/2 phosphorylation after 72 hrs and 7 days exposure, however this was non-significant (P=N.S., **Fig. 5.11**). Between cell types, there were no significant differences in ERK1/2 phosphorylation basally, as reported originally in Sharples *et al.* (2011) or for all other treatments in the present study at either time point.

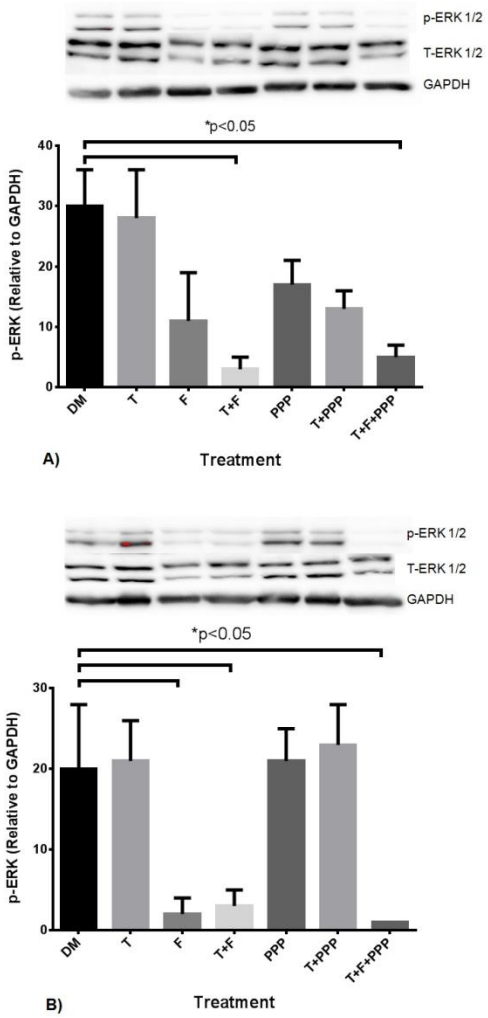

Fig 5.10 The effect of exogenous testosterone and co-incubations on total and phosphorylated ERK1/2 in CON myoblasts after 72 hrs (**A**) and 7 days (**B**) exposure. **A**) The presence of flutamide was detrimental in ERK1/2 activation (*P<0.05). Exogenous testosterone did not significantly alter ERK1/2 activation levels. **B**) Similar to 72 hrs, at 7 days flutamide administration continued to be detrimental for ERK1/2 phosphorylation (*P < 0.05). There were no alterations in total ERK protein at either time points. There were no differences between cell types (CON vs. PD) for any time point/condition.

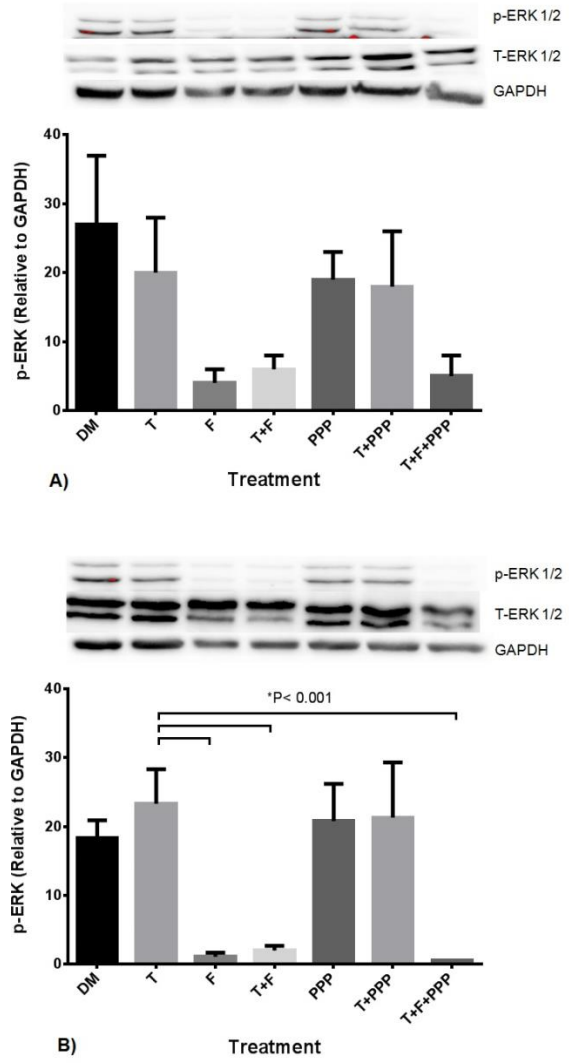

Fig 5.11 The effect of exogenous testosterone and co-incubations on total and phosphorylated ERK1/2 in PD myoblasts after 72 hrs (**A**) and 7 days (**B**) exposure. **A**) There were no statistically significant alterations in with any treatment after 72 hrs, although all flutamide conditions displayed a trend towards reduced ERK1/2 activation. **B**) At 7 days the presence of flutamide was significantly detrimental for ERK1/2 phosphorylation (*P < 0.05). There were no alterations in total ERK protein at either time points.

In CON cells, after 72 hrs there were significant reductions in phosporylated Akt with the presence of flutamide in treatments (CON DM 93.5 ± 0.5% vs. F 24.5 ± 19.5%; T+F 19 ± 17%; T+F+PPP 33 ± 11.5%; $P \leq 0.05$, **Fig. 5.12**). The presence of testosterone had no effect on Akt phosphorylation at either time points in CON cells (P=N.S.). After 7 days administration, there were no statistically significant alterations with any of the treatments, notably an increase

in phosphorylated Akt with Picropodophyllin (P=N.S., **Fig. 5.12**), although this was non-significant. In comparison, a testosterone stimulus applied to the PD myoblasts lead to observed increases in Akt phosphorylation (although not statistically significant), after 72hrs exposure. These increases after testosterone administration were also present with the co-incubation of Picropodophyllin, yet the presence of flutamide significantly reduced Akt phosphorylation (PD T+PPP 72.5 ± 10.5% vs. F 6 ± 5%; T+F 8.5 ± 5%; T+F+PPP 10.5 ± 5.5%; $P \leq 0.05$, **Fig. 5.13**). At 7 days, the increases in Akt phosphorylation with a testosterone stimulus were no longer present. However, the presence of flutamide was still detrimental to Akt phosphorylation (PD DM 93 ± 4% vs. F 9 ± 4%; T+F 7 ± 5%; T+F+PPP 1 ± 1%; $P \leq 0.05$, **Fig. 5.13**). Between cell types, there were significant differences in Akt phosphorylation for basal treatments in CON and PD myoblasts, where there was a significant reduction after 72 hrs in PD myoblasts (CON DM 93.5 ± 0.5% vs PD DM 37.5 ± 19.5; $P \leq 0.01$). However at 7 days, Akt phosphorylation was significantly increased in PD myoblasts compared to basal CON cells highlighting a delayed response and may explain the delay in fusion within this cell type (PD DM 93 ± 5 vs. CON DM 23 ± 5; $P \leq 0.001$). For all other treatments between the cell types, no significant differences were observed at either time point.

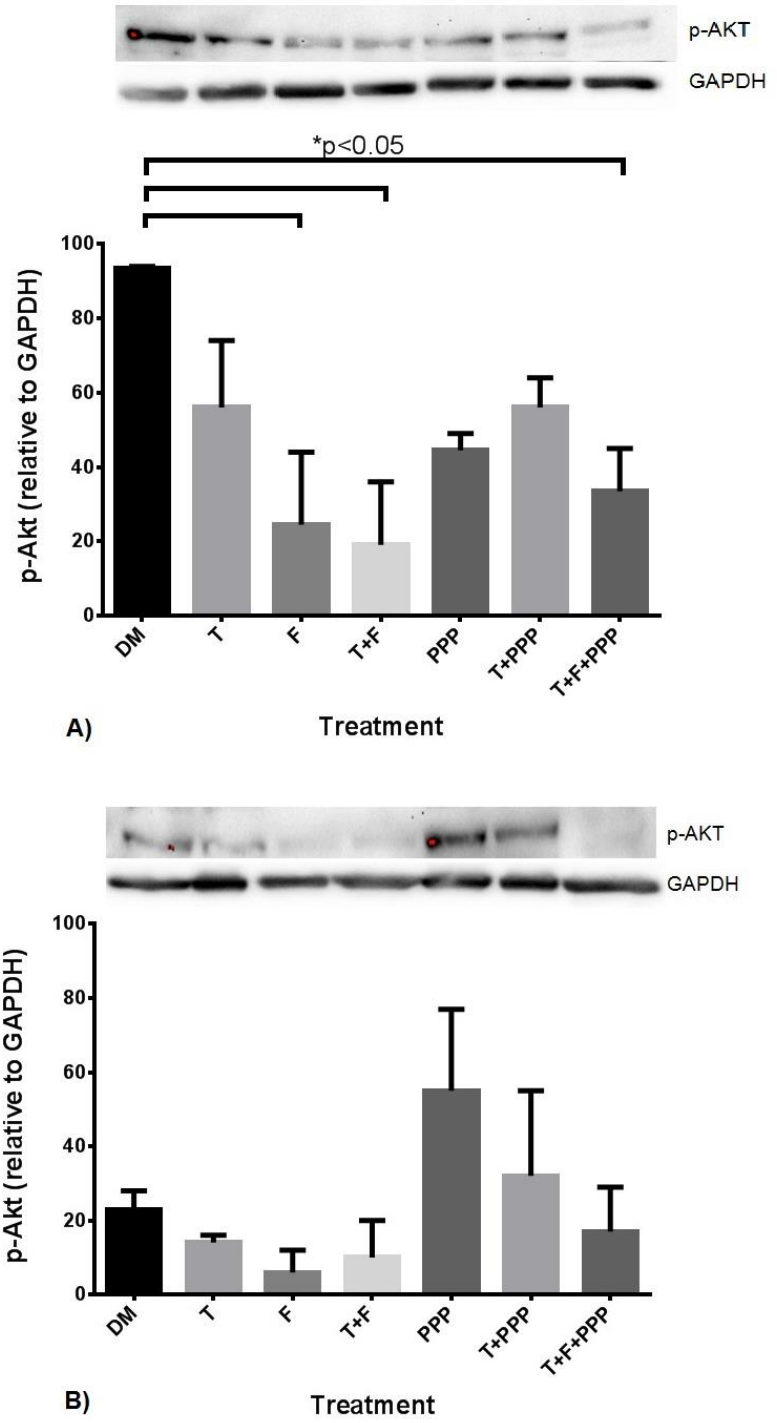

Fig 5.12 The effect of testosterone administration and co-incubations on phosphorylated Akt in CON myoblasts after 72 hrs (**A**) and 7 days (**B**). After 72 hrs (A), flutamide presence significantly reduced Akt phosphorylation compared to un-treated CON myoblast (*P< 0.05). Exogenous testosterone had no impact on alterations in Akt phosphorylation. At 7 days (**B**), there were no statistically significant alterations in phosphorylated Akt in PD myoblasts. Values presented as Mean ± S.E.M.

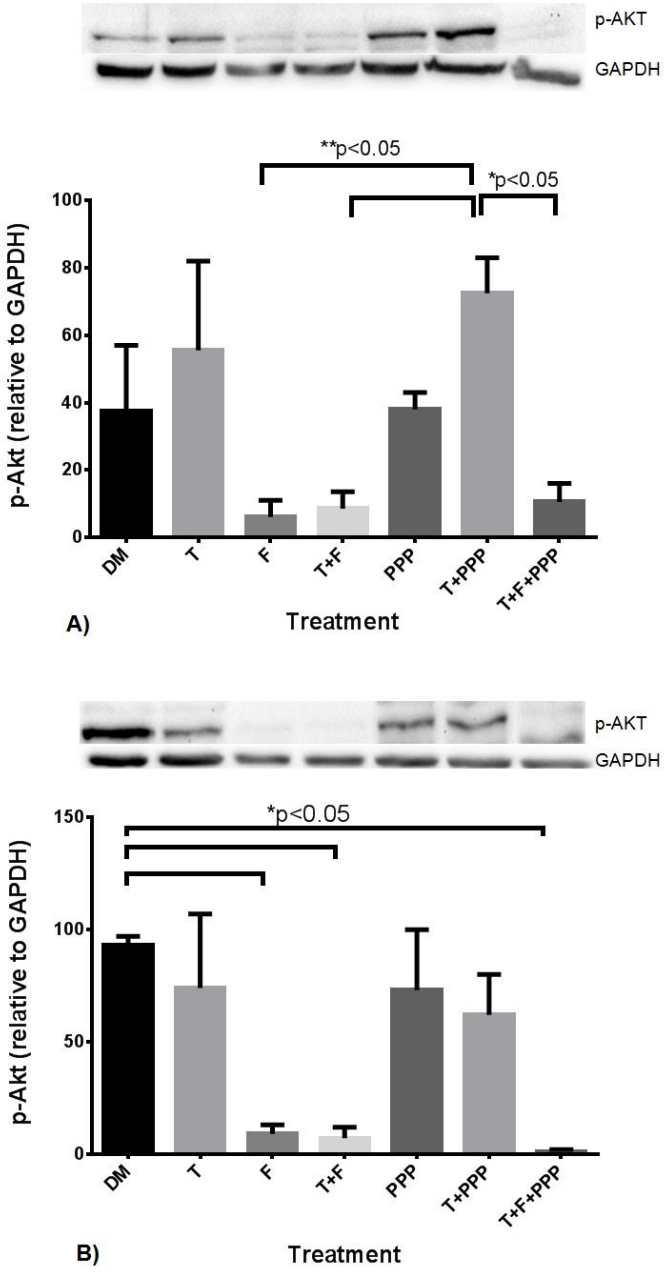

Fig 5.13 The effect of exogenous testosterone and co-incubations on phosphorylated Akt in PD myoblasts after 72 hrs (**A**) and 7 days (**B**). After 72 hrs (**A**), exogenous testosteron*et al*one increased Akt phosphorylation (although not statistically significant). The co-incubation of testosterone and Picropodophyllin significantly increased phosphorylated Akt levels which were reduced in the presence of flutamide (*P< 0.05). At 7 days (**B**), the presence of flutamide significantly reduced the levels of phosphorylated Akt in PD myoblasts (*P < 0.05). Values presented as Mean ± S.E.M.

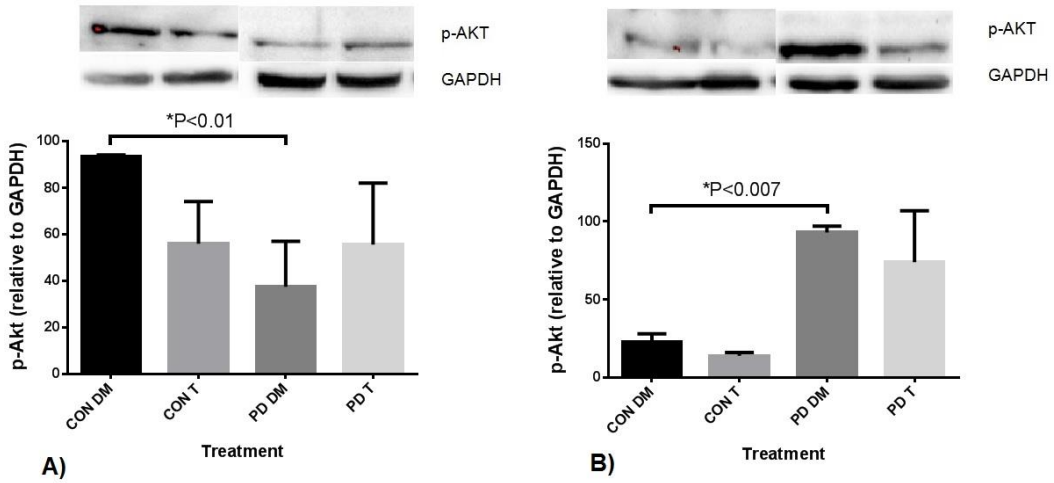

Fig 5.14 Comparison between Akt phosphorylation in basal and testosterone treated myoblasts after 72 hrs (**A**) and 7 days (**B**). A) Akt phosphorylation was significantly reduced in PD myoblasts compared to basal CON cells after 72 hrs (*P ≤ 0.01). B) After 7 days culture phosphorylated Akt increased in basal PD myoblasts compared to CON cells (*P ≤ 0.007), highlighting a delayed response in Akt signalling within the PD cell type. Values presented as Mean ± S.E.M.

Finally, p706SK was investigated. In CON and PD myoblasts, testosterone had no significant effect on p70S6K phosphorylation after 72 hrs or 7 days treatment. After 72hrs the presence of flutamide alone, and in co-incubations with testosterone and and combined (T+F+PPP) significantly decreased phosphorylation levels compared to basal conditions (CON DM 38 ± 14% vs. F 7± 4%, T+F 3± 2%; T+F+PPP 4± 3%; P ≤ 0.05, **Fig. 5.15**). After 7 days treatment, the pattern for flutamide administration being detrimental on p70S6K phosphorylation was still evident, although not statistically significant in CON cells. In PD myoblasts, the presence of flutamide was detrimental to p70S6K phosphorylation at both exposure points, although not statistically significant (P=N.S., **Fig. 5.16**). Between cell types, there were no significant differences in p70S6K phosphorylation observed for all treatments at either time point.

Overall, the alterations in protein signalling provide evidence towards that a functional AR receptor is required for normal myotube formation and hypertrophy in control and age phenotypic myoblasts, as flutamide reduces these parameters with associated reductions in phosphorylation of ERK, Akt and p70S6K.

Inhibition of the IGF-IR (although reducing ERK and Akt acutely after 15 mins in chapter 4) by 72 hrs had little impact on the downstream signaling molecules assessed here (indeed Akt actually increased, non-significantly, with PPP in CON and PD myoblasts at 72hrs, perhaps as a delayed response following inhibition at earlier time points). Importantly, testosteron*et al*one itself had little impact on increasing these signaling proteins (except for Akt in PD myoblasts, which is a further investigated in chapter 6). Overall suggesting the requirement of a functional androgen receptor for testosterone induced adaptation and not IGF-IR or associated signaling.

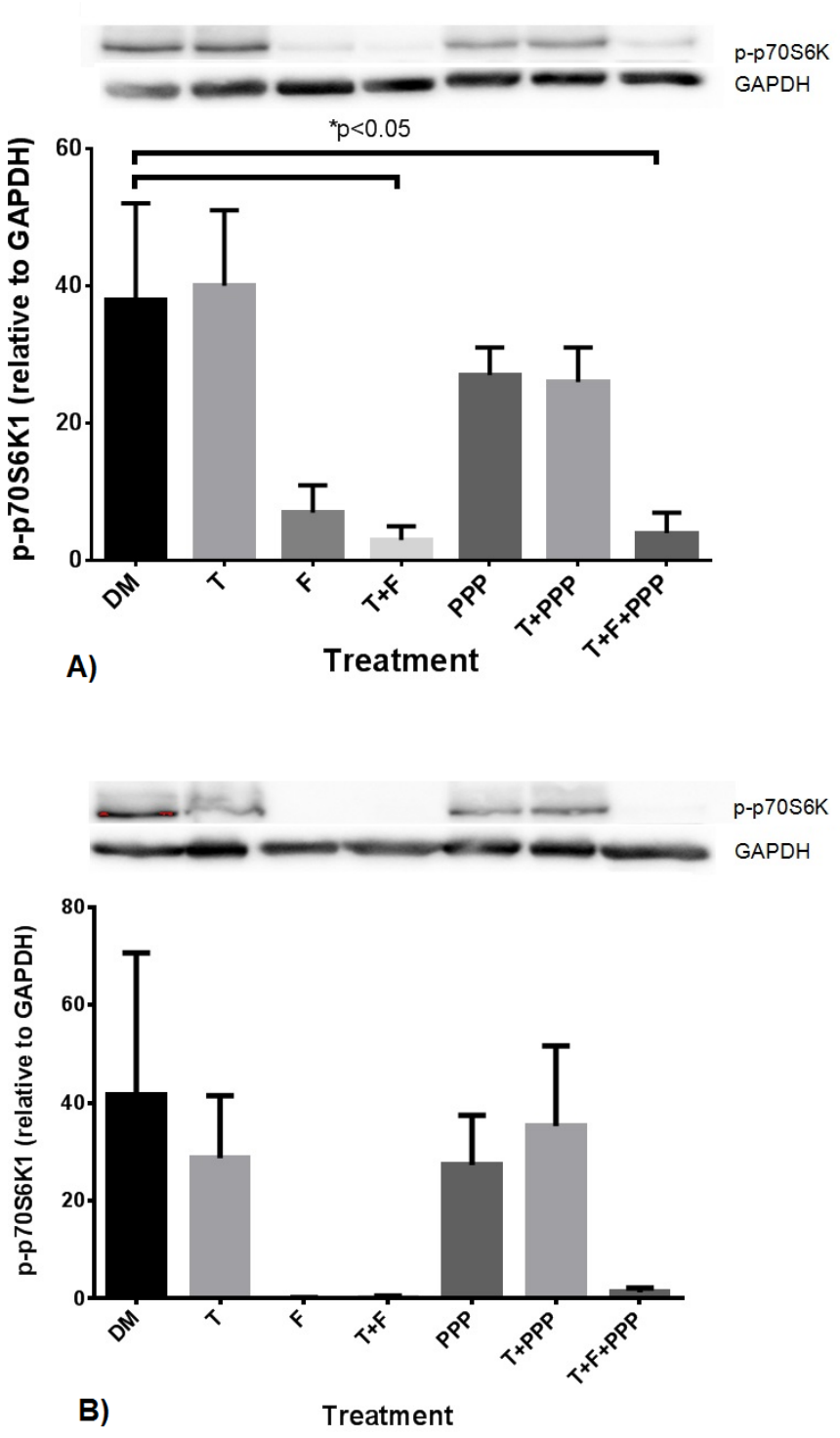

Fig 5.15 The effect of testosterone administration and co-incubations on phosphorylated p70S6K in CON myoblasts after 72 hrs (**A**) and 7 days (**B**) exposure. **A**) The presence of flutamide was significantly detrimental to p70S6K activation compared to un-treated myoblasts (*P < 0.05) **B**) There were no statistically significant alterations detected at 7 days. Values presented as Mean ± S.E.M.

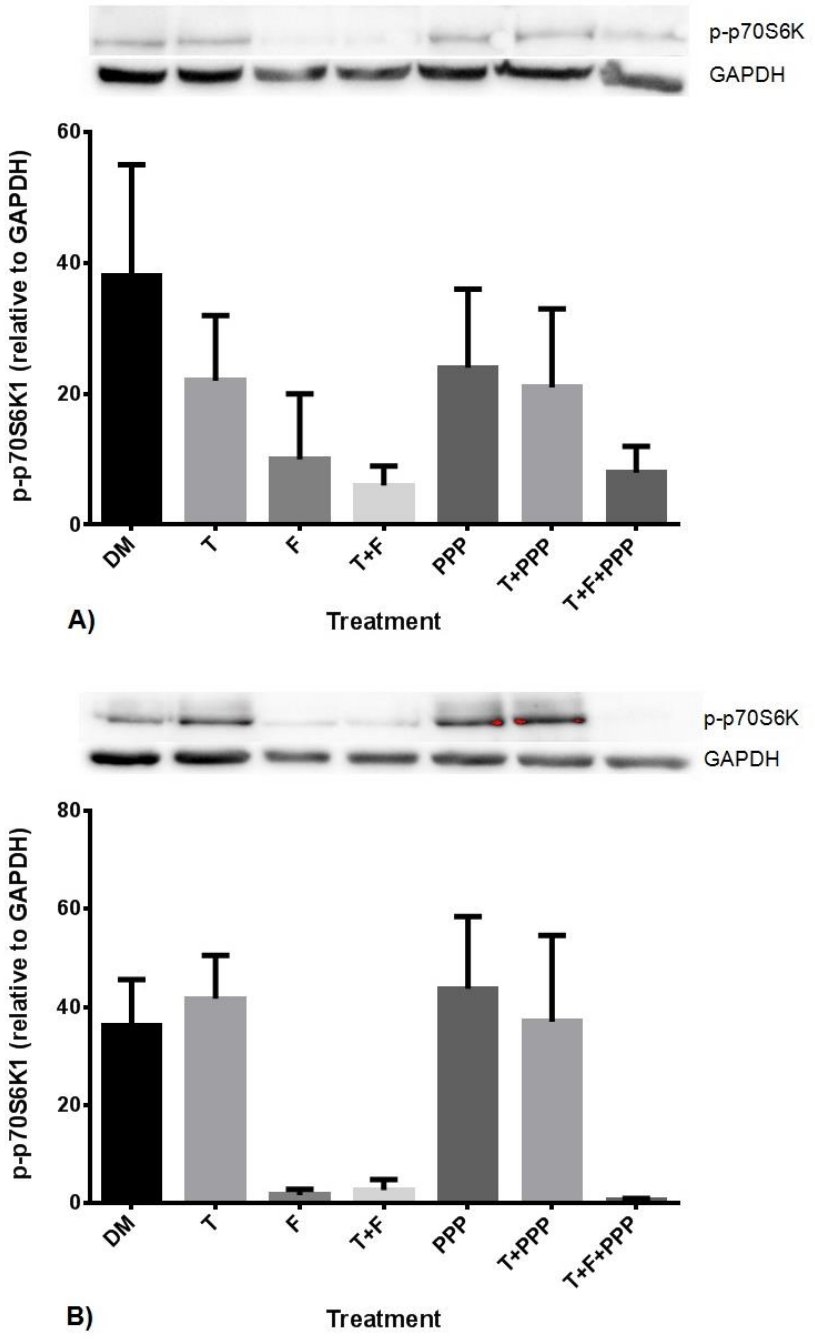

Fig 5.16 The effect of exogenous testosterone administration and co-incubations on total and phosphorylated p70S6K in PD myoblasts after 72 hrs (**A**) and 7 days (**B**) exposure. At both time points, no statistically significant alterations were observed between treatments, although the inclusion of flutamide in the cell culture media appeared to have a detrimental effect. Values presented as Mean ± S.E.M.

5.3.5 Effects of testosterone administration on gene transcripts in control and PD myoblasts.

Gene transcripts (mRNA) were analyzed to determine the impact of treatments on important genes involved in muscle differentiation and hypertrophy in both CON and PD myoblasts. Testosterone significantly increased myogenin mRNA expression in both CON (DM 75.86 ± 12.67 vs. T 108.36 ± 18.34; $P \leq 0.001$, **Fig 5.17A**) and PD (DM 27.03 ± 3.02 vs. T 34.05 ± 5.03; $P \leq 0.05$, **Fig 5.17B**) myoblasts after 72 hrs exposure. After 7 days exposure, the observed increases in *myogenin* with testosterone treatment were no longer present in either cell type (P=N.S.). In basal conditions, CON cells had significantly higher expression of *myogenin* after 72 hrs compared to PD myoblasts (CON DM 75.86 ± 12.67 vs. PD DM 27.03 ± 3.02; $P \leq 0.01$, **Fig. 5.17**), with this effect not observed at 7days (P=N.S, **Fig 5.16**). The observations with testosterone administration increasing myogenin expression support the evidence detailed in chapter 4 and importantly, show that such treatment can exert a positive effect in cells displaying an ageing phenotype. Gene transcripts for *MyoD*, *Igf1* receptor and *myostatin*, the administration of testosterone had no impact in either cell type (P=N.S). In PD myoblasts, testosterone treatment significantly reduced AR mRNA levels after 72 hrs exposure (DM 4.07 ± 2.04 vs. T 1.28 ± 0.05; $P \leq 0.001$, **Fig. 5.18B**), which is opposite to the observations at the protein level above (**Fig 5.8**).

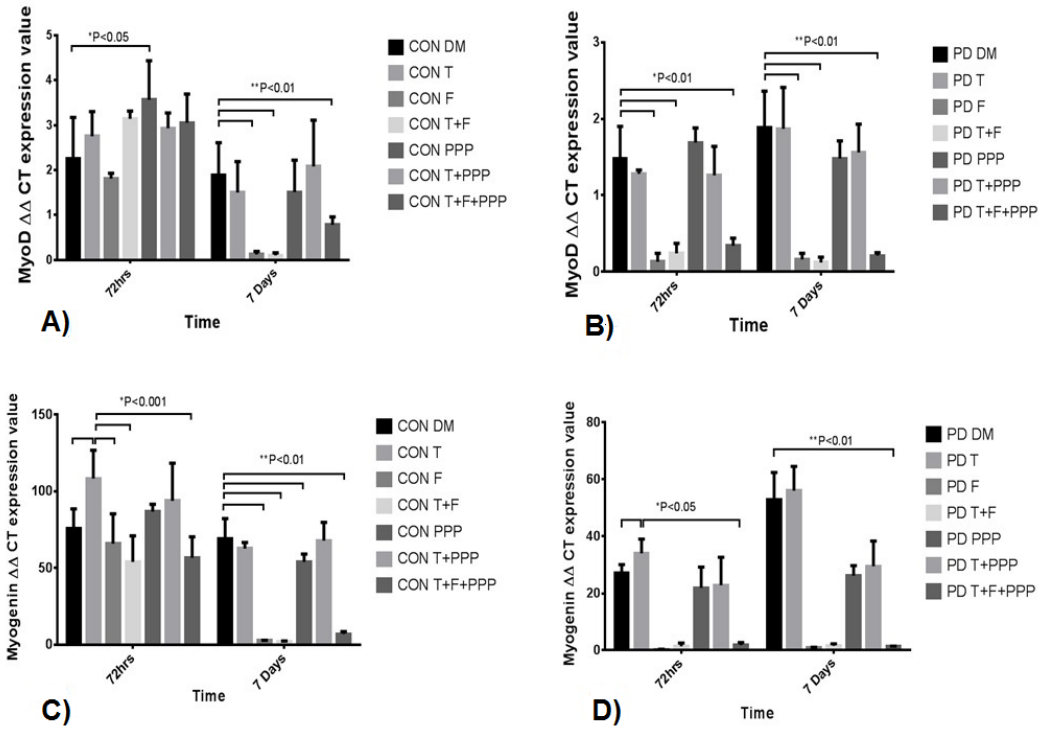

Fig 5.17 Impact of exogenous testosterone and AR (Flutamide/F) /IGF-IR (picropodophyllin/PPP) inhibitor co-incubations on MyoD and myogenin mRNA transcripts in CON and PD myoblasts after 72 hrs and 7 days. **A**) Picropodophyllin alone significantly increased MyoD levels after 72 hrs (*P < 0.05). At 7days, the presence of flutamide reduced MyoD expression levels in CON myoblasts (**P < 0.01) **B**) In PD myoblasts, testosterone had no impact on MyoD levels at either time point. The presence of flutamide significantly reduced expression levels after 72 hrs (*P < 0.01) and 7 days (**P <0.01). **C**) Testosterone treatment significantly increased myogenin expression levels in CON myoblasts after 72hrs (*P < 0.001). The presence of flutamide significantly reduced testosterone induced increases in myogenin (*P < 0.001). The presence of PPP did not significantly reduce increases in myogenin under a testosterone stimulus after 72 hrs culture. **D**) In PD myoblasts, testosterone administration increased myogenin levels (P < 0.05) compared to un-treated cells. This observation was abrogated by the presence of flutamide and Picropodophyllin (*P < 0.05). At 7 days, there were no increases in myogenin expression with testosterone, however the presence of flutamide resulted in reduced levels (**P < 0.01)

5.3.6 Flutamide administration significantly impacted on gene transcription levels

The presence of flutamide alone had a significant impact on genes investigated within the current chapter for both cell types. Specifically, flutamide was detrimental for transcripts involved in muscle differentiation (*MyoD* and *myogenin*). For *MyoD* mRNA expression, In CON cells, significant reductions

compared to DM conditions were observed with the presence of flutamide after 7 days exposure (CON DM 1.88 ± 0.73 vs. F 0.12 ± 0.07; T+F 0.10 ± 0.06; T+F+PPP 0.78 ± 0.18; P ≤ 0.01, **Fig 5.17C**). A similar pattern occurred in the PD myoblasts after 72hrs (PD DM 1.48 ± 0.42 vs. F 0.13 ± 0.11; T+F 0.24 ± 0.13; T+F+PPP 0.34 ± 0.10; P ≤ 0.01, **Fig 5.17D**) and 7 days (PD DM 1.88 ± 0.48 vs. F 0.16 ± 0.08; T+F 0.12 ± 0.07; T+F+PPP 0.21 ± 0.04; P ≤ 0.01, **Fig 5.17D**) exposure with treatments including flutamide for *MyoD* mRNA expression.

After 7 days exposure, myogenin expression was significantly decreased in CON cells compared to basal treatments (CON DM 69.07 ± 13.15 vs. F 2.84 ± 0.11; T+F 2.06 ± 0.33; T+F+PPP 6.99 ± 1.54; P ≤ 0.01, **Fig. 5.17A**). The reduction (~95%) in *myogenin* with flutamide completely inhibited CON myoblast fusion. Additionally, the detrimental effect with flutamide administration on myogenin expression was observed in PD myoblasts after 72 hrs (PD DM 34.05 ± 5.03 vs. F 0.30 ± 0.11; T+F 1.44 ± 1.14; T+F+PPP 1.83 ± 0.91; P ≤ 0.01, **Fig. 5.17B**) and 7 days (PD DM 56.04 ± 8.50 vs. F 1.02 ± 0.08; T+F 1.60 ± 0.73; T+F+PPP 1.39 ± 0.10; P ≤ 0.01, **Fig. 5.17B**) exposure.

Between cell types, PD myoblasts appeared to be more susceptible to flutamide treatment than CON cells. *MyoD* expression was significantly reduced in PD myoblasts administered with flutamide compared to the same condition in CON myoblasts (PD+F 0.13 ± 0.11 vs. CON+F 1.81 ± 0.12; P ≤ 0.05) after 72 hrs culture, although this phenomenon was no longer present after 7 days culture. A similar trend for *MyoD* expression was observed in both testosterone plus flutamide (PD T+F 0.24 ± 0.13 vs. CON T+F 3.14 ± 0.17; P ≤ 0.05) and picropodophyllin (PD T+F+PPP 0.34 ± 0.10 vs. CON T+F+PPP 3.05 ± 0.64; P ≤ 0.05) co-incubations after 72 hrs culture. Furthermore, the alterations in *myogenin* expression, supports the increased susceptibility of PD myoblasts to flutamide administration. *Myogenin* expression was significantly decreased after 72 hrs in PD myoblasts with flutamide compared to CON treated myoblasts (PD+F 0.30 ± 0.11 vs. CON+F 65.95 ± 19.37; P ≤ 0.05). This pattern was further observed at 72 hrs in treatments where flutamide was present (PD T+F 1.44 ± 1.14 vs. CON T+F 53.98 ± 16.97; PD T+F+PPP 1.83 ± 0.91 vs. CON T+F+PPP 56.68 ± 13.65; P ≤ 0.05). Overall, the presence of flutamide completely abolishes MyoD and

myogenin expression after 72 hrs and 7 days in CON and PD myoblasts, factors which are fundamental in the fusion of myoblasts.

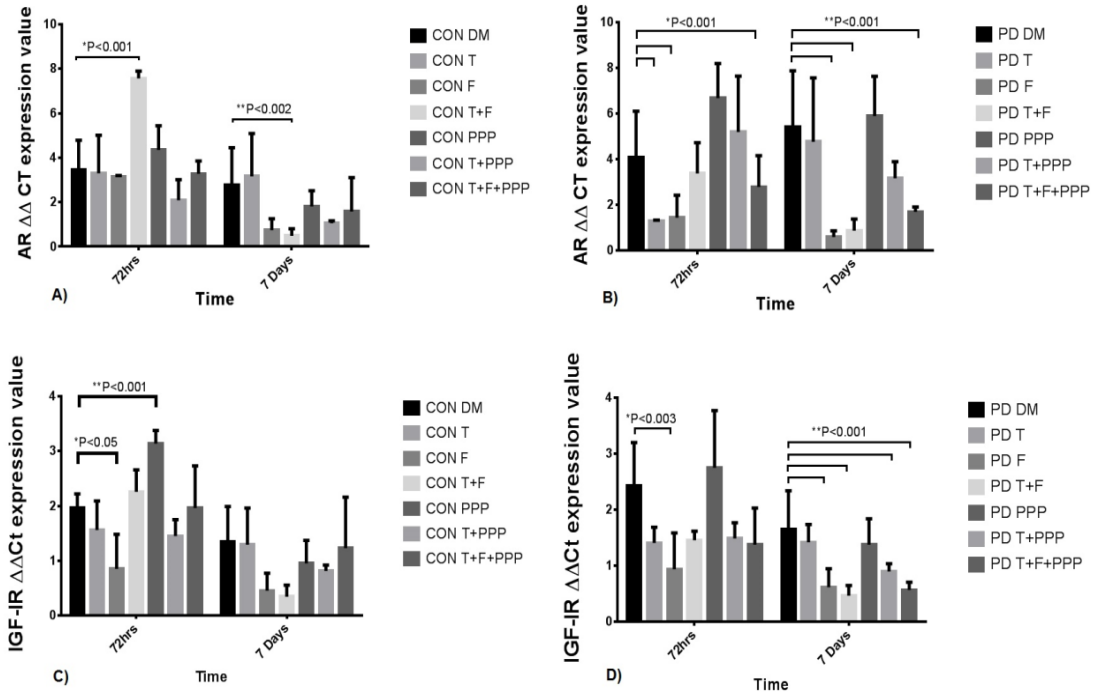

Fig 5.18 The effect of testosterone administration and inhibitor co-incubations on androgen receptor (AR) and IGF-I receptor (IGF-IR) gene transcripts in CON and PD myoblasts after 72 hrs and 7 days. **A**) Testosterone co-incubated with flutamide significantly increased *AR* mRNA expression levels after 72hrs in CON myoblasts (*P < 0.001). This effect was significantly reduced after 7 days (**P < 0.002). **B**) In PD myoblasts, there significant reductions in AR expression with testosteron*et al*one and the presence flutamide after 72 hrs (*P < 0.001). At 7 days, the addition of flutamide alone and co-incubated resulted in *AR* expression remaining decreased (**P < 0.001). **C**) In CON myoblasts, flutamide significantly reduced IGF-IR expression (*P < 0.05) and Picropodophyllin significantly increased IGF-IR levels at the same time point (**P < 0.001). There were no observed alterations at 7 days exposure. **D**) Flutamide significantly reduced IGF-IR expression after 72 hrs in PD myoblasts compared to un-treated cells (*P < 0.003). The presence of flutamide, after 7 days treatment, resulted in significant reductions in IGF-IR expression compared to basal conditions (**P < 0.01).

In CON cells, *AR* expression was significantly reduced when co-incubated with testosterone after 7 days exposure (CON DM 2.76 ± 1.69 vs. T+F 0.49 ± 0.32; P ≤ 0.002, **Fig. 5.18A**). To note, the administration of Picropodophyllin significantly increased *AR* mRNA expression after 72hrs exposure (CON DM

2.76 ± 1.69 vs. PPP 4.35 ± 1.09; P ≤ 0.001, Fig 5.18A). In the PD myoblasts, both the presence of testosterone and flutamide significantly reduced *AR* mRNA after 72hrs (PD DM 4.07 ± 2.04 vs. T 1.28 ± 0.05; F 1.44 ± 0.99; T+F+PPP 2.79 ± 1.37; P ≤ 0.001, **Fig. 5.18B**). For 7 days, the presence of flutamide in treatments significantly reduced *AR* expression (PD DM 5.42 ± 2.46 vs. F 0.59 ± 0.27; T+F 0.87 ± 0.51; T+F+PPP 1.70 ± 0.21; P ≤ 0.001, **Fig. 5.18B**).

The *Igf1* receptor was significantly reduced with flutamide administration after 72 hrs exposure in CON cells (CON DM 1.96 ± 0.26 vs. F 0.85 ± 0.63; P ≤ 0.05, **Fig 5.18C**). The addition of Picropodophyllin significantly increased *Igf1* receptor expression in CON cells at 72 hrs (CON DM 1.96 ± 0.26 vs. PPP 0.95 ± 0.42; P ≤ 0.001, **Fig. 5.18C**), highlighting a possible negative feedback loop. The presence of flutamide significantly reduced *Igf1* receptor expression in PD myoblasts after 7 days exposure (PD DM 1.65 ± 0.69; F 0.62 ± 0.33; T+F 0.47 ± 0.18; T+F+PPP 0.57 ± 0.14; P ≤ 0.001, **Fig 5.18D**). Furthermore, testosterone co-incubated with Picropodophyllin decreased IGF-I receptor mRNA expression after 7 days (PD DM 1.65 ± 0.69 vs. T+PPP 0.90 ± 0.14; P ≤ 0.001, **Fig. 5.18D**). Overall, the presence of flutamide had a significantly detrimental impact on IGF-I and androgen receptors in both cell types. Overall, testosteron*et al*one or in combination had very little impact on these receptors at the mRNA transcript level.

Finally, as myostatin has recently been shown to be responsive to androgens (Dubois *et al*., 2014) the observations in myotube morphology with flutamide administration may be explained by the alterations in *myostatin* mRNA levels. The presence of flutamide significantly increased *myostatin* expression after 7 days exposure in CON myoblasts (CON DM 2.78 ± 1.32 vs. F 8.30 ± 0.85; T+F 7.44 ± 0.52; T+F+PPP 6.01 ± 2.52; P ≤ 0.001, **Fig. 5.19A**). Although not significant, there were trends for myostatin increased levels with the presence of flutamide after 72 hrs in CON myoblasts. Similarly in PD myoblasts, treatments containing flutamide increased *myostatin* expression at both time points, although not statistically significant. After 72 hrs, flutamide co-incubated with testosterone significantly increased *myostatin* expression in PD myoblasts (PD DM 3.83 ± 1.17 vs. T+F 11.39 ± 2.49; P ≤ 0.001, **Fig. 5.19B**). In this experiment, testosterone

and Picropodophyllin had no impact on myostatin expression in either cell type. There were significant differences in myostatin expression between basal CON and PD myoblasts after 7 days culture (CON DM 2.78 ± 1.32 vs. PD DM 8.99 ± 0.47; $P \leq 0.01$). Myostatin has been observed to be detrimental in myotube size and inhibiting muscle differentiation, thus potentially explaining the lack of myotube formation in the current chapter (Trendelenburg *et al*., 2009).

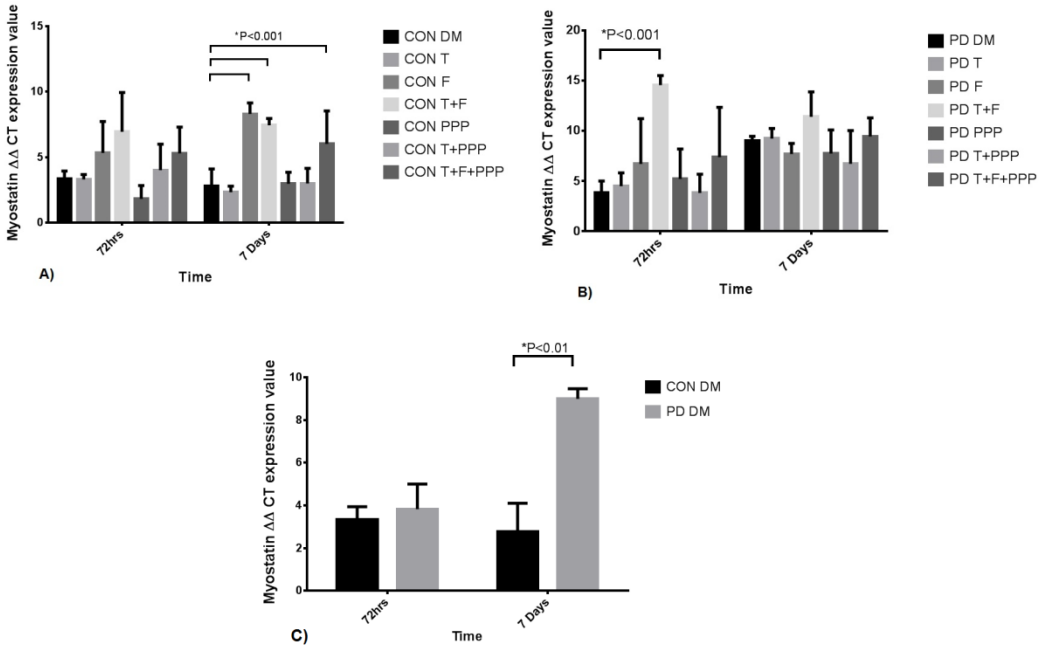

Fig 5.19 The effect of testosterone administration and inhibitor co-incubations on *myostatin* mRNA levels in CON and PD myoblasts after 72 hrs and 7 days. **A**) There were no statistically significant differences in *myostatin* levels between treatments in CON myoblasts after 72 hrs. At 7 days, there were sizeable increases in *myostatin* levels with flutamide presence compared to basal conditions (*$P < 0.001$). **B**) After 72 hrs, the co-incubation of testosterone and flutamide increased myostatin significantly compared to un-treated PD cells ($P < 0.001$). At 7 days, there were no statistically different changes between treatments in PD myoblasts. **C**) There was a significant increase in *myostatin* mRNA levels after 7 days culture between basal CON and PD myoblasts (*$P \leq 0.01$).

5.4 DISCUSSION

This chapter sought to investigate the predominate pathway for mediating testosterone induced hypertrophy as commonly the AR and IGF-I pathway have been investigated independently (Serra *et al*., 2011, White *et al*., 2012, Wu *et al*.,

2010a). The alterations in myotube morphology and protein signalling (discussed below) provide evidence towards a pivotal role for a functional androgen receptor being required in myotube formation and hypertrophy in control and aged phenotypic myoblasts and thus the original hypothesis for both AR and IGF-IR being pivotal in testosterone induced hypertrophy was rejected.

Secondly, the effect of testosterone administration in rescuing an ageing phenotype at the cellular level using a model of cells displaying impaired regeneration and hypertrophy was investigated. The observations in this chapter provide novel insights into the ability of exogenous testosterone to enhance impaired hypertrophy and rescue an ageing phenotype confirming our original hypothesis. Testosterone administration has been utilized in clinical populations where muscle wasting is present (Casaburi *et al*., 2004, Bhasin *et al*., 2000, Sinha-Hikim *et al*., 2006, Atkinson *et al*., 2010). Furthermore, the mechanisms which may be involved in the hypertrophic effect of testosterone were addressed.

5.4.1 Exogenous testosterone administration rescues an ageing phenotype via the androgen receptor and Akt

Similar to the observations observed in Chapter 1, exogenous testosterone had a hypertrophic effect on C_2C_{12} muscle cells highlighted by increases in myotube diameter and myonuclear accretion. In the current chapter, testosterone was able to rescue an ageing phenotype as increases in hypertrophic variables were observed such as myotube diameter. The positive effect of a testosterone stimulus on myotube morphology in CON and MPD myoblasts was accompanied by heightened *myogenin* expression, similar results in chapter 1 and previous literature (Lee, 2002, Wannenes *et al*., 2008). At the transcriptional level, exogenous testosterone had little impact on other genes investigated. Although AR mRNA was significantly down-regulated in the PD myoblasts after 72 hrs culture, opposing the increased alterations observed in total AR protein following testosterone. At the protein level, testosterone significantly increased androgen receptor levels in PD myoblasts, even in the presence of the IGF-I inhibitor (Picropodophyllin). The AR increases in PD myoblasts were significantly greater compared to testosterone stimulated CON myoblasts and provide evidence

towards the rescuing of the ageing phenotype via the androgen receptor. This was accompanied via increases in myogenin, plus when the AR was inhibited alterations in MyoD occurred, providing evidence towards the morphological changes observed.

Recently, Serra and colleagues (2011) highlighted the role of IGF-I signalling in mediating the effects of testosterone on skeletal muscle mass. The authors noted that a testosterone stimulus was mediated via IGF-IR signalling. The inhibition of IGF-IR was achieved through small interference RNA compared to the current chapter which utilized a substrate competitor inhibitor (Picropodophyllin). Contrary to the findings of Serra *et al*, (2011) we observed testosterone induced hypertrophy in both cell types even in the presence of the IGF-I receptor inhibitor, supported by the findings of Wu *et al*. (2010a). The most recent evidence has alluded to the potential role of Akt/mTOR signalling in testosterone induce hypertrophy (Basualto-Alarcón *et al*., 2013, White *et al*., 2012) and it has been proposed a functional IGF-I receptor is not required for skeletal muscle hypertrophy in-vivo (Spangenburg *et al*., 2008). Within the current chapter, mean increases in downstream IGF—IR signaling (Akt phosphorylation) were apparent in the PD myoblasts only with testosterone administration after 72 hrs culture, an observation that continued even in the presence of the IGF-IR inhibitor (PPP), suggesting a direct activation of Akt independently of upstream IGF-IR. PD myoblasts also had basally reduced phosphor Akt at key time points in differentiation (72 hrs) *verses* control myoblasts and therefore Akt may be a mediating target for the testosterone mediated rescue in differentiation of the ageing phenotype myoblasts. The role of testosterone and Akt was investigated in chapter 6.

5.4.2 The critical role of the androgen receptor in skeletal muscle hypertrophy

The androgen receptor (AR) has been observed to be important in skeletal muscle development and muscle differentiation (Wannenes *et al*., 2008), as the knockout of muscle-specific AR results in reduced muscle mass and strength (MacLean *et al*., 2008). In the present chapter, flutamide (AR antagonist)

administration alone was detrimental to myotube formation in both CON and PD myoblasts. The presence of flutamide significantly impacted on Akt, ERK1/2 and p70S6K activation in both cell types which provides evidence towards the reduced protein synthesis required for differentiation and hypertrophy (Adi *et al*., 2002, Baar and Esser, 1999, Jones *et al*., 2001, Rommel *et al*., 2001). Furthermore, the presence of flutamide abrogated testosterone induced hypertrophy in both cell types, even with Picropodophyllin co-incubation, supporting AR in being a critical pathway for muscle hypertrophy under a testosterone stimulus.

Finally, the alterations in gene transcripts may provide an explanation for the impact of flutamide and thus an AR mechanism. In both CON and PD myoblasts with the presence of flutamide, there was a significant increase in myostatin levels. Myostatin has been observed to be a negative regulator of muscle mass and more specifically inhibit muscle differentiation and myotube size (Amthor *et al*., 2004, McCroskery *et al*., 2003, Trendelenburg *et al*., 2009). Although in testosteron*et al*one had no impact on myostatin levels in the current chapter, in other chapters (3 and 6), a testosterone stimulus was observed to reduce myostatin levels. Recently Braga and colleagues (2012), reported the effects of testosterone on TGF-β signalling (pathway detailed in 1.4.4) where testosterone stimulation of muscle proliferation and differentiation occurred due to inhibition of this pathway via follistatin up-regulation. Furthermore, Dubois and colleagues (2014) have highlighted the androgen receptor as a direct target for myostatin expression through using a satellite-cell specific AR knockout mice. Therefore, in relation to the current chapter, the inhibition of the AR may have contributed towards increased myostatin levels as the receptor has previously been observed to regulate follistatin levels, a factor that inhibits the TGF-β family member, myostatin (Amthor *et al*., 2004, Singh *et al*., 2009).

5.4.3 Chapter Summary

In summary, this chapter has highlighted the impact of testosterone in rescuing an ageing phenotype with cells displaying impaired regeneration and hypertrophy. Importantly, the results provide evidence towards the mechanisms for testosterone

induced hypertrophy, where in the presence of testosterone a functional androgen receptor seems fundamental in regulating appropriate myoD, myogenin and myostatin expression in the control of myotube differentiation and hypertrophy. The increases in androgen receptor protein levels in PD myoblasts under a testosterone stimulus highlight the responsiveness of aged myoblasts to a hypertrophic stimulus which may partly explain the use of testosterone as an effective clinical treatment in muscle wasting disease. Finally, myotube hypertrophy occurred in both cell types with testosterone administration even in the presence of an IGF-I receptor inhibitor suggesting a limited role of the IGF-IR and associated signaling in testosterones mediated increases in differentiation and hypertrophy. Testosterone did appear however to increase Akt phosphorylation in cells that show a prior impaired regenerative capacity (PD) only. Therefore in the final chapter (6) the downstream target Akt will be investigated to provide more insight into whether its activity is directly involved in mediating a testosterone stimulus and rescuing an ageing phenotype observed in the present chapter.

6. THE ROLE OF AKT IN TESTOSTERONE-INDUCED HYPERTROPHY IN AGED PHENOTYPE MYOBLASTS

6.1 INTRODUCTION

Recent studies suggest testosterone induced hypertrophy may be mediated by the AR and Akt/mTOR/p70S6K pathway as recent evidence has observed activation of this particular pathway through a testosterone stimulus (Basualto-Alarcón *et al*., 2013, White *et al*., 2012). It is worth noting that the present study suggests that inhibition of the IGF-IR using Picropodophyllin, albeit only knocking down associated IGF-I signaling (Akt/ERK) by 60% and 40% respectively, did not impact on testosterone ability to induce myotube differentiation and hypertrophy. However, Akt was only significantly elevated with testosterone in the cells that display a prior aged phenotype (PD) vs. control cells, even in the presence of the IGF-IR inhibitor, suggesting that Akt could be directly activated by testosterone administration, independently of upstream input from the IGF-IR. The study by White and colleagues (2012) utilized an both an animal castration model and the C_2C_{12} muscle cell line to address the impact of androgen availability on the aforementioned signalling pathway (the AR was not considered within this particular study). Loss of testosterone in the animal model resulted in significantly reduced skeletal muscle mass which was accompanied by reductions in Akt phosphorylation, GSK3, PRAS40 and FoxO3a (all Akt targets). Furthermore, administration of testosterone (5-500 nM) induced activation of Akt in C_2C_{12} muscle cells with 24hrs exposure. Complementary to these findings, Basualto-Alarcón *et al*. (2013) observed an increase Akt phosphorylation after 15 minutes testosterone (100 nM) stimulation. The present data, as eluded to above, from chapter 5, suggests that Akt is not significantly increased with testosterone in control cells but only increased in aged cells and PD cells show a reduction in Akt basally at 72hrs *verses* un-aged controls. Therefore, it appears that Akt seems to be fundamental in testosterones action in aged cells even when the IGF-IR is inhibited (chapter 5). This interaction, if not by IGF-IR, maybe mediated by myostatin, where increases in myostatin has been liked with directly inhibiting Akt (Dubois *et al*., 2014, Léger *et al*., 2008, Morissette *et al*., 2009), and in the

present study we see an increase in myostatin mRNA and corresponding decrease in pAkt when AR's (via flutamide) action is inhibited and the protein level of AR is low (chapter 5). As myostatin has recently been shown to be transcriptionally regulated by AR (Dubois *et al*., 2014) the role of testosterones action in the ability to 1) restore regeneration in aged myoblasts via increasing Akt (chapter 5) and reducing myostatin (present chapter) maybe the important mechanism of action for testosterones restoration of myotube differentiation and hypertrophy in aged cells.

In order to investigate this we cultured control and PD cells in the presence of T and T +/- LY294002 a PI3K/Akt inhibitor and measured the impact on myoblast/myotube morphology and transcriptional regulators of differentiation and hypertrophy (myogenin, mTOR, AR and myostatin). We hypothesized that by inhibiting PI3K/Akt, testosterone's ability to restore differentiation and hypertrophy in PD cells only would be negated.

6.2. MATERIALS AND METHODS

6.2.1 Cell Culture

Mouse C_2C_{12} skeletal muscle myoblasts (CON and PD; outlined in 2.4.2) were resurrected as described in 2.6 and cultured as outlined in 2.4.1. Cells at the time points of 0, 72 hrs and 7 days were fixed for morphological analysis (outlined in 2.10), isolated for RNA (outlined in 2.14.2 and 2.11).

6.2.2 Cell Treatments

All treatments were administered in DM described above. The treatments comprised of a vehicle control (DMSO at a concentration of 0.01%), Testosteron*et al*one (T) 100 nM (Tocris Bioscience, Bristol, UK), PI3K inhibitor (LY) 5 μM (LY294002- Calbiochem, Middlesex, UK), 100 nM T + 5 μM LY. DMSO was used as the solvent for T reconstitution at the same concentration as the vehicle (0.01%). For results and figure legends the following nomenclature will be used DMSO, T, LY and T + LY respectively. All treatments were added at 0 hrs and existing media was further supplemented at 72 hrs. The inhibitor, LY at a dose of 5 μM has been extensively shown to be highly specific and effective in

C_2C_{12} cells in inhibiting PI3K and downstream Akt (Al-Shanti *et al*., 2011, Coolican *et al*., 1997, Frost *et al*., 2009, Lee, 2009, Li *et al*., 2005a, Zeng *et al*., 2012).

6.2.3 RNA Isolation

6 well plates for each time point (0hrs, 72hrs and 7 days) were washed with 1ml per well of Phosphate Buffer Saline (PBS) and extracted for RNA by placing 300µl of TRIzol™ Reagent (Sigma, St Louis) in each well. RNA extraction and quantification was performed as stated in chapter 3,4 and 5.

6.2.4 Reverse Transcription Quantitative Real Time Polymerase Chain Reaction (rt-qRT-PCR)

Seventy nanograms of RNA were taken from each sample and real time, reverse transcription polymerase chain reaction (RT-rt-PCR) was performed as detailed in 2.12.3. Primer sequences for genes of interest are shown in **table 2.1** and were checked for specificity according to 2.12.2. Analysis was performed as detailed in Chapter 3, 4 and 5.

6.2.5 Morphological Analysis

Following media aspiration and 2 × PBS washes (1 ml/well), cells were fixed by adding 1 ml methanol/acetone (1:1) to 1 ml PBS in each well in a drop-wise manner and incubated for 10 mins RT. Following aspiration, 2 ml methanol and acetone (1:1) were added to each well and incubated for a further 10 mins. Finally PBS (2ml/well) was added after removal of the methanol and acetone mix and plates were stored at 4^oC until further analyses. This fixing process allows nuclei to become discernible under light microscopy alone, without the need for additional nuclear staining. Quantification was performed as outlined in 2.10.3 and chapter 4.

6.2.6 Statistical Analyses

Experiments were performed separate times (n = 3) in triplicate. Data are presented as mean $\pm$ S.D. Morphology data at 72 hrs were assessed using a (2×2) mixed two-way factorial ANOVA (GraphPad Software, Inc., San Diego, USA)

for interactions between cell type (PD, CON) and treatments (DMSO, T). LY and T+LY treatment were excluded from the aforementioned analysis, as there were no observable myotubes at 72 hrs in these conditions. Morphology data at 7 days were assessed using a (2×4) mixed two-way factorial ANOVA for interactions between cell type (PD, CON) and treatments (DMSO, T, LY and T + LY). Gene expression data were assessed using a (2×2×4) mixed three-way factorial ANOVA for interactions between cell type (PD, CON), time (72 hrs and 7 days) and treatments (DMSO, T, LY and T + LY). Bonferroni post hoc analyses were performed where main effects for treatment or cell type occurred, without a significant interaction between treatment and cell type. If significant interactions were present, independent t-tests were conducted to confirm statistical significance between variables of interest. Furthermore, paired-sample t-tests were undertaken for variable of interests within cell type and treatment. Myonuclear Accretion (fusion index) measures were analysed using Chi Square to investigate whether myotube categories (3-4 nuclei or 5+ nuclei) differed from one another based on treatment exposure. A P-value of ≤ 0.05 was considered to represent a statistically significant difference.

6.3. RESULTS

6.3.1 Exogenous T treatment increases myotube hypertrophy in both CON and PD cells

The administration of exogenous DMSO, T, LY, T+LY to CON and PD cells brought about morphological changes in differentiation (**Figs 6.1 & 6.2**). Firstly, it is important to mention that in support of previous observations showing reductions in differentiation in PD vs. CON cells (Sharples *et al*., 2011) as well as chapter 4 and 5; a significant difference for mean myotube diameter at 72 hrs was again observed in the present study (CON 17.32 ± 2.56 vs. PD 14.58 ± 2.66, P = 0.01, **Fig. 6.3A**), supporting the ageing phenotype observed previously in PD cells (Sharples *et al*., 2011, Sharples *et al*., 2012) as well as in chapter 4 and 5. Importantly, in the present study, T administration appeared to increase hypertrophy (myotube diameter) in both cell types. Statistical analyses confirmed the morphological observations in **Fig. 6.1** and **6.2** and revealed that a T-stimulus

significantly increased myotube diameter in both CON and PD cells after 72 hrs (CON+T 21.02 ± 1.89 vs. CON 17.32 ± 2.56; PD+T 18.29 ± 3.08 vs. PD 14.58 ± 2.66, P = 0.01, **Fig. 6.3A**) and 7 days (CON+T 22.03 ± 2.65 vs. CON 17.50 ± 2.38; PD+T 20.49 ± 1.99 vs. PD 15.70 ± 1.59, P = 0.01, **Fig. 6.3A**) compared with non-treated cells, respectively.

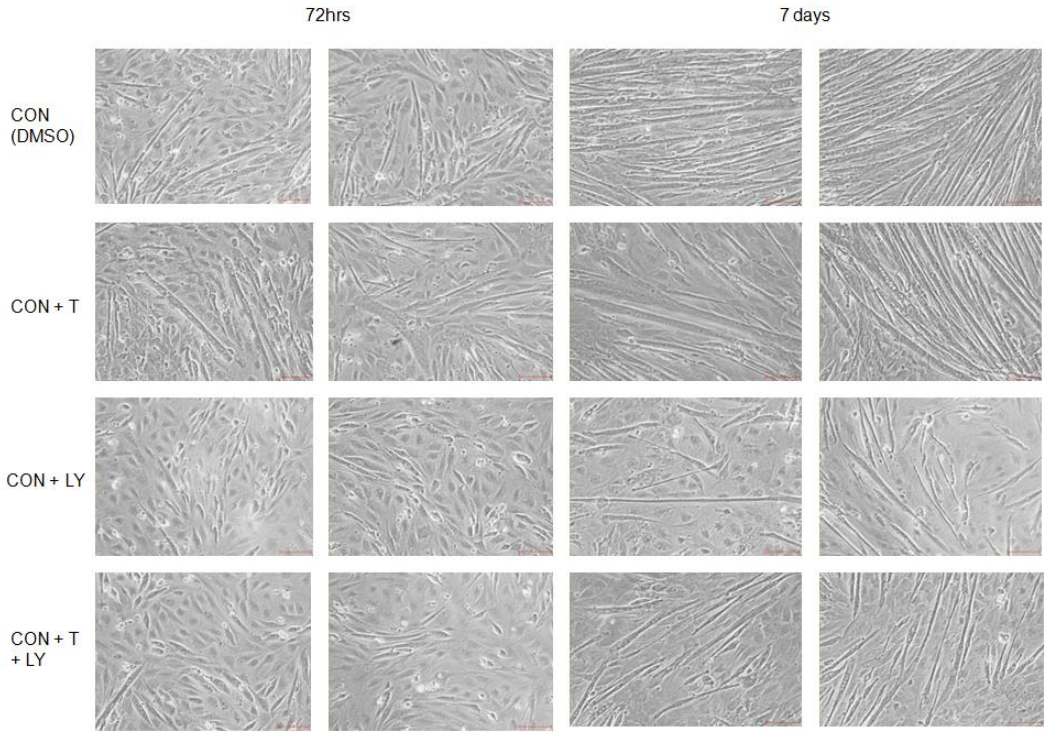

Fig 6.1 Representative light microscope images (x10 magnification) of treatments (DMSO, T, LY, T+LY) exposed to the CON cell type after 72 hrs and 7 days. The presence of T increased myotube number and size after 72hrs and 7 days culture. The presence of LY abrogated the hypertrophic effects of T.

Importantly, the magnitude of change between both cell models in response to T administration and compared with their respective baseline controls was not significantly different at either time points, with T increasing myotube diameter in both PD (+25% and +23%) and CON (+21% and +20%) cells to the same extent after 72 hrs (**Fig. 6.3A**) and 7 days (**Fig. 6.3C**); respectively, confirming the findings in Chapter 5 where we showed T increasing myotube diameter in both PD (23% and 17%) and CON (15% and 16%) after 72 hrs (**Fig 5.5E**) and 7 days (**Fig. 5.5E**). Overall, this suggests that cells with a reduced differentiation phenotype have the same capacity to undergo hypertrophy in

response to exogenous testosterone administration as CON cells as previously reported in chapter 5. Furthermore, the addition of T significantly increased myotube number in CON cells (CON+T 2.90 ± 0.72 vs. CON 2.23 ± 0.68, P ≤ 0.05, **Fig. 6.3D**) after 7 days exposure only (at 72 hrs although there were mean increases this was not statistically significant (P = N.S.)). There were no significant changes in myotube number in PD cells after 72 hours or 7 days exposure (P = N.S.). This suggests testosterone increases hypertrophy (myotube diameter) in both cells types; however, T only enhanced myotube number in CON cells at 7 days.

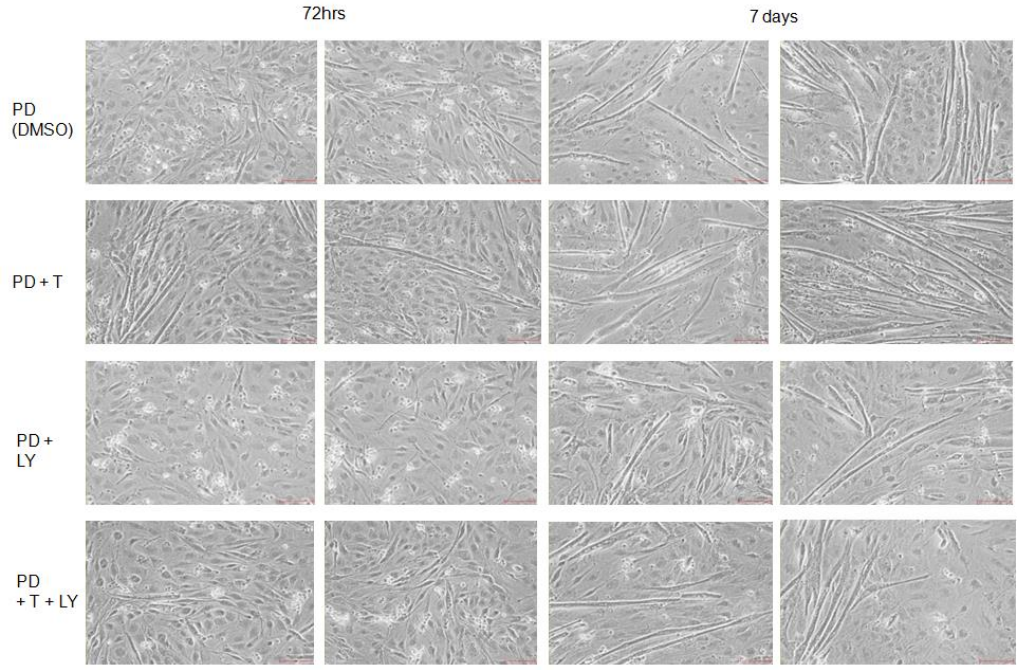

Fig 6.2 Representative light microscope images (x10 magnification) of treatments (DMSO, T, LY, T+LY) exposed to the PD cell type after 72 hrs and 7 days. The administration of T was able to reverse the aged phenotype observed in PD myoblasts at both time points. The presence of LY negated the hypertrophic effect of T, suggesting the role of Akt in mediating the effects of T.

Together with the changes in myotube diameter at both 72 hrs and 7 days, T significantly increased the mean number of nuclei per myotube in CON cells (CON 3.77 ± 0.86 vs. CON+T 4.98 ± 1.76, P ≤ 0.001, **Fig. 6.3B**) at 72 hrs and at 7 days (CON 3.68 ± 0.67 vs. CON+T 4.91 ± 1.10, P ≤ 0.01, **Fig. 6.3B**). Furthermore, in the PD cells, a similar response was observed for nuclei/tube in the presence of T at 72 hrs (PD+T 4.27 ± 1.03 vs. PD 3.33 ± 0.71, P = 0.03, **Fig.**

6.3B), and 7 days (PD+T 5.18 ± 1.31 vs. PD 3.84 ± 0.71, P ≤ 0.001 **Fig. 6.3B**) exposure compared to non-treated cells. Interestingly, again there were similar magnitude increases in CON and PD cells in the presence of T vs. basal conditions at 72 hrs (24.3% CON vs. 22% PD) and 7 days (25.1% CON vs. 25.9% PD), confirming the observations in chapter 5.

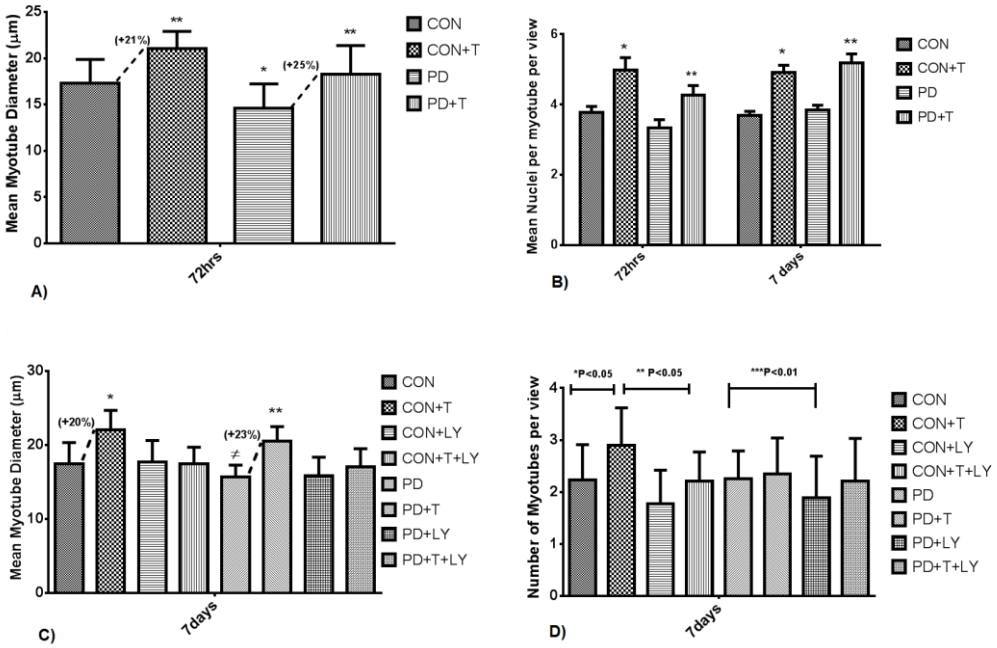

Fig 6.3 The effect of T-stimulus on CON and PD cells on various morphology variables after 72 hrs and 7 days exposure. **A**) The effect of T-stimulus on mean myotube diameter for CON and PD cells after 72 hrs exposure. *Reduced mean myotube diameter between CON and PD cells (P ≤ 0.01). **T-stimulus significantly increased mean myotube diameter vs. non-treated CON and PD (P ≤ 0.01). Dash line represents magnitude change in mean myotube diameter with T-stimulus, similar in both CON (+21%) and PD (+25%) cells. A similar pattern was observed at 7 days (CON +20%; PD +23%). **B**) The changes in mean nuclei per myotube at 72 hrs and 7 days with and without exogenous T administration. *T significantly increased mean nuclei per myotube in CON (+24%; P ≤ 0.001) cells after 72 hrs and 7 days (+25%; P ≤ 0.001) exposure vs. non-treated cells. **Furthermore T-treatment in PD cells increased mean nuclei per myotube after 72 hrs (+22%; P = 0.033) and 7 days exposure (+25%; P ≤ 0.001). **C**) The effect of T in the presence of LY is attenuated for mean myotube diameter after 7 days culture. *The presence of LY significantly reduced the effect of T on myotube diameter (P ≤ 0.05) in CON cells. **A similar effect was observed in PD cells (P ≤ 0.05). ≠ Myotube diameter significantly remained reduced in PD vs. CON cells, similar to that observed at 72 hrs (see Fig. 2A) (P ≤ 0.05). Dash line represents magnitude change in mean myotube diameter with T-stimulus, similar in both CON (+20%) and PD (+23%) cells. It appears that T's action on myotube hypertrophy requires the activity of the

PI3K/Akt pathway in both cell types. **D)** The effect of T and LY treatment on myotube number in CON and PD cells at 7 days. *T-treated CON cells significantly exhibited a greater number of myotubes compared to non-treated cells ($P \leq 0.05$). **The addition of LY alone and in the presence of T significantly reduced the number of myotubes compared to T-treated CON cells ($P \leq 0.05$). ***In PD cells, LY alone significantly reduced myotube number ($P \leq 0.01$) at 7 days, with all other treatments showed no significant effects.

6.3.2 PI3K/Akt inhibitor (LY) inhibits testosterone-induced increases in differentiation and hypertrophy for CON and PD cells

The presence of LY inhibitor alone led to a lack of differentiation with no quantifiable myotubes being present in both CON and PD cells at 72 hrs (**Fig. 6.1 & 6.2**). As highlighted above; the addition of T significantly increased differentiation shown by enhanced myotube number in CON cells (CON+T 2.90 ± 0.72 vs. CON 2.23 ± 0.68, $P \leq 0.05$, **Fig. 6.3D**) after 7 days exposure. The presence of LY co-incubated with T significantly reduced the effect on myotube number (CON+T+LY 2.21 ± 0.56 vs. CON+T 2.90 ± 0.72, $P \leq 0.05$, **Fig. 6.3D**). LY alone was also able to reduce myotube number vs. T treatment (CON+LY 1.77 ± 0.65 vs. CON+T 2.90 ± 0.72, $P \leq 0.05$, **Fig 6.3D**) and non-treated controls (2.23 ± 0.68, $P \leq 0.01$, **Fig 6.3D**). Interestingly, T in the presence of the LY inhibitor was unable to restore differentiation, shown by non-significant differences with LY alone conditions (P = N.S.) and non-treated CON cells (**Fig. 6.3D**). These observations highlight that Ts increase in myotube number in CON cells, as previously observed, is blunted in the presence of the LY inhibitor; returning differentiation back to basal levels. As previously highlighted there were no significant changes in myotube number after T administration in PD cells. However, LY alone was able to reduce myotube number vs. T treatment (PD+LY 1.89 ± 0.80 vs. PD+T 2.35 ± 0.69, $P \leq 0.05$, **Fig 6.3D**) and non-treated controls (PD 2.26 ± 0.53, P = 0.05, **Fig 6.3D**). Overall, T's action appears to require the activity of the PI3K/AKT pathway in order to differentiate in both CON and PD myoblasts.

Following these observations for indices of differentiation we next wished to ascertain the impact of T in the presence of the PI3K inhibitor (LY) on myotube hypertrophy. At 7 days, as previously highlighted above, the addition of T

significantly increased myotube diameter in CON and PD cells (**Fig. 6.3C**). The presence of LY co-incubated with T significantly reduced the effect on myotube diameter in both CON (CON+T+LY 17.49 ± 2.21 vs. CON+T 22.03 ± 2.65, P ≤ 0.05, **Fig. 6.3C**) and PD cells (PD+T+LY 17.10 ± 2.40 vs. PD+T 20.49 ± 1.99, P ≤ 0.05, **Fig. 6.3C**). LY alone was also able to reduce myotube diameter vs. T treatment in CON cells (CON+T 22.03 ± 2.65 vs. CON+LY 17.7 ± 2.91, P ≤ 0.05, **Fig 6.3C**). Similar observations were observed in PD cells (PD+T 20.49 ± 1.99 vs. PD+LY 15.83 ± 2.53, P ≤ 0.05, **Fig 6.3C**). Interestingly, T was unable to restore myotube diameter in the presence of the LY inhibitor shown by non-significant differences with LY alone conditions in CON cells and non-treated CON cells (P = N.S, **Fig. 6.3C**). The same observations were mirrored in PD cells where T was unable to restore myotube diameter in the presence of the LY inhibitor shown by non-significant differences with LY alone conditions in PD cells (P = N.S, **Fig. 6.3C**). Overall, this shows that T's observed increases in hypertrophy was blunted in the presence of the LY inhibitor returning myotube diameter back to basal levels in both cell types.

6.3.3 T-treatment enhancement in differentiation and hypertrophy is accompanied by increases in cell fusion

To address the effects of the various treatments on cell fusion, myonuclear accretion was calculated. The administration of T resulted in a greater percentage of myotubes expressing 5+ nuclei for both CON (CON+T 67.9% vs. CON 32.1%, χ_1^2= 32.99, P ≤ 0.05) and PD cells (PD+T 67.2% vs. PD 32.8%, χ_1^2= 20.58, P ≤ 0.05) compared to untreated cells after 7 days exposure (**Fig 6.4A & 6.4B** respectively). Furthermore, the addition of LY with T treatment reduced the percentage of myotubes expressing 5+ nuclei back to similar levels of LY-alone treated cells (CON+T+LY 28.1% vs. CON+LY 15.2%, χ_1^2= 2.53, P = N.S; PD+T+LY 37.5% vs. PD+LY 21.6%, χ_1^2= 3.4, P=N.S, **Fig 6.4A & 6.4B** respectively). In accordance with these observations, there was no significant difference in total nuclei counts for all treatments in either cell type at both time points (P = N.S). There was however a significant interaction between cell type as the PD cells had a significantly higher total nuclei count (P ≤ 0.05) compared to

CON cells at both time points, a finding confirmed previously by Sharples *et al.* (2011), who highlighted a continued proliferation at the expense of exiting the cell cycle in G1 and differentiating.

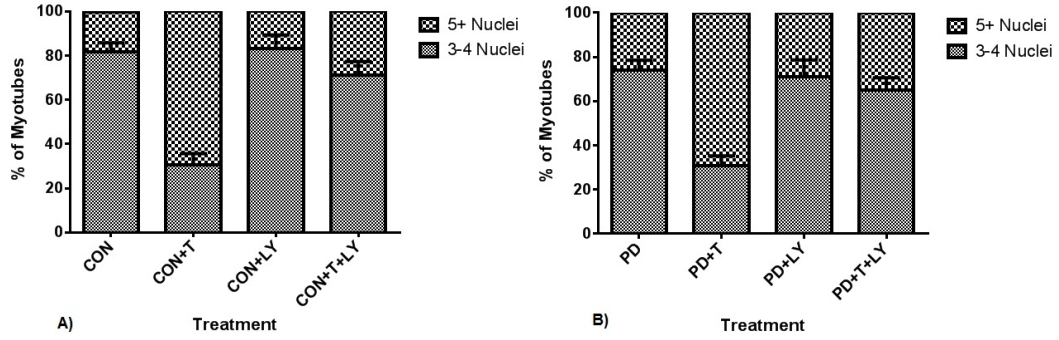

Fig 6.4 The effect of T and LY treatment on fusion index in CON (A) and PD (B) cells after 7 days exposure. T-treatment significantly increased the percentage of myotubes expressing 5+ nuclei in both cell types ($P \leq 0.05$). The co-incubation of T and LY reduced the percentage of 5+ multi-nucleated myotubes back to similar levels of un-treated cells in both cell types at the same time point.

6.3.4 Expression of *myogenin* mRNA increases after T-administration in both PD and CON cells

There was a significant difference in *myogenin* transcript expression levels between CON and PD cells after 72 hrs (CON 191.51 ± 12.84 vs. PD 48.58 ± 8.14, $P \leq 0.001$, **Fig. 6.5A**) and 7 days exposure (CON 128.36 ± 27.11 vs. PD 59.22 ± 4.57, $P \leq 0.001$, **Fig. 6.5A**). Whilst still remaining significantly different, the expression of *myogenin* significantly increased in both CON and PD cells when treated with T (CON+T 222.18 ± 36.63 vs. CON 191.51 ± 12.84; PD+T 67.00 ± 5.35 vs. PD 48.58 ± 8.14, $P \leq 0.05$, **Fig. 6.5A**) after 72 hrs. The increase in *myogenin* mRNA expression also continued at 7 days in PD treated cells (PD + T 74.15 ± 8.13 vs. PD 59.22 ± 4.57, $P \leq 0.001$, **Fig. 6.5A**), yet there was no difference in *myogenin* mRNA expression at this time point between non-treated and T-treated CON cells. However, absolute levels of *myogenin* transcript expression were basally significantly higher (shown above) in CON treated cells *verses* PD treated (CON+T 131.46 ± 24.53 vs. PD+T 67.00 ± 5.35, $P = 0.001$) cells at 7 days. The presence of LY, significantly reduced *myogenin* expression

after 72 hrs exposure in CON cells (CON+LY 134.38 ± 16.13 vs. CON 191.51 ± 16.00, P ≤ 0.05 **Fig. 6.5A**), with no reductions being observed in PD cells at the same time point. Furthermore, LY alone had no effect on *myogenin* mRNA expression after 7 days culture in either cell type (P = N.S **Fig. 6.5A**).

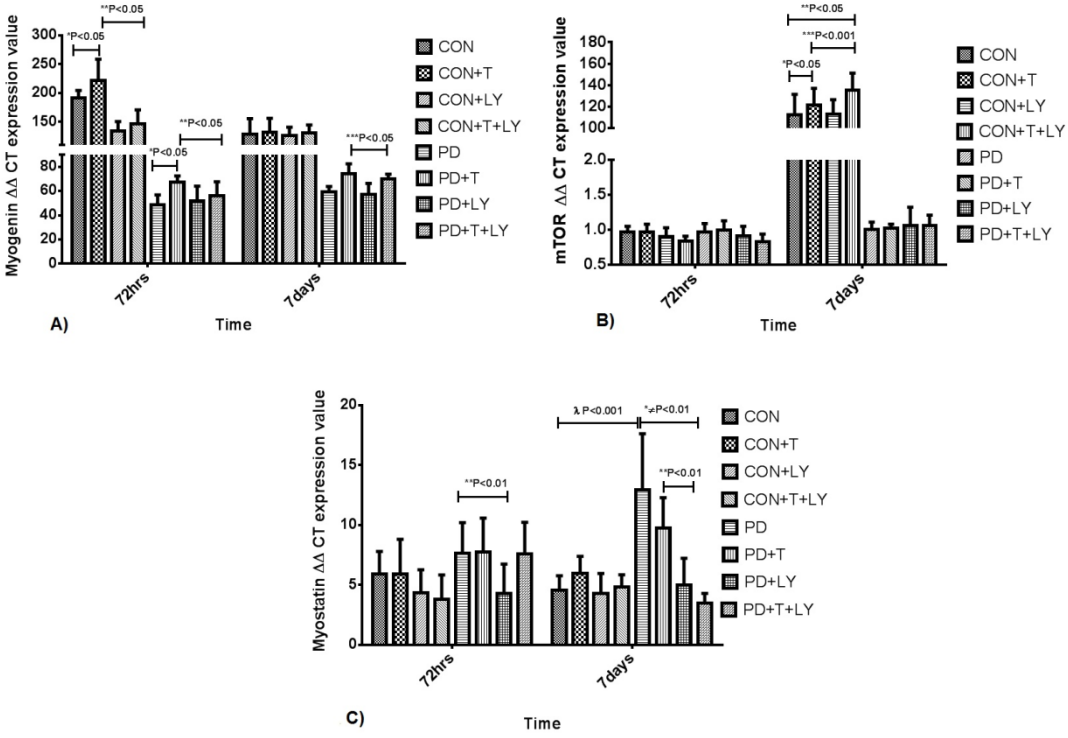

Fig 6.5 The effect of T-stimulus on transcript mRNA expression for *myogenin* (**A**), *mTOR* (**B**) and *myostatin* (**C**) in CON and PD cells. **A)** The effect of T-stimulus on *myogenin* mRNA expression levels after 72 hrs exposure. *T-stimulus significantly increased myogenin expression in CON and PD cells compared to non-treated cells (P ≤ 0.05). **The presence of LY with T treatment significantly attenuated T's effect in CON cells (P ≤ 0.05). ***T exposure continued to increase *myogenin* mRNA in PD cells after 7 days culture, even in the presence of LY (P ≤ 0.05). **B)** Changes in *mTOR* mRNA expression with various treatments to CON and PD cells after 7 days culture. *CON+T and **CON+T+LY significantly increased *mTOR* expression vs. CON untreated cells (P ≤ 0.05). ***There was a significant difference in *mTOR* expression between CON+LY and CON+T+LY (P ≤ 0.001). Additionally there was a significant difference in *mTOR* expression between untreated CON and PD cells in 7 days culture. There were no changes in PD cells with the same treatments at either time points. **C**) The effect of T-stimulus on myostatin mRNA expression after 7 days exposure. *T significantly reduced *myostatin* expression in the PD treated cells after 7 days (P ≤ 0.01). **LY alone significantly reduced myostatin levels (P ≤ 0.01) at 72 hrs and 7 days. ≠ Plus with the addition of T to LY, this reduction was heightened (P ≤ 0.01) compared to non-treated PD cells.

T in the presence of LY inhibitor significantly attenuated *myogenin* expression after 72 hrs when compared with T alone in both cell types (CON+T 222.18 ± 36.63 vs. CON+T+ LY 146.09 ± 24.58, $P \leq 0.05$; PD+T 67.00 ± 5.35 vs. PD+T+LY 56.04 ± 11.50, $P \leq 0.05$, **Fig. 6.5A**). At 7 days, there were no significant changes for any treatment conditions in CON cells (P = N.S for all comparisons) for *myogenin* expression. However in PD cells, T further enhanced myogenin expression significantly, even when administered in the presence of LY (PD 59.22 ± 4.57 vs. PD+T+LY 69.93 ± 3.98, $P \leq 0.05$; PD+LY 57.04 ± 9.22 vs. PD+T+LY 69.93 ± 3.98, $P \leq 0.05$, **Fig. 6.5A**). Thus, T caused an increase in *myogenin* expression in both cells types, whether LY was present or absent. This may suggest at the molecular level at least, that T elevates *myogenin* expression, independently of PI3K/Akt, but appears to be not sufficient enough to rescue morphological differentiation/hypertrophy in PD cells.

6.3.5 Testosterone increases mTOR expression in the presence of PI3K inhibitor in CON cells

The expression of *mTOR* did not change after 72 hrs in either cell type (CON 0.97 ± 0.08 vs. PD 0.97 ± 0.12, **Fig. 6.5B**). After 7 days exposure, T administration alone significantly increased *mTOR* mRNA expression compared to CON non-treated cells (CON+T 121.08 ± 15.87 vs. CON 111.95 ± 19.36, $P \leq 0.05$ **Fig. 6.5B**). Furthermore, the treatment of T + LY significantly increased *mTOR* mRNA compared to LY alone (CON+T +LY 135.14 ± 16.08 vs. CON+LY 112.70 ± 13.62, $P \leq 0.001$, **Fig. 6.5B**) and untreated controls (CON+T +LY 135.14 ± 16.08 vs. CON 111.95 ± 19.36, $P \leq 0.05$). This highlights T administration increases in *mTOR* expression even in the presence of LY. In the PD cells, all treatments were without effect on *mTOR* expression at 7 days exposure (**Fig. 6.5B**). However, at 7 days under basal conditions, CON cells displayed significantly higher *mTOR* expression than PD cells (CON 111.95 ± 19.36 vs. PD 1.01 ± 0.10, $P \leq 0.05$, **Fig. 6.5B**).

6.3.6 T-stimulus reduces negative muscle mass regulator myostatin in PD cells only

Myostatin transcript expression was slightly elevated in PD cells after 72 hrs compared to CON, although these elevations were not statistically significant (CON 5.93 ± 1.87 vs. PD 7.63 ± 2.58, **Fig. 6.5C**). However, at 7 days, statistically significant observations were observed for increases in *myostatin* mRNA expression in PD cells compared to CON cells (PD 12.93 ± 4.69 vs. CON 4.57 ± 1.20, $P \leq 0.001$ **Fig. 6.5C**), confirming the findings in chapter 5. This novel finding suggests that under basal conditions, myostatin may block differentiation in these myoblasts and thus contribute towards reduced myotube hypertrophy. In CON cells, T treatments, LY alone or co-incubations of T+LY at 72 hrs did not alter *myostatin* mRNA expression (**Fig. 6.5C**). The presence of LY alone was the only treatment to significantly reduce *myostatin* mRNA expression after 72 hrs exposure to PD cells (PD+LY 4.27 ± 2.47 vs. PD 7.63 ± 2.58, $P \leq 0.01$ **Fig. 6.5C**).

At 7 days, there were no changes in *myostatin* mRNA expression in CON cells (CON 4.57 ± 1.20; CON+T 5.99 ± 1.40; CON+LY 4.32 ± 1.65; CON+T+LY 4.84 ± 1.01, **Fig. 6.5C**). However in the PD cells, T treatment significantly impaired elevations in *myostatin* expression compared to PD non-treated cells (PD + T 9.73 ± 2.56 vs. PD 12.93 ± 4.69, $P \leq 0.05$, **Fig. 6.5C**). The reduction in *myostatin* transcript expression was significantly larger in magnitude with the addition of T with LY (-36%) in PD cells at the 7 day time point (PD + T + LY 3.47 ± 0.83 vs. PD 12.93 ± 4.69, $P \leq 0.01$ **Fig. 6.5C**), yet similar effects were not observed in CON cells. However, the presence of LY alone also brought about reductions in *myostatin* expression (PD+LY 4.98 ± 2.25 vs. PD 12.93 ± 4.69, $P \leq 0.001$, **Fig. 6.5C**) and the reductions were similar to T+LY (P = N.S). Overall, suggesting both LY and testosteron*et al*one reduce myostatin expression in PD cells only. It therefore appears that T potentially reduces myostatin expression in aged PD cells only suggesting a potential mechanism that may explain the increase in differentiation/hypertrophy seen in this cell type, whereas in CON cells, the increases with T are independent of myostatin expression.

6.4 DISCUSSION

The present chapter supports the findings in chapter 5, for testosterone in enhancing myogenic differentiation and myotube hypertrophy (Lee, 2002, Singh *et al*., 2003, Singh *et al*., 2009, Sinha-Hikim *et al*., 2003, Sinha-Hikim *et al*., 2006, Wannenes *et al*., 2008). In the current chapter and chapter 5, testosterone was observed to rescue the ageing phenotype with increases in hypertrophic variables such as myotube diameter in the PD myoblasts. Enhanced myotube hypertrophy (chapter 5) in PD myoblasts was accompanied by increased Akt phosphorylation, for which the Akt/mTOR pathway has most recently been linked to mediating the effects of testosterone (Basualto-Alarcón *et al*., 2013, White *et al*., 2012). Thus the current chapter of work set out to inhibit Akt using LY294002, the results of which are discussed in more detail in section 6.4.1.

Interestingly, testosterone improved hypertrophy (myotube diameter) to the same magnitude in both cell types at 72 hrs and 7 day time points, confirming the findings reported in chapter 5. Thus, despite PD cells having undergone multiple population doublings *verses* their controls, and therefore displaying a reduced basal differentiation capacity as previously described in Sharples *et al*. (Sharples *et al*., 2011, Sharples *et al*., 2012); testosterone was able to exert similar magnitude increases in myotube hypertrophy. Despite this interesting observation, testosterone was unable to fully restore differentiation (myotube number) to the level observed in untreated control cells at 7 days; perhaps suggesting testosterones predominant role in hypertrophy rather than differentiation in this model. Indeed in chapter 5, testosterone was not able to enhance myotube differentiation (unable to quantify myotube number) but did enhance hypertrophy in myotubes observed after 72 hrs culture. Furthermore, in line with previous findings, the current chapter and data presented in chapters 4 and 5, the PD cells had reduced myogenin expression vs. CON cells (Sharples *et al*., 2011, Sharples *et al*., 2012), with the present chapter also supporting previous morphological and biochemical (reduced CK activity, marker of differentiation) findings (Sharples *et al*., 2011, Sharples *et al*., 2012), as myotube diameter was reduced in the PD cells. Overall, the findings in both chapters 5 and 6 further consolidate the use of these

cells as a representative model to investigate cellular and molecular mechanisms of aged (PD) phenotypes.

6.4.1 The Impact of testosterone induced hypertrophy and Akt inhibition

Importantly, testosterone mediated increases in myotube hypertrophy were potentiated via the PI3K/Akt pathway, where inhibition of this pathway in the presence of testosterone rendered the hormone unable to exert its potent influence on myotube hypertrophy in both cell types. This study supports previous work where the PI3K/Akt pathway has been implicated in testosterones action in L6 myoblasts (Wu *et al*., 2010a) and human skeletal myoblasts (Serra *et al*., 2011) where the same PI3K inhibitor (LY294002) also reduced testosterone induced hypertrophy. Kovacheva and colleagues (2010) have also previously reported that Akt signalling downstream of PI3K was restored by testosterone administration in elderly mice. The present study further supports that testosterones action in myotube hypertrophy is mediated via PI3K/Akt pathway, especially where reductions in Akt activation have been previously reported in this model (i.e. lower in PD vs. CON) (Sharples *et al*., 2011). Indeed in chapter 5, Akt phosphorylation was significantly altered between basal CON and PD myoblasts after 72 hrs and 7 days (**Fig 5.14**), highlighted a delayed response in Akt signalling. Overall, these observations further suggest that the manipulation of this pathway by testosterone may be imperative for therapeutic restoration of muscle atrophy (Bodine *et al*., 2001).

Interestingly, exogenous testosterone improved myogenin expression independent of the PI3K inhibitor (LY294002) suggesting testosterone-mediated activation of myogenin independently of the PI3K/Akt signalling pathway. Testosterone has previously been shown to increase myogenin in C_2C_{12} cells (Lee, 2002, Wannenes *et al*., 2008). Indeed, community-dwelling older men treated with grades doses of testosterone show increases in muscle fibre size accompanied by increased myogenin expression (Bhasin *et al*., 2005, Sinha-Hikim *et al*., 2006). Despite this, testosterone induced increases in myogenin observed in the presence of PI3K inhibitor were unable to restore the differentiation/hypertrophy impinged by the PI3K inhibitor alone. Therefore,

suggesting that myogenin was not the main mechanism of action in testosterone-induced increases in differentiation and hypertrophy. Despite this in chapter 5 myogenin is severely reduced where androgen receptor function is inhibited via flutamide administration alone, suggesting functional AR is required for appropriate myogenin expression without testosterone. However, in chapter 5, there are also observed increases in AR protein levels under a testosteron*et al*one stimulus with increases in myogenin in CON cells in chapters 5 & 6. Therefore this suggests an association with testosterone, functional AR and myogenin expression. Absolute levels of myogenin were severely reduced in PD vs. CON cells with testosterone unable to rescue absolute myogenin expression levels in the cells that display an aged phenotype (PD's) to those observed in untreated control cells. Thus, perhaps highlighting myogenin's more pertinent role in differentiation (not hypertrophy) as testosterone was unable to restore absolute levels of myogenin and corresponding myotube numbers in PD cells *verses* untreated control levels.

6.4.2 Possible involvement of mTOR in mediating Testosterone induced hypertrophy

In addition, testosterone increased mTOR expression in CON cells at 7 days, previously testosterone has been shown to increase mTOR phosphorylation in both L6 rat (Wu *et al*., 2010a) and in C_2C_{12} (White *et al*., 2012) myoblasts. Indeed, mTOR mRNA expression in CON cells was increased in the presence of testosterone plus PI3K inhibitor (LY), perhaps suggesting an important role for testosterone in increasing mTOR independently of PI3K/Akt. Furthermore, White and colleagues (2012) also observed increases in mTOR phosphorylation with incremental doses of T in C_2C_{12} cells, independently of Akt activation. However, mTOR expression was not increased in PD cells in the presence of testosteron*et al*one or in combination with the PI3K inhibitor suggesting impaired *mTOR* transcript expression in response to exogenous testosterone in the aged, reduced differentiation phenotype PD vs. control cells. Previously, it has been observed that reduced IGF-I transcript expression with corresponding reductions in Akt phosphorylation in PD myoblasts (Sharples *et al*., 2011) and in chapter 5 (**Fig**

5.14). As Akt is upstream of mTOR this suggests Akt may be involved in the reduction of mTOR observed between CON and PD myoblasts basally at 7 days. However, activity of mTOR was not directly assessed in the present chapter and warrants further investigation.

The observations towards mTOR expression may have implications towards the findings in chapter 5 and in the current chapter as myostatin over-expression has previously been reported to down-regulate Akt/mTOR signalling (Amirouche *et al*., 2009) as well as the Akt/mTOR/p70S6K pathway inhibiting myostatin (Welle *et al*., 2009). Therefore the involvement of testosterone in stimulating mTOR may explain the reductions in myostatin in the current chapter, but also may explain the increases in myostatin with the inhibition of the AR, as flutamide treatments (chapter 5) resulted in significant reductions in Akt and p70S6K phosphorylation. However, the role in which mTOR interacts with AR, Akt and myostatin remains to be elucidated in this model. The combined observations in chapter 5 and 6, do provide evidence towards a cross talk between the AR and Akt/mTOR/p70S6K pathway with regards to myostatin regulation.

6.4.3 Testosterone suppresses the myostatin levels in aged myoblasts

Myostatin is a negative regulator of muscle mass in many species (Dominique and Gérard, 2006, McPherron *et al*., 1997, McPherron and Lee, 1997, Schuelke *et al*., 2004). There is evidence indicating that myostatin inhibits satellite cell activation, proliferation, and differentiation (Kawada *et al*., 2006, Sinha-Hikim *et al*., 2006, Wagner *et al*., 2005), possibly mediated through perturbation of Akt and mTORC1 signalling (Trendelenburg *et al*., 2009). Therefore reductions in myostatin, as previously observed with testosterone administration (Kawada *et al*., 2006), can enhance muscle mass regulation in muscle wasting diseases such as cachexia and sarcopenia (Liu *et al*., 2008, Siriett *et al*., 2006, Siriett *et al*., 2007). Interestingly, in the current chapter, myostatin mRNA expression was reduced in the presence of T in myoblasts expressing impaired differentiation, with observable increases in myotube hypertrophy. These reductions in myostatin mRNA under a testosterone stimulus support the observations in chapter 3. Interestingly, the inhibition of AR (through flutamide)

resulted in increases in myostatin expression (chapter 5). Additionally, Akt phosphorylation was up regulated with a testosterone stimulus in PD cells and down regulated in the presence of flutamide. Therefore the regulation of muscle hypertrophy under a testosterone stimulus appears to be controlled by AR, Akt and myostatin interactions. The reduction in *myostatin* mRNA expression at 7 days with T treatment was accompanied by increases in myogenin mRNA expression in PD cells, which is supported recent literature highlighting myostatin's role for inhibiting myogenic differentiation (Gao *et al*., 2013, McFarlane *et al*., 2011, Trendelenburg *et al*., 2009). Despite this, testosterone did not return absolute levels of myostatin expression to the low levels observed in the control cells. These observations suggest that although testosterone may reduce myostatin expression, it is not entirely responsible for the improved hypertrophy observed in the atrophic phenotype cells. Furthermore, the PI3K inhibitor (LY) alone also substantially reduced myostatin expression where there is a distinct lack of differentiation and hypertrophy. This is in contrast to recent studies where there was a reduction in the activity of Akt observed in the presence of exogenous myostatin in human myoblasts (Trendelenburg *et al*., 2009). Therefore, if myostatin was reduced, PI3K/Akt activity may be expected to increase. Although in chapter 5, the increased levels of *myostatin* expression with flutamide, occurred with reductions in Akt phosphorylation.

6.4. Chapter Summary

In this chapter, exogenous testosterone was able to increase hypertrophy in myoblasts with reduced differentiation potential (PD cells) to a similar magnitude as the control cells, confirming the findings in chapter 5. Testosterone induced myotube hypertrophy was mediated via the PI3K/Akt pathway, where inhibition of this pathway in the presence of testosterone rendered the hormone unable to exhibit its potent influence on myotube hypertrophy in both phenotypically aged and control cells. Similarly, in chapter 5, PD myoblasts were most responsive to testosterone stimulus highlighted by the significant increases in AR expression. Exogenous testosterone increased *myogenin* expression in both cell types. Myostatin expression was reduced in the presence of testosterone in aged cells

only. Overall, based on the observations in the current chapter and chapter 5, administration of testosterone shows strong potential to enhance hypertrophy in ageing myoblasts directly via the AR and alternatively through the PI3K/Akt pathway, that is not via upstream IGF-IR (as shown in chapter 5), but potentially through mTOR.

7. GENERAL DISCUSSION

The data collected and presented in this thesis provides evidence towards the mechanisms of action for testosterone induced hypertrophy, but most importantly the potential role for testosterone administration in preserving muscle mass from a cellular and molecular perspective. The ultimate goal of this research is to understand the mechanisms in skeletal muscle which are driven by a testosterone stimulus. Indeed, with testosterone administration in vivo, adverse events (discussed in section 7.3.2) can occur and thus understanding the mechanisms in skeletal muscle will aid in the advancement of tissue specific treatments in clinical populations where muscle wasting is present. The work undertaken in this thesis has identified molecular targets/pathways through which a testosterone stimulus is mediated and importantly provides evidence for the intrinsic ability of aged muscle cells to respond to this anabolic stimulus.

Between the 1990's to 2000's, there has been extensive literature conducted highlighting the positive benefits of testosterone administration in various clinical populations such as Andropause (low testosterone levels). The major benefits centre on enhanced muscle mass. Recent studies have highlighted an increase in satellite cell number with testosterone administration, providing evidence how testosterone may interact with skeletal muscle and increase muscle growth. Human in vivo studies only allow for partial mechanistic questions to be addressed. More recently, in vitro studies have utilized various techniques to inhibit particular pathways and thus explore testosterone mechanisms in more detail. However evidence is lacking towards the role of potential pathways mediating a testosterone stimulus in skeletal muscle regeneration and ageing. Thus a deeper understanding of the regulation of the identified molecular targets in this thesis will, with future research, begin to enhance the progression of our understanding towards testosterone as a therapeutic treatment for muscle mass preservation.

7.1 KEY FINDINGS

Recent literature has addressed various pathways (AR, IGF-I/Akt/mTOR and TGF-β family etc) towards understanding the molecular and cellular mechanisms

which drive testosterone-induced muscle hypertrophy using in vitro cell culture (Basualto-Alarcón *et al*., 2013, Sculthorpe *et al*., 2012, Serra *et al*., 2011, White *et al*., 2012). However there is limited evidence which has addressed these proposed mechanisms in the context of ageing and muscle wasting (Serra *et al*., 2013). In light of this, an in vitro cell culture model was utilised which replicates an ageing phenotype to address the ability of a testosterone stimulus to rescue/enhance myotube differentiation and hypertrophy. Prior to this however, both testosterone and inhibitor doses were characterised in C_2C_{12} muscle cells to be used in later experiments, assessing molecular and cellular targets e.g. myotube number, mean nuclei per myotube, diameter etc. These initial experiments provided an inhibitor dose for androgen receptor and IGF-I receptor. The administration of flutamide (40μM) significantly reduced myotube hypertrophy and differentiation in cells expressing hypertrophic CON and atrophic (PD) phenotypes. The detrimental effect was accompanied by alterations in gene transcripts for muscle differentiation, IGF-I and the androgen receptor itself. In the instance of Picropodophyllin administration, a 150nM dose had a negative effect on muscle differentiation. Although low levels of AR protein have previously been observed in the literature within the C_2C_{12} muscle cell line (Altuwaijri *et al*., 2004, Lee, 2002), inhibiting the AR appeared to have catastrophic effects on morphological and transcriptional markers of differentiation and hypertrophy, eluding to the importance of a functional AR in myotube formation and hypertrophy in skeletal muscle (Mitchell *et al*., 2013, Sheppard *et al*., 2011).

The data presented in this thesis, supports the role for testosterone in enhancing myogenic differentiation and myotube hypertrophy (Lee, 2002, Singh *et al*., 2003, Singh *et al*., 2009, Sinha-Hikim *et al*., 2003, Sinha-Hikim *et al*., 2006, Wannenes *et al*., 2008) but more importantly, shows the capacity to improve hypertrophy and myonuclear accretion in a previously established model displaying impaired differentiation and hypertrophy similar to that of atrophic phenotypes such as ageing (Sharples *et al*., 2011, Sharples *et al*., 2012). Interestingly, testosterone improved hypertrophy (myotube diameter) to the same magnitude in both cell types (chapter 5 and 6). Thus, despite PD cells having undergone multiple population doublings *vs*. their controls, and therefore

displaying a reduced basal differentiation capacity as previously described in Sharples *et al*. (2011, 2012); testosterone was able to exert similar magnitude increases in myotube hypertrophy.

The mechanisms which regulate testosterone induced hypertrophy were investigated within the ageing phenotype (PD model). The role of the androgen receptor, IGF-I receptor (chapter 5) and Akt (chapter 6) were addressed as they have all be proposed to have a role in mediating testosterone's anabolic effect (Basualto-Alarcón *et al*., 2013, Serra *et al*., 2011, White *et al*., 2012). Testosterone significantly up-regulated androgen receptor expression in cells displaying an ageing phenotype, even in the presence of the IGF-I receptor being inhibited. Thus it appears even in an ageing phenotype, the responsiveness to a testosterone stimulus remains and is not IGF-I receptor mediated. Interestingly, AR inhibition alone resulted in increases in myostatin levels which may explain the lack of myotube formation (Braga *et al*., 2012, Trendelenburg *et al*., 2009). Additionally testosterone was observed to decrease myostatin levels in the aged cells and thus may have contributed to enhancing myotube hypertrophy. Finally, the inhibition of Akt (upstream of mTOR pathway) lead to testosterone induced myotube hypertrophy being diminished, lending support to role of the Akt/mTOR pathway (White *et al*., 2012). Interestingly, *mTOR* mRNA expression increased even in the presence of LY294002 under a testosterone stimulus and thus testosterone may directly activate mTOR signalling directly (discussed in more detail below 7.3.1). In light of these mechanistic observations, a proposed figure of testosterone's mechanism of action is detailed below (**Fig 7.1**):

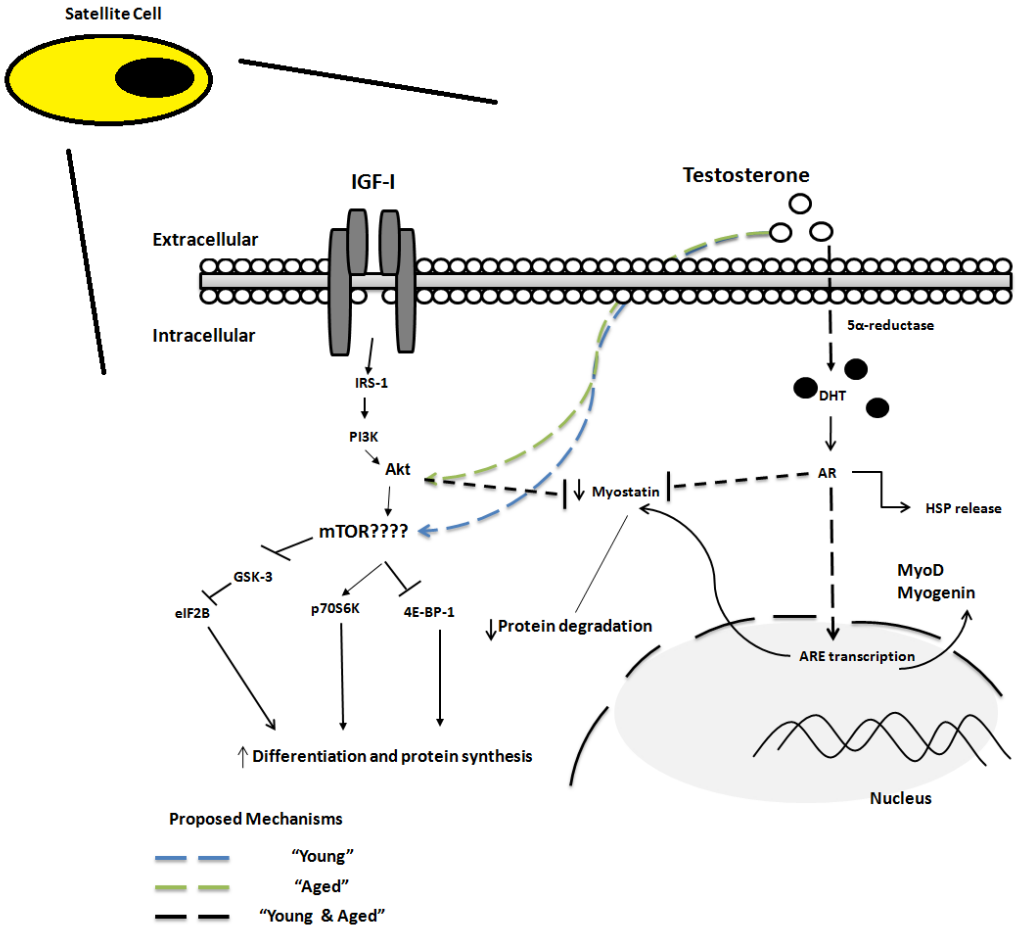

Fig 7.1 Proposed mechanisms for testosterone induced myotube hypertrophy in rescuing an ageing phenotype. Testosterone action appears to be mediated via the Akt/mTOR pathway and via the androgen receptor which ultimately lead to reduced myostatin levels. Therefore, this signalling cascade, triggered by testosterone, provides a net positive balance for myotube hypertrophy to occur.

7.2 LIMITATIONS TO THE PRESENT WORK

In chapter 4, the use of Picropodophyllin to inhibit the IGF-I receptor may not have been fully effective as only a 60% and 40% approx. reduction in IGF-I downstream (Akt and ERK ½ respectively) signalling was observed. Of course, the dose selected for experiments was based on the dose response experiment performed where reductions in myotube morphological parameters was observed. Indeed, the dose used was higher than doses previously implemented within C_2C_{12} muscle cells (Deldicque *et al.*, 2007, Galluzzo *et al.*, 2009). Effectively the limitation lies within the nature of the inhibitor as it acts as a substrate competitor

to compete for binding to the receptor and thus reduced tyrosine kinase activity (Duan *et al*., 2009, Girnita *et al*., 2004). Thus although a high dose was implemented, there may have still been some residual activation of the IGF-I receptor.

In chapter 5, the total protein levels for Akt and p70S6K were only completed for n=1. However, between treatments the totals appeared to be effected by each treatment. Ideally replicates (n=3) for the proteins would have been produced and thus the phosphorylated proteins could have been analysed relative to total levels instead of GAPDH, as was performed in the chapter. Furthermore, previous studies have addressed testosterone induced signalling after 12 hrs (Basualto-Alarcón *et al*., 2013) and 24hrs (White *et al*., 2012) and thus the time points (72 hrs and 7 days) in the current thesis may have not captured all the protein signalling involved in testosterone induced hypertrophy.

Finally, the mechanistic work presented in this thesis has been performed within cell culture models. The adoption of muscle cells lines vs. primary human culture to address cell behaviour may facilitate different responses to androgen treatment between primary cultures and cell lines with myoblast proliferation and differentiation capacity impacting on variation in mechanisms observed (Serra *et al*., 2011). Even the comparison between muscle cells of the same species is difficult with varying androgen-responsiveness in varying muscle itself (De Naeyer *et al*., 2014, Johansen *et al*., 2007, Kadi *et al*., 2000). Culture systems are commonly monolayer, yet within the body, cell-cell and cell-matrix interactions occur within a 3-D environment. The role of the vascular network in skeletal muscle is another factor which limits current monolayer and 3D culture. Another limit is the lack of various other cell types, such as fibroblasts and motor neurons, which may play a role in skeletal muscle androgen-responsiveness (Mosler *et al*., 2012, Serra *et al*., 2011). Overall, the mechanistic work presented provides an initial start point for subsequent studies (discussed below).

7.3 FUTURE DIRECTIONS

7.3.1 Testosterone as a "kick starter" in muscle hypertrophy

Recent evidence in vitro has suggested testosterone enhances mTOR activation in contributing towards muscle hypertrophy (Basualto-Alarcón *et al*., 2013, Wu *et al*., 2010a) and increases at the mRNA level were observed in chapter 6. In the ageing muscle of elderly men, mTOR and its downstream targets have been observed to be reduced in activation by -30 to 50% (Cuthbertson *et al*., 2005) compared to young counterparts. Furthermore, there is a reduced response in muscle contraction-induced mTOR signalling in aged models (Drummond *et al*., 2008, Fry *et al*., 2011, Parkington *et al*., 2004). The inhibition of mTOR through rapamycin has been observed to inhibit muscle protein synthesis (Drummond *et al*., 2009a). Therefore subsequent future studies may look to investigate the interaction between Testosterone and mTOR in the context of ageing, as testosterone-induced hypertrophy appears to be dependent on upon mTOR activation (Wu *et al*., 2010a, White *et al*., 2012).

In Chapter 6, mTOR expression in CON cells was increased in the presence of testosterone plus PI3K inhibitor (LY) (albeit mRNA expression and not protein activity), other studies have shown that mTOR activation can occur via signals independent of canonical IGF-I/Akt, via a pathway involving phospholipase D, phosphatidic acid and a downstream regulator Rheb (ras homologue enriched brain) (Anthony *et al*., 2000a, Anthony *et al*., 2000b, Hornberger *et al*., 2006, Sun *et al*., 2010). Redd 2 may also be important in inhibiting mTOR via the tuberous sclerosis 1 (TSC1) and 2 (TSC2) complex (DeYoung *et al*., 2008). As mTOR mRNA expression is increased in CON vs. PD cells, testosterone increases mTOR expression in CON cells which is blunted in PD cells at 7 days, and mTOR transcript expression is still increased with testosterone even the presence of PI3K/Akt inhibitor it begs the question as to the role of testosterone in regulating phospholipase D, phosphatidic acid, Rheb and Redd2 and their subsequent interaction with mTOR. Especially in light of recent data where following mechanical overload Redd2 is reduced to enable mTOR to initiate p70S6K activity, which is involved in protein synthesis and hypertrophy, a

process that is impaired in the elderly (Drummond *et al*., 2009b) who have impaired regenerative capacity.

Testosterone supplementation has been observed to increase satellite cell number in young and elderly individuals (Sinha-Hikim *et al*., 2003, Sinha-Hikim *et al*., 2006). In aged mice, there were observed increases in satellite cell activation (PCNA marker) with testosterone treatment compared to aged match controls (Kovacheva *et al*., 2010). A factor to consider is that the satellite cell provides the predominant location for androgen receptor expression (Chen *et al*., 2005, Sinha-Hikim *et al*., 2004). Within type II muscle fibres, satellite cell content in elderly individuals has been observed to be reduced (Verdijk *et al*., 2007) and an overall decline in satellite cell number is observed (Sajko *et al*., 2004, Kadi *et al*., 2004). Indeed, in this thesis, data points towards testosterone induced hypertrophy being driving by myoblast fusion (heightened myogenin expression similar to human observations (Sinha-Hikim *et al*., 2006)) via the androgen receptor. Thus, as the AR has most recently been correlated as a marker of muscle hypertrophy (Mitchell *et al*., 2013), it seems pertinent that future studies may focus more on the role of the AR in the context of ageing and satellite cell activation through primary cell culture or clinical human studies.

7.3.2 Hormone based therapies for muscle wasting with age

Testosterone replacement therapy in males has been observed to increase skeletal muscle mass and strength in various clinical populations (e.g. sarcopenia) (Bhasin *et al*., 2005). Despite potential benefits, adverse events (such as haemoglobin/hematocrits alterations and prostate cancer where muscle wasting is observed) can occur with such treatment (Bhasin *et al*., 2005). Therefore, maximizing the muscle-specific benefits of testosterone administration is highly important and such future enhancements will stem from understanding the mechanisms of hormonal action in skeletal muscle. Recent literature, including work presented in this thesis, suggests the cross talk between the androgen receptor and Pi3K/Akt/mTOR cell signalling pathway in mediating effects of testosterone (Basualto-Alarcón *et al*., 2013, White *et al*., 2012).

Importantly, testosterone administration is also unfavorable for female patients, therefore in post-menopausal females HRT (oestrogen/progesterone) is

administered as an alternative. Interestingly, similar to testosterone, HRT has been observed to elicit skeletal muscle strength gains and to enhance regeneration in humans (Ronkainen *et al*., 2009, Sipila *et al*., 2001, Taaffe *et al*., 2005). However, empirical data is sparse and it has only been alluded to that oestrogen specifically creates a pro-anabolic skeletal muscle environment (Velders and Diel, 2013), where reductions in inflammatory factors such TNF-α and NF-$_{K\beta}$ have been observed (Ghisletti *et al*., 2005). However, mechanistically how both testosterone and/or oestrogen/progesterone (HRT) may influence the chronically inflamed skeletal muscle niche remains to be elucidated, especially in relation to mechanisms of action.(Lach-Trifilieff *et al*., 2014, Watt *et al*., 2010)(Lach-Trifilieff *et al*., 2014)(Watt *et al*., 2010)(Bhasin *et al*., 2006, Bhasin and Jasuja, 2009, Dalton *et al*., 2011)

7.4 CONCLUSION

The work described in this thesis has detailed potential mechanisms towards testosterone induced hypertrophy through the utilization of an in vitro cell model which mimics an ageing phenotype. These observations provided evidence towards the impact testosterone administration can have on preserving muscle mass. The positive effect of testosterone on rescuing cells displaying impaired regeneration was accompanied by increases in AR protein, myogenin expression plus the involvement of Akt/mTOR signaling, independently of the IGF-IR appeared to be pivotal in mediating the effects of testosterone. AR inhibition alone resulted in interesting results which future studies may look to investigate regarding muscle hypertrophy. This thesis provides evidence towards unravelling key cellular and molecular mechanisms of testosterone regulation, for which the potential to harness the un-refutable power of this hormone in order to implement interventions for sarcopenia and muscle wasting diseases is pertinent.

8. REFERENCES

ADAMS, G. R. 2002. Invited Review: Autocrine/paracrine IGF-I and skeletal muscle adaptation. *Journal of Applied Physiology,* 93**,** 1159-1167.

ADI, S., BIN-ABBAS, B., WU, N.-Y. & ROSENTHAL, S. M. 2002. Early stimulation and late inhibition of extracellular signal-regulated kinase 1/2 phosphorylation by IGF-I: a potential mechanism mediating the switch in IGF-I action on skeletal muscle cell differentiation. *Endocrinology,* 143**,** 511-516.

AHTIAINEN, J. P., HULMI, J. J., KRAEMER, W. J., LEHTI, M., NYMAN, K., SELÄNNE, H., ALEN, M., PAKARINEN, A., KOMULAINEN, J. & KOVANEN, V. 2011. Heavy resistance exercise training and skeletal muscle androgen receptor expression in younger and older men. *Steroids,* 76**,** 183-192.

AIZAWA, K., IEMITSU, M., MAEDA, S., OTSUKI, T., SATO, K., USHIDA, T., MESAKI, N. & AKIMOTO, T. 2010. Acute exercise activates local bioactive androgen metabolism in skeletal muscle. *Steroids,* 75**,** 219-223.

AL-SHANTI, N., FAULKNER, S. H., SAINI, A., LORAM, I. & STEWART, C. E. 2011. A semi-automated programme for tracking myoblast migration following mechanical damage: manipulation by chemical inhibitors. *Cellular Physiology and Biochemistry,* 27**,** 625-636.

AL-SHANTI, N. & STEWART, C. E. 2008. PD98059 enhances C2 myoblast differentiation through p38 MAPK activation: a novel role for PD98059. *J Endocrinol,* 198**,** 243-52.

ALTUWAIJRI, S., LEE, D. K., CHUANG, K.-H., TING, H.-J., YANG, Z., XU, Q., TSAI, M.-Y., YEH, S., HANCHETT, L. A. & CHANG, H.-C. 2004. Androgen receptor regulates expression of skeletal muscle-specific proteins and muscle cell types. *Endocrine,* 25**,** 27-32.

AMIROUCHE, A., DURIEUX, A.-C., BANZET, S., KOULMANN, N., BONNEFOY, R., MOURET, C., BIGARD, X., PEINNEQUIN, A. & FREYSSENET, D. 2009. Down-regulation of Akt/mammalian target of rapamycin signaling pathway in response to myostatin overexpression in skeletal muscle. *Endocrinology,* 150**,** 286-294.

AMTHOR, H., NICHOLAS, G., MCKINNELL, I., KEMP, C. F., SHARMA, M., KAMBADUR, R. & PATEL, K. 2004. Follistatin complexes Myostatin and antagonises Myostatin-mediated inhibition of myogenesis. *Dev Biol,* 270**,** 19-30.

ANTHONY, J. C., ANTHONY, T. G., KIMBALL, S. R., VARY, T. C. & JEFFERSON, L. S. 2000a. Orally administered leucine stimulates protein synthesis in skeletal muscle of postabsorptive rats in association with increased eIF4F formation. *The Journal of Nutrition,* 130**,** 139-145.

ANTHONY, J. C., YOSHIZAWA, F., ANTHONY, T. G., VARY, T. C., JEFFERSON, L. S. & KIMBALL, S. R. 2000b. Leucine stimulates translation initiation in skeletal muscle of postabsorptive rats via a rapamycin-sensitive pathway. *The Journal of Nutrition,* 130**,** 2413-2419.

ARGILÉS, J. M., BUSQUETS, S., GARCÍA-MARTÍNEZ, C. & LÓPEZ-SORIANO, F. J. 2005. Mediators involved in the cancer anorexia-cachexia syndrome: past, present, and future. *Nutrition,* 21**,** 977-985.

ATES, K., YANG, S. Y., ORRELL, R. W., SINANAN, A. C., SIMONS, P., SOLOMON, A., BEECH, S., GOLDSPINK, G. & LEWIS, M. P. 2007. The IGF-I splice variant MGF increases progenitor cells in ALS, dystrophic, and normal muscle. *FEBS Lett,* 581**,** 2727-32.

ATKINSON, R. A., SRINIVAS-SHANKAR, U., ROBERTS, S. A., CONNOLLY, M. J., ADAMS, J. E., OLDHAM, J. A., WU, F. C., SEYNNES, O. R., STEWART, C. E. & MAGANARIS, C. N. 2010. Effects of testosterone on skeletal muscle architecture in intermediate-frail and frail elderly men. *The Journals of Gerontology Series A: Biological Sciences and Medical Sciences,* 65**,** 1215-1219.

AVERSA, Z., BONETTO, A., PENNA, F., COSTELLI, P., DI RIENZO, G., LACITIGNOLA, A., BACCINO, F. M., ZIPARO, V., MERCANTINI, P. & FANELLI, F. R. 2012. Changes in myostatin signaling in non-weight-losing cancer patients. *Annals of surgical oncology,* 19**,** 1350-1356.

BAAR, K. & ESSER, K. 1999. Phosphorylation of p70S6k correlates with increased skeletal muscle mass following resistance exercise. *American Journal of Physiology-Cell Physiology,* 276**,** C120-C127.

BASARIA, S., COVIELLO, A. D., TRAVISON, T. G., STORER, T. W., FARWELL, W. R., JETTE, A. M., EDER, R., TENNSTEDT, S., ULLOOR, J. & ZHANG, A. 2010. Adverse events associated with testosterone administration. *New England Journal of Medicine,* 363**,** 109-122.

BASUALTO-ALARCÓN, C., JORQUERA, G., ALTAMIRANO, F., JAIMOVICH, E. & ESTRADA, M. 2013. Testosterone Signals through mTOR and Androgen Receptor to Induce Muscle Hypertrophy. *Medicine and science in sports and exercise*.

BECCAFICO, S., RIUZZI, F., PUGLIELLI, C., MANCINELLI, R., FULLE, S., SORCI, G. & DONATO, R. 2011. Human muscle satellite cells show age-related differential expression of S100B protein and RAGE. *Age,* 33**,** 523-541.

BEGGS, M. L., NAGARAJAN, R., TAYLOR-JONES, J. M., NOLEN, G., MACNICOL, M. & PETERSON, C. A. 2004. Alterations in the TGFβ signaling pathway in myogenic progenitors with age. *Aging Cell,* 3**,** 353-361.

BENNETT, N. C., GARDINER, R. A., HOOPER, J. D., JOHNSON, D. W. & GOBE, G. C. 2010. Molecular cell biology of androgen receptor signalling. *The international journal of biochemistry & cell biology,* 42**,** 813-827.

BHASIN, S., CALOF, O. M., STORER, T. W., LEE, M. L., MAZER, N. A., JASUJA, R., MONTORI, V. M., GAO, W. & DALTON, J. T. 2006. Drug insight: testosterone and selective androgen receptor modulators as anabolic therapies for chronic illness and aging. *Nature Reviews Endocrinology,* 2**,** 146-159.

BHASIN, S. & JASUJA, R. 2009. Selective androgen receptor modulators (SARMs) as function promoting therapies. *Current opinion in clinical nutrition and metabolic care,* 12**,** 232.

BHASIN, S., STORER, T. W., BERMAN, N., CALLEGARI, C., CLEVENGER, B., PHILLIPS, J., BUNNELL, T. J., TRICKER, R., SHIRAZI, A. & CASABURI, R. 1996. The effects of supraphysiologic doses of testosterone on muscle size and strength in normal men. *New England Journal of Medicine,* 335**,** 1-7.

BHASIN, S., STORER, T. W., JAVANBAKHT, M., BERMAN, N., YARASHESKI, K. E., PHILLIPS, J., DIKE, M., SINHA-HIKIM, I., SHEN, R. & HAYS, R. D. 2000. Testosterone replacement and resistance exercise in HIV-infected men with weight loss and low testosterone levels. *JAMA: the journal of the American Medical Association,* 283**,** 763-770.

BHASIN, S., TRAVISON, T. G., STORER, T. W., LAKSHMAN, K., KAUSHIK, M., MAZER, N. A., NGYUEN, A.-H., DAVDA, M. N., JARA, H. & AAKIL, A. 2012. Effect of Testosterone Supplementation With and Without a Dual 5α-Reductase Inhibitor on Fat-Free Mass in Men With Suppressed Testosterone Production A Randomized Controlled Trial. *JAMA: the journal of the American Medical Association,* 307**,** 931-939.

BHASIN, S., WOODHOUSE, L., CASABURI, R., SINGH, A. B., BHASIN, D., BERMAN, N., CHEN, X., YARASHESKI, K. E., MAGLIANO, L. & DZEKOV, C. 2001. Testosterone dose-response relationships in healthy young men. *American Journal of Physiology-Endocrinology and Metabolism,* 281**,** E1172-E1181.

BHASIN, S., WOODHOUSE, L., CASABURI, R., SINGH, A. B., MAC, R. P., LEE, M., YARASHESKI, K. E., SINHA-HIKIM, I., DZEKOV, C. & DZEKOV, J. 2005. Older men are as responsive as young men to the anabolic effects of graded doses of testosterone on the skeletal muscle. *Journal of Clinical Endocrinology & Metabolism,* 90**,** 678-688.

BIGOT, A., JACQUEMIN, V., DEBACQ-CHAINIAUX, F., BUTLER-BROWNE, G. S., TOUSSAINT, O., FURLING, D. & MOULY, V. 2008. Replicative aging down-regulates the myogenic regulatory factors in human myoblasts. *Biology of the Cell,* 100**,** 189-199.

BLAU, H. M., PAVLATH, G. K., HARDEMAN, E. C., CHIU, C. P., SILBERSTEIN, L., WEBSTER, S. G., MILLER, S. C. & WEBSTER, C. 1985. Plasticity of the differentiated state. *Science,* 230**,** 758-66.

BODINE, S. C., STITT, T. N., GONZALEZ, M., KLINE, W. O., STOVER, G. L., BAUERLEIN, R., ZLOTCHENKO, E., SCRIMGEOUR, A., LAWRENCE, J. C. & GLASS, D. J. 2001. Akt/mTOR pathway is a crucial regulator of skeletal muscle hypertrophy and can prevent muscle atrophy in vivo. *Nature cell biology,* 3**,** 1014-1019.

BORST, S. E., DE HOYOS, D. V., GARZARELLA, L., VINCENT, K., POLLOCK, B. H., LOWENTHAL, D. T. & POLLOCK, M. L. 2001. Effects of resistance training on insulin-like growth factor-I and IGF binding proteins. *Medicine and science in sports and exercise,* 33**,** 648.

BRAGA, M., BHASIN, S., JASUJA, R., PERVIN, S. & SINGH, R. 2012. Testosterone inhibits transforming growth factor-β signaling during myogenic differentiation and proliferation of mouse satellite cells: potential role of follistatin in mediating testosterone action. *Molecular and cellular endocrinology,* 350**,** 39-52.

BRODSKY, I., BALAGOPAL, P. & NAIR, K. S. 1996. Effects of testosterone replacement on muscle mass and muscle protein synthesis in hypogonadal men--a clinical research center study. *Journal of Clinical Endocrinology & Metabolism,* 81**,** 3469-3475.

BROWN, D., HIKIM, A. P. S., KOVACHEVA, E. L. & SINHA-HIKIM, I. 2009. Mouse model of testosterone-induced muscle fiber hypertrophy: involvement of p38 mitogen-activated protein kinase-mediated Notch signaling. *Journal of endocrinology,* 201**,** 129-139.

BRUUNSGAARD, H., LADELUND, S., PEDERSEN, A. N., SCHROLL, M., JØRGENSEN, T. & PEDERSEN, B. 2003. Predicting death from tumour necrosis factor-alpha and interleukin-6 in 80-year-old people. *Clinical & Experimental Immunology,* 132**,** 24-31.

CALLEWAERT, F., BOONEN, S. & VANDERSCHUEREN, D. 2010. Sex steroids and the male skeleton: a tale of two hormones. *Trends in Endocrinology & Metabolism,* 21**,** 89-95.

CARLSON, M. E. & CONBOY, I. M. 2007. Loss of stem cell regenerative capacity within aged niches. *Aging Cell,* 6**,** 371-382.

CASABURI, R., BHASIN, S., COSENTINO, L., PORSZASZ, J., SOMFAY, A., LEWIS, M. I., FOURNIER, M. & STORER, T. W. 2004. Effects of testosterone and resistance training in men with chronic obstructive pulmonary disease. *American journal of respiratory and critical care medicine,* 170**,** 870-878.

CHAKKALAKAL, J. V., JONES, K. M., BASSON, M. A. & BRACK, A. S. 2012. The aged niche disrupts muscle stem cell quiescence. *Nature,* 490**,** 355-60.

CHAMBON, C., DUTEIL, D., VIGNAUD, A., FERRY, A., MESSADDEQ, N., MALIVINDI, R., KATO, S., CHAMBON, P. & METZGER, D. 2010. Myocytic androgen receptor controls the strength but not the mass of limb muscles. *Proceedings of the National Academy of Sciences,* 107**,** 14327-14332.

CHEN, Y., ZAJAC, J. D. & MACLEAN, H. E. 2005. Androgen regulation of satellite cell function. *Journal of endocrinology,* 186**,** 21-31.

CHENG, Z., ADI, S., WU, N., HSIAO, D., WOO, E., FILVAROFF, E., GUSTAFSON, T. & ROSENTHAL, S. 2000. Functional inactivation of the IGF-I receptor delays differentiation of skeletal muscle cells. *Journal of endocrinology,* 167**,** 175-182.

CLEMMONS, D. R. 2009. Role of IGF-I in skeletal muscle mass maintenance. *Trends in Endocrinology & Metabolism,* 20**,** 349-356.

CONBOY, I. M., CONBOY, M. J., SMYTHE, G. M. & RANDO, T. A. 2003. Notch-mediated restoration of regenerative potential to aged muscle. *Science,* 302**,** 1575-1577.

CONBOY, I. M., CONBOY, M. J., WAGERS, A. J., GIRMA, E. R., WEISSMAN, I. L. & RANDO, T. A. 2005. Rejuvenation of aged progenitor cells by exposure to a young systemic environment. *Nature,* 433**,** 760-764.

CONRAADS, V., HOYMANS, V. Y. & VRINTS, C. J. 2007. Heart failure and cachexia: insights offered from molecular biology. *Frontiers in bioscience: a journal and virtual library,* 13**,** 325-335.

COOLICAN, S. A., SAMUEL, D. S., EWTON, D. Z., MCWADE, F. J. & FLORINI, J. R. 1997. The mitogenic and myogenic actions of insulin-like growth factors utilize distinct signaling pathways. *Journal of Biological Chemistry,* 272**,** 6653-6662.

CORNELISON, D. & WOLD, B. J. 1997. Single-cell analysis of regulatory gene expression in quiescent and activated mouse skeletal muscle satellite cells. *Developmental biology,* 191**,** 270-283.

CROWN, A., HE, X., HOLLY, J., LIGHTMAN, S. & STEWART, C. 2000. Characterisation of the IGF system in a primary adult human skeletal muscle cell model, and comparison of the effects of insulin and IGF-I on protein metabolism. *Journal of endocrinology,* 167**,** 403-415.

CRUZ-JENTOFT, A. J., LANDI, F., TOPINKOVA, E. & MICHEL, J.-P. 2010. Understanding sarcopenia as a geriatric syndrome. *Current Opinion in Clinical Nutrition & Metabolic Care,* 13**,** 1-7.

CUTHBERTSON, D., SMITH, K., BABRAJ, J., LEESE, G., WADDELL, T., ATHERTON, P., WACKERHAGE, H., TAYLOR, P. M. & RENNIE, M. J. 2005. Anabolic signaling deficits underlie amino acid resistance of wasting, aging muscle. *The FASEB Journal,* 19**,** 422-424.

DALTON, J. T., BARNETTE, K. G., BOHL, C. E., HANCOCK, M. L., RODRIGUEZ, D., DODSON, S. T., MORTON, R. A. & STEINER, M. S. 2011. The selective androgen receptor modulator GTx-024 (enobosarm) improves lean body mass and physical function in healthy elderly men and postmenopausal women: results of a double-blind, placebo-controlled phase II trial. *Journal of cachexia, sarcopenia and muscle,* 2**,** 153-161.

DE NAEYER, H., LAMON, S., RUSSELL, A., EVERAERT, I., DE SPAEY, A., VANHEEL, B., TAES, Y. & DERAVE, W. 2014. Androgenic and estrogenic regulation of Atrogin-1, MuRF1 and myostatin expression in different muscle types of male mice. *European journal of applied physiology***,** 1-11.

DEANE, C. S., HUGHES, D. C., SCULTHORPE, N., LEWIS, M. P., STEWART, C. E. & SHARPLES, A. P. 2013. Impaired hypertrophy in myoblasts is improved with testosterone administration. *J Steroid Biochem Mol Biol,* 138**,** 152-61.

DEANS, C. & WIGMORE, S. J. 2005. Systemic inflammation, cachexia and prognosis in patients with cancer. *Current Opinion in Clinical Nutrition & Metabolic Care,* 8**,** 265-269.

DEGENS, H. 2010. The role of systemic inflammation in age-related muscle weakness and wasting. *Scandinavian journal of medicine & science in sports,* 20**,** 28-38.

DEGENS, H. & ALWAY, S. E. 2003. Skeletal muscle function and hypertrophy are diminished in old age. *Muscle & nerve,* 27**,** 339-347.

DELDICQUE, L., THEISEN, D., BERTRAND, L., HESPEL, P., HUE, L. & FRANCAUX, M. 2007. Creatine enhances differentiation of myogenic C2C12 cells by activating both p38 and Akt/PKB pathways. *American Journal of Physiology-Cell Physiology,* 293**,** C1263-C1271.

DEYOUNG, M. P., HORAK, P., SOFER, A., SGROI, D. & ELLISEN, L. W. 2008. Hypoxia regulates TSC1/2–mTOR signaling and tumor suppression through REDD1-mediated 14–3–3 shuttling. *Genes & development,* 22**,** 239-251.

DIEL, P., BAADNERS, D., SCHLÜPMANN, K., VELDERS, M. & SCHWARZ, J. 2008. C2C12 myoblastoma cell differentiation and proliferation is stimulated by androgens and associated with a modulation of myostatin and Pax7 expression. *Journal of molecular endocrinology,* 40**,** 231-241.

DILLON, E. L., BASRA, G., HORSTMAN, A. M., CASPERSON, S. L., RANDOLPH, K. M., DURHAM, W. J., URBAN, R. J., DIAZ-ARRASTIA, C., LEVINE, L. & HATCH, S. S. 2012. Cancer cachexia and anabolic interventions: a case report. *Journal of cachexia, sarcopenia and muscle,* 3**,** 253-263.

DILLON, E. L., DURHAM, W. J., URBAN, R. J. & SHEFFIELD-MOORE, M. 2010. Hormone treatment and muscle anabolism during aging: androgens. *Clinical Nutrition,* 29**,** 697-700.

DOMINIQUE, J.-E. & GÉRARD, C. 2006. Myostatin regulation of muscle development: molecular basis, natural mutations, physiopathological aspects. *Experimental cell research,* 312**,** 2401-2414.

DOUMIT, M. E., COOK, D. R. & MERKEL, R. A. 1996. Testosterone up-regulates androgen receptors and decreases differentiation of porcine myogenic satellite cells in vitro. *Endocrinology,* 137**,** 1385-1394.

DREYER, H. C., BLANCO, C. E., SATTLER, F. R., SCHROEDER, E. T. & WISWELL, R. A. 2006. Satellite cell numbers in young and older men 24 hours after eccentric exercise. *Muscle & nerve,* 33**,** 242-253.

DRUMMOND, M. J., DREYER, H. C., PENNINGS, B., FRY, C. S., DHANANI, S., DILLON, E. L., SHEFFIELD-MOORE, M., VOLPI, E. & RASMUSSEN, B. B. 2008. Skeletal muscle protein anabolic response to resistance exercise and essential amino acids is delayed with aging. *Journal of Applied Physiology,* 104**,** 1452-1461.

DRUMMOND, M. J., FRY, C. S., GLYNN, E. L., DREYER, H. C., DHANANI, S., TIMMERMAN, K. L., VOLPI, E. & RASMUSSEN, B. B. 2009a. Rapamycin

administration in humans blocks the contraction-induced increase in skeletal muscle protein synthesis. *The Journal of physiology,* 587**,** 1535-1546.

DRUMMOND, M. J., MIYAZAKI, M., DREYER, H. C., PENNINGS, B., DHANANI, S., VOLPI, E., ESSER, K. A. & RASMUSSEN, B. B. 2009b. Expression of growth-related genes in young and older human skeletal muscle following an acute stimulation of protein synthesis. *Journal of Applied Physiology,* 106**,** 1403-1411.

DUAN, Z., CHOY, E., HARMON, D., YANG, C., RYU, K., SCHWAB, J., MANKIN, H. & HORNICEK, F. J. 2009. Insulin-like growth factor-I receptor tyrosine kinase inhibitor cyclolignan picropodophyllin inhibits proliferation and induces apoptosis in multidrug resistant osteosarcoma cell lines. *Molecular cancer therapeutics,* 8**,** 2122-2130.

DUBOIS, V., LAURENT, M. R., SINNESAEL, M., CIELEN, N., HELSEN, C., CLINCKEMALIE, L., SPANS, L., GAYAN-RAMIREZ, G., DELDICQUE, L., HESPEL, P., CARMELIET, G., VANDERSCHUEREN, D. & CLAESSENS, F. 2014. A satellite cell-specific knockout of the androgen receptor reveals myostatin as a direct androgen target in skeletal muscle. *Faseb J,* 26**,** 26.

DUDGEON, W., PHILLIPS, K., CARSON, J., BREWER, R., DURSTINE, J. L. & HAND, G. 2006. Counteracting muscle wasting in HIV-infected individuals. *HIV medicine,* 7**,** 299-310.

ERIKSSON, A., KADI, F., MALM, C. & THORNELL, L.-E. 2005. Skeletal muscle morphology in power-lifters with and without anabolic steroids. *Histochemistry and cell biology,* 124**,** 167-175.

EVANS, N. A. 2004. Current concepts in anabolic-androgenic steroids. *The American Journal of Sports Medicine,* 32**,** 534-542.

FERNANDEZ-BALSELLS, M. M., MURAD, M. H., LANE, M., LAMPROPULOS, J. F., ALBUQUERQUE, F., MULLAN, R. J., AGRWAL, N., ELAMIN, M. B., GALLEGOS-OROZCO, J. F. & WANG, A. T. 2010. Adverse effects of testosterone therapy in adult men: a systematic review and meta-analysis. *The Journal of Clinical Endocrinology & Metabolism,* 95**,** 2560-2575.

FERNÁNDEZ, A. M., DUPONT, J., FARRAR, R. P., LEE, S., STANNARD, B. & LE ROITH, D. 2002. Muscle-specific inactivation of the IGF-I receptor induces compensatory hyperplasia in skeletal muscle. *Journal of Clinical Investigation,* 109**,** 347-355.

FERRANDO, A. A., SHEFFIELD-MOORE, M., YECKEL, C. W., GILKISON, C., JIANG, J., ACHACOSA, A., LIEBERMAN, S. A., TIPTON, K., WOLFE, R. R. & URBAN, R. J. 2002. Testosterone administration to older men improves muscle function: molecular and physiological mechanisms. *American Journal of Physiology-Endocrinology and Metabolism,* 282**,** E601-E607.

FERRANDO, A. A., TIPTON, K. D., DOYLE, D., PHILLIPS, S. M., CORTIELLA, J. & WOLFE, R. R. 1998. Testosterone injection stimulates net protein synthesis but not tissue amino acid transport. *American Journal of Physiology-Endocrinology and Metabolism,* 275**,** E864-E871.

FINK, H. A., EWING, S. K., ENSRUD, K. E., BARRETT-CONNOR, E., TAYLOR, B. C., CAULEY, J. A. & ORWOLL, E. S. 2006. Association of testosterone and estradiol deficiency with osteoporosis and rapid bone loss in older men. *Journal of Clinical Endocrinology & Metabolism,* 91**,** 3908-3915.

FROST, R. A., HUBER, D., PRUZNAK, A. & LANG, C. H. 2009. Regulation of REDD1 by insulin-like growth factor-I in skeletal muscle and myotubes. *Journal of Cellular Biochemistry,* 108**,** 1192-1202.

FROST, R. A., NYSTROM, G. J., JEFFERSON, L. S. & LANG, C. H. 2007. Hormone, cytokine, and nutritional regulation of sepsis-induced increases in atrogin-1 and MuRF1 in skeletal muscle. *American Journal of Physiology-Endocrinology and Metabolism,* 292**,** E501-E512.

FRY, C. S., DRUMMOND, M. J., GLYNN, E. L., DICKINSON, J. M., GUNDERMANN, D. M., TIMMERMAN, K. L., WALKER, D. K., DHANANI, S., VOLPI, E. & RASMUSSEN, B. B. 2011. Aging impairs contraction-induced human skeletal muscle mTORC1 signaling and protein synthesis. *Skelet Muscle,* 1**,** 11-11.

GALLUZZO, P., RASTELLI, C., BULZOMI, P., ACCONCIA, F., PALLOTTINI, V. & MARINO, M. 2009. 17β-Estradiol regulates the first steps of skeletal muscle cell

differentiation via ER-α-mediated signals. *American Journal of Physiology-Cell Physiology,* 297**,** C1249-C1262.

GAO, F., KISHIDA, T., EJIMA, A., GOJO, S. & MAZDA, O. 2013. Myostatin acts as an autocrine/paracrine negative regulator in myoblast differentiation from human induced pluripotent stem cells. *Biochemical and biophysical research communications,* 431**,** 309-314.

GENNARI, L., MERLOTTI, D., MARTINI, G., GONNELLI, S., FRANCI, B., CAMPAGNA, S., LUCANI, B., DAL CANTO, N., VALENTI, R. & GENNARI, C. 2003. Longitudinal association between sex hormone levels, bone loss, and bone turnover in elderly men. *Journal of Clinical Endocrinology & Metabolism,* 88**,** 5327-5333.

GENTILE, M. A., NANTERMET, P. V., VOGEL, R. L., PHILLIPS, R., HOLDER, D., HODOR, P., CHENG, C., DAI, H., FREEDMAN, L. P. & RAY, W. J. 2010. Androgen-mediated improvement of body composition and muscle function involves a novel early transcriptional program including IGF1, mechano growth factor, and induction of β-catenin. *Journal of molecular endocrinology,* 44**,** 55-73.

GEORGE, T., VELLOSO, C. P., ALSHARIDAH, M., LAZARUS, N. R. & HARRIDGE, S. D. 2010. Sera from young and older humans equally sustain proliferation and differentiation of human myoblasts. *Experimental gerontology,* 45**,** 875-881.

GHISLETTI, S., MEDA, C., MAGGI, A. & VEGETO, E. 2005. 17β-Estradiol inhibits inflammatory gene expression by controlling NF-κB intracellular localization. *Molecular and cellular biology,* 25**,** 2957-2968.

GIRNITA, A., GIRNITA, L., DEL PRETE, F., BARTOLAZZI, A., LARSSON, O. & AXELSON, M. 2004. Cyclolignans as inhibitors of the insulin-like growth factor-1 receptor and malignant cell growth. *Cancer research,* 64**,** 236-242.

GOBINET, J., POUJOL, N. & SULTAN, C. 2002. Molecular action of androgens. *Molecular and cellular endocrinology,* 198**,** 15-24.

GRAD, J. M., LE DAI, J., WU, S. & BURNSTEIN, K. L. 1999. Multiple androgen response elements and a Myc consensus site in the androgen receptor (AR) coding region are involved in androgen-mediated up-regulation of AR messenger RNA. *Molecular Endocrinology,* 13**,** 1896-1911.

HAMEED, M., ORRELL, R., COBBOLD, M., GOLDSPINK, G. & HARRIDGE, S. 2003. Expression of IGF-I splice variants in young and old human skeletal muscle after high resistance exercise. *The Journal of physiology,* 547**,** 247-254.

HARTGENS, F. & KUIPERS, H. 2004. Effects of androgenic-anabolic steroids in athletes. *Sports Medicine,* 34**,** 513-554.

HASSELGREN, P.-O., MENCONI, M. J., FAREED, M. U., YANG, H., WEI, W. & EVENSON, A. 2005. Novel aspects on the regulation of muscle wasting in sepsis. *The international journal of biochemistry & cell biology,* 37**,** 2156-2168.

HERON-MILHAVET, L., MAMAEVA, D., LEROITH, D., LAMB, N. J. & FERNANDEZ, A. 2010. Impaired muscle regeneration and myoblast differentiation in mice with a muscle-specific KO of IGF-IR. *Journal of cellular physiology,* 225**,** 1-6.

HILL, M. & GOLDSPINK, G. 2003. Expression and Splicing of the Insulin-Like Growth Factor Gene in Rodent Muscle is Associated with Muscle Satellite (stem) Cell Activation following Local Tissue Damage. *The Journal of physiology,* 549**,** 409-418.

HORNBERGER, T., CHU, W., MAK, Y., HSIUNG, J., HUANG, S. & CHIEN, S. 2006. The role of phospholipase D and phosphatidic acid in the mechanical activation of mTOR signaling in skeletal muscle. *Proceedings of the National Academy of Sciences of the United States of America,* 103**,** 4741-4746.

HUANG, Z., CHEN, D., ZHANG, K., YU, B., CHEN, X. & MENG, J. 2007. Regulation of myostatin signaling by c-Jun N-terminal kinase in C2C12 cells. *Cellular signalling,* 19**,** 2286-2295.

HULMI, J. J., AHTIAINEN, J. P., SELÄNNE, H., VOLEK, J. S., HÄKKINEN, K., KOVANEN, V. & MERO, A. A. 2008. Androgen receptors and testosterone in men—effects of protein ingestion, resistance exercise and fiber type. *The Journal of steroid biochemistry and molecular biology,* 110**,** 130-137.

INOUE, K., YAMASAKI, S., FUSHIKI, T., OKADA, Y. & SUGIMOTO, E. 1994. Androgen receptor antagonist suppresses exercise-induced hypertrophy of skeletal muscle. *European journal of applied physiology and occupational physiology,* 69**,** 88-91.

JOHANSEN, J., BREEDLOVE, S. & JORDAN, C. 2007. Androgen receptor expression in the levator ani muscle of male mice. *Journal of neuroendocrinology,* 19**,** 823-826.

JONES, N. C., FEDOROV, Y. V., ROSENTHAL, R. S. & OLWIN, B. B. 2001. ERK1/2 is required for myoblast proliferation but is dispensable for muscle gene expression and cell fusion. *Journal of cellular physiology,* 186**,** 104-115.

KADI, F. 2008. Cellular and molecular mechanisms responsible for the action of testosterone on human skeletal muscle. A basis for illegal performance enhancement. *British journal of pharmacology,* 154**,** 522-528.

KADI, F., BONNERUD, P., ERIKSSON, A. & THORNELL, L.-E. 2000. The expression of androgen receptors in human neck and limb muscles: effects of training and self-administration of androgenic-anabolic steroids. *Histochemistry and cell biology,* 113**,** 25-29.

KADI, F., CHARIFI, N., DENIS, C. & LEXELL, J. 2004. Satellite cells and myonuclei in young and elderly women and men. *Muscle & nerve,* 29**,** 120-127.

KADI, F., CHARIFI, N., DENIS, C., LEXELL, J., ANDERSEN, J. L., SCHJERLING, P., OLSEN, S. & KJAER, M. 2005. The behaviour of satellite cells in response to exercise: what have we learned from human studies? *Pflügers Archiv,* 451**,** 319-327.

KADI, F., ERIKSSON, A., HOLMNER, S., BUTLER-BROWNE, G. S. & THORNELL, L.-E. 1999. Cellular adaptation of the trapezius muscle in strength-trained athletes. *Histochemistry and cell biology,* 111**,** 189-195.

KADI, F. & THORNELL, L.-E. 2000. Concomitant increases in myonuclear and satellite cell content in female trapezius muscle following strength training. *Histochemistry and cell biology,* 113**,** 99-103.

KALISTA, S., SCHAKMAN, O., GILSON, H., LAUSE, P., DEMEULDER, B., BERTRAND, L., PENDE, M. & THISSEN, J.-P. 2011. The type 1 insulin-like growth factor receptor (IGF-IR) pathway is mandatory for the follistatin-induced skeletal muscle hypertrophy. *Endocrinology,* 153**,** 241-253.

KAWADA, S., OKUNO, M. & ISHII, N. 2006. Testosterone causes decrease in the content of skeletal muscle myostatin. *International Journal of Sport and Health Science,* 4**,** 44-48.

KHOSLA, S., MELTON, L. J., ROBB, R. A., CAMP, J. J., ATKINSON, E. J., OBERG, A. L., ROULEAU, P. A. & RIGGS, B. L. 2005. Relationship of volumetric BMD and structural parameters at different skeletal sites to sex steroid levels in men. *Journal of Bone and Mineral Research,* 20**,** 730-740.

KIM, H., BARTON, E., MUJA, N., YAKAR, S., PENNISI, P. & LEROITH, D. 2005. Intact insulin and insulin-like growth factor-I receptor signaling is required for growth hormone effects on skeletal muscle growth and function in vivo. *Endocrinology,* 146**,** 1772-1779.

KIM, H. H. Regulation of gonadotropin-releasing hormone gene expression. Seminars in reproductive medicine, 2007. Copyright© 2007 by Thieme Medical Publishers, Inc., 333 Seventh Avenue, New York, NY 10001, USA., 313-325.

KIM, H. J. & LEE, W. J. 2009a. Insulin-like growth factor-I induces androgen receptor activation in differentiating C2C12 skeletal muscle cells. *Molecules and cells,* 28**,** 189-194.

KIM, H. J. & LEE, W. J. 2009b. Ligand-independent activation of the androgen receptor by insulin-like growth factor-I and the role of the MAPK pathway in skeletal muscle cells. *Molecules and cells,* 28**,** 589-593.

KOVACHEVA, E. L., HIKIM, A. P. S., SHEN, R., SINHA, I. & SINHA-HIKIM, I. 2010. Testosterone supplementation reverses sarcopenia in aging through regulation of myostatin, c-Jun NH2-terminal kinase, Notch, and Akt signaling pathways. *Endocrinology,* 151**,** 628-638.

KRAEMER, W. J. & RATAMESS, N. A. 2005. Hormonal responses and adaptations to resistance exercise and training. *Sports Medicine,* 35**,** 339-361.

KVORNING, T., ANDERSEN, M., BRIXEN, K., SCHJERLING, P., SUETTA, C. & MADSEN, K. 2007. Suppression of testosterone does not blunt mRNA expression of myoD, myogenin, IGF, myostatin or androgen receptor post strength training in humans. *The Journal of physiology,* 578**,** 579-593.

LABRIE, F. 1991. Intracrinology. *Molecular and cellular endocrinology,* 78**,** C113-C118.

LABRIE, F. 2010. The intracrine sex steroid biosynthesis pathways. *Progress in brain research,* 181**,** 177-192.

LACH-TRIFILIEFF, E., MINETTI, G. C., SHEPPARD, K., IBEBUNJO, C., FEIGE, J. N., HARTMANN, S., BRACHAT, S., RIVET, H., KOELBING, C. & MORVAN, F. 2014. An antibody blocking activin type II receptors induces strong skeletal muscle hypertrophy and protects from atrophy. *Molecular and cellular biology,* 34**,** 606-618.

LAEMMLI, U. K. 1970. Cleavage of structural proteins during the assembly of the head of bacteriophage T4. *Nature,* 227**,** 680-685.

LASSAR, A. B. 2009. The p38 MAPK family, a pushmi-pullyu of skeletal muscle differentiation. *The Journal of cell biology,* 187**,** 941-943.

LAWLOR, M. A., FENG, X., EVERDING, D. R., SIEGER, K., STEWART, C. E. & ROTWEIN, P. 2000. Dual control of muscle cell survival by distinct growth factor-regulated signaling pathways. *Molecular and cellular biology,* 20**,** 3256-3265.

LEE, D. K. 2002. Androgen receptor enhances myogenin expression and accelerates differentiation. *Biochemical and biophysical research communications,* 294**,** 408-413.

LEE, W. J. 2009. Insulin-like growth factor-I-induced androgen receptor activation is mediated by the PI3K/Akt pathway in C2C12 skeletal muscle cells. *Molecules and cells,* 28**,** 495-499.

LEES, S. J., ZWETSLOOT, K. A. & BOOTH, F. W. 2009. Muscle precursor cells isolated from aged rats exhibit an increased tumor necrosis factor- alpha response. *Aging Cell,* 8**,** 26-35.

LÉGER, B., DERAVE, W., DE BOCK, K., HESPEL, P. & RUSSELL, A. P. 2008. Human sarcopenia reveals an increase in SOCS-3 and myostatin and a reduced efficiency of Akt phosphorylation. *Rejuvenation research,* 11**,** 163-175B.

LEWIS, M. I., FOURNIER, M., STORER, T. W., BHASIN, S., PORSZASZ, J., REN, S.-G., DA, X. & CASABURI, R. 2007. Skeletal muscle adaptations to testosterone and resistance training in men with COPD. *Journal of Applied Physiology,* 103**,** 1299-1310.

LI, B.-G., HASSELGREN, P.-O. & FANG, C.-H. 2005a. Insulin-like growth factor-I inhibits dexamethasone-induced proteolysis in cultured L6 myotubes through PI3K/Akt/GSK-3β and PI3K/Akt/mTOR-dependent mechanisms. *The international journal of biochemistry & cell biology,* 37**,** 2207-2216.

LI, Y.-P., CHEN, Y., JOHN, J., MOYLAN, J., JIN, B., MANN, D. L. & REID, M. B. 2005b. TNF-α acts via p38 MAPK to stimulate expression of the ubiquitin ligase atrogin1/MAFbx in skeletal muscle. *The FASEB Journal,* 19**,** 362-370.

LI, Y.-P., LECKER, S. H., CHEN, Y., WADDELL, I. D., GOLDBERG, A. L. & REID, M. B. 2003. TNF-α increases ubiquitin-conjugating activity in skeletal muscle by up-regulating UbcH2/E220k. *The FASEB Journal,* 17**,** 1048-1057.

LIU, C., YANG, Z., LIU, C., WANG, R., TIEN, P., DALE, R. & SUN, L. 2008. Myostatin antisense RNA-mediated muscle growth in normal and cancer cachexia mice. *Gene therapy,* 15**,** 155-160.

LIU, J.-P., BAKER, J., PERKINS, A. S., ROBERTSON, E. J. & EFSTRATIADIS, A. 1993. Mice carrying null mutations of the genes encoding insulin-like growth factor I (< i> Igf-1</i>) and type 1 IGF receptor (< i> Igf1r</i>). *Cell,* 75**,** 59-72.

LIVAK, K. J. & SCHMITTGEN, T. D. 2001. Analysis of Relative Gene Expression Data Using Real-Time Quantitative PCR and the 2< sup>− ΔΔCT</sup> Method. *methods,* 25**,** 402-408.

LOVELOCK, J. E. & BISHOP, M. W. 1959. Prevention of freezing damage to living cells by dimethyl sulphoxide. *Nature,* 183**,** 1394-5.

MACLEAN, H. E., CHIU, W. M., NOTINI, A. J., AXELL, A.-M., DAVEY, R. A., MCMANUS, J. F., MA, C., PLANT, D. R., LYNCH, G. S. & ZAJAC, J. D. 2008. Impaired skeletal muscle development and function in male, but not female, genomic androgen receptor knockout mice. *The FASEB Journal,* 22**,** 2676-2689.

MASIELLO, D., CHENG, S., BUBLEY, G. J., LU, M. L. & BALK, S. P. 2002. Bicalutamide functions as an androgen receptor antagonist by assembly of a transcriptionally inactive receptor. *Journal of Biological Chemistry,* 277**,** 26321-26326.

MCCALL, G. E., BYRNES, W. C., FLECK, S. J., DICKINSON, A. & KRAEMER, W. J. 1999. Acute and chronic hormonal responses to resistance training designed to promote muscle hypertrophy. *Canadian Journal of Applied Physiology,* 24**,** 96-107.

MCCAULLEY, G. O., MCBRIDE, J. M., CORMIE, P., HUDSON, M. B., NUZZO, J. L., QUINDRY, J. C. & TRIPLETT, N. T. 2009. Acute hormonal and neuromuscular responses to hypertrophy, strength and power type resistance exercise. *European journal of applied physiology,* 105**,** 695-704.

MCCROSKERY, S., THOMAS, M., MAXWELL, L., SHARMA, M. & KAMBADUR, R. 2003. Myostatin negatively regulates satellite cell activation and self-renewal. *The Journal of cell biology,* 162**,** 1135-1147.

MCFARLANE, C., HUI, G. Z., AMANDA, W. Z. W., LAU, H. Y., LOKIREDDY, S., XIAOJIA, G., MOULY, V., BUTLER-BROWNE, G., GLUCKMAN, P. D. & SHARMA, M. 2011. Human myostatin negatively regulates human myoblast growth and differentiation. *American Journal of Physiology-Cell Physiology,* 301**,** C195.

MCPHERRON, A. C., LAWLER, A. M. & LEE, S.-J. 1997. Regulation of skeletal muscle mass in mice by a new TGF-p superfamily member.

MCPHERRON, A. C. & LEE, S.-J. 1997. Double muscling in cattle due to mutations in the myostatin gene. *Proceedings of the National Academy of Sciences,* 94**,** 12457-12461.

MENDLER, L., BAKA, Z., KOVÁCS-SIMON, A. & DUX, L. 2007. Androgens negatively regulate myostatin expression in an androgen-dependent skeletal muscle. *Biochemical and biophysical research communications,* 361**,** 237-242.

MILLER, W. L. 1988. Molecular biology of steroid hormone synthesis. *Endocrine reviews,* 9**,** 295-318.

MITCHELL, C. J., CHURCHWARD-VENNE, T. A., BELLAMY, L., PARISE, G., BAKER, S. K. & PHILLIPS, S. M. 2013. Muscular and Systemic Correlates of Resistance Training-Induced Muscle Hypertrophy. *PloS one,* 8**,** e78636.

MITCHELL, W. K., WILLIAMS, J., ATHERTON, P., LARVIN, M., LUND, J. & NARICI, M. 2012. Sarcopenia, dynapenia, and the impact of advancing age on human skeletal muscle size and strength; a quantitative review. *Frontiers in physiology,* 3.

MIYAZAKI, M., MCCARTHY, J. J., FEDELE, M. J. & ESSER, K. A. 2011. Early activation of mTORC1 signalling in response to mechanical overload is independent of phosphoinositide 3-kinase/Akt signalling. *The Journal of physiology,* 589**,** 1831-1846.

MORISSETTE, M. R., COOK, S. A., BURANASOMBATI, C., ROSENBERG, M. A. & ROSENZWEIG, A. 2009. Myostatin inhibits IGF-I-induced myotube hypertrophy through Akt. *American Journal of Physiology-Cell Physiology,* 297**,** 1124-1132.

MORSE, C. I., THOM, J. M., MIAN, O. S., MUIRHEAD, A., BIRCH, K. M. & NARICI, M. V. 2005. Muscle strength, volume and activation following 12-month resistance training in 70-year-old males. *European journal of applied physiology,* 95**,** 197-204.

MOSLER, S., PANKRATZ, C., SEYFRIED, A., PIECHOTTA, M. & DIEL, P. 2012. The anabolic steroid methandienone targets the hypothalamic–pituitary–testicular axis and myostatin signaling in a rat training model. *Archives of toxicology,* 86**,** 109-119.

MUSCARITOLI, M., BOSSOLA, M., AVERSA, Z., BELLANTONE, R. & ROSSI FANELLI, F. 2006. Prevention and treatment of cancer cachexia: new insights into an old problem. *European Journal of Cancer,* 42**,** 31-41.

OPHOFF, J., VAN PROEYEN, K., CALLEWAERT, F., DE GENDT, K., DE BOCK, K., BOSCH, A. V., VERHOEVEN, G., HESPEL, P. & VANDERSCHUEREN, D. 2009. Androgen signaling in myocytes contributes to the maintenance of muscle mass and fiber type regulation but not to muscle strength or fatigue. *Endocrinology,* 150**,** 3558-3566.

PARKINGTON, J. D., LEBRASSEUR, N. K., SIEBERT, A. P. & FIELDING, R. A. 2004. Contraction-mediated mTOR, p70S6k, and ERK1/2 phosphorylation in aged skeletal muscle. *Journal of Applied Physiology,* 97**,** 243-248.

PAYNE, A. H. & HALES, D. B. 2004. Overview of steroidogenic enzymes in the pathway from cholesterol to active steroid hormones. *Endocrine reviews,* 25**,** 947-970.

PHILIPPOU, A., HALAPAS, A., MARIDAKI, M. & KOUTSILIERIS, M. 2007. Type I insulin-like growth factor receptor signaling in skeletal muscle regeneration and hypertrophy. *J Musculoskelet Neuronal Interact,* 7**,** 208-218.

PIETRANGELO, T., PUGLIELLI, C., MANCINELLI, R., BECCAFICO, S., FANÒ, G. & FULLE, S. 2009. Molecular basis of the myogenic profile of aged human skeletal muscle satellite cells during differentiation. *Experimental gerontology,* 44**,** 523-531.

PRONSATO, L., BOLAND, R. & MILANESI, L. 2013. Non-classical localization of androgen receptor in the C2C12 skeletal muscle cell line. *Archives of biochemistry and biophysics,* 530**,** 13-22.

QIN, W., PAN, J., WU, Y., BAUMAN, W. A. & CARDOZO, C. 2010. Protection against dexamethasone-induced muscle atrophy is related to modulation by testosterone of

FOXO1 and PGC-1α. *Biochemical and biophysical research communications,* 403**,** 473-478.

RANTANEN, T., HARRIS, T., LEVEILLE, S. G., VISSER, M., FOLEY, D., MASAKI, K. & GURALNIK, J. M. 2000. Muscle strength and body mass index as long-term predictors of mortality in initially healthy men. *The Journals of Gerontology Series A: Biological Sciences and Medical Sciences,* 55**,** M168-M173.

RATAMESS, N. A., KRAEMER, W. J., VOLEK, J. S., MARESH, C. M., VANHEEST, J. L., SHARMAN, M. J., RUBIN, M. R., FRENCH, D. N., VESCOVI, J. D. & SILVESTRE, R. 2005. Androgen receptor content following heavy resistance exercise in men. *The Journal of steroid biochemistry and molecular biology,* 93**,** 35-42.

ROMMEL, C., BODINE, S. C., CLARKE, B. A., ROSSMAN, R., NUNEZ, L., STITT, T. N., YANCOPOULOS, G. D. & GLASS, D. J. 2001. Mediation of IGF-1-induced skeletal myotube hypertrophy by PI(3)K/Akt/mTOR and PI(3)K/Akt/GSK3 pathways. *Nat Cell Biol,* 3**,** 1009-13.

RONKAINEN, P. H., KOVANEN, V., ALÉN, M., PÖLLÄNEN, E., PALONEN, E.-M., ANKARBERG-LINDGREN, C., HÄMÄLÄINEN, E., TURPEINEN, U., KUJALA, U. M. & PUOLAKKA, J. 2009. Postmenopausal hormone replacement therapy modifies skeletal muscle composition and function: a study with monozygotic twin pairs. *Journal of Applied Physiology,* 107**,** 25-33.

RØNNESTAD, B. R., NYGAARD, H. & RAASTAD, T. 2011. Physiological elevation of endogenous hormones results in superior strength training adaptation. *European journal of applied physiology,* 111**,** 2249-2259.

RUBINSKY, B. 2003. Principles of low temperature cell preservation. *Heart Fail Rev,* 8**,** 277-84.

RUSS, D. & LANZA, I. 2011. The impact of old age on skeletal muscle energetics: supply and demand. *Current aging science,* 4**,** 234-247.

SACHECK, J. M., OHTSUKA, A., MCLARY, S. C. & GOLDBERG, A. L. 2004. IGF-I stimulates muscle growth by suppressing protein breakdown and expression of atrophy-related ubiquitin ligases, atrogin-1 and MuRF1. *American Journal of Physiology-Endocrinology and Metabolism,* 287**,** E591-E601.

SAINI, A., AL-SHANTI, N., FAULKNER, S. H. & STEWART, C. E. 2008. Pro- and anti-apoptotic roles for IGF-I in TNF-alpha-induced apoptosis: a MAP kinase mediated mechanism. *Growth Factors,* 26**,** 239-53.

SAINI, A., FAULKNER, S., AL-SHANTI, N. & STEWART, C. 2009. Powerful signals for weak muscles. *Ageing research reviews,* 8**,** 251-267.

SAJKO, Š., KUBÍNOVÁ, L., CVETKO, E., KREFT, M., WERNIG, A. & ERŽEN, I. 2004. Frequency of M-cadherin-stained satellite cells declines in human muscles during aging. *Journal of Histochemistry & Cytochemistry,* 52**,** 179-185.

SAKUMA, K. & YAMAGUCHI, A. 2013. Sarcopenic Obesity and Endocrinal Adaptation with Age. *International journal of endocrinology,* 2013.

SARBASSOV, D. D., ALI, S. M. & SABATINI, D. M. 2005. Growing roles for the mTOR pathway. *Current opinion in cell biology,* 17**,** 596-603.

SARBASSOV, D. D. & PETERSON, C. A. 1998. Insulin receptor substrate-1 and phosphatidylinositol 3-kinase regulate extracellular signal-regulated kinase-dependent and-independent signaling pathways during myogenic differentiation. *Molecular Endocrinology,* 12**,** 1870-1878.

SATO, K., IEMITSU, M., AIZAWA, K. & AJISAKA, R. 2008. Testosterone and DHEA activate the glucose metabolism-related signaling pathway in skeletal muscle. *American Journal of Physiology-Endocrinology and Metabolism,* 294**,** E961-E968.

SATTLER, F., BHASIN, S., HE, J., CHOU, C.-P., CASTANEDA-SCEPPA, C., YARASHESKI, K., BINDER, E., SCHROEDER, E. T., KAWAKUBO, M. & ZHANG, A. 2011. Testosterone threshold levels and lean tissue mass targets needed to enhance skeletal muscle strength and function: the HORMA trial. *The Journals of Gerontology Series A: Biological Sciences and Medical Sciences,* 66**,** 122-129.

SCHMITTGEN, T. D. & LIVAK, K. J. 2008. Analyzing real-time PCR data by the comparative CT method. *Nature protocols,* 3**,** 1101-1108.

SCHUELKE, M., WAGNER, K. R., STOLZ, L. E., HÜBNER, C., RIEBEL, T., KÖMEN, W., BRAUN, T., TOBIN, J. F. & LEE, S.-J. 2004. Myostatin mutation associated with gross muscle hypertrophy in a child. *New England Journal of Medicine,* 350**,** 2682-2688.

SCULTHORPE, N., SOLOMON, A. M., SINANAN, A. C., BOULOUX, P. M., GRACE, F. & LEWIS, M. P. 2012. Androgens affect myogenesis in vitro and increase local IGF-1 expression. *Med Sci Sports Exerc,* 44**,** 610-5.

SERRA, C., BHASIN, S., TANGHERLINI, F., BARTON, E. R., GANNO, M., ZHANG, A., SHANSKY, J., VANDENBURGH, H. H., TRAVISON, T. G. & JASUJA, R. 2011. The role of GH and IGF-I in mediating anabolic effects of testosterone on androgen-responsive muscle. *Endocrinology,* 152**,** 193-206.

SERRA, C., TANGHERLINI, F., RUDY, S., LEE, D., TORALDO, G., SANDOR, N. L., ZHANG, A., JASUJA, R. & BHASIN, S. 2013. Testosterone improves the regeneration of old and young mouse skeletal muscle. *The Journals of Gerontology Series A: Biological Sciences and Medical Sciences,* 68**,** 17-26.

SHARPLES, A. P., AL-SHANTI, N., LEWIS, M. P. & STEWART, C. E. 2011. Reduction of myoblast differentiation following multiple population doublings in mouse C2C12 cells: A model to investigate ageing? *Journal of Cellular Biochemistry,* 112**,** 3773-3785.

SHARPLES, A. P., AL-SHANTI, N. & STEWART, C. E. 2010. C2 and C2C12 murine skeletal myoblast models of atrophic and hypertrophic potential: relevance to disease and ageing? *Journal of cellular physiology,* 225**,** 240-250.

SHARPLES, A. P., PLAYER, D. J., MARTIN, N. R., MUDERA, V., STEWART, C. E. & LEWIS, M. P. 2012. Modelling in vivo skeletal muscle ageing in vitro using three-dimensional bioengineered constructs. *Aging Cell,* 11**,** 986-995.

SHARPLES, A. P. & STEWART, C. E. 2011. Myoblast models of skeletal muscle hypertrophy and atrophy. *Current Opinion in Clinical Nutrition & Metabolic Care,* 14**,** 230-236.

SHEFFIELD-MOORE, M., URBAN, R. J., WOLF, S. E., JIANG, J., CATLIN, D. H., HERNDON, D. N., WOLFE, R. R. & FERRANDO, A. A. 1999. Short-term oxandrolone administration stimulates net muscle protein synthesis in young men. *Journal of Clinical Endocrinology & Metabolism,* 84**,** 2705-2711.

SHEPPARD, R. L., SPANGENBURG, E. E., CHIN, E. R. & ROTH, S. M. 2011. Androgen receptor polyglutamine repeat length affects receptor activity and C2C12 cell development. *Physiological genomics,* 43**,** 1135-1143.

SINANAN, A., BUXTON, P. G. & LEWIS, M. P. 2006. Muscling in on stem cells. *Biology of the Cell,* 98**,** 203-214.

SINGH, R., ARTAZA, J. N., TAYLOR, W. E., GONZALEZ-CADAVID, N. F. & BHASIN, S. 2003. Androgens stimulate myogenic differentiation and inhibit adipogenesis in C3H 10T1/2 pluripotent cells through an androgen receptor-mediated pathway. *Endocrinology,* 144**,** 5081-5088.

SINGH, R., BHASIN, S., BRAGA, M., ARTAZA, J. N., PERVIN, S., TAYLOR, W. E., KRISHNAN, V., SINHA, S. K., RAJAVASHISTH, T. B. & JASUJA, R. 2009. Regulation of myogenic differentiation by androgens: cross talk between androgen receptor/ beta-catenin and follistatin/transforming growth factor-beta signaling pathways. *Endocrinology,* 150**,** 1259-68.

SINHA-HIKIM, I., ARTAZA, J., WOODHOUSE, L., GONZALEZ-CADAVID, N., SINGH, A. B., LEE, M. I., STORER, T. W., CASABURI, R., SHEN, R. & BHASIN, S. 2002. Testosterone-induced increase in muscle size in healthy young men is associated with muscle fiber hypertrophy. *American Journal of Physiology-Endocrinology and Metabolism,* 283**,** E154-E164.

SINHA-HIKIM, I., CORNFORD, M., GAYTAN, H., LEE, M. L. & BHASIN, S. 2006. Effects of testosterone supplementation on skeletal muscle fiber hypertrophy and satellite cells in community-dwelling older men. *Journal of Clinical Endocrinology & Metabolism,* 91**,** 3024-3033.

SINHA-HIKIM, I., ROTH, S. M., LEE, M. I. & BHASIN, S. 2003. Testosterone-induced muscle hypertrophy is associated with an increase in satellite cell number in healthy, young men. *American Journal of Physiology-Endocrinology and Metabolism,* 285**,** E197-E205.

SINHA-HIKIM, I., TAYLOR, W. E., GONZALEZ-CADAVID, N. F., ZHENG, W. & BHASIN, S. 2004. Androgen receptor in human skeletal muscle and cultured muscle satellite cells: up-regulation by androgen treatment. *Journal of Clinical Endocrinology & Metabolism,* 89**,** 5245-5255.

SIPILA, S., TAAFFE, D. R., CHENG, S., PUOLAKKA, J., TOIVANEN, J. & SUOMINEN, H. 2001. Effects of hormone replacement therapy and high-impact physical exercise on

skeletal muscle in post-menopausal women: a randomized placebo-controlled study. *Clinical Science,* 101**,** 147-157.

SIRIETT, V., PLATT, L., SALERNO, M. S., LING, N., KAMBADUR, R. & SHARMA, M. 2006. Prolonged absence of myostatin reduces sarcopenia. *Journal of cellular physiology,* 209**,** 866-873.

SIRIETT, V., SALERNO, M. S., BERRY, C., NICHOLAS, G., BOWER, R., KAMBADUR, R. & SHARMA, M. 2007. Antagonism of myostatin enhances muscle regeneration during sarcopenia. *Molecular Therapy,* 15**,** 1463-1470.

SMITH, C., JANNEY, M. & ALLEN, R. 1994. Temporal expression of myogenic regulatory genes during activation, proliferation, and differentiation of rat skeletal muscle satellite cells. *Journal of cellular physiology,* 159**,** 379-385.

SMITH, G. I., YOSHINO, J., REEDS, D. N., BRADLEY, D., BURROWS, R. E., HEISEY, H. D., MOSELEY, A. C. & MITTENDORFER, B. 2013. Testosterone and Progesterone, But Not Estradiol, Stimulate Muscle Protein Synthesis in Postmenopausal Women. *The Journal of Clinical Endocrinology & Metabolism,* 99**,** 256-265.

SMITH, P. K., KROHN, R. I., HERMANSON, G. T., MALLIA, A. K., GARTNER, F. H., PROVENZANO, M. D., FUJIMOTO, E. K., GOEKE, N. M., OLSON, B. J. & KLENK, D. C. 1985. Measurement of protein using bicinchoninic acid. *Anal Biochem,* 150**,** 76-85.

SPANGENBURG, E. E., LE ROITH, D., WARD, C. W. & BODINE, S. C. 2008. A functional insulin-like growth factor receptor is not necessary for load-induced skeletal muscle hypertrophy. *The Journal of physiology,* 586**,** 283-291.

SPIERING, B. A., KRAEMER, W. J., VINGREN, J. L., RATAMESS, N. A., ANDERSON, J. M., ARMSTRONG, L. E., NINDL, B. C., VOLEK, J. S., HÄKKINEN, K. & MARESH, C. M. 2009. Elevated endogenous testosterone concentrations potentiate muscle androgen receptor responses to resistance exercise. *The Journal of steroid biochemistry and molecular biology,* 114**,** 195-199.

STEVENSON, E. J., KONCAREVIC, A., GIRESI, P. G., JACKMAN, R. W. & KANDARIAN, S. C. 2005. Transcriptional profile of a myotube starvation model of atrophy. *Journal of Applied Physiology,* 98**,** 1396-1406.

SUN, Y., BILAN, P. J., LIU, Z. & KLIP, A. 2010. Rab8A and Rab13 are activated by insulin and regulate GLUT4 translocation in muscle cells. *Proceedings of the National Academy of Sciences,* 107**,** 19909-19914.

TAAFFE, D. R., SIPILÄ, S., CHENG, S., PUOLAKKA, J., TOIVANEN, J. & SUOMINEN, H. 2005. The effect of hormone replacement therapy and/or exercise on skeletal muscle attenuation in postmenopausal women: a yearlong intervention. *Clinical physiology and functional imaging,* 25**,** 297-304.

TING, H.-J. & CHANG, C. 2008. Actin associated proteins function as androgen receptor coregulators: an implication of androgen receptor's roles in skeletal muscle. *The Journal of steroid biochemistry and molecular biology,* 111**,** 157-163.

TISDALE, M. J. 2009. Mechanisms of cancer cachexia. *Physiological Reviews,* 89**,** 381-410.

TRAISH, A. M., MINER, M. M., MORGENTALER, A. & ZITZMANN, M. 2011. Testosterone deficiency. *The American journal of medicine,* 124**,** 578-587.

TRENDELENBURG, A. U., MEYER, A., ROHNER, D., BOYLE, J., HATAKEYAMA, S. & GLASS, D. J. 2009. Myostatin reduces Akt/TORC1/p70S6K signaling, inhibiting myoblast differentiation and myotube size. *American Journal of Physiology-Cell Physiology,* 296**,** C1258-C1270.

URBAN, R. J., BODENBURG, Y. H., GILKISON, C., FOXWORTH, J., COGGAN, A. R., WOLFE, R. R. & FERRANDO, A. 1995. Testosterone administration to elderly men increases skeletal muscle strength and protein synthesis. *American Journal of Physiology-Endocrinology and Metabolism,* 269**,** E820-E826.

VANDENPUT, L. & OHLSSON, C. 2010. Sex steroid metabolism in the regulation of bone health in men. *The Journal of steroid biochemistry and molecular biology,* 121**,** 582-588.

VASILCANU, D., GIRNITA, A., GIRNITA, L., VASILCANU, R., AXELSON, M. & LARSSON, O. 2004. The cyclolignan PPP induces activation loop-specific inhibition of tyrosine phosphorylation of the insulin-like growth factor-1 receptor. Link to the phosphatidyl inositol-3 kinase/Akt apoptotic pathway. *Oncogene,* 23**,** 7854-7862.

VELDERS, M. & DIEL, P. 2013. How sex hormones promote skeletal muscle regeneration. *Sports Medicine,* 43**,** 1089-1100.

VERDIJK, L. B., KOOPMAN, R., SCHAART, G., MEIJER, K., SAVELBERG, H. H. & VAN LOON, L. J. 2007. Satellite cell content is specifically reduced in type II skeletal muscle fibers in the elderly. *American Journal of Physiology-Endocrinology and Metabolism,* 292**,** E151-E157.

VINGREN, J. L., KRAEMER, W. J., HATFIELD, D. L., VOLEK, J. S., RATAMESS, N. A., ANDERSON, J. M., HÄKKINEN, K., AHTIAINEN, J., FRAGALA, M. S. & THOMAS, G. A. 2009. Effect of resistance exercise on muscle steroid receptor protein content in strength-trained men and women. *Steroids,* 74**,** 1033-1039.

VINGREN, J. L., KRAEMER, W. J., RATAMESS, N. A., ANDERSON, J. M., VOLEK, J. S. & MARESH, C. M. 2010. Testosterone physiology in resistance exercise and training. *Sports Medicine,* 40**,** 1037-1053.

WAGNER, K. R., LIU, X., CHANG, X. & ALLEN, R. E. 2005. Muscle regeneration in the prolonged absence of myostatin. *Proceedings of the National Academy of Sciences of the United States of America,* 102**,** 2519-2524.

WANNENES, F., CAPRIO, M., GATTA, L., FABBRI, A., BONINI, S. & MORETTI, C. 2008. Androgen receptor expression during C2C12 skeletal muscle cell line differentiation. *Molecular and cellular endocrinology,* 292**,** 11-19.

WARD, K. A., PYE, S. R., ADAMS, J. E., BOONEN, S., VANDERSCHUEREN, D., BORGHS, H., GAYTANT, J., GIELEN, E., BÁRTFAI, G. & CASANUEVA, F. F. 2011. Influence of age and sex steroids on bone density and geometry in middle-aged and elderly European men. *Osteoporosis international,* 22**,** 1513-1523.

WATT, K. I., JASPERS, R. T., ATHERTON, P., SMITH, K., RENNIE, M. J., RATKEVICIUS, A. & WACKERHAGE, H. 2010. SB431542 treatment promotes the hypertrophy of skeletal muscle fibers but decreases specific force. *Muscle & nerve,* 41**,** 624-629.

WELLE, S., BURGESS, K. & MEHTA, S. 2009. Stimulation of skeletal muscle myofibrillar protein synthesis, p70 S6 kinase phosphorylation, and ribosomal protein S6 phosphorylation by inhibition of myostatin in mature mice. *American Journal of Physiology-Endocrinology and Metabolism,* 296**,** E567.

WEST, D. & PHILLIPS, S. M. 2010. Anabolic processes in human skeletal muscle: restoring the identities of growth hormone and testosterone. *The Physician and sportsmedicine,* 38**,** 97.

WEST, D. W., BURD, N. A., CHURCHWARD-VENNE, T. A., CAMERA, D. M., MITCHELL, C. J., BAKER, S. K., HAWLEY, J. A., COFFEY, V. G. & PHILLIPS, S. M. 2012. Sex-based comparisons of myofibrillar protein synthesis after resistance exercise in the fed state. *Journal of Applied Physiology,* 112**,** 1805-1813.

WEST, D. W., BURD, N. A., TANG, J. E., MOORE, D. R., STAPLES, A. W., HOLWERDA, A. M., BAKER, S. K. & PHILLIPS, S. M. 2010. Elevations in ostensibly anabolic hormones with resistance exercise enhance neither training-induced muscle hypertrophy nor strength of the elbow flexors. *Journal of Applied Physiology,* 108**,** 60-67.

WEST, D. W., KUJBIDA, G. W., MOORE, D. R., ATHERTON, P., BURD, N. A., PADZIK, J. P., DE LISIO, M., TANG, J. E., PARISE, G. & RENNIE, M. J. 2009. Resistance exercise-induced increases in putative anabolic hormones do not enhance muscle protein synthesis or intracellular signalling in young men. *The Journal of physiology,* 587**,** 5239-5247.

WEST, D. W. & PHILLIPS, S. M. 2012. Associations of exercise-induced hormone profiles and gains in strength and hypertrophy in a large cohort after weight training. *European journal of applied physiology,* 112**,** 2693-2702.

WHITE, J. P., GAO, S., PUPPA, M. J., SATO, S., WELLE, S. L. & CARSON, J. A. 2012. Testosterone regulation of Akt/mTORC1/FoxO3a signaling in skeletal muscle. *Molecular and cellular endocrinology*.

WIECHELMAN, K. J., BRAUN, R. D. & FITZPATRICK, J. D. 1988. Investigation of the bicinchoninic acid protein assay: identification of the groups responsible for color formation. *Analytical biochemistry,* 175**,** 231-237.

WIERMAN, M. E. 2007. Sex steroid effects at target tissues: mechanisms of action. *Advances in physiology education,* 31**,** 26-33.

WILKINSON, S. B., TARNOPOLSKY, M. A., GRANT, E. J., CORREIA, C. E. & PHILLIPS, S. M. 2006. Hypertrophy with unilateral resistance exercise occurs without increases in endogenous anabolic hormone concentration. *European journal of applied physiology,* 98**,** 546-555.

WU, Y., BAUMAN, W. A., BLITZER, R. D. & CARDOZO, C. 2010a. Testosterone-induced hypertrophy of L6 myoblasts is dependent upon Erk and mTOR. *Biochemical and biophysical research communications,* 400**,** 679-683.

WU, Y., ZHAO, W., ZHAO, J., PAN, J., WU, Q., ZHANG, Y., BAUMAN, W. A. & CARDOZO, C. P. 2007. Identification of androgen response elements in the insulin-like growth factor I upstream promoter. *Endocrinology,* 148**,** 2984-2993.

WU, Y., ZHAO, W., ZHAO, J., ZHANG, Y., QIN, W., PAN, J., BAUMAN, W. A., BLITZER, R. D. & CARDOZO, C. 2010b. REDD1 is a major target of testosterone action in preventing dexamethasone-induced muscle loss. *Endocrinology,* 151**,** 1050-1059.

XU, T., SHEN, Y., PINK, H., TRIANTAFILLOU, J., STIMPSON, S. A., TURNBULL, P. & HAN, B. 2004. Phosphorylation of p70s6 kinase is implicated in androgen-induced levator ani muscle anabolism in castrated rats. *J Steroid Biochem Mol Biol,* 92**,** 447-54.

YAFFE, D. & SAXEL, O. 1977. Serial passaging and differentiation of myogenic cells isolated from dystrophic mouse muscle. *Nature,* 270**,** 725-7.

YIN, H.-N., CHAI, J.-K., YU, Y.-M., SHEN, C.-A., WU, Y.-Q., YAO, Y.-M., LIU, H., LIANG, L.-M., TOMPKINS, R. G. & SHENG, Z.-Y. 2009. Regulation of signaling pathways downstream of IGF-I/insulin by androgen in skeletal muscle of glucocorticoid-treated rats. *The Journal of Trauma and Acute Care Surgery,* 66**,** 1083-1090.

ZENG, X.-Q., ZHANG, C.-M., TONG, M.-L., CHI, X., LI, X.-L., JI, C.-B., ZHANG, R. & GUO, X.-R. 2012. Knockdown of NYGGF4 increases glucose transport in C2C12 mice skeletal myocytes by activation IRS-1/PI3K/AKT insulin pathway. *Journal of bioenergetics and biomembranes,* 44**,** 351-355.

ZHAO, W., PAN, J., ZHAO, Z., WU, Y., BAUMAN, W. A. & CARDOZO, C. P. 2008. Testosterone protects against dexamethasone-induced muscle atrophy, protein degradation and MAFbx upregulation. *The Journal of steroid biochemistry and molecular biology,* 110**,** 125-129.

9. APPENDIX

9.1 APPENDIX 1

Table 9.1 Raw C_T values obtained for Myogenin, AR, IGF-I and myostatin transcripts. These data were used to construct Fig 3.5

	Sample	Myogenin mean C_T	AR mean C_T	IGF-I mean C_T	Myostatin mean C_T	RP2 mean C_T
72 hrs	DM	21.93	29.71	20.23	26.09	20.19
	50 nM T	21.01	29.78	20.29	26.16	19.84
	500 nM T	21.30	29.46	20.14	25.84	19.54
7 days	DM	22.47	30.66	20.24	25.01	20.59
	50 nM T	22.38	31.47	20.91	24.13	21.40
	500 nM T	22.76	31.59	20.96	25.44	21.40

9.2 APPENDIX 2

Table 9.2 Raw C_T values obtained for Myogenin, AR and IGF-I transcripts in CON and PD myoblasts treated with and without flutamide (F). These data were used to construct fig 4.3.

	Cell type	Treatment	Myogenin mean C_T	AR mean C_T	IGF-I mean C_T	RP2 mean C_T
72 hrs	CON	DM	16.39	22.47	17.71	17.11
		40 μM F	17.24	23.47	18.21	17.09
	PD	DM	18.28	21.32	19.11	16.17
		40 μM F	21.91	21.85	20.48	16.90
7 days	CON	DM	16.41	22.85	16.01	16.42
		40 μM F	17.99	21.70	17.42	16.75
	PD	DM	17.19	19.90	17.66	16.09
		40 μM F	22.27	22.75	19.15	16.59

9.3 APPENDIX 3

Copy of peer reviewed journal article including data from chapter 6 (Deane *et al*., 2013).

Title: Impaired Hypertrophy in myoblasts is improved with testosterone administration

Journal: The Journal of Steroid Biochemistry and Molecular Biology

Issue: 138

Pages: 152-161

See Overleaf

Journal of Steroid Biochemistry & Molecular Biology 138 (2013) 152–161

Contents lists available at SciVerse ScienceDirect

Journal of Steroid Biochemistry and Molecular Biology

journal homepage: www.elsevier.com/locate/jsbmb

Impaired hypertrophy in myoblasts is improved with testosterone administration

Colleen S. Deane[b,c,1], David C. Hughes[a,b,1], Nicholas Sculthorpe[d], Mark P. Lewis[b,e,f,g], Claire E. Stewart[a], Adam P. Sharples[a,*]

[a] Stem Cells, Ageing & Molecular Physiology (SCAMP) Unit, Research Institute for Sport and Exercise Sciences (RISES), School of Sport and Exercise Sciences, Liverpool John Moores University, Tom Reilly Building, Byrom Street, Liverpool, UK
[b] Muscle Cellular and Molecular Physiology Research Group (MCMPRG), Institute of Sport and Physical Activity Research (ISPAR), University of Bedfordshire, UK
[c] School of Health and Social Care, Bournemouth University, UK
[d] Institute for Clinical Exercise and Health Science (ICEHS), University of the West of Scotland, Hamilton, UK
[e] Cellular and Molecular Physiology, Musculoskeletal Biology Research Group, School of Sport, Exercise and Health Science, Loughborough University, Loughborough, UK
[f] Cranfield Health, Cranfield University, Cranfield, Bedfordshire, UK
[g] School of Life and Medical Sciences, University College London (UCL), UK

ARTICLE INFO

Article history:
Received 21 February 2013
Received in revised form 8 May 2013
Accepted 14 May 2013

Keywords:
Satellite cell
Muscle stem cell
PI3K
Akt
mTOR
Myostatin

ABSTRACT

We investigated the ability of testosterone (T) to restore differentiation in multiple population doubled (PD) murine myoblasts, previously shown to have a reduced differentiation in monolayer and bioengineered skeletal muscle cultures vs. their parental controls (CON) (Sharples et al., 2011, 2012 [7,26]). Cells were exposed to low serum conditions in the presence or absence of T (100 nM) ± PI3K inhibitor (LY294002) for 72 h and 7 days (early and late muscle differentiation respectively). Morphological analyses were performed to determine myotube number, diameter (μm) and myonuclear accretion as indices of differentiation and myotube hypertrophy. Changes in gene expression for myogenin, mTOR and myostatin were also performed. Myotube diameter in CON and PD cells increased from 17.32 ± 2.56 μm to 21.02 ± 1.89 μm and 14.58 ± 2.66 μm to 18.29 ± 3.08 μm ($P \leq 0.05$) respectively after 72 h of T exposure. The increase was comparable in both PD (+25%) and CON cells (+21%) suggesting a similar intrinsic ability to respond to exogenous T administration. T treatment also significantly increased myonuclear accretion (% of myotubes expressing 5+ nuclei) in both cell types after 7 days exposure ($P \leq 0.05$). Addition of PI3K inhibitor (LY294002) in the presence of T attenuated these effects in myotube morphology (in both cell types) suggesting a role for the PI3K pathway in T stimulated hypertrophy. Finally, PD myoblasts showed reduced responsiveness to T stimulated mRNA expression of mTOR vs. CON cells and T also reduced myostatin expression in PD myoblasts only. The present study demonstrates testosterone administration improves hypertrophy in myoblasts that basally display impaired differentiation and hypertrophic capacity vs. their parental controls, the action of testosterone in this model was mediated by PI3K/Akt pathway.

1. Introduction

Muscle wasting occurs within many life-threatening diseases such as cancer (termed cancer cachexia) [1], AIDS [2], sepsis [3], heart failure [4] and ageing (sarcopenia) [5–7]. Individuals that experience muscle loss during these various disease states have a reduced physiological and functional capacity, altered metabolism [8,9] and a reduction in circulating levels of growth hormone, insulin-like-growth factor-I (IGF-I) and testosterone [2]. These accumulative factors manifest themselves in increased frailty and morbidity and therefore reduced quality of life that subsequently leads to earlier mortality [10,11]. In the instance of cancer approximately 50% of patients suffer with muscle atrophy (cachexia), which alone accounts for 25% of all cancer deaths [12–14]. The regulation of skeletal muscle mass is reliant on the balance between hypertrophy (e.g. protein synthesis/anabolism) and atrophy (e.g. protein breakdown/catabolism). A potential clinical intervention for promoting a positive net balance in the favour of protein synthesis is testosterone (T) administration [15,16]. T replacement therapy has been observed to increase muscle strength and mass in various clinical populations including patients with AIDS, COPD and sarcopenia [12,17–20]. However, a limited number of studies have investigated the role of T in skeletal muscle hypertrophy and atrophy [21–23] at the cellular level.

Skeletal muscle fibre numbers are set in-utero, i.e. fibres are terminally differentiated or post mitotic and unable to divide. Skeletal

* Corresponding author at: Stem Cells, Ageing & Molecular Physiology (SCAMP) Unit, Research Institute for Sport and Exercise Sciences (RISES), School of Sport and Exercise Sciences, Liverpool John Moores University, Tom Reilly Building, Byrom Street, Liverpool L3 3AF, UK. Tel.: +44 7812732670.
E-mail address: a.p.sharples@googlemail.com (A.P. Sharples).
[1] These authors are considered joint primary authors of this article.

0960-0760/$ – see front matter © 2013 Elsevier Ltd. All rights reserved.
http://dx.doi.org/10.1016/j.jsbmb.2013.05.005

muscles regenerative capacity therefore occurs as a result of a specialised cell type, the satellite cell, which resides underneath the basal lamina of the mature fibre and has mitotic potential. With the relevant cues, satellite cells are activated (termed myoblasts), then proliferate or return to quiescence for subsequent regenerative bouts. Activated myoblasts repair the muscle by fusing with the existing fibres, a process known as differentiation [24,25]. Most recently, our laboratories have highlighted two myoblast models to study reduced differentiation capacity [7,26,27]. The first investigated the parental mouse C_2 myoblasts vs. their subclone, the C_2C_{12} cells. Despite their shared origins, we observed differences in morphological and biochemical responses between the C_2 and C_2C_{12} cells. The C_2 cells displayed slower and diminished differentiation profiles compared to the C_2C_{12} cells and were also more susceptible to TNF-α-induced inhibition of differentiation and induction of apoptosis [27]. Because muscle wasting is associated with reduced muscle mass [28,29] and increased susceptibility to TNF-induced muscle protein degradation [30–32], this comparative model provided us with an excellent representation of muscle atrophy, hypertrophy and adaptability, thus, enabling the determination of potential regulators associated with muscle wasting. The second model utilised C_2C_{12} cells that had undergone multiple population doublings (PD) vs. parental control cells (CON), which have undergone no doublings relative to the PD cells [7]. These cells also display impaired differentiation in monolayer [7] and in three dimensional culture systems [26] vs. their parental controls. We reported that the PD cells had a significantly reduced number of cells exiting the cell cycle in G1, a prerequisite for fusion, with corresponding decreases in transcript expression of IGF-I, myoD, myogenin and reduced activation of Akt with increases in IGFBP5 mRNA and JNK activation vs. control cells [7]. Interestingly, similar morphology, transcript and signalling processes were also observed in cells isolated from aged human muscle [33–35] and in whole tissue biopsies [36,37]. Thus, these cells can be used as a representative model to investigate mechanisms of atrophic phenotypes (PD) vs. parental control cells (CON) that display hypertrophic phenotypes [7].

In the present study we utilised the latter model to investigate T administration on PD cells displaying impaired differentiation. As the PD cells display a reduction in Akt activation [7], the PI3K/Akt/mTOR pathway was investigated in the present study, as it is inextricably involved in protein synthesis [38] and most recently linked to T's regulation of muscle hypertrophy [23].

The aims were to: (1) improve the impaired differentiation and hypertrophy profiles observed previously in PD cells using T administration; and (2) manipulate the role of PI3K/Akt in Ts regulation of differentiation in PD and CON cells. We hypothesised that T would induce improved differentiation and hypertrophy in CON cells and would improve the impaired differentiation in the PD cells. Further by inhibiting PI3K, testosterone's ability to restore differentiation action would be negated in both cell types. The overall objective of the research was to utilise an in vitro model that is representative of impaired differentiation (PD) in order to elucidate the ability of T to improve differentiation and hypertrophy and to investigate the cellular and molecular mechanisms of its action.

2. Materials and methods

2.1. Cell culture

Mouse C_2C_{12} [39,40] (ATCC, Rockville, MD, USA) skeletal muscle myoblasts were seeded at 80,000 cells per ml in 2 ml of growth media (GM) per well (Dulbecco's modified eagle's medium, DMEM (Sigma, Dorset, UK)), 20% foetal bovine serum (FBS) (PAA, Somerset, UK), 1% PenStrep (Invitrogen, Paisley, UK)) onto 0.2% porcine gelatin-coated (Sigma, Dorset, UK) 6-well plates (Fisher Scientific, Loughborough, UK) and grown in a humidified 5% CO_2 atmosphere at 37 °C. Population doubled (PD) cells and their parental controls (CON) were developed as detailed in Sharples et al. [7,26]. Briefly, PD cells underwent an extra 58–60 population doublings vs. their CON cells. Once confluent, the myoblasts were changed from growth media to low serum media/differentiation media (DM; composed of: DMEM, 2% horse serum (HS), 1% Penstrep and 1% L-glutamine) which promotes the fusion of the myoblasts into multinucleated myotubes. C_2C_{12} myoblasts undergo spontaneous differentiation into myotubes on serum withdrawal, and do not require growth factor addition to stimulate the process [40]. Cells were incubated in DM for 30 min at 37 °C in a 5% CO_2 atmosphere with this period of equilibration denoted as, 0 h time point. Cells at the time points of 72 h and 7 days (early and late muscle differentiation respectively) were fixed (see below) for subsequent morphology analyses or isolated for reverse transcription quantitative real-time polymerase chain reaction (RT-PCR).

2.2. Cell treatments

All treatments were administered in 2 ml DM per well. The treatments comprised of a vehicle control (DMSO at a concentration of 0.01%), testosterone alone (T) 100 nM (Tocris Bioscience, Bristol, UK), PI3K inhibitor (LY) 5 μM (LY294002 – Calbiochem, Middlesex, UK), 100 nM T + 5 μM LY. DMSO was used as the solvent for T reconstitution at the same concentration as the vehicle (0.01%). For results and figure legends the following nomenclature will be used DMSO, T, LY and T + LY All treatments were added at 0 h and existing media was further supplemented at 72 h with 1 ml of DM containing the aforementioned treatments conditions. The inhibitor, LY at a dose of 5 μM has been extensively shown to be highly specific and effective in C_2C_{12} cells in inhibiting PI3K and downstream Akt [41–46].

2.3. RNA isolation

Plates for each time point (0 h, 72 h and 7 days) were washed twice with 1 ml/well phosphate buffer saline (PBS) (Fisher Scientific, Loughborough, UK) and extracted for RNA using 250 μl TRIzol™ Reagent (Sigma, Dorset, UK) per well. RNA was extracted following manufacturer's instructions. RNA concentration and purity were assessed through UV spectroscopy at ODs of 260 and 280 nm, using the Nanodrop spectrophotometer 3000 (Fisher, Rosklide, Denmark). Only samples with a 260:280 ratio of between 1.9 and 2.15 were carried forward for reverse transcription and PCR amplification detailed below.

2.4. Primer design

Primer sequences (Table 1) were identified using Gene (NCBI, www.ncbi.nlm.nih.gov/gene) and designed using both web-based OligoPerfect™ Designer (Invitrogen, Carlsbad, CA, USA) and Primer-BLAST (NCBI, http://www.ncbi.nlm.nih.gov/tools/primer-blast). Sequence homology searches ensured specificity. Three or more GC bases in the last 5 bases at the 3′ end of the primer were avoided. Secondary structure interactions (hairpins, self-dimer and cross dimer) within the primer were also avoided. All primers ranged between 18 and 23 bp and amplified a product between 173 and 197 bp. GC content was between 36.3 and 55.5% (Table 1). Primers without the requirement of further purification were purchased from Sigma (Suffolk, UK).

Table 1
Primer sequences for genes of interest.

Gene	Primer sequence (5′–3′)	Ref. sequence number	Amplicon length (bp)	GC% content
Myostatin	**F:** TACTCCGAATAGAAGCCATAA	NM_010834	194	36.3
	R: GTAGCGTGATAACGTCATC			45
mTOR	**F:** CACTCCACTATCCTGTTACCT	NM_020009	190	47.6
	R: GAGATCCTTGGCACACCT			55.5
Myogenin	**F:** CCAACTGAGATTGTCTGTC	NM_031189	173	47.3
	R: GGTGTTAGCCTTATGTGAAT			40
RP-IIβ	**F:** GGTCAGAAGGGAACTTGTGGTAT	NM_153798.1	197	50
	R: GCATCATTAAATGGAGTAGCGTC			44.4

2.5. Reverse transcription quantitative real time polymerase chain reaction (rt-qRT-PCR)

70 ng of RNA/sample was reverse transcribed and amplified using QuantiFast™ SYBR® Green RT-PCR one-step kit on a Rotogene 3000Q (Qiagen, Crawley, UK) supported by Rotogene software (Hercules, CA, USA). rt-qRT-PCR was performed as follows: 10 min, 50 °C (reverse transcription), 5 min 95 °C (transcriptase inactivation and initial denaturation), followed by: 10 s, 95 °C (denaturation), 30 s, 60 °C (annealing and extension) for 40 cycles. Following completion, melting curve analyses were performed to exclude primer–dimer and non-specific amplification (all melt analysis in this study presented single reproducible peaks). All PCR efficiencies were comparable (standard deviation ± 0.03%) across all conditions and genes. Relative mRNA expression was quantified for myogenin, mTOR and myostatin (Table 1) using the comparative Ct ($^{\Delta\Delta}$ct) method [7,47] against a stable reference gene of RP-IIb (combined Ct value for all runs across experimental conditions 16.63 ± 0.38) and calibrator of CON treatment at 0 h.

2.6. Morphological analysis

Following media aspiration and 2× PBS washes (1 ml/well), cells were fixed by adding 1 ml methanol/acetone (1:1) to 1 ml PBS in per well in a drop-wise manner and incubated for 10 min at RT. Following aspiration, 2 ml methanol and acetone (1:1) were added to each well and incubated for a further 10 min. Finally PBS (2 ml/well) was added after removal of the methanol and acetone solution and plates were stored at 4 °C until further analyses. This fixing process allowed nuclei to become discernible under light microscopy alone, without the need for additional nuclear staining. A total of 30 fields per condition for each time point were captured with a cell imaging system at 10× magnification (Inverso-TC, CETI, Medline Scientific Limited, Oxon, UK) and analysed using Image J (Java) software (National Institutes of Health, USA). Morphology was assessed by determination of myotube diameter, number of myotubes per view, mean number of nuclei per myotube per field of view, fusion index (cell fusion) and total nuclei counts (changes in total cell number and therefore an indices for proliferation). A myotube was defined as containing 3+ nuclei encapsulated within cellular structures, so to avoid counting of cells undergoing mitosis. Myotube diameter (μm) was determined by measuring the diameter of 3 equidistant points on each myotube (left end, middle, right end) and determining the mean of the 3 values as previously described [48,49]. An indicator of myonuclear accretion (fusion index) was calculated by dividing myotubes into two classes; myotubes which contained 3–4 nuclei or myotubes which expressed 5+ nuclei.

2.7. Statistical analyses

Experiments were performed 3× (n = 3) in triplicate. Data are presented as mean + S.D. Morphology data at 72 h were assessed using a (2 × 2) mixed two-way factorial ANOVA (GraphPad Software, Inc., San Diego, USA) for interactions between cell type (PD, CON) and treatments (DMSO, T). LY and T + LY treatment were excluded from the aforementioned analysis, as there were no observable myotubes at 72 h in these conditions. Morphology data at 7 days were assessed using a (2 × 4) mixed two-way factorial ANOVA for interactions between cell type (PD, CON) and treatments (DMSO, T, LY and T + LY). Gene expression data were assessed using a (2 × 2 × 4) mixed three-way factorial ANOVA for interactions between cell type (PD, CON), time (72 h and 7 days) and treatments (DMSO, T, LY and T + LY). Bonferroni post hoc analyses were performed where main effects for treatment or cell type occurred, without a significant interaction between treatment and cell type. If significant interactions were present, independent t-tests were conducted to confirm statistical significance between variables of interest. Furthermore, paired-sample t-tests were undertaken for variable of interests within cell type and treatment. Myonuclear accretion (fusion index) measures were analysed using Chi Square to investigate whether myotube categories (3–4 nuclei or 5+ nuclei) differed from one another based on treatment exposure. A P-value of $\leq$0.05 was considered to represent a statistically significant difference.

3. Results

3.1. Exogenous T treatment increases myotube hypertrophy in both CON and PD cells

The administration of exogenous DMSO, T, LY, T + LY to CON and PD cells brought about morphological changes in differentiation (Figs. 1 and 2). Firstly, it is important to mention that in support of previous observations showing reductions in differentiation in PD vs. CON cells [7]; a significant difference for mean myotube diameter at 72 h was again observed in the present study (CON 17.32 ± 2.56 vs. PD 14.58 ± 2.66, P = 0.01, Fig. 3A, supporting the atrophic phenotype observed previously in PD cells [7,26]. Importantly, in the present study, T administration appeared to increase hypertrophy (myotube diameter) in both cell types. Statistical analyses confirmed the morphological observations in Figs. 1 and 2 and revealed that a T-stimulus significantly increased myotube diameter in both CON and PD cells after 72 h (CON + T 21.02 ± 1.89 vs. CON 17.32 ± 2.56; PD + T 18.29 ± 3.08 vs. PD 14.58 ± 2.66, P = 0.01, Fig. 3A) and 7 days (CON + T 22.03 ± 2.65 vs. CON 17.50 ± 2.38; PD + T 20.49 ± 1.99 vs. PD 15.70 ± 1.59, P = 0.01, Fig. 3A) compared with non-treated cells, respectively.

Importantly, the magnitude of change between both cell models in response to T administration and compared with their respective baseline controls was not significantly different at either time points, with T increasing myotube diameter in both PD (+25% and +23%) and CON (+21% and +20%) cells to the same extent after 72 h (Fig. 3A) and 7 days (Fig. 3C) respectively. Overall, this suggests that cells with a reduced differentiation phenotype have the same capacity to undergo hypertrophy in response to exogenous testosterone administration as CON cells. Furthermore, the addition of T significantly increased myotube number in CON cells (CON + T 2.90 ± 0.72 vs. CON 2.23 ± 0.68, $P \leq$ 0.05, Fig. 3D)

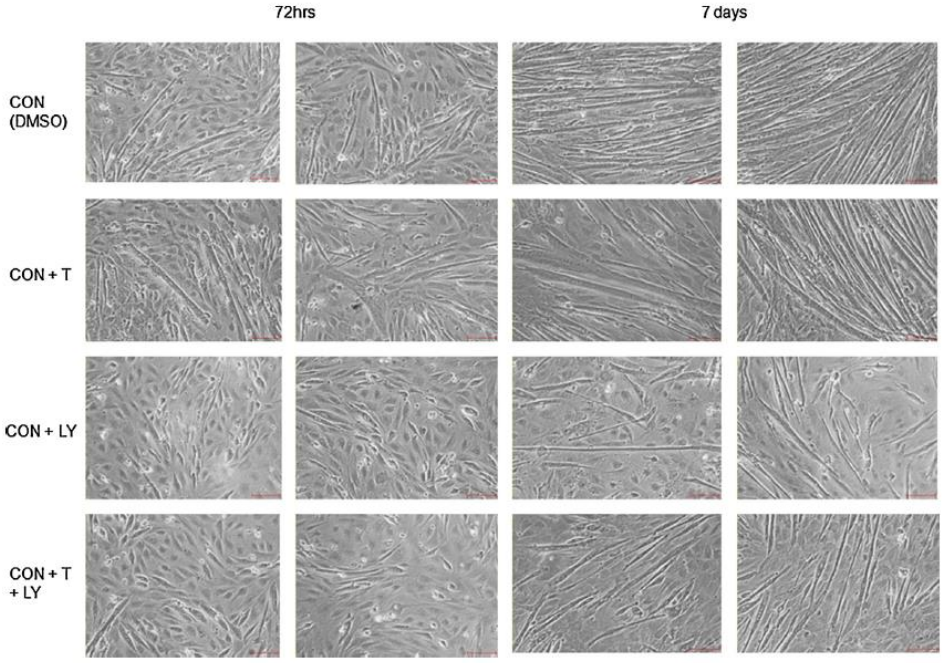

Fig. 1. Representative light microscope images (10× magnification) of treatments (DMSO, T, LY, T+LY) exposed to the CON cell type after 72 h and 7 days.

after 7 days exposure only (at 72 h although there were mean increases this was not statistically significant (P= N.S.)). There were no significant changes in myotube number in PD cells after 72 h or 7 days exposure (P= N.S.). This suggests testosterone increases hypertrophy (myotube diameter) in both cells types; however, T only enhanced myotube number in CON cells at 7 days.

Together with the changes in myotube diameter at both 72 h and 7 days, T significantly increased the mean number of nuclei per myotube in CON cells (CON 3.77 ± 0.86 vs. CON + T 4.98 ± 1.76, $P \leq 0.001$, Fig. 3B) at 72 h and at 7 days (CON 3.68 ± 0.67 vs. CON + T 4.91 ± 1.10, $P \leq 0.01$, Fig. 3B); again substantiating the morphological observation that hypertrophy, rather than hyperplasia was occurring in response to T administration. Furthermore, in the PD cells, a similar response was observed for nuclei/myotube in the presence of T at 72 h (PD + T 4.27 ± 1.03 vs. PD 3.33 ± 0.71, P= 0.03, Fig. 3B), and 7 days (PD + T 5.18 ± 1.31 vs. PD 3.84 ± 0.71, $P \leq 0.001$ Fig. 3B) compared to non-treated cells. Interestingly, again there were similar magnitude increases in CON and PD cells in the presence of T vs. basal conditions at 72 h (24.3% CON vs. 22% PD) and 7 days (25.1% CON vs. 25.9% PD).

3.2. PI3K/Akt inhibitor (LY) inhibits testosterone-induced increases in differentiation and hypertrophy in both CON and PD cells

The presence of LY inhibitor alone led to a lack of differentiation with no quantifiable myotubes being present in both CON and PD cells at 72 h (Figs. 1 and 2). As highlighted above; the addition of T significantly increased differentiation shown by enhanced myotube number in CON cells (CON + T 2.90 ± 0.72 vs. CON 2.23 ± 0.68, $P \leq 0.05$, Fig. 3D) after 7 days exposure. The presence of LY co-incubated with T significantly reduced myotube number vs. testosterone alone conditions (CON + T + LY 2.21 ± 0.56 vs. CON + T 2.90 ± 0.72, $P \leq 0.05$, Fig. 3D). LY alone was also able to reduce myotube number vs. T treatment (CON + LY 1.77 ± 0.65 vs. CON + T 2.90 ± 0.72, $P \leq 0.05$, Fig. 3D) and non-treated controls (2.23 ± 0.68, $P \leq 0.01$, Fig. 3D). Interestingly, T in the presence of the LY inhibitor was unable to restore differentiation, shown by non-significant differences with LY alone conditions (P= N.S.) and non-treated CON cells (Fig. 3D). These observations highlight that Ts increase in myotube number in CON cells, is blunted in the presence of the LY inhibitor; returning differentiation back to basal levels. As previously highlighted there were no significant changes in myotube number after T administration in PD cells. However, LY alone was able to reduce myotube number vs. T treatment (PD + LY 1.89 ± 0.80 vs. PD + T 2.35 ± 0.69, $P \leq 0.05$, Fig. 3D) and non-treated controls (PD 2.26 ± 0.53, P= 0.05, Fig. 3D).

Following these observations for indices of differentiation we next wished to ascertain the impact of T in the presence of the PI3K inhibitor (LY) on myotube hypertrophy. At 7 days, as previously highlighted above, the addition of T significantly increased myotube diameter in CON and PD cells (Fig. 3C). The presence of LY co-incubated with T significantly reduced testosterone's effect on myotube diameter in both CON (CON + T + LY 17.49 ± 2.21 vs. CON + T 22.03 ± 2.65, $P \leq 0.05$, Fig. 3C) and PD cells (PD + T + LY 17.10 ± 2.40 vs. PD + T 20.49 ± 1.99, $P \leq 0.05$, Fig. 3C). LY alone was also able to reduce myotube diameter vs. T treatment in CON cells (CON + T 22.03 ± 2.65 vs. CON + LY 17.7 ± 2.91, $P \leq 0.05$, Fig. 3C). Similar observations were observed in PD cells (PD + T 20.49 ± 1.99 vs. PD + LY 15.83 ± 2.53, $P \leq 0.05$, Fig. 3C). Interestingly,

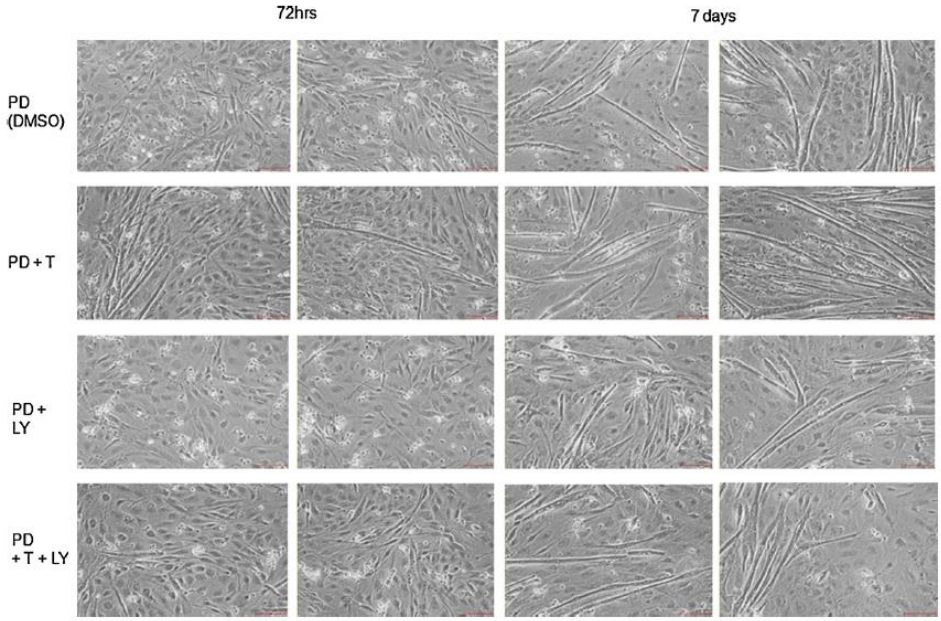

Fig. 2. Representative light microscope images (10× magnification) of treatments (DMSO, T, LY, T + LY) to population doubled cells after 72 h and 7 days.

T was unable to restore myotube diameter in the presence of the LY inhibitor shown by non-significant differences with LY alone conditions in CON cells and non-treated CON cells (P = N.S., Fig. 3C). The same observations were mirrored in PD cells where T was unable to restore myotube diameter in the presence of the LY inhibitor shown by non-significant differences with LY alone conditions in PD cells (P = N.S., Fig. 3C). Overall, this shows that T's observed increases in hypertrophy was blunted in the presence of the LY inhibitor returning myotube diameter back to basal levels in both cell types.

3.3. T-treatments enhancement in differentiation and hypertrophy is accompanied by increases in myonuclear accretion

To address the effects of the various treatments on the capacity to undergo cell fusion, myonuclear accretion was calculated. The administration of T resulted in a greater percentage of myotubes expressing 5+ nuclei for both CON (CON + T 67.9% vs. CON 32.1%, $\chi^2_1 = 32.99$, $P \leq 0.05$) and PD cells (PD + T 67.2% vs. PD 32.8%, $\chi^2_1 = 20.58$, $P \leq 0.05$) compared to untreated cells after 7 days exposure (Fig. 4A and B respectively). Furthermore, the addition of LY with T treatment reduced the percentage of myotubes expressing 5+ nuclei back to similar levels of LY-alone treated cells (CON + T + LY 28.1% vs. CON + LY 15.2%, $\chi^2_1 = 2.53$, P = N.S.; PD + T + LY 37.5% vs. PD + LY 21.6%, $\chi^2_1 = 3.4$, P = N.S., Fig. 4A and B respectively). In accordance with these observations, there was no significant difference in total nuclei counts for all treatments in either cell type at both time points (P = N.S.). There was however a significant interaction between cell type where PD cells had a significantly higher total nuclei count ($P \leq 0.05$) compared to CON cells at both time points, a finding confirmed previously by Sharples et al. [7], who highlighted a continued proliferation at the expense of exiting the cell cycle in G1 and differentiating.

3.4. Expression of myogenin mRNA increases after T-administration in both PD and CON cells

There was a significant difference in myogenin transcript expression levels between CON and PD cells after 72 h (CON 191.51 ± 12.84 vs. PD 48.58 ± 8.14, $P \leq 0.001$, Fig. 5A) and 7 days exposure (CON 128.36 ± 27.11 vs. PD 59.22 ± 4.57, $P \leq 0.001$, Fig. 5A). Whilst still remaining significantly different, the expression of myogenin significantly increased in both CON and PD cells when treated with T (CON + T 222.18 ± 36.63 vs. CON 191.51 ± 12.84; PD + T 67.00 ± 5.35 vs. PD 48.58 ± 8.14, $P \leq 0.05$, Fig. 5A) after 72 h. The increase in myogenin mRNA expression also continued at 7 days in PD treated cells (PD + T 74.15 ± 8.13 vs. PD 59.22 ± 4.57, $P \leq 0.001$, Fig. 5A), yet there was no difference in myogenin mRNA expression at this time point between non-treated and T-treated CON cells. However, absolute levels of myogenin transcript expression were basally significantly higher (shown above) in CON treated cells vs. PD treated (CON + T 131.46 ± 24.53 vs. PD + T 67.00 ± 5.35, P = 0.001) cells at 7 days. The presence of LY, significantly reduced myogenin expression after 72 h exposure in CON cells (CON + LY 134.38 ± 16.13 vs. CON 191.51 ± 16.00, $P \leq 0.05$ Fig. 5A), with no reductions being observed in PD cells at the same time point. Furthermore, LY alone had no effect on myogenin mRNA expression after 7 days culture in either cell type (P = N.S. Fig. 5A).

T in the presence of LY inhibitor significantly attenuated myogenin expression after 72 h when compared with T alone in both cell types (CON + T 222.18 ± 36.63 vs. CON + T + LY 146.09 ± 24.58, $P \leq 0.05$; PD + T 67.00 ± 5.35 vs. PD + T + LY 56.04 ± 11.50, $P \leq 0.05$, Fig. 5A). At 7 days, there were no significant changes for any treatment conditions in CON cells (P = N.S. for all comparisons) for myogenin expression. However in PD cells, T further enhanced myogenin expression significantly, even when administered in

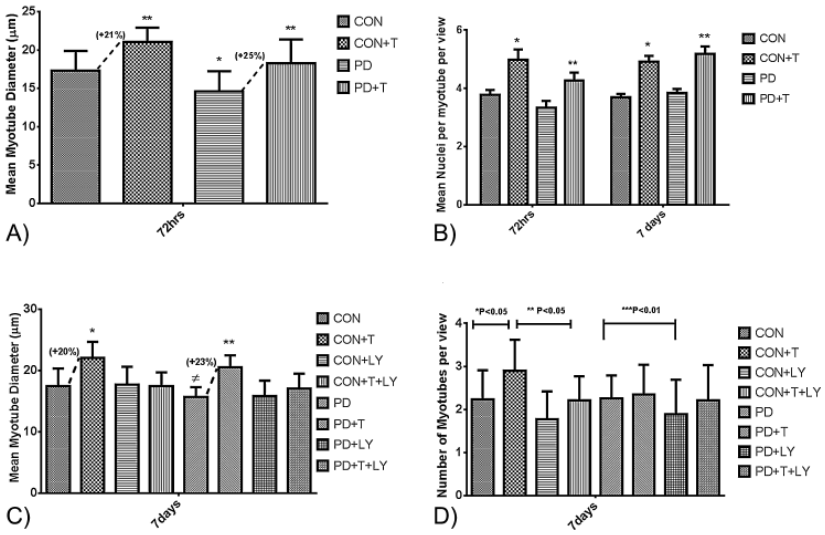

Fig. 3. The effect of T-stimulus on CON and PD cells on various morphology variables after 72 h and 7 days exposure. (A) The effect of T-stimulus on mean myotube diameter for CON and PD cells after 72 h exposure. *Reduced mean myotube diameter between CON and PD cells ($P \leq 0.01$). **T-stimulus significantly increased mean myotube diameter in CON cells vs. non-treated CON and PD ($P \leq 0.01$). Dash line represents magnitude change in mean myotube diameter with T-stimulus, similar in magnitude for both CON (+21%) and PD (+25%) cells. A similar pattern was observed at 7 days (CON +20%; PD +23%). (B) The changes in mean nuclei per myotube at 72 h and 7 days with and without exogenous T administration. *T significantly increased mean nuclei per myotube in CON (+24%; $P \leq 0.001$) cells after 72 h and 7 days (+25%; $P \leq 0.001$) exposure vs. non-treated cells. **T-treatment in PD cells increased mean nuclei per myotube after 72 h (+22%; $P = 0.033$) and 7 days exposure (+25%; $P \leq 0.001$). (C) Myotube number is attenuated when LY is co-incubated with T at 7 days. *The presence of LY significantly reduced the effect of T on myotube diameter ($P \leq 0.05$) in CON cells. **A similar effect was observed in PD cells ($P \leq 0.05$). ≠ Myotube diameter significantly reduced in PD vs. CON cells, similar to that observed at 72 h (see Fig. 2A) ($P \leq 0.05$). Dash line represents magnitude change in mean myotube diameter with T-stimulus, similar in both CON (+20%) and PD (+23%) cells. It appears that T's action on myotube hypertrophy requires the activity of the PI3K/Akt pathway in both cell types. (D) The effect of T and LY treatment on myotube number in CON and PD cells at 7 days. *T-treated CON cells significantly exhibited a greater number of myotubes compared to non-treated cells ($P \leq 0.05$). **The addition of LY alone and in the presence of T significantly reduced the number of myotubes compared to T-treated CON cells ($P \leq 0.05$). ***In PD cells, LY alone significantly reduced myotube number ($P \leq 0.01$) at 7 days, with all other treatments showed no significant effects.

the presence of LY (PD 59.22 ± 4.57 vs. PD + T + LY 69.93 ± 3.98, $P \leq 0.05$; PD + LY 57.04 ± 9.22 vs. PD + T + LY 69.93 ± 3.98, $P \leq 0.05$, Fig. 5A). Thus, T caused an increase in myogenin expression in both cells types, whether LY was present or absent. This may suggest at the molecular level at least, that T elevates myogenin expression, independently of PI3K/Akt, but appears to be not sufficient enough to rescue morphological differentiation/hypertrophy in PD cells.

3.5. Testosterone increases mTOR expression in the presence of PI3K inhibitor in CON cells

The expression of mTOR did not change after 72 h in either cell type (CON 0.97 ± 0.08 vs. PD 0.97 ± 0.12, Fig. 5B). After 7 days exposure, T administration alone significantly increased mTOR mRNA expression compared to CON non-treated cells (CON + T 121.08 ± 15.87 vs. CON 111.95 ± 19.36, $P \leq 0.05$ Fig. 5B).

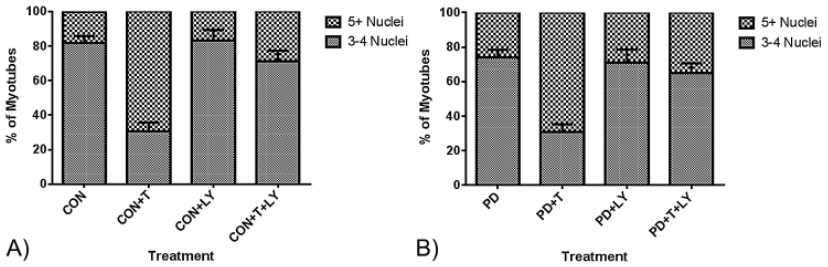

Fig. 4. The effect of T and LY treatment on myonuclear accretion in CON (A) and PD (B) cells after 7 days exposure. T-treatment significantly increased the percentage of myotubes expressing 5+ nuclei in both cell types ($P \leq 0.05$). LY alone reduced the percentage of 5+ nucleated myotubes back to baseline levels in both cell types. T in the presence of PI3K inhibitor (LY) was unable to to restore the number of 5+ nucleated myotubes to the levels induced by T alone.

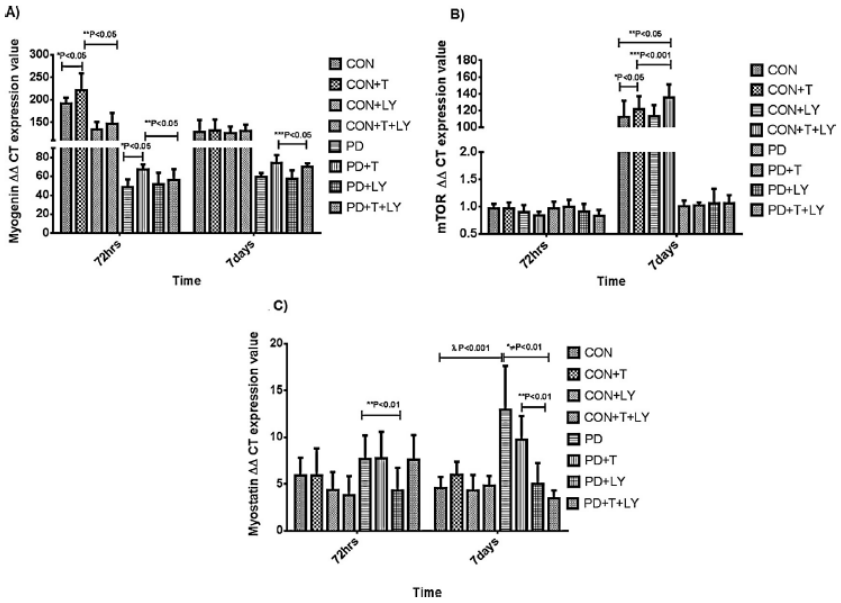

Fig. 5. The effect of T-stimulus on mRNA expression of myogenin (A), mTOR (B) and myostatin (C) in CON and PD cells. (A) The effect of T-stimulus on myogenin mRNA expression levels after 72 h exposure. *T-stimulus significantly increased myogenin expression in CON and PD cells compared to non-treated cells ($P \leq 0.05$). **The presence of LY with T treatment significantly attenuated T's effect in CON cells ($P \leq 0.05$). ***T exposure continued to increase myogenin mRNA in PD cells after 7 days culture, even in the presence of LY ($P \leq 0.05$). B) Changes in mTOR mRNA expression with the various treatments to CON and PD cells after 7 days culture. *CON + T and **CON + T + LY significantly increased mTOR expression vs. CON untreated cells ($P \leq 0.05$). ***There was a significant difference in mTOR expression between CON + LY and CON + T + LY ($P \leq 0.001$). Additionally there was a significant difference in mTOR expression between untreated CON and PD cells in 7 days culture. There were no changes in PD cells with the same treatments at either time points. (C) The effect of T-stimulus on myostatin mRNA expression after 7 days exposure. *T significantly reduced myostatin expression in the PD treated cells after 7 days ($P \leq 0.01$). **LY alone significantly reduced myostatin levels ($P \leq 0.01$) at 72 h and 7 days. ≠ Plus with the addition of T to LY, this reduction was heightened ($P \leq 0.01$) compared to non-treated PD cells.^λ Basal PD cells had significantly elevated myostatin mRNA levels at 7 days vs. parental controls ($P \leq 0.001$).

Furthermore, the treatment of T + LY significantly increased mTOR mRNA compared to LY alone (CON + T + LY 135.14 ± 16.08 vs. CON + LY 112.70 ± 13.62, $P \leq 0.001$, Fig. 5B) and untreated controls (CON + T + LY 135.14 ± 16.08 vs. CON 111.95 ± 19.36, $P \leq 0.05$). This highlights T administration increases in mTOR expression even in the presence of LY. In the PD cells, all treatments were without effect on mTOR expression at 7 days exposure (Fig. 5B). However, at 7 days under basal conditions, CON cells displayed significantly higher mTOR expression than PD cells (CON 111.95 ± 19.36 vs. PD 1.01 ± 0.10, $P \leq 0.05$, Fig. 5B).

3.6. T-stimulus reduces negative muscle mass regulator myostatin in PD cells only

Myostatin transcript expression was slightly elevated in PD cells after 72 h compared to CON, although these elevations were not statistically significant (CON 5.93 ± 1.87 vs. PD 7.63 ± 2.58, Fig. 5C). However, at 7 days, statistically significant observations were observed for increases in myostatin mRNA expression in PD cells compared to CON cells (PD 12.93 ± 4.69 vs. CON 4.57 ± 1.20, $P \leq 0.001$, Fig. 5C). This novel finding suggests that under basal conditions, myostatin may block differentiation in these myoblasts and thus contribute towards reduced myotube hypertrophy. In CON cells, T treatments, LY alone or co-incubations of T + LY at 72 h did not alter myostatin mRNA expression (Fig. 5C). The presence of LY alone was the only treatment to significantly reduce myostatin mRNA expression after 72 h exposure to PD cells (PD + LY 4.27 ± 2.47 vs. PD 7.63 ± 2.58, $P \leq 0.01$, Fig. 5C).

At 7 days, there were no changes in myostatin mRNA expression in CON cells (CON 4.57 ± 1.20; CON + T 5.99 ± 1.40; CON + LY 4.32 ± 1.65; CON + T + LY 4.84 ± 1.01, Fig. 5C). However in the PD cells, T treatment significantly impaired elevations in myostatin expression compared to PD non-treated cells (PD + T 9.73 ± 2.56 vs. PD 12.93 ± 4.69, $P \leq 0.05$, Fig. 5C). The reduction in myostatin transcript expression was significantly larger in magnitude with the addition of T with LY (−36%) in PD cells at the 7 day time point (PD + T + LY 3.47 ± 0.83 vs. PD 12.93 ± 4.69, $P \leq 0.01$, Fig. 5C), yet similar effects were not observed in CON cells. However, the presence of LY alone also brought about reductions in myostatin expression (PD + LY 4.98 ± 2.25 vs. PD 12.93 ± 4.69, $P \leq 0.001$, Fig. 5C) and the reductions were similar to T + LY (P = N.S.). Overall, suggesting both LY and testosterone alone reduce myostatin expression in PD cells only. It therefore appears that T potentially reduces myostatin expression in atrophied PD cells only suggesting a potential mechanism that may explain the increase in differentiation/hypertrophy seen in this cell type, whereas in CON cells, the increases with T are independent of myostatin expression.

4. Discussion

The present study supports a role for testosterone in enhancing myogenic differentiation and myotube hypertrophy [50–55] but more importantly, shows the capacity to improve hypertrophy and

myonuclear accretion in a previously established model displaying impaired differentiation and hypertrophy similar to that of atrophic phenotypes such as those observed in ageing [7,26]. Furthermore, testosterone treatment enhanced hypertrophy shown by increases in myotube diameter, nuclei per myotube and a larger number of myotubes with 5 or more nuclei in both control (CON) and multiple population doubling (PD) cells. Interestingly, testosterone improved hypertrophy (myotube diameter) to the same magnitude in both cell types at 72 h and 7 day time points. Thus, despite PD cells having undergone multiple population doublings vs. their controls, and therefore displaying a reduced basal differentiation capacity as previously described in Sharples et al. [7,26]; testosterone was able to exert similar magnitude increases in myotube hypertrophy. Despite this interesting observation, testosterone was unable to fully restore differentiation (myotube number) to the level observed in untreated control cells at 7 days; perhaps suggesting testosterones predominant role in hypertrophy rather than differentiation in this model. Furthermore, in line with previous findings, the current study showed that PD cells had reduced myogenin expression vs. CON cells [7,26], with the present study also supporting previous morphological and biochemical (reduced CK activity) findings [7,26], showing myotube diameter was reduced in the PD cells. This further consolidates the use of these cells as a representative model to investigate cellular and molecular mechanisms of atrophic (PD) vs. hypertrophic phenotypes (CON).

Importantly, testosterone mediated increases in myotube hypertrophy were potentiated via the PI3K/Akt pathway, where inhibition of this pathway in the presence of testosterone rendered the hormone unable to exert its potent influence on myotube hypertrophy in both cell types. This study supports previous work where the PI3K/Akt pathway has been implicated in testosterones action in L6 myoblasts [22] and human skeletal myoblasts [56] where the same PI3K inhibitor (LY294002) also reduced testosterone induced hypertrophy. Kovacheva and colleagues [57] have also previously reported that Akt signalling downstream of PI3K was restored by testosterone administration in elderly mice. The present study further supports that testosterones action in myotube hypertrophy is mediated via PI3K/Akt pathway, especially where reductions in Akt activation have been previously reported in this model (i.e. lower in PD vs. CON) [7]. Overall, these observations further suggest that the manipulation of this pathway by testosterone may be imperative for therapeutic restoration of muscle atrophy [38].

Interestingly, exogenous testosterone improved myogenin expression in both CON and PD cells types, whether the PI3K inhibitor (LY294002) was present or absent, suggesting testosterone-mediated activation of myogenin occurs independently of the PI3K/Akt signalling pathway. Testosterone has previously been shown to increase myogenin in C_2C_{12} cells [50,51]. Indeed, community-dwelling older men treated with grades doses of testosterone show increases in muscle fibre size accompanied by increased myogenin expression [55]. Despite this, testosterone induced increases in myogenin observed in the presence of PI3K inhibitor were unable to restore the reduced differentiation/hypertrophy impinged by the PI3K inhibitor alone. Therefore, suggesting that myogenin was not the main mechanism of action in testosterone-induced increases in hypertrophy. Overall however, absolute levels of myogenin were severely reduced in PD vs. CON cells, with testosterone unable to rescue absolute myogenin expression levels in the cells that display atrophic phenotypes (PD's) to levels observed in untreated control cells. Thus, perhaps highlighting myogenins more pertinent role in differentiation (not hypertrophy) as testosterone was unable to restore absolute levels of myogenin and corresponding myotube numbers in PD cells vs. untreated control levels. Although, as discussed above, testosterone was able to improve myotube diameter, i.e. hypertrophy.

In addition to this, testosterone increased mTOR expression in CON cells at 7 days, Previously testosterone has been shown to increase mTOR phosphorylation in both L6 rat [22] and in C_2C_{12} [23] myoblasts. Indeed, mTOR mRNA expression in CON cells was increased in the presence of testosterone plus PI3K inhibitor (LY), perhaps suggesting an important role for testosterone in increasing mTOR independently of PI3K/Akt. Furthermore, White and colleagues [23] also observed increases in mTOR phosphorylation with incremental doses of testosterone in C_2C_{12} cells, independently of Akt activation. However, mTOR expression was not increased in PD cells in the presence of testosterone alone or in combination with the PI3K inhibitor suggesting impaired mTOR transcript expression in response to exogenous testosterone in the atrophic, reduced differentiation phenotype PD vs. control cells. Previously, in our labs we have observed reduced IGF-I transcript expression with corresponding reductions in Akt phosphorylation in PD myoblasts [7]. As Akt is upstream of mTOR this suggests Akt may be involved the reduction of mTOR observed between CON and PD myoblasts basally at 7 days. However, activity of mTOR was not directly assessed in the present study and warrants further investigation.

In agreement with the present study where mTOR expression in CON cells was increased in the presence of testosterone plus PI3K inhibitor (LY) (albeit mRNA expression and not protein activity), other studies have shown that mTOR activation can occur via signals independent of canonical IGF-I/Akt, via a pathway involving phospholipase D, phosphatidic acid and a downstream regulator Rheb (ras homologue enriched brain) [58–61]. Redd 2 may also be important in inhibiting mTOR via the tuberous sclerosis 1 (TSC1) and 2 (TSC2) complex [62]. As mTOR mRNA expression is increased in CON vs. PD cells; testosterone increase mTOR expression in CON cells which is blunted in PD cells at 7 days, and mTOR transcript expression is still increased with testosterone even the presence of PI3K/Akt inhibitor, it begs the question as to the role of testosterone in regulating phospholipase D, phosphatidic acid, Rheb and Redd2 and their subsequent interaction with mTOR. Especially in light of recent data where following mechanical overload Redd2 is reduced to enable mTOR to initiate p70S6K activity, which is involved in protein synthesis and hypertrophy, a process that is impaired in the elderly [63].

Myostatin is a negative regulator of muscle mass in many species [64–67]. There is evidence indicating that myostatin inhibits satellite cell activation, proliferation, and differentiation [55,68,69], possibly mediated through perturbation of Akt and mTOR signalling [49]. Therefore reductions in myostatin, as previously observed with testosterone administration [69], can enhance muscle mass regulation in muscle wasting diseases such as cachexia and sarcopenia [70–72]. Interestingly, in the current study myostatin mRNA expression was reduced in myoblasts that have basally impaired hypertrophy (PD cells) when administered with testosterone with corresponding increases in myotube hypertrophy. The reduction in myostatin mRNA expression at 7 days with T treatment was accompanied by increases in myogenin mRNA expression in PD cells, which is supported recent literature highlighting myostatin's role for inhibiting myogenic differentiation [49,73,74]. Despite this, testosterone did not return absolute levels of myostatin expression to the low levels observed in the control (CON) cells. These observations suggest that although testosterone may reduce myostatin expression, it is not entirely responsible for the improved hypertrophy observed in the atrophic (PD) phenotype cells. Furthermore, the PI3K inhibitor (LY) alone also substantially reduced myostatin expression where there is a distinct lack of differentiation and hypertrophy. This is in contrast to recent studies where there was a reduction in the activity of Akt observed in the presence of exogenous myostatin in human myoblasts [49]. Therefore, if myostatin was reduced, PI3K/Akt activity may be expected to increase. Although inhibition of PI3K in the present study makes

it difficult to compare with the aforementioned study, this phenomenon requires further investigation in the current model.

It is important to note the potential effect of testosterone breakdown which may occur within the cell culture media as the steroidogenic enzymes 5-α reductase and aromatase are critical in converting T to dihydrotestosterone (DHT) and estradiol respectively [75,76]. Therefore, knowing if testosterone is the active steroid compound stimulating hypertrophy in the current model is a limiting factor. Future studies may address the impact of other steroid hormones such as DHT in rescuing impaired differentiation and hypertrophy via the PI3K/Akt pathway.

5. Conclusion

In the present study exogenous testosterone was able to increase hypertrophy in myoblasts with reduced differentiation potential (PD cells) to a similar magnitude as the control cells. Testosterone induced myotube hypertrophy was mediated via the PI3K/Akt pathway, where inhibition of this pathway in the presence of testosterone rendered the hormone unable to exhibit its potent influence on myotube hypertrophy in phenotypically atrophic (PD) and hypertrophic control (CON) cells Testosterone-induced hypertrophy was also accompanied by increased myonuclear accretion in both cell types, with corresponding increases in myogenin expression. Furthermore,blunted mTOR expression was observed in response to exogenous testosterone administration in atrophic myotubes (PD) vs. control (CON) myotubes. Myostatin expression was reduced in the presence of testosterone in atrophic cells only. Overall, administration of testosterone shows strong potential to enhance hypertrophy in a previously atrophic cell type myoblasts via the PI3K/Akt pathway.

Acknowledgements

The laboratory work was carried out within the Stem Cells, Ageing & Molecular Physiology (SCAMP) Unit, Research Institute for Sport and Exercise Sciences (RISES), School of Sport and Exercise Sciences, Liverpool John Moores University, Tom Reilly Building, Byrom Street, Liverpool, UK and the MCMPRG, Bedford, UK. .The manuscript was prepared within SCAMP, RISES, LJMU.

References

[1] C.L. Donohoe, A.M. Ryan, J.V. Reynolds, Cancer cachexia: mechanisms and clinical implications, Gastroenterology Research and Practice (2011), http://dx.doi.org/10.1155/2011/601434.
[2] W.D. Dudgeon, K.D. Philips, J.A. Carson, R.B. Brewer, J.L. Durstine, et al., Counteracting muscle wasting in HIV-infected individuals, Trends in Immunology 25 (2006) 4–7.
[3] P.O. Hasselgren, M.J. Menconi, M.U. Fareed, H. Yang, W. Wei, et al., Novel aspects on the regulation of muscle wasting in sepsis, International Journal of Biochemistry and Cell Biology 37 (2005) 2156–2168.
[4] V.M. Conraads, V.Y. Hoymans, C.J. Vrints, Heart failure and cachexia: insights offered from molecular biology, Frontiers in Bioscience 13 (2008) 325–335.
[5] A. Saini, S. Faulkner, N. Al-Shanti, C. Stewart, Powerful signals for weak muscles, Ageing Research Reviews 8 (2009) 251–267.
[6] A.J. Cruz-Jentoft, F. Landi, E. Topkinkova, J.P. Michel, Understanding sarcopenia as a geriatric syndrome, Current Opinion in Clinical Nutrition and Metabolic Care 13 (2010) 1–7.
[7] A.P. Sharples, N. Al-Shanti, M.P. Lewis, C.E. Stewart, Reduction of myoblast differentiation following multiple population doublings in mouse C(2)C(12) cells: a model to investigate ageing? Journal of Cellular Biochemistry 112 (2011) 3773–3785.
[8] M.J. Tisdale, Cancer cachexia, Physiological Reviews 81 (2009) 381–440.
[9] D.W. Russ, I.R. Lanza, The impact of old age on skeletal muscle energetic: supply and demand, Current Aging Science 4 (2011) 234–247.
[10] T. Rantanen, T. Harris, S.G. Leveille, M. Visser, D. Foley, et al., Muscle strength and body mass index as long-term predictors of mortality in initially healthy men, Journals of Gerontology Series A: Biological Sciences and Medical Sciences 55 (2000) 168–173.
[11] C. Deans, S.J. Wigmore, Systemic inflammation, cachexia and prognosis in patients with cancer, Current Opinion in Clinical Nutrition and Metabolic Care 8 (2005) 256–259.
[12] E.L. Dillon, G. Basra, A.M. Horstman, S.L. Casperson, K.M. Randolph, et al., Cancer cachexia and anabolic interventions: a case report, Journal of Cachexia, Sarcopenia and Muscle 3 (2012) 253–263.
[13] M. Muscaritoli, M. Bossola, Z. Aversa, R. Bellantone, F. Rossi Fanelli, Prevention and treatment of cancer cachexia: new insights into an old problem, European Journal of Cancer 42 (2006) 31–41.
[14] J.M. Argiles, S. Busquets, C. Garcia-Martinez, F.J. Lopez-Soriano, Mediators involved in the cancer anorexia–cachexia syndrome: past, present and future, Nutrition 21 (2005) 977–985.
[15] I.G. Brodsky, P. Balagopal, K.S. Nair, Effects of testosterone replacement on muscle mass and muscle protein synthesis in hypogonadal men—a clinical research center study, Journal of Clinical Endocrinology & Metabolism 81 (1996) 3469–3475.
[16] M. Sheffield-Moore, R.J. Urban, S.E. Wolfe, J. Jiang, D.H. Catlin, et al., Short-term oxandrolone administration stimulates net muscle protein synthesis in young men, Journal of Clinical Endocrinology & Metabolism 84 (1999) 2705–2711.
[17] S. Bashin, T.W. Storer, M. Javanbakht, N. Berman, K.E. Yarasheski, et al., Testosterone replacement and resistance exercise in HIV-infected men with weight loss and low testosterone levels, JAMA 283 (2000) 763–770.
[18] R. Casaburi, S. Bashin, L. Cosentino, J. Porszasz, A. Somfay, et al., Effects of testosrerone and resistance training in men with chronic obstructive pulmonary disease, American Journal of Respiratory and Critical Care Medicine 170 (2004) 870–878.
[19] A. Ferrando, M. Sheffield-Moore, C. Yeckel, C. Gilkison, J. Jiang, et al., Testosterone administration to older men improves muscle function: molecular and physiological mechanisms, American Journal of Physiology: Endocrinology and Metabolism 282 (2002) E601–E607.
[20] F. Sattler, S. Bashin, J. Hue, C. Chou, C. Castenada-Sceppa, et al., Testosterone threshold levels and lean tissue mass targets needed to enhance skeletal muscle strength and function: the HORMA trial, Journal of Gerontology: Medical Sciences 66A (1) (2011) 122–129.
[21] C. Serra, F. Tangherlini, S. Rudy, D. Lee, G. Toraldo, et al., Testosterone improves the regeneration of old and young mouse skeletal muscle, Journals of Gerontology Series A: Biological Sciences and Medical Sciences 68 (2013) 17–26.
[22] Y. Wu, W.A. Bauman, R.D. Blitzer, C. Cardozo, Testosterone-induced hypertrophy of L6 myoblasts is dependant upon erk and mTORC1, Biochemical and Biophysical Research Communications 400 (2010) 679–683.
[23] J.P. White, S. Gao, M.J. Puppa, S. Sato, S.L. Welle, et al., Testosterone regulation of Akt/mTORC1C1/FoxO3a signalling in skeletal muscle, Molecular and Cellular Endocrinology 365 (2012) 174–186.
[24] A. Mauro, Satellite cell of skeletal muscle fibers, Journal of Biophysical and Biochemical Cytology 9 (1961) 493–495.
[25] T.J. Hawke, D.J. Garry, Myogenic satellite cells: physiology to molecular biology, Journal of Applied Physiology 91 (2001) 534–551.
[26] A.P. Sharples, D.J. Player, N.R. Martin, V. Mudera, C.E. Stewart, M.P. Lewis, Modelling in-vivo skeletal muscle ageing in-vitro using three dimensional bioengineered constructs, Aging Cell 11 (2012) 986–996.
[27] A.P. Sharples, N. Al-Shanti, C.E. Stewart, C2 and C2C12 murine skeletal muscle myoblast models of atrophic and hypertrophic potential: relevance to disease and ageing? Journal of Cellular Physiology 225 (2010) 240–250.
[28] H. Degens, S.E. Always, Skeletal muscle function and hypertrophy are diminished in old age, Muscle and Nerve 27 (2003) 339–347.
[29] C.I. Morse, J.M. Thom, O.S. Mian, A. Muirhead, K.M. Birch, et al., Muscle strength, volume and activation following 12-month resistance training in 70-year old males, European Journal of Applied Physiology 95 (2005) 197–204.
[30] H. Bruunsgaard, K. Andersen-Ranberg, J.B. Hjelmborg, B.K. Pedersen, B. Jeune, Elevated levels of tumour necrosis factor alpha and mortality in centenarians, American Journal of Medicine 115 (2003) 278–283.
[31] H. Bruunsgaard, S. Ladelund, A.N. Pedersen, M. Schroll, T. Jorgensen, et al., Predicting death from tumour necrosis factor alpha and interleukin-6 in 80-year old people, Clinical and Experimental Immunology 132 (2003) 24–31.
[32] S.J. Lees, K.A. Zwetsloot, F.W. Booth, Muscle precursor cells isolated from aged rats exhibit an increased TNF-alpha response, Aging Cell 8 (2009) 26–35.
[33] A. Bigot, V. Jacquemin, F. Debacq-Chainiaux, G. Butler-Browne, O. Toussaint, et al., Replicative aging down-regulates the myogenic regulatory factors in human myoblasts, Biologie Cellulaire 100 (2008) 189–199.
[34] T. Pietrangelo, C. Puglielli, R. Mancinelli, S. Beccafico, G. Fano, et al., Molecular basis of the myogenic profile of aged human skeletal muscle satellite cells during differentiation, Experimental Gerontology 44 (2009) 523–531.
[35] S. Beccafico, F. Riuzzi, C. Puglielli, R. Mancinelli, S. Fulle, et al., Human muscle satellite cells show age-related differential expression of S100B protein and RAGE, Age (Dordrecht, Netherlands) 33 (4) (2011) 523–541.
[36] D. Cuthbertson, K. Smith, J. Babraj, G. Leese, T. Waddell, et al., Anabolic signaling deficits underlie amino acid resistance of wasting, aging muscle, FASEB Journal 19 (2005) 422–424.
[37] B. Léger, W. Derave, K. De Bock, P. Hespel, A.P. Russell, Human sarcopenia reveals an increase in SOCS-3 and myostatin and a reduced efficiency of Akt phosphorylation, Rejuvenation Research 11 (1) (2008) 163B–175B.
[38] S.C. Bodine, T.N. Stitt, M. Gonzalez, W.O. Kline, G.L. Stover, R. Bauerlein, E. Zlotchenko, A. Scrmgeour, J.C. Lawrence, D.J. Glass, G.D. Yancopoulos, Akt/mTORC1 pathway is a crucial regulator of skeletal muscle hypertrophy

and can prevent muscle atrophy *in vivo*, Nature Cell Biology 3 (2001) 1014–1019.
[39] D. Yaffe, O. Saxel, Serial passaging and differentiation of myogenic cells isolated from dystrophic mouse muscle, Nature 270 (1977) 725–727.
[40] H.M. Blau, G.K. Pavlath, E.C. Hardeman, C.P. Chiu, L. Silberstein, et al., Plasticity of the differentiated state, Science 230 (1985) 758–766.
[41] N. Al-Shanti, S.H. Faulkner, A. Saini, I. Loram, C.E. Stewart, A semi-automated programme for tracking myoblast migration following mechanical damage: manipulation by chemical inhibitors, Cellular Physiology and Biochemistry 27 (6) (2011) 625–636.
[42] S.A. Coolican, D.S. Samuel, D.Z. Ewton, F.J. McWade, J.R. Florini, The mitogenic and myogenic actions of insulin-like growth factors utilize distinct signalling pathways, Journal of Biological Chemistry 272 (10) (1997) 6653–6662.
[43] R.A. Frost, D. Huber, A. Pruznak, C.H. Lang, Regulation of REDD1 by insulin-like growth factor-I in skeletal muscle and myotubes, Journal of Cellular Biochemistry 108 (5) (2009) 1192–1202.
[44] W. Lee, Insulin-like growth factor-I induced androgen receptor activation is mediated by the PI3/Akt pathway in C2C12 skeletal muscle cells, Molecules and Cells 28 (5) (2009) 495–499.
[45] B.G. Li, P.O. Hasselgren, C.H. Fang, Insulin-like growth factor-I inhibits dexamethasone-induced proteolysis in cultured L6 myotubes through PI3K/Akt/GSK-3beta and PI3K/Akt/mTORC1-dependent mechanisms, International Journal of Biochemistry and Cell Biology 37 (10) (2005) 2207–2216.
[46] X.Q. Zeng, C.M. Zhang, M.L. Tong, X. Chi, X.L. Li, et al., Knockdown of NYGGF4 increases glucose transport in C2C12 mice skeletal myocytes by activation IRS-1/PI3K/AKT insulin pathway, Journal of Bioenergetics and Biomembranes 44 (3) (2012) 351–355.
[47] T.D. Schmittgen, K.J. Livak, Analyzing real-time PCR data by the comparative C(T) method, Nature Protocols 3 (6) (2008) 1101–1108.
[48] E.J. Stevenson, A. Koncarevic, P.G. Giresi, R.W. Jackman, S.C. Kandarian, Transcriptional profile of a myotube starvation model of atrophy, Journal of Applied Physiology 98 (2005) 1396–1406.
[49] A.U. Trendelenburg, A. Meyer, D. Rohner, J. Boyle, S. Hatakeyama, et al., Myostatin reduces Akt/TORC1/p70S6K signaling, inhibiting myoblast differentiation and myotube size, American Journal of Physiology: Cell Physiology 296 (2009) C1258–C1270.
[50] D. Lee, Androgen receptor enhances myogenin expression and accelerates differentiation, Biochemical and Biophysical Research Communications 294 (2) (2002) 408–413.
[51] F. Wannenes, M. Caprio, L. Gatta, A. Fabbri, S. Bonini, et al., Androgen receptor expression during C2C12 skeletal muscle cell line differentiation, Molecular and Cellular Endocrinology 292 (2008) 11–19.
[52] I. Sinha-Hikim, S.M. Roth, M.I. Lee, S. Bhasin, Testosterone induced muscle hypertrophy is associated with an increase in satellite cell number in healthy, young men, American Journal of Physiology: Endocrinology and Metabolism 285 (2003) E197–E205.
[53] R. Singh, J.N. Artaza, W.E. Taylor, N.F. Gonzalez-Cadavid, S. Bashin, Androgens stimulate myogenic differentiation and inhibit adipogenesis in C3H 10T1/2 pluripotent cells through an androgen receptor-mediated pathway, Endocrinology 144 (2003) 5081–5088.
[54] R. Singh, S. Bashin, M. Braga, J.N. Artaza, S. Pervin, et al., Regulation of myogenic differentiation by androgens: cross talk between androgen receptor/β-catenin and follistatin/transforming growth factor-β signaling pathways, Endocrinology 150 (2009) 1259–1268.
[55] I. Sinha-Hikim, M. Cornford, H. Gaytan, M.L. Lee, S. Bhasin, Effects of testosterone supplementation on skeletal muscle fiber hypertrophy and satellite cells in community dwelling, older men, Journal of Clinical Endocrinology and Metabolism 91 (2006) 3024–3033.
[56] C. Serra, S. Bashin, F. Tangherlini, E.R. Barton, M. Ganno, et al., The role of GH and IGF-I in mediating anabolic effects of testosterone on androgen-responsive muscle, Endocrinology 152 (2011) 193–206.
[57] E.L. Kovacheva, A.M.S. Hikim, R. Shen, I. Shinha, I. Sinha-Hikim, Testosterone supplementation reverses sarcopenia in aging through regulation of myostatin, c-jun NH_2 Terminal kinase, notch, and Akt signaling pathways, Endocrinology 151 (2010) 628–638.
[58] T.A. Hornberger, W.K. Chu, Y.W. Mak, et al., The role of phospholipase D and phosphatidic acid in the mechanical activation of mTORC1 signaling in skeletal muscle, Proceedings of the National Academy of Science 103 (2006) 4741–4746.
[59] Y. Sun, P.J. Bilan, Z. Liu, Klip A. Rab8A, Rab13 are activated by insulin and regulate GLUT4 translocation in muscle cells, Proceedings of the National Academy of Science 107 (2010) 19909–19914.
[60] J.C. Anthony, F. Yoshizawa, T.G. Anthony, et al., Leucine stimulates translation initiation in skeletal muscle of postabsorptive rats via a rapamycin-sensitive pathway, Journal of Nutrition 130 (2000) 2413–2419.
[61] J.C. Anthony, T.G. Anthony, S.R. Kimball, et al., Orally administered leucine stimulates protein synthesis in skeletal muscle of post absorptive rats in association with increased eIF4F formation, Journal of Nutrition 130 (2000) 139–145.
[62] M.P. DeYoung, P. Horak, A. Sofer, et al., Hypoxia regulates TSC1/2-mTORC1 signaling and tumor suppression through REDD1-mediated 14-3-3 shuttling, Genes and Development 22 (2008) 239–251.
[63] M.J. Drummond, M. Miyazaki, H.C. Dreyer, B. Pennings, S. Dhanani, et al., Expression of growth-related genes in young and older human skeletal muscle following an acute stimulation of protein synthesis, Journal of Applied Physiology 106 (2009) 1403–1411.
[64] A.C. McPherron, A.M. Lawler, S.J. Lee, Regulation of skeletal muscle mass in mice by a new TGF-beta superfamily member, Nature 387 (1997) 83–90.
[65] A.C. McPherron, S.J. Lee, Double muscling in cattle due to mutations in the myostatin gene, Proceedings of the National Academy of Science 94 (1997) 12457–12461.
[66] M. Schuelke, K.R. Wagner, L.E. Stolz, C. Hubner, et al., Myostatin mutation associated with gross muscle hypertrophy in a child, New England Journal of Medicine 350 (2004) 2682–2688.
[67] D. Joulia-Ekaza, G. Cabello, Myostatin regulation of muscle development: molecular basis, natural mutations, physiopathological aspects, Experimental Cell Research 312 (13) (2006) 2401–2414.
[68] K.R. Wagner, X. Liu, X. Chang, R.E. Allen, Muscle regeneration in the prolonged absence of myostatin, Proceedings of the National Academy of Science 102 (7) (2005) 2519–2524.
[69] S. Kawada, M. Okuno, N. Ishii, Testosterone causes the decrease in the content of skeletal muscle myostatin, International Journal of Sport and Health Science 4 (2006) 44–48.
[70] V. Siriett, L. Platt, M.S. Salerno, N. Ling, et al., Prolonged absence of myostatin reduces sarcopenia, Journal of Cellular Physiology 209 (3) (2006) 866–873.
[71] V. Siriett, M.S. Salerno, C. Berry, G. Nicholas, et al., Antagonism of myostatin enhances muscle regeneration during sarcopenia, Molecular Therapy 15 (8) (2007) 1463–1470.
[72] C.M. Liu, Z. Yang, C.W. Liu, R. Wang, P. Tien, et al., Myostatin antisense RNA-mediated muscle growth in normal and cancer cachexia mice, Gene Therapy 15 (2008) 155–160.
[73] F. Gao, T. Kishida, A. Ejima, S. Gojo, O. Mazda, Myostatin acts as an autocrine/paracrine negative regulator in myoblast differentiation from human induced pluripotent stem cells, Biochemical and Biophysical Research Communications 431 (2013) 309–314.
[74] C. McFarlane, G.Z. Hui, W.Z. Amanda, H.Y. Lau, S. Lokireddy, et al., Human myostatin negatively regulates human myoblast growth and differentiation, American Journal of Physiology: Cell Physiology 301 (2011) C195–C203.
[75] V. Luu-The, F. Labrie, The intracrine sex steroid biosynthesis pathways, Progress in Brain Research 181 (2010) 177–192.
[76] L. Vandenput, C. Ohlsson, Sex steroid metabolism in the regulation of bone health in men, Journal of Steroid Biochemistry and Molecular Biology 121 (2010) 582–588.